Synthesis and Interactions of Sulfated C5a-receptor and CHIPS Mimics

Anton Bunschoten

Synthesis and Interactions of Sulfated C5a-receptor and CHIPS mimics

Anton Bunschoten

PhD thesis with summary in Dutch

Department of Medicinal Chemistry and Chemical Biology

Utrecht University, Utrecht, The Netherlands

Augustus 2010

ISBN: 978-90-8891-190-3

Cover design: Hans Ippel, Anton Bunschoten

Published by: Uitgeverij BOXPress, Oisterwijk

Printed by: Proefschriftmaken.nl / Printyourthesis.com

The research described in this thesis was financially supported by the Dutch Technology Foundation STW, Applied Science Division of NWO, and the Technology Program of the Ministry of Economic Affairs (UKG.06609).

Synthesis and Interactions of Sulfated C5a-receptor and CHIPS Mimics

Synthese en interacties van gesulfateerde C5a-receptor en CHIPS mimetica

(met samenvatting in het Nederlands)

Proefschrift

ter verkrijging van de graad van doctor aan de Universiteit Utrecht
op gezag van de rector magnificus, prof. dr. J. C. Stoof,
ingevolge het besluit van het college voor promoties
in het openbaar te verdedigen
op maandag 30 augustus 2010 des middags te 2.30 uur

door

Anton Bunschoten

geboren op 28 september 1981 te Soest

Promotor:	Prof. dr. R. M. J. Liskamp
Co-promotoren:	Dr. J. Kemmink
	Dr. ir. J. A. W. Kruijtzer

List of abbreviations

Amino acids

Ala	A	L-alanine
Arg	R	L-arginine
Asn	N	L-asparagine
Asp	D	L-aspartic acid
Cys	C	L-cysteine
Gln	Q	L-glutamine
Glu	E	L-glutamic acid
Gly	G	glycine
His	H	L-histidine
Ile	I	L-isoleucine
Leu	L	L-leucine
Lys	K	L-lysine
Met	M	L-methionine
Phe	F	L-phenylalanine
Pro	P	L-proline
D-Pro	p	D-proline
Ser	S	L-serine
Thr	T	L-threonine
Trp	W	L-tryptophan
Tyr	Y	L-tyrosine
Val	V	L-valine

General

AIBN	azobisisobutyronitrile
Alloc	allyloxycarbonyl
ASST	arylsulfate sulfotransferase
Boc	*tert*-butyloxycarbonyl
BOP	benzotriazol-1-yloxytris(dimethylamino)-phosphonium hexafluorophosphate
^{t}Bu	*tert*-butyl
br	broad
C5aR	complement 5a receptor
CD	circular dichroism
CHIPS	chemotaxis inhibitory protein of S*taphylococcus aureus*
CHOPS	chemotaxis inhibitory construct protein of *Staphylococcus aureus*
CID	collision induced dissociation
d	doublet
DBU	1,8-Diazabicyclo[5.4.0]undec-7-ene
DCE	1,2-dichloroethane
DCM	dichloromethane
DCV	dichlorovinyl
DIPEA	*N*,*N*-diisopropyl-*N*-ethylamine
DMA	N,N-dimethylacetamide

DMAP	4-dimetylaminopyridine
Dmbz	2,6-dimethoxybenzoyl
DMF	N,N-dimethylformamide
DMSO	dimethylsulfoxide
DTT	dithiothreitol
ECD	electron capture dissociation
EDD	electron detachment dissociation
EDTA	ethylenediaminetetraacetic acid
ER	endoplasmatic reticulum
ESI	electro spray ionisation
ETD	electron transfer dissociation
Fmoc	9-fluorenylmethoxycarbonyl
Fmoc-OSu	*N*-(9-fluorenylmethoxycarbonyloxy)succinimide
GPCR	G protein-coupled receptor
HBTU	2-(1*H*-benzotriazol-1-yl)-1,1,3,3-tetramethyluronium hexafluorophosphate
HOBt·H_2O	*N*-hydroxybenzotriazol hydrate
HPLC	high performance liquid chromatography
HSQC	heteronuclear single quantum correlation
ITC	isothermal titration calorimetry
Kd	dissociation constant
LH	luteinizing hormone
m	multiplet
MALDI	matrix assisted laser desorption/ionisation
MD	molecular dynamics
MHz	megahertz
MS	mass spectrometry
MTBE	methyl-*tert*-butyl ether
NBS	*N*-bromosuccinimide
NMP	*N*-methylpyrrolidone
NMR	nuclear magnetic resonance
N-OH-AA	*N*-hydroxy arylamines
NOE	nuclear overhauser effect
NOESY	nuclear overhauser effect spectroscopy
NP	neopentyl
*o*NBS	*O*-nitrobenzenesulfonyl
PAH	polycyclic aromatic hydrocarbons
PAPS	3’-phosphoadenosine 5’-phosphosulfate
PAP	3’-phosphoadenosine 5’-phosphate
PAS	pyridinium acetyl sulfate
PB	periodic boundary
Pbf	2,2,4,6,7-pentamethyldihydrobenzofuran-5-sulfonyl
PDB	protein data bank
*p*NPS	*p*-nitrophenyl sulfate
ppm	parts per million
q	quartet
rms	root mean square

Rt	retention time
s	singlet
SDS-PAGE	sodium dodecyl sulfate – poly acrylamide gel electrophoresis
SPPS	solid phase peptide synthesis
t	triplet
TAC	triazacyclophane
TBAB	tetrabutylammonium bromide
TEA	triethylamine
TFA	trifluoroacetic acid
TIS	triisopropylsilane
TLC	thin layer chromatography
TMS	tetramethylsilane
TOCSY	total correlation spectroscopy
TOF	time of flight
TPST	tyrosyl protein sulfotransferase
Trt	triphenylmethyl or trityl.

Chapter 1

General Introduction

1

1.1 Introduction

Post-translational modifications (PTM´s) of proteins are nature´s way of expanding the diversity of proteins encoded in the approx 23.000 genes of the humane genome even more.[1, 2] By modifying side-chains or introducing new functionalities, proteins can interact with an enormous variety of targets, catalyze a vast number of reactions and relay several types of signals. Moreover, the reversibility of several PTM´s gives the possibility for fine tuning of interactions and turning pathways on and off. For instance the formation of disulfide bonds can be crucial for the tertiary structure of proteins, the acetylation and deacetylation of histones are crucial for their function in gene transcription,[3] and the phosphorylation of serine, threonine and tyrosine functions as an on/off switch for multiple intracellular signaling pathways.[4, 5]

Understanding the introduction and function of these PTM´s, of which phosphorylation is an outstanding example, is crucial for our understanding of human physiology. Extensive research has been and still is invested in studying phosphorylation, which has resulted in an enormous amount of knowledge in this area. Phosphorylation has been shown to be crucial in intracellular communication and has been identified as a very important process to interfere with in e.g. anti-cancer therapies.[6] A considerable part of the successes in the field of protein phosphorylation lies in the development of synthetic procedures and methodologies to produce, reliably and conveniently, phosphorylated peptides. The availability of these methods has opened up the way for researchers to study the functions of these phosphate groups in a range of biological processes.

The sulfate group is, at first glance, a quite similar moiety compared to the phosphate group. It is widely applied in human physiology and is present on a vast range of molecular structures: from the smallest aromatic compounds like phenol to the very large and complex carbohydrates and proteins. Next to their structural similarity to a phosphate group, sulfates and phosphates also share the possibility to adapt and modify the function of peptides and proteins by post-translational modification. Similar to phosphorylation, the hydroxyl functionality of tyrosine residues, but also of serine and threonine can be sulfated.[7] Although it is believed that up to 1% of all tyrosine residues can be sulfated in vivo,[8] still little is known about which peptides and proteins are sulfated and about the function of sulfation.

In this introduction sulfation *in vivo* will be discussed, starting with the sulfation of small compounds, then sulfation of carbohydrates and finally the sulfation of peptides and proteins. The focus will be on sulfation as a post-translational modification, the analysis of sulfated peptides and proteins and the synthesis of these structures. Our interest in sulfated peptides and proteins originates from the sulfated C5a-receptor (C5aR), a crucial receptor in the human complement system, and from the inhibitory action of Chemotaxis Inhibitory Protein of *Staphylococcus aureus* (CHIPS) on the C5a-receptor. This very specific and potent inhibitory action of CHIPS on the C5aR can be used as a molecular source of inspiration towards the development of new anti-inflammatory drugs.

1.2 Sulfation *in vivo*

The presence of sulfated molecules, mainly aromatic compounds, in the human body was first described by Baumann in 1876, who analyzed sulfated phenolic compounds in human urine. He also identified one of the functions of sulfation: detoxification. Patients who were treated with phenol, used as an antiseptic agent at that time, excreted exclusively sulfated phenol.[9] It was realized that inorganic sulfate was not the sulfating agent *in vivo* and in 1957 Robbins et al. concluded that the active sulfate source in humans is 3´-phosphoadenosine 5´-phosphosulfate (PAPS), which donates a sulfonate group to the hydroxyl functionality of the molecule to be sulfated.[10] Although the name for this reaction should therefore be sulfonation, the historically used term sulfation is still the preferred and most widely used one. PAPS itself is synthesized from ATP, which is sulfated by ATP-

sulfurylase and phosphorylated on the 5´-position by APS-kinase (Fig. 1.1). After delivering its sulfonate group to its target molecule, the resulting PAP is degraded to 5´-AMP by PAP-nucleotidase.[11]

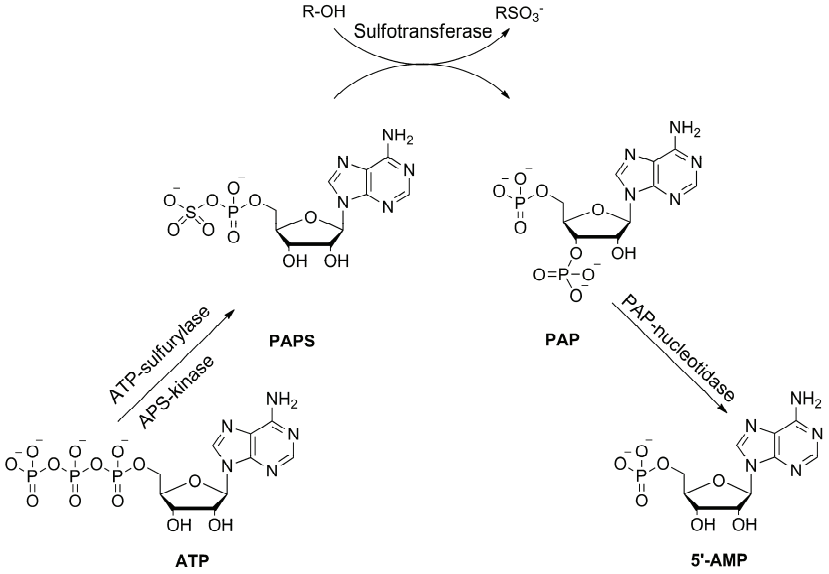

Figure 1.1 Biosynthesis, action and degradation of 3´-phosphoadenosine 5´-phosphosulfate.

In that same period the study of sulfokinases was started, which are the enzymes responsible for transferring the sulfonate group form PAPS to the substrates. Gradually the name "sulfotransferase" was more accepted instead of "sulfokinase", probably because it was often confused with (phospho)kinase. Sulfotransferases and the enzymes necessary for PAPS synthesis are found in almost all human tissues and lack of PAPS synthesis has been described as lethal.[12, 13] Next to animals, sulfotransferases have also been identified in insects, bacteria and even in plants.[14-18] Human sulfotransferases can be divided in two classes, namely cytosolic soluble sulfotransferases and membrane bound sulfotransferases.

Cytosolic Sulfotransferases introduce sulfate groups onto small endo- and exogenous compounds

Soluble cytosolic sulfotransferases were the first to be discovered and are the most frequently studied sulfotransferases. They are soluble globular proteins (Fig. 1.2) found in almost all tissues and organisms. They are named "SULT" followed by the number of one of the enzyme families and a designation (A, B etc.) for the subfamily, e.g. 1E1 and 2A1 (Fig. 1.2).[19] Families 1-200 are found in animals, families 201-400 are found within plant species, families 401 and higher are reserved for prokaryotes. The SULT´s have ca. 45% amino acid homology within a family and ca. 60% amino acid homology within subfamilies. Especially the binding site for PAPS is highly preserved within the SULT´s and within other classes of sulfotransferases.[19, 20]

The SULT´s are quite promiscuous in accepting substrates and can sulfate a wide variety of endogenous and exogenous compounds, e.g. hormones, neurotransmitters, drugs and xenobiotics.[21] As indicated earlier, the first role assigned to the SULT´s was that of detoxification exogenous compounds as a chemical defense mechanism.[22] Addition of a sulfate group to mainly aromatic hydroxyl functionalities results in increased water solubility and therefore facilitates excretion. In most cases sulfation also results in a decrease in biological activity of the ligand although also the activation of compounds by sulfation has been described. The anti-hypertensive drug minoxidil is converted to its active metabolite by sulfation.[23] On the other hand, some xenobiotics like e.g. hydroxymethyl polycyclic aromatic hydrocarbons (PAHs) and N-hydroxy arylamines (N-OH-AAs) are converted in mutagenic and carcinogenic metabolites by sulfation.[24]

The importance of sulfation as a biological reaction was emphasized even more when the important role of SULT´s in the metabolism, regulation and activity of steroid hormones was discoverd. The regulation of dehydroepiandrosterone (DHEA) is the most important example of this function of sulfation.[22, 25, 26] An imbalance in the activity of these steroid sulfotransferases and their complementary sulfatases is considered to be the cause of hormone-dependent breast cancer.[27, 28]

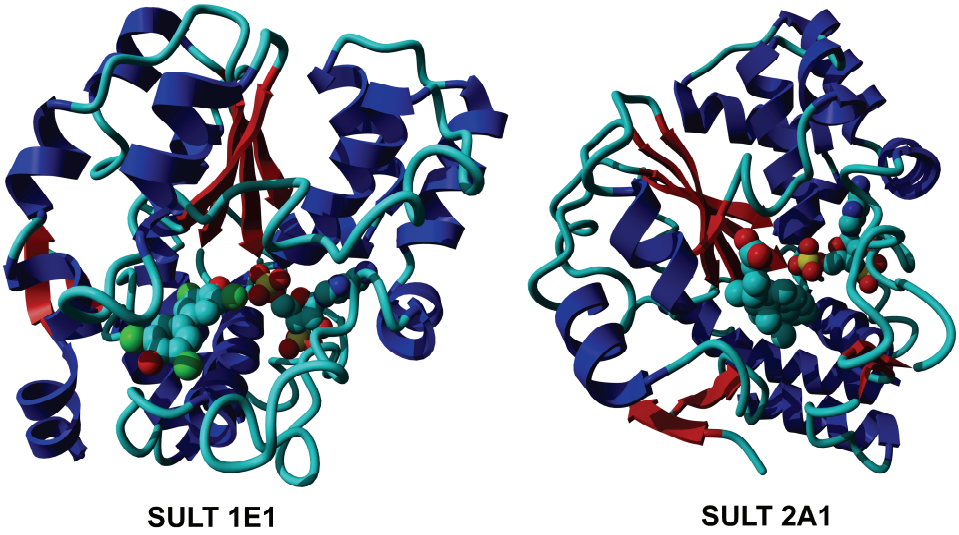

Figure 1.2 Crystal structures of two typical cytosolic sulfotransferases in complex with PAP and a substrate, both depicted as ball-structures. Structures obtained from Protein Data Bank, 1G3M and 3F3Y, respectively.

Membrane bound sulfotransferases sulfate large biomolecules

Two types of membrane bound sulfotransferases are described in the literature: Carbohydrate sulfotransferases and tyrosyl protein sulfotransferases. Most of the membrane bound sulfotransferases are involved in sulfating (large) carbohydrate (containing) structures. The luteinizing hormone (LH)

was the first glycoprotein shown to be sulfated on its carbohydrate moieties. The sulfated carbohydrate part did not influence the function of the hormone, but did regulate its clearance from the bloodstream.[29]

An example of a large carbohydrate structure sulfated *in vivo* is heparan sulfate (Fig. 1.3), which is a very common constituent of the extra-cellular matrix and is extensively involved in cellular recognition. As such it is connected to embryonic development, angiogenesis, blood coagulation, cell adhesion, etc. [30] Heparan consists of alternating hexuronic acid or l-iduronic acid and d-glucosamine residues and can be *N*-sulfated on glucosamine and *O*-sulfated on the 2-, 3- and 6-position of each carbohydrate building blocks. Each of these sulfations is carried out by its own sulfotransferase, e.g. HS-3-*O*-ST (heparin sulfate D-glucosaminyl 3-*O*-Sulfotransferase) and HS-2-*O*-ST (heparin sulfate idouronic acid 2-*O*-Sulfotransferase). The sulfation pattern of these types of extracellular carbohydrates can be fine tuned by extracellular sulfatases.[31]

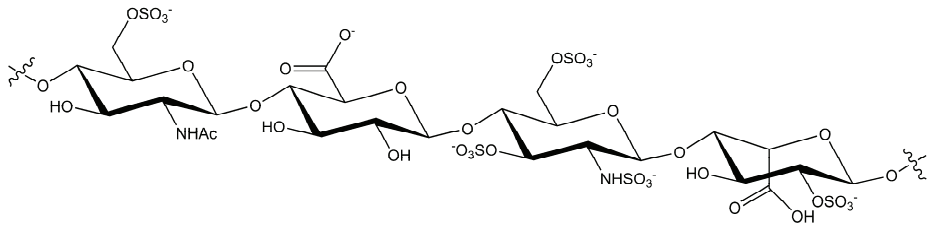

Figure 1.3 Fragment of heparan sulfate depicting the different building blocks: GlnNAc, GlcA, $GlcNH_2$ and IdoA, with the possible sulfation patterns.[32]

Peptides and proteins are sulfated by tyrosyl protein sulfotransferases

The first peptide containing a sulfated tyrosine residue was discovered in 1954 by Bettelheim. He described the observation that bovine fibrinogen contained a tyrosine that was blocked in the natural peptide, but could be liberated via mild acid hydrolysis and formation of inorganic sulfate salts was observed.[33] Since then several small peptides have been discovered containing a sulfated tyrosine, for example: gastrin, phyllokinin, cholecystokinin, caerulein, hirudin and Leu-enkephalin.[34-39] Tyrosine sulfation became known as a widespread post-translational modification after the publication of Huttner, who described that sulfated proteins were found in all tissues he had examined.[40] Later Baeuerle and Huttner determined that the proteome of the fruit fly *Drosophila melanogaster* contained up to 1% of sulfated tyrosine residues and this number has since been used as an argument to illustrate the importance of protein sulfation.[8] The same group also discovered that, although the function of most sulfated peptides/proteins was unknown, most if not all were secretory or membrane bound sulfated peptides/proteins.[41]

Medzhiradszky recently described the sulfation of serine and threonine *in vivo*, which was observed by high resolution mass spectrometry.[7] However, so far no further observations or biological functions have been reported.

In 1983 the isolation of a particulate fraction of PC12 cells was described, which was capable of catalyzing the sulfation of proteins with ^{35}S-labelled PAPS as a sulfate donor. It was concluded that the enzyme responsible for sulfation of proteins was isolated and named it tyrosylprotein sulfotransferase (TPST).[42] This enzyme is membrane bound and located in the Golgi complex with its catalytic domain directed to the lumen of the Golgi.[43] One of the functions of the Golgi complex is the covalent modification of proteins destined for lysosomes, secretory granules, and the plasma membrane, which supports the hypothesis that mainly secretory peptides and proteins are being sulfated. Later on the sulfation reaction was localized in the trans-Golgi network, the last part of the Golgi before peptides and proteins get transported to their intended locations (Fig. 1.4).[44]

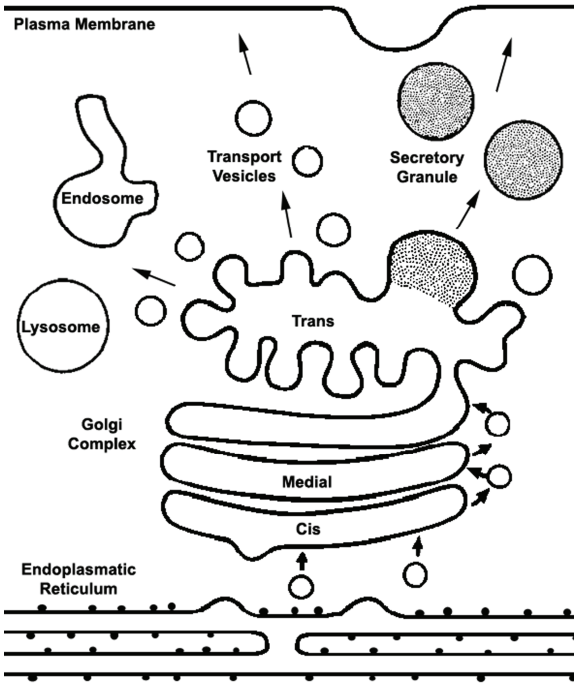

Figure 1.4 The transport of proteins, synthesized in the ER, via the Golgi to lysosomes and the plasma membrane.

In 1998 Ouyang et al. cloned human TPST and presented the amino acid sequence of the 370-amino acid long N-glycosylated protein.[45] Later, TPST-2 was independently discovered by two research groups by aligning DNA-sequences.[46, 47] TPST-2 consists of 377 amino acids and is 67% homologous

to TPST-1. Based on gene homology studies it is not expected that more similar TPST enzymes will be uncovered.[48]

Both TPST´s contain a small transmembrane domain and a short cytosolic tail by which the protein is anchored in the membrane of the trans-Golgi network. This topology classifies both enzymes as type II transmembrane proteins. No real substrate specificity has been established for both TPST´s, although some small differences have been observed in the sequence and reaction rates by which multiple sulfated proteins get sulfated.[49] TPST-2 was shown to be up-regulated in comparison to TPST-1 in shear stress experiment with blood vessel endothelial cells (HUVEC).[50] Differences between the two sulfotransferases are observed in mice capable of producing only one of both enzymes.[51, 52] Double knockout mice were born alive, but most died shortly after birth, demonstrating the importance of sulfations *in vivo*.[53] The TPST´s show a different optimal pH, (pH 6.5 and pH 6.0), a different response to the presence and concentrations of Mg^{2+} and Mn^{2+} and different kinetic constants for several peptide substrates.[54] Although the expression levels varied, both TPST´s were found in all 20 examined human tissues examined by Mishiro et al.[54]

So far there is no exact acceptor sequence known for TPST´s, although it was recognized already in 1985 that the tyrosines to be sulfated should be surrounded by acidic amino acids.[43] Based on several peptides and proteins known to contain sulfated or unsulfated tyrosine residues, a set of sequence characteristics was formulated (Table 1.1). Based on these characteristics a position-specific scoring matrix (PSSM) and a prediction program, called ´the sulfinator´, were created.[55, 56] The PSSM was effective in ´predicting´ known sulfated sequences, but its static scoring of the surrounding sequence was less effective in recognizing new patterns. The ´sulfinator´ is more flexible in predicting the position of sulfated tyrosines within a peptide sequence with an overall accuracy of 98% of known sulfated and unsulfated sequences.[56] Two problems are not addressed by these predictors: proteins containing a possible sulfation site need to have that specific sequence surface exposed and have to travel through the Golgi in order to be sulfated.[57] Because of this, false positives can be generated when protein sequences are scanned for sulfation sites.

Table 1.1 Consensus sequence characteristics for tyrosine sulfation

Feature	Position from tyrosine	Description
Acidic residue	± 5	Acidic residue adjacent to tyrosine and at least three within five residues
Basic residue	± 5	No more than one basic residue within 5 residues
Turn inducing	± 7	Presence of a turn inducing residue within 7 residues
Disulfide	± 7	No disulfide bonds within 7 residues
Sugar	± 7	No glycosylation sites within 7 residues of
Hydrophobic	± 5	No more than three hydrophobic residues within 5 residues

Until now around fifty sulfated human proteins and peptides have been identified, mainly based on direct evidence or based on similarity with known sulfated sequences. Among these sulfated proteins are hormones, extracellular matrix proteins, blood coagulants or anticoagulants, complement proteins, GPCR´s and adhesion proteins.[48] Unfortunately, for most of these sulfated proteins the role of the sulfate group is unknown, although a limited number of sulfated proteins have been studied in detail, of which PSGL-1 and CCR5 are the best examples.

P-selecting glycoprotein ligand 1

The migration of circulating leukocytes from the blood stream into infected tissues depends on the adhesion of leukocytes to the wall of blood vessels. This adhesion is mediated by the binding of P-selectin glycoprotein ligand 1 (PSGL-1), a membrane bound protein on the surface of neutrophils, to P-selectin, a membrane bound protein on the surface of endothelial cells. Next to crucial glycosylation, the N-terminus of mature PSGL-1 contains three tyrosines, each of which can be sulfated.[58] ^{35}S-sulfate is incorporated in PSGL-1 *in vivo* and experiments with N-terminal peptides demonstrated that all three sulfated tyrosine residues were necessary to obtain an identical binding affinity to P-selecting compared to soluble PSGL-1.[58-61]

CC-chemokine receptor 5

HIV-1 infection starts by binding of the viral glycoprotein gp120 to CD4 of the host cell. Glycoprotein gp120 is connected to the virus via a gp41 transmembrane protein. Subsequent conformational rearrangements of gp120 lead to binding to the chemokine receptor CCR5. The binding of the gp120:CD4 complex to this CCR5 co-receptor allows gp41 to bind to the membrane of the host cell and promote fusion of the membranes and entry of the viral content (Fig. 1.5).[62] The N-terminus of the CCR5-receptor contains four tyrosine residues surrounded by acidic amino acids of which especially tyrosines 10 and 14 are sulfated and crucial for binding of CD4/gp120 and finally viral infection.[63] This sulfation of CCR5 is also mimicked by the human immune system in this case, tyrosine sulfated antibodies against gp120 were identified in two HIV-1 infected patients.[64]

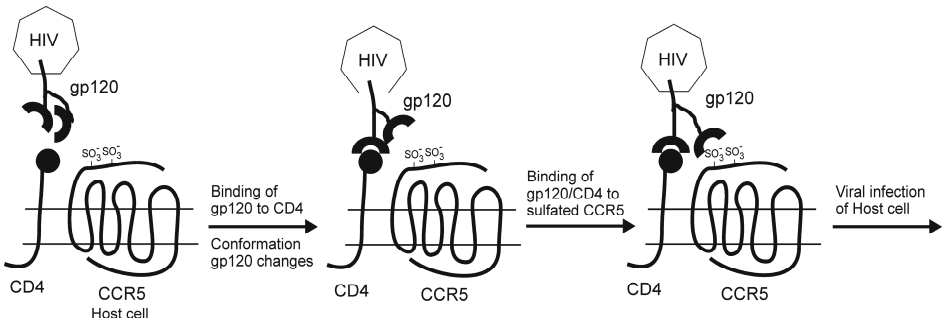

Figure 1.5 HIV-1 infection of a host cell. Gp120 binds to CD4, upon which a binding site for the N-terminus of CCR5 is exposed. Binding of gp120:CD4 to CCR5 will lead to viral entry.

1.3 Stability of sulfated tyrosines

Arylsulfates are acid-labile compounds; a proposed mechanism for the hydrolysis of arylsulfates comprises the protonation of the monoester and subsequent hydrolysis (Fig. 1.6).[65] 95% of sulfated tyrosine is hydrolyzed within 5 minutes in 1M HCl at 100 °C.[66] However, under milder acidic conditions sulfated tyrosine residues are less labile and Balsved et al. demonstrated that the peptide gastrin is largely unharmed at pH 1 when stored below 25 °C.[67] The stability of sulfotyrosine residues can be increased by increasing the length of the sulfated peptide, by the introduction of large cations, and by basic residues close to sulfotyrosine in the peptide sequence. However, this acid-lability is still a large obstacle for the detection, analysis and synthesis of sulfated peptides.[65, 68]

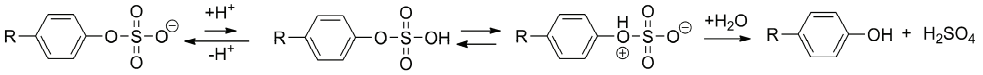

Figure 1.6 Proposed mechanism for the acid hydrolysis of sulfate arylmonoesters.[65]

In vivo, sulfotyrosine residues are remarkably stable and this PTM is even believed to be irreversible.[48] Sulfotyrosine and its sulfated metabolites are normal constituents of human urine.[69] Because tyrosine itself is not efficiently sulfated *in vivo* it was soon suggested that the sulfotyrosine found in urine had to originate from degraded peptides containing sulfated tyrosine residues.[70] Several researches have shown that peptides containing sulfated tyrosine residues and sulfotyrosine itself are degraded and are excreted (human, mouse, rats, rabbits, pigs) in urine as sulfated tyrosine metabolites.[70-73] Sulfotyrosine is also hardly hydrolyzed by the sulfatases known in 1959.[74] Although some *in vitro* sulfatase activity against sulfotyrosine has been described for sulfatase A and B, no sulfatase has been uncovered that shows activity towards peptides or proteins containing sulfated tyrosine residues. [26, 75]

1.4 Analysis of sulfated peptides/proteins

In order to study the sulfation of peptides and proteins in vivo it is very important to be able to show tyrosine sulfation and to determine the position of a sulfated tyrosine residue within a peptide sequence in case of multiple tyrosine residues that can be sulfated. Several techniques and approaches have been described in the literature, and will be briefly discussed below.

Isotope labeling reveals the presence of sulfotyrosine

A very reliable and much applied method for identifying sulfated proteins is using the knowledge of the incorporation of inorganic sulfate into PAPS after which it will be incorporated in the target molecule (Fig. 1.1). By supplying cells with ^{35}S-enriched sulfate, which will be incorporated in PAPS, sulfated molecules will be labeled with a radio isotope and are therefore traceable.[66] In order to distinguish sulfated tyrosines from glycoproteins with sulfated carbohydrates, the glycosylation can be inhibited or the protein can be hydrolyzed under alkaline conditions after which sulfotyrosine can be identified by e.g. HPLC.[58] Sometimes co-labeling with [^{3}H]tyrosine or [^{14}C]tyrosine is used to

determine whether the ^{35}S-sulfate is indeed incorporated in sulfotyrosine.[8] Although a much used and very reliable method, isotope labeling will not reveal the location of the sulfated tyrosine residues within a peptide or protein.

Inhibition of sulfations reveals biological role of sulfation

The presence and importance of sulfated tyrosine residues can be determined by the inhibition of sulfation. Inhibition of sulfation in general can be accomplished by a sulfate analogue like selenate (SeO_4^{2-}), however selenates were too toxic for use in living cells.[76] Chlorate (ClO_3^-) on the other hand could be applied in living cells and its inhibition was reversible, which was demonstrated by the removal of the chlorate.[77, 78] Introduction of chlorate will result in a blocked active site of ATP-sulfurylase and therefore an impaired synthesis of PAPS (Fig. 1.1). Unfortunately, this method does not discriminate between sulfated proteins or carbohydrates, because PAPS is the universal sulfate source for both sulfations. A more selective way to show the involvement of a sulfated tyrosine residue would be to remove selectively the sulfate groups from a particular tyrosine residue and evaluate the resulting biological activity. This has been accomplished by the use of an arylsulfatase from *Aerobacter aerogenes*, which has been shown to remove sulfate groups selectively from tyrosine residues.[58]

Anti-sulfotyrosine antibodies recognize sulfated sequences

Antibodies that can selectively recognize a sulfated tyrosine residue are very powerful tool in identifying sulfated proteins in the proteome. It was already possible to raise antibodies against sulfated peptides, unfortunately sequences of around 10 residues surrounding a sulfated tyrosine residue were necessary to raise antibodies successfully. Therefore these antibodies will not be sequence independent. The first sequence independent antibodies against sulfated tyrosines were developed simultaneously by two groups. In 2006 both Kehoe et al. and Hoffhines et al. developed, by phage display methods, selective antibodies that were able to bind to sulfated peptides with different sequences.[79, 80] These selective antibodies open up the way for sulfoproteomics, the proteome wide search for sulfated proteins, but no reports have been published yet.

Analysis of sulfated proteins by mass spectrometry

A very powerful technique in proteomics and studies into many post-translational modifications of proteins is mass spectrometry. There are, however, several problems with the identification of sulfotyrosine containing peptides and proteins by mass spectrometry. The standard conditions used for MALDI or ESI mass spectrometry often lead to desulfation of sulfotyrosines caused by the acidic sample conditions as well as ´in-source decay´. Measurements in the negative ion mode, with neutral or basic sample conditions have been shown to produce mass spectra containing dominantly the sulfated product peak as for instance shown by Wolfender et al.[81] But successful detection of proteins or peptides without the loss of the sulfate group will need optimization for each experiment.

Although the loss of a sulfate group, when detected, can be evidence of sulfation, identification of the position of sulfated residues will not be possible by standard methods. The weak sulfate monoester bond would break before fragmentation of the peptide backbone would occur. Besides, the mass difference of 80 Da ($-SO_3$) detected upon fragmentation of a sulfate group is the same as the mass difference upon fragmentation of a phosphate group ($-HPO_3$).[82] Several strategies have been developed to be able to apply mass spectrometry in the identification of sulfated residues in proteins.

Discrimination between sulfation and phosphorylation can be made by determining the difference in lability and fragmentation of the sulfate group compared to the phosphate group. The level of fragmentation upon a measurement in the negative ion mode compared to positive ion mode may give an indication whether the loss of 80 Da originates from the more stable phosphorylated residue or the labile sulfated residue,[83, 84] although this can be tricky because of the unknown stability of sulfates in different peptide sequences and sample conditions. Nonetheless, this method has been applied to screen for sulfated fragments in protein digests.[85]

Another approach to determine whether the loss of 80 Da originates from a phosphate group or from a sulfate group is to perform ultra-high accuracy mass measurements, because there is a small mass difference of 9.5 mDa (loss of $-SO_3$ ΔM = 79.9568 Da, loss of $-HPO_3$ ΔM = 79.9663 Da). For these types of measurements very accurate mass equipment will be necessary, like for instance a Fourier transform ion cyclotron resonance (FT-ICR) mass spectrometer and these types of measurements will be challenging on (crude) protein or peptide mixtures. With this method Medzihradszky et al. showed the presence of sulfated serine and threonine residues within proteins isolated from different types of eukaryotes.[7]

The above mentioned approaches might tell you whether there is a sulfated residue present in a certain peptide or protein, but it will not reveal the position of the sulfated residue when multiple tyrosine, serine or threonine residues are present. Several new fragmentation methods show promising results with the sequencing of peptides containing labile post-translational modifications. Electron capture dissociation (ECD), electron detachment dissociation (EDD) and electron transfer dissociation (ETD) are mild fragmentation techniques. Peptide fragments are created, respectively, by the addition of low energy electrons to peptide cations, by the detachment of electrons by bombardment of negatively charged peptides by fast electrons or by the transfer of electrons from radical anions to peptide cations.[86-88] These methods result mainly in the fragmentation of the peptide backbone instead of fragmentation of the weakest bonds, which is mainly observed in collision-induced dissociation (CID). Leaving the post-translational modifications intact during fragmentation of the peptide backbone would reveal crucial information about the location of the PTM within the peptide sequence. Promising results have been published but no extensive study into sulfoproteomics has been reported yet.[87-89]

Recently a combination of chemical labeling and MS/MS measurements was reported for the determination of *O*-sulfation sites within peptides. Tyrosine residues containing a free hydroxyl group were efficiently acetylated with sulfosuccinimidyl acetate (S-NHSAc) and imidazole. Thus tyrosine residues containing a free hydroxyl group detected after an MS/MS experiment were originally sulfated and were desulfated during the mass spectromic analysis.[90] In case of the possible presence of a phosphorylated tyrosine residue in the peptide, treatment with alkaline phosphatase was performed before the acetylation step.

1.5 Synthesis of sulfated peptides

In addition to a convenient and reliable analysis, the availability of synthetic sulfated peptides is essential for studies into the biological function of sulfated peptides and proteins. The available methods are still fairly limited and comprise the use of global sulfating reagents, unprotected sulfated building blocks, harsh deprotection conditions or enzymatic sulfations. The most often applied methods in the literature are summarized below.

Global sulfating reagents

The most general method for introducing sulfate groups is by global sulfation with sulfating reagents. One of the oldest procedures to introduce sulfate groups on amino acids or peptides is treatment with concentrated sulfuric acid. In 1946 the effect of sulfuric acid on amino acids and peptides was described.[91] It was noticed that little hydrolysis occurred, instead sulfate groups were added mainly to the hydroxyl containing amino acids. A major side-reaction of tyrosine when treated with sulfuric acid was sulfonation of the aromatic ring, but this could be limited by performing the reaction at low temperature and this method has successfully been applied in the synthesis of small sulfated peptides.[74, 92] Milder reagents for the synthesis of sulfated peptides and building blocks were soon discovered. Penke et al. introduced pyridinium acetyl sulfate (PAS) as a new sulfating reagent, but it has not been applied by others.[93] The pyridine or DMF sulfurtrioxide complexes are more widely used sulfating reagents also applied in peptide synthesis.[94-97] However, these reagents will react with all hydroxyl functionalities as well as with free amines in an unprotected peptide. The synthesis of complex peptides with these general sulfating reagents requires a suitable protecting strategy.

A successful strategy has been applied by Futaki and Kitagawa in the synthesis of cionin. They protected the reactive side chains with sulfinyl-based protecting groups. (Fig. 1.7A) Those protecting groups are acid stable, but during sulfation with sulfurtrioxide the added ethanedithiol reduces the sulfoxides after which they become acid-labile.[98, 99] Another interesting strategy was described by Young and Kiessling, in which all other functional groups within the peptide were protected with benzyl protecting groups and the tyrosine residue to be sulfated was introduced with an azidomethyl (Azm) protecting group on the phenolic position (Fig. 1.7B).[100] After removal of the Azm-group with tinchloride and thiophenol under basic conditions the resulting free tyrosine side chain was sulfated with $DMF{\cdot}SO_3$. Then, the sulfated peptide was cleaved from the resin under mild acidic conditions

and was deprotected by hydrogenolysis.[97] Although this is an elegant method, not all building blocks are readily available and especially the Azm-protected tyrosine has to be synthesized in 6-7 steps.[97] Moreover, the use of benzyl-protected amino acids in Fmoc/*t*Bu SPPS is not the preferred protecting group strategy.

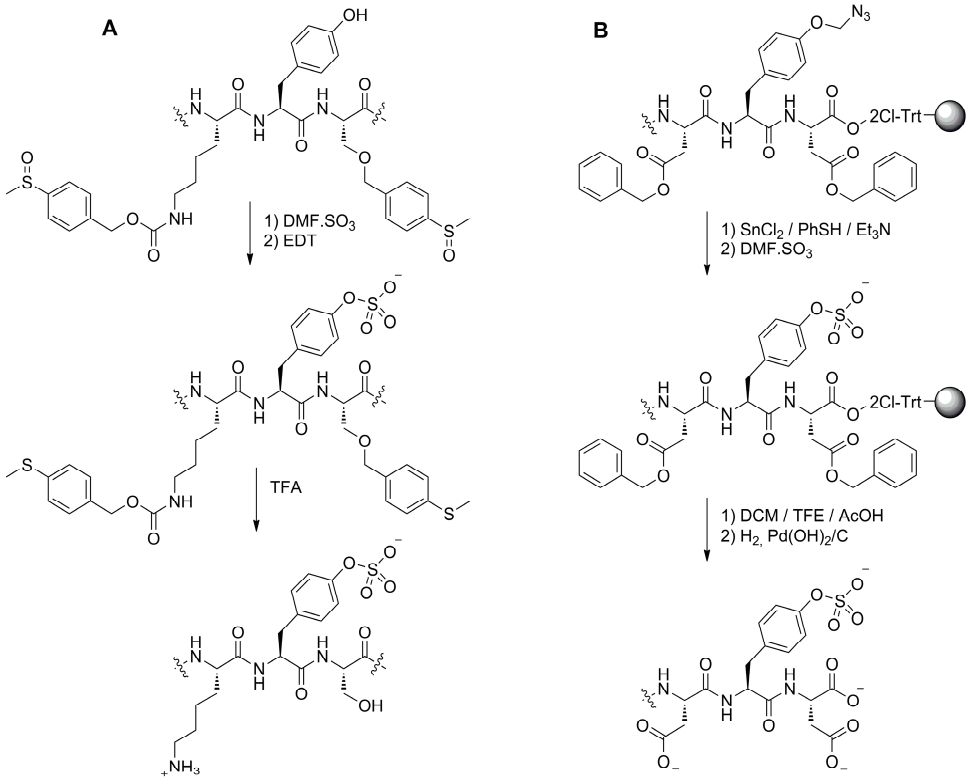

Figure 1.7 Protection strategies for the application of sulfating reagents on peptide sequences. A) application of sulfinyl-based protecting groups which become acid labile after reduction,[98] B) application of the Azm protecting group to selectively deprotect the tyrosine hydroxyl-functionality.[97]

Incorporation of sulfated tyrosine building blocks

The incorporation of a sulfated tyrosine building block would be the ideal strategy, because no additional protection or deprotections steps would be required. The first successful application of sulfated tyrosine building blocks dates from 1979. Moroder et al. applied a Cbz-protected sulfated barium salt of tyrosine for the synthesis of small sulfated peptides.[101] With the development of Fmoc/*t*Bu SPPS also side-chain unprotected sulfated tyrosine building blocks for Fmoc/*t*Bu SPPS were described (Fig. 1.8A). Although they have been applied in the synthesis of sulfated peptides, the acid-lability of the sulfate ester is still a complicating factor. In principal the sulfate monoester can be preserved during the final prolonged treatment with TFA to cleave the peptide from the solid phase

and deprotect the amino acid side-chains, but the right conditions have to be determined for each peptide-sequence to achieve complete cleavage and deprotection while obtaining as little sulfate ester hydrolysis as possible. Short deprotection times, low temperatures and exclusion of sulfur-based scavengers have been moderately successful.[60, 102-105] Diminishing of sulfate group hydrolysis by the formation of sodium, barium and tetrabutylammonium salts of Fmoc-Tyr(SO_3^-)-OH has been attempted (Fig 1.8A).[60, 65, 101] Although this approach has been applied several times, solubility problems and low coupling-yields are mentioned in the literature.[59, 97] Moreover, hydrolysis of the sulfate monoester and incomplete deprotection of the other amino acid side chains will be a large obstacle for the synthesis of complex peptides containing several sulfated tyrosine residues.

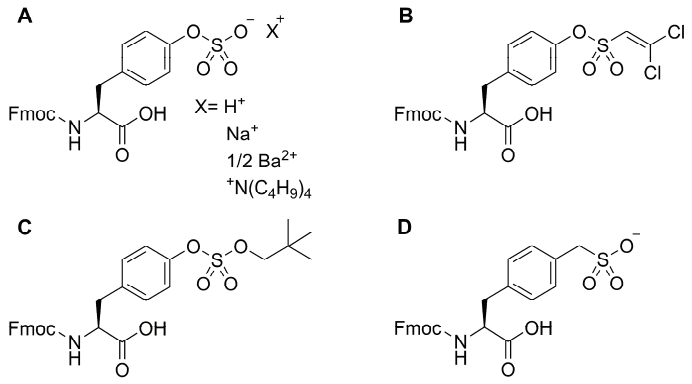

Figure 1.8 Sulfated building blocks for Fmoc/*t*Bu solid phase peptide synthesis. A) Fmoc-tyrosine sulfate salts, B) dichlorovinyl-protected sulfotyrosine, C) neopentyl-protected sulfotyrosine, D) sulfonate isostere of sulfotyrosine.

Incorporation of protected sulfated tyrosine building blocks

In 2004, Liu et al. described the use of 2,2,2-trichloroethyl chlorosulfate as a reagent to introduce a protected sulfate moiety into steroids and carbohydrates.[106, 107] Unfortunately, the TCE protecting group is not stable during the piperidine deprotection steps applied in Fmoc/*t*Bu SPPS and its application in Boc SPPS has not been reported.

In 2009, at the same time we described our new method (Chapter 2),[108] Ali and Taylor reported the application of a derivative of TCE, the dichlorovinyl protecting group (Dcv)(Fig. 1.8B). A sulfated tyrosine building block protected with the Dcv group proved to be stable in Fmoc/*t*Bu SPPS when piperidine was replaced with 2-methylpiperidine for deprotection of the Fmoc group. Removal of the Dcv-group was performed with Pd/C and hydrogen gas in the presence of a high concentration ammonium formate or triethylamine at room temperature.[109, 110] The use of ammonium formate was expected to be problematic in the presence of methionine, cysteine and tryptophan residues.[109] By introducing triethylamine, sulfated peptides with methionine and tryptophan residues could be synthesized, but no comments on the incorporation of cysteine were made.[110]

In 2006, Simpson and Widlanski described the synthesis of neopentyl- and isobutyl-protected sulfated carbohydrates and tyrosine (Fig. 1.8C), but found that isobutyl protection was not stable under basic conditions (6% piperidine) and deprotection conditions for the neopentyl group were too harsh for application in peptide chemistry (azide or cyanide nucleophiles in hot DMF).[111]

Serendipitously, at the same time we described our new method (Chapter 2),[108] they discovered that the very stable and sterically hindered neopentyl protecting group was removed from sulfotyrosine by incubation for 6-12 hours at 37 ºC in 1-2 M ammonium acetate.[112] Although the mechanism is not well understood, they successfully applied this approach for the synthesis of several sulfated peptides and reported complete stability of the neopentyl protecting group under Fmoc/*t*Bu SPPS conditions.

Application of sulfotyrosine isosteres

An approach to circumvent the acid lability of the sulfotyrosine is replacement with an isostere of sulfotyrosine. In 1989 Marseigne et al. described the replacement of sulfotyrosine with a sulfonate isostere, Phe(*p*-CH_2SO_3Na)(Fig. 1.8D), in CCK8 peptides. These peptides, with the non-hydrolysable sulfonate group, showed similar binding affinities towards the native receptor.[113, 114] Recently, Roosenburg et al. used this same CCK8 peptide with sulfonate groups for peptide receptor imaging by attaching a radiolabel.[115] Also in the construction of CCR5 N-terminal peptides, the sulfonate isostere could replace the sulfated tyrosine residue successfully.[116]

Enzymatic sulfation by sulfotransferases

Sulfated peptides can also be synthesized by an enzymatic route. In 1990, Niehrs et al. described the first broad application of enzymatic sulfation of synthetic peptides.[117] Golgi-enriched membranes were isolated from bovine adrenal medulla and the substrate-specificity of TPST was explored with around 20 synthetic peptides known or expected to be sulfated or phosphorylated. The synthetic application of the TPST´s was made more conveniently by the cloning and over-expression of TPST-1 and TPST-2 in 1998.[45-47] Cloned and isolated soluble versions of TPST-1 and TPST-2 have shown to be very valuable tools in different types of sulfation-procedures. Although it is still an expensive method and therefore limited to small scale peptide synthesis, mainly on µmole scale, it is extremely valuable for the synthesis of complex (glyco)peptides, ^{15}N- and ^{13}C-labeled peptides and for mimicking *in vivo* sulfations to determine location and functionality. Isolated TPST-1 was used for the synthesis of the N-terminal region of PSGL-1, a 23-residue long peptide which contains three sulfated tyrosine residues next to a glycosylated threonine.[59] Several studies with isolated TPST´s have been carried out to resolve the *in vivo* sulfation pattern of peptides containing multiple tyrosine residues.[49, 118, 119] ^{15}N- and ^{13}C-labelled peptides can be very useful tools for studying protein structures and protein-peptide interactions, but the synthesis of peptides by SPPS using labeled amino acids is very expensive. Protein expression in e.g. *E. coli* with labeled nutrients is much cheaper and will yield labeled peptides and proteins which can be sulfated after isolation by treatment with TPST and PAPS.[118]

Employing human TPST´s, enzymatic peptide sulfation will be limited to the sequences sulfated *in vivo*, however there is also a bacterial sulfotransferase isolated that has different sequence requirements compared to human TPST´s. This enzyme, isolated form *Eubacterium* A-44[15, 18] does not require PAPS as sulfate source but uses other easier obtainable sulfated arylsulfates, e.g. *p*-nitrophenyl sulfate (*p*NPS). Therefore this type of enzyme is called arylsulfate sulfotransferases (ASST). Besides sulfations of several small biomolecules, it is also capable of sulfating several peptide-sequences specifically on tyrosine, for example Leu-enkephalin and CCK-8.[120] An agarose immobilized version of this ASST was shown to be more stable and could reach higher yields compared to a soluble ASST.[121] A cloned version of this ASST was expressed in *E. coli* and evaluated for the use in an industrial setting and although the produced enzyme was not as active as reported earlier, the authors believed it can be used for the production of sulfated peptides.[122] Unfortunately it is difficult to predict which sequences will be sulfated by this ASST.

1.6 Sulfation in the human complement system

As was described above, sulfation is a widespread post-translational modification especially of extracellular peptides and proteins. In addition to the discussed sulfations of CCR5 and PSGL-1, the C5a-receptor is another very important membrane bound protein that is sulfated *in vivo*.[123] This G protein-coupled receptor plays a dominant role in the complement system, which is a crucial part of the host innate or non-specific immune system and is often described as ´the first line of defense´. Although it was believed to be only a small mechanism to ´complement´ antibodies in eradicating pathogens, it is now considered as an important defense-mechanism bridging the innate and adaptive immune systems.[124] Complement consists of at least 30 soluble and membrane bound proteins which, upon activation of the complement cascade, are involved in attacking, neutralizing and removing invading pathogens. In addition they regulate the adaptive immune system and repair cellular damage. The complement system can be activated in three ways: by 1) formation of antigen-antibody complexes denoted as the classical pathway, 2) spontaneous hydrolysis of complement factor 3 (C3) denoted as the alternative pathway, and 3) by the binding of microbial carbohydrate structures denoted as the mannose-binding lectin pathway.[125, 126] The whole cascade converges around C3 which is cleaved into C3a and C3b by C3 convertase. During the process C5 convertase is formed from several different activated factors and starts producing C5a and C5b from C5. C3b is, next to formation of C5 convertase, responsible for covalently marking pathogen surfaces for opsonisation. C5b forms, together with C6-9, the membrane attack complex, which causes lysis of the bacterial membrane. C3a, C4a and C5a are called anyphylatoxins and are responsible for the recruitment and activation of leukocytes (chemotaxis) (Fig. 1.9A). [125, 127] Anyphylatoxin C5a is a 100-times more potent as C3a and is believed to be the main chemotactic agent for neutrophils.[128]

The complement system provides a very powerful immune response that has to be controlled very carefully, for instance the activity of C5a is rapidly diminished by removing the C-terminal arginine (C5a desArg).[129, 130] A small disruption in the balance of the complement system can lead to

unnecessary or excessive activation and results in inflammation and cell lysis of host tissue. Numerous inflammatory, autoimmune and infectious diseases have been associated with complement activation (Fig. 1.9 B) and the C5a-receptor plays an important role in many of them.[127, 131, 132]

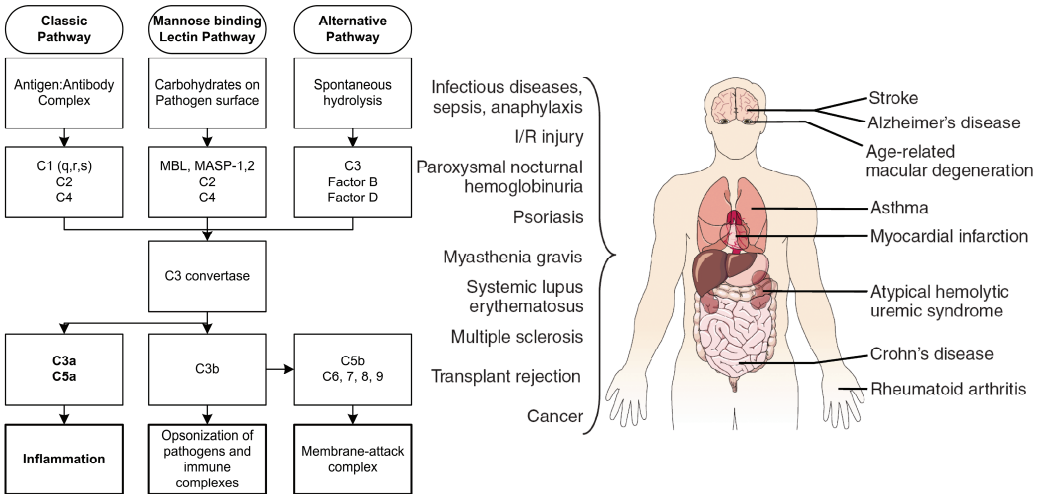

Figure 1.9 A) Schematic overview of the complement system. B) Diseases linked to the activity of the complement system. (Figure reprinted with permission of Nature Publishing Group[133]

1.7 C5a-receptor

The very potent chemotactic agent C5a, a 74-residue long α-helical glycoprotein, performs its function by activating the C5a-receptor (C5aR). This receptor is mainly present on the membrane of neutrophils, monocytes and macrophages, but is also present on several other types of cells and tissues.[134] The C5aR, a 350-residue long G protein-coupled receptor with an intracellular C-terminus and an extracellular N-terminus, was first cloned and sequenced in 1991 (Fig. 1.10).[135, 136] In 2000 a second C5a-binding receptor, that is C5L2, was described with a 35% amino acid homology with C5aR.[137] This receptor seems not to be coupled to G protein signaling pathways.[138] On the other hand, the receptor does show coupling to β-arrestin, which is believed to attenuate G protein-coupled signaling and is part of a separate signaling pathway.[139] Although it has been shown that C5L2 is necessary for optimal action of C5a, no distinct biological function for this receptor has been identified so far.[139-141] It is believed that the C5L2 receptor, in contrast to C5aR, is a decoy receptor competing with C5aR for C5a and C5a desArg. In contrast to C5aR, the C5L2 has a similar binding affinity for C5a and C5a desArg.[142]

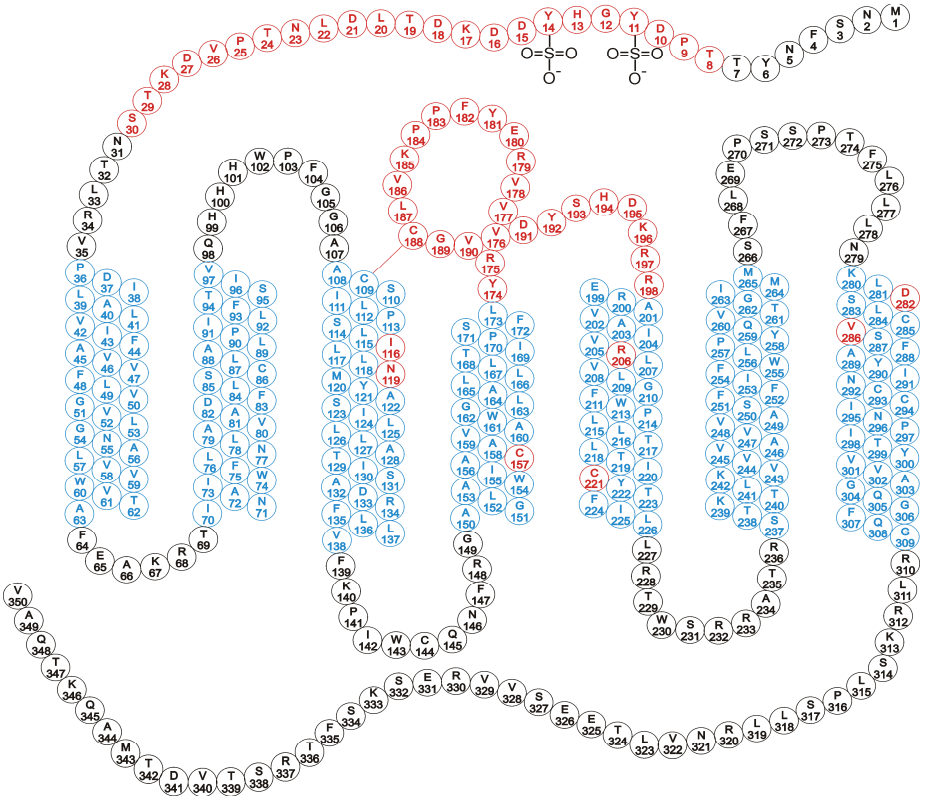

Figure 1.10 Model of the C5a-Receptor. Residues involved in α-helices passing trough the membrane are in blue. Residues involved in binding of C5a are in red.[143]

The extracellular N-terminus of the C5aR contains two tyrosine residues (11 and 14) which are post-translationally modified by sulfation.[123] C5a is believed to bind first to the extracellular N-terminus of the C5a-receptor, where the sulfated tyrosine residues have been shown to be crucial for binding,[123] and then C-terminus of C5a is inserted into the receptor core where it activates the receptor.[144] Upon activation of the C5aR on the surface of white blood cells, the cells will start moving towards an increasing concentration of C5a, which is called chemotaxis. This will lead them to the site of complement activation, which is normally the site of infection. When these white blood cells arrive at the site of infection they have a complete arsenal of ´weapons´ to deal with the cause of the infection: Reactive oxygen species (ROS), reactive nitrogen species (RNS), hydrolytic enzymes and antimicrobial peptides.[145] All of these measures are directed towards invading pathogens, but are also harmful for host tissues especially when the response is unnecessary, excessive or chronic.[145] Activation of complement in general and the activation of the C5aR by C5a specifically has been linked to several inflammatory diseases e.g. asthma,[131] (myocardial) ischemia / reperfusion injury,[132, 146] inflammatory bowel disease,[147, 148] and rheumatoid arthritis.[149-151] Therefore an active search for

C5aR antagonists is still going on. Several reports have appeared, describing small molecules and peptide C5aR antagonists, like PMX-53, PMX-205, W-54011, aniline-substituted tetrahydroquinolines, NDT 9513727 and bis-sulfonamides (Fig. 1.11).[152-156] One of them, the cyclic peptide AcF[OPdChaWR] or PMX-53, has successfully passed phase I and II clinical trials and has shown to be save and well tolerated, although it is sensitive to enzymatic degradation.[157] PMX-53 is still subject of pre-clinical trials, however, Arana therapeutics reported some disappointing activities in treatment of Age-Related Macular Degeneration (AMD) and announced halting the development of PMX-53 for this disease.[158] A more hydrophobic and more stable variant of PMX-53, that is PMX-205, containing a hydrocinnamate moiety instead of an acetylated phenylalanine residue, is possibly still under development.[159] In 2008 G2 Therapies and Novo Nordisk announced the start of clinical trials with C5aR antibodies for the treatment of rheumatoid arthritis and systemic lupus eruthematosus.[160] Finally, at Jerini AG and Mitsubishi Pharma, C5aR antagonists are under development for several indications.

Most, if not all, inhibitors are directed towards the activation site within the core of the C5a-receptor. Interfering with the extracellular N-terminal part of the receptor might also be a very promising strategy, which may also be the mode of action of C5aR antibodies. Another inhibitor directed towards the N-terminus of the C5aR has been identified in the arsenal of immune modulating proteins of the bacterium *Staphylococcus aureus* by van Strijp and coworkers. This discovered inhibitory protein was named Chemotaxis Inhibitory Protein of *Staphylococcus aureus* (CHIPS).[161]

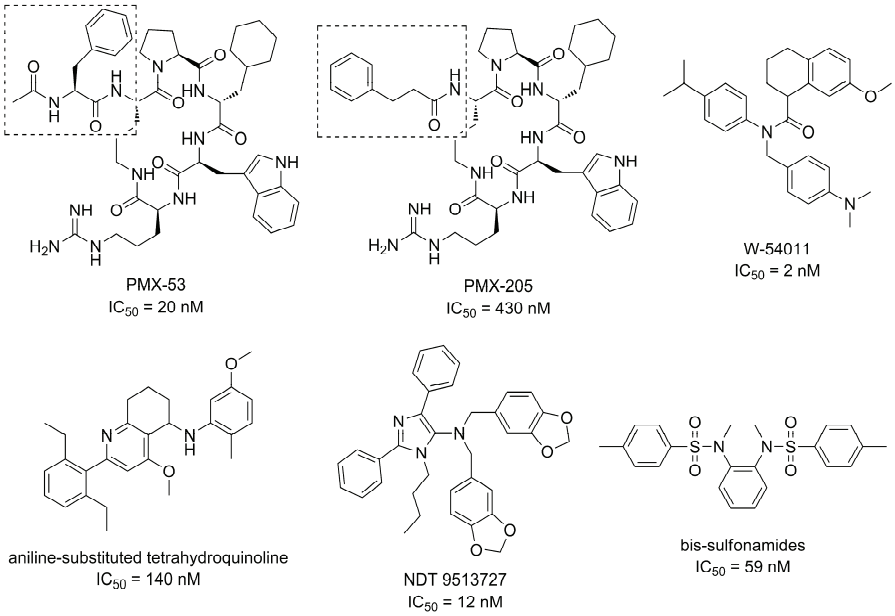

Figure 1.11 Literature examples of potent C5aR antagonists: In order: PMX-53,[152] PMX-205,[159] W-54011,[153] aniline-substituted tetrahydroquinoline,[155] NDT 9513727,[154] bis-sulfonamides.[156]

1.8 CHIPS

Like all organisms, bacteria have two main goals: survive and reproduce. Especially this drive to survive has led to the development of highly specialized bacterial defense-proteins to evade the human immune system.[162] To survive the first attack of the human immune system, bacteria have to evade the innate immune system. Inhibition of the complement system is a necessary step in bacterial survival. In 2000 Veldkamp et al. discovered that the supernatant of *Staphylococcus aureus*, a very common but potentially lethal bacterium,[163] contained a potent inhibitor of chemotaxis of neutrophils triggered by C5a and fMLP.[164] This inhibitor was identified as a 121-residue long protein and was named CHIPS.[161] CHIPS is a very specific and potent inhibitor of the Formylated Peptide Receptor (FPR) and de C5a-Receptor (C5aR) with dissociation constants of 35.4 and 1.1 nM, respectively.[165] Because of its high affinity and selectivity, CHIPS was recognized as a potential new anti-inflammatory compound.[161] Although no adverse effects of CHIPS were observed in pre-clinical animal toxicity studies, administration of 0.1 mg/kg to four human volunteers caused in one subject an anaphylactoid reaction caused by the presence of anti-CHIPS antibodies.[166] It was shown that, because of the widespread colonization of humans by *S. aureus*, most individuals have high levels of anti-CHIPS antibodies in their circulation.[166, 167] Despite this severe side-reaction, inhibition of the C5aR and the FPR receptor was observed *in vivo* upon administration of CHIPS to human volunteers and further investigations into its structure and mechanism of action continued.[166] During the investigations into the structure of CHIPS, it was discovered that the inhibitory activity towards the FPR was conserved in the N-terminal part of CHIPS,[168] and the inhibitory activity towards the C5aR was conserved in a truncated CHIPS lacking the first 30 residues ($CHIPS_{31-121}$).[169] The structure of $CHIPS_{31-121}$ was elucidated in our group (Fig. 1.12) and appeared to have a high structural similarity with other bacterial immune-modulating proteins such as the staphylococcal superantigen-like proteins 5 and 7 and the staphylococcal and streptococcal superantigens TSST-1 and SPE-C.[169]

Based on the knowledge of the potency and the structure of CHIPS, a project was started to elucidate the molecular mechanism of action of CHIPS on the C5a-receptor with the aim to develop CHIPS-based anti-inflammatory compounds with less immunogenic properties. Besides the results presented in this thesis, Erika Gustafsson recently described in her thesis the identification of several immunogenic epitopes on the surface of CHIPS.[170] By directed evolution using FIND® technology, several active CHIPS proteins with a decreased interaction with pre-existing anti-CHIPS antibodies have been developed.[171, 172]

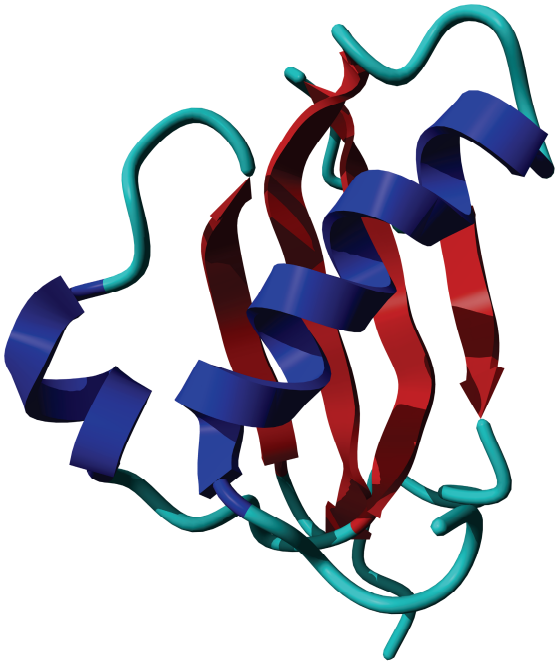

Figure 1.12 Solution-structure of $CHIPS_{31-121}$ solved by NMR (PDB code 1XEE).[169] α-Helices are depicted in blue, β-sheets in red and loops and the termini in cyan.

1.9 Aim and outline of this thesis

In conclusion, CHIPS is a very interesting and inspirational protein containing valuable information for the development of new anti-inflammatory compounds based on the inhibition of the C5a-receptor. To learn more about how CHIPS is inhibiting the C5aR, information on the molecular interactions between these two proteins is of crucial importance. The aim of the research described in this thesis was therefore to explore the inhibitory interactions of CHIPS with the C5a-receptor and to develop the necessary chemistry for the synthesis of sulfated C5a-receptor mimics. Based upon the gained knowledge from these studies, CHIPS mimics have been designed, synthesized and tested for binding to the C5a-receptor.

The chemistry to reliably and conveniently synthesize multiple tyrosine sulfated C5a-receptor mimics was developed and is described in **chapter 2** of this thesis. For this synthesis of sulfated peptides, 2,2,2-trichloroethyl chlorosulfate is used as a reagent to introduce a protected sulfate group onto the free hydroxyl functionality of tyrosine. Next to this reagent, also the application of the more stable 2,2,2-trichloroethyl methylimidazoliumsulfate salt is explored. The developed strategy is first tested on the synthesis of sulfated Leu-enkephalin. After the very promising results with this small peptide, the new method was successfully applied in synthesis of a small collection of C5a-receptor mimics containing a high degree of functional amino acids. The selected C5aR mimics differed in length of

the selected part of the C5aR N-terminus (from 9 to 35 amino acid residues) and in the pattern of sulfation. In addition also the compatibility of our new method with the cysteine side chain was tested. With some small adjustments in the HPLC purification, a cysteine-containing peptide with multiple sulfated tyrosine residues was successfully synthesized.

In **chapter 3** the binding of CHIPS to the collection of sulfated and unsulfated C5aR mimics, which are described in chapter 2, is evaluated. The ITC binding experiments clearly show the importance of both the sulfated tyrosine residues within the C5aR N-terminus, resulting in a 400-fold increase of binding affinity. Based on ITC studies and biological assays with a C5aR expressing cell line, the best mimic for the C5a-receptor, $C5aR_{7\text{-}28}S_2$, was selected. CHIPS has a high affinity for $C5aR_{7\text{-}28}S_2$ (8.4 nM), close to the affinity for the native C5aR (1.1 nM). The binding of CHIPS to this sulfated C5a-receptor mimic is studied in more detail with NMR spectroscopy and resulted in the elucidation of the structure of the complex $CHIPS_{31\text{-}121}$:$C5aR_{7\text{-}28}S_2$ (PDB: 2K3U). Within this structure the involvement of the crucial sulfate groups was distinct. With the information enclosed in the complex structure, the activities of previous and new mutants of CHIPS (R44A, K95A, Y97A and S106A) could be explained. Next to this, the structure of the $CHIPS_{31\text{-}121}$:$C5aR_{7\text{-}28}S_2$ complex opened up the way for the design of CHIPS mimics as a new class of C5aR inhibitors.

In **chapter 4** the replacement of the sulfate groups, within the best C5a-receptor mimics, with the more stable phosphate groups is explored. $C5aR_{7\text{-}28}P^{11}$, $C5aR_{7\text{-}28}P^{14}$ and $C5aR_{7\text{-}28}P_2$ were successfully synthesized. Binding of these phosphorylated C5a-receptor mimics to CHIPS was studied by ITC and NMR and the findings are compared with the results obtained with sulfated C5a-receptor mimics. The phosphorylated C5aR mimics show similar binding affinities for $CHIPS_{31\text{-}121}$ compared to the sulfated C5aR mimics. Also the chemical shift perturbations within the ^{15}N-HSQC spectra, as observed in a titration experiment, were strikingly similar. However, in a cell-based assay the phosphorylated C5aR mimics performed significantly less compared to the sulfated C5aR mimics.

The information about the interactions of CHIPS with the C5a-receptor opens up the way for the development of new CHIPS-based anti-inflammatory compounds. **Chapter 5** describes the design, synthesis and binding studies of a first generation peptide mimic of CHIPS, designated as CHOPS. The parts of CHIPS which had no interactions with the C5aR mimic, as determined from the structure presented in chapter 3, were removed. The two remaining fragments, which showed interactions with our C5a mimic, are successfully linked together by a β-turn inducing D-Pro-Gly linker to form a single peptide. After its successful synthesis by automated SPPS its affinity for our C5aR mimic was determined and its structure was studied with NMR. Although CHOPS did not have any distinct structure in solution, it became structured upon binding to $C5aR_{7\text{-}28}S_2$. The complex had a dissociation constant of 3.6 μM, which is a promising result for a first generation CHIPS mimic.

After this promising result, even smaller CHIPS mimics were designed and synthesized as described in **chapter 6**. A different approach to develop these CHIPS mimics was chosen. Crucial parts of CHIPS were selected and arranged on the TAC-scaffold in a similar pattern compared to the native protein. These scaffold-based mimics of CHIPS were successfully synthesized on the solid support For one of these TAC-based CHIPS mimics a new approach was applied for the synthesis of a peptide connected to the TAC-scaffold in the ´reversed´ order. Despite their successful synthesis, the TAC-based CHIPS mimics showed no affinity for our best C5aR mimic. However, based on the affinity found for CHOPS, scaffold-based mimics which can induce a CHIPS-like topology more are still interesting target structures.

1.10 References

[1] I. H. G. S. Consortium, Finishing the euchromatic sequence of the human genome, *Nature* **2004**, *431*, 931.

[2] C. T. Walsh, S. Garneau-Tsodikova, G. J. Gatto, Protein posttranslational modifications: The chemistry of proteome diversifications, *Angew. Chem. Int. Ed.* **2005**, *44*, 7342.

[3] M. Grunstein, Histone acetylation in chromatin structure and transcription, *Nature* **1997**, *389*, 349.

[4] A. S. Kim, E. J. Miller, L. H. Young, AMP-activated protein kinase: a core signalling pathway in the heart, *Acta Phys.* **2009**, *196*, 37.

[5] P. Kreis, J. V. Barnier, PAK signalling in neuronal physiology, *Cell. Signal.* **2009**, *21*, 384.

[6] P. Cohen, Protein kinases - the major drug targets of the twenty-first century?, *Nat. Rev. Drug Discovery* **2002**, *1*, 309.

[7] K. F. Medzihradszky, Z. Darula, E. Perlson, M. Fainzilber, R. J. Chalkley, H. Ball, D. Greenbaum, M. Bogyo, D. R. Tyson, R. A. Bradshaw, A. L. Burlingame, O-sulfonation of serine and threonine - Mass spectrometric detection and characterization of a new posttranslational modification in diverse proteins throughout the eukaryotes, *Mol. Cell. Proteomics* **2004**, *3*, 429.

[8] P. A. Baeuerle, W. B. Huttner, Tyrosine sulfation of yolk proteins 1, 2, and 3 in *Drosophila melanogaster*, *J. Biol. Chem.* **1985**, *260*, 6434.

[9] E. Baumann, Ueber sulfosauren im harn, *Berichte der Deutchen Chemischen Gesellschaft zu Berlin* **1876**, *9*, 54.

[10] P. W. Robbins, F. Lipmann, Isolation and identification of active sulfate, *J. Biol. Chem.* **1957**, *229*, 837.

[11] C. D. Klaassen, J. W. Boles, Sulfation and sulfotransferases .5. The importance of 3'-phosphoadenosine 5'-phosphosulfate (PAPS) in the regulation of sulfation, *Faseb J.* **1997**, *11*, 404.

[12] G. M. Pacifici, M. Franchi, C. Colizzi, L. Giuliani, A. Rane, Sulfotransferase in humans - Development and tissue distribution, *Pharmacology* **1988**, *36*, 411.

[13] A. Superti-Furga, A defect in the metabolic activation of sulfate in a patient with achondrogenesis type IB, *Am. J. Hum. Genet.* **1994**, *55*, 1137.

[14] F. Grun, N. Noy, U. Hammerling, J. Buck, Purification, cloning, and bacterial expression of retinol dehydratase from *Spodoptera frugiperda*, *J. Biol. Chem.* **1996**, *271*, 16135.

[15] K. Kobashi, T. Akao, S. Takebe, Y. Fukaya, D. H. Kim, Sulfation of phenolic compounds with arylsulfotransferase derived from bacteria in human colonic flora *Sulfur Amino Acids / Ganryu Aminosan* **1984**, *7*, 437.

[16] Y. Matsubayashi, H. Hanai, O. Hara, Y. Sakagami, Active fragments and analogs of the plant growth factor, phytosulfokine: Structure-activity relationships, *Biochem. Biophys. Res. Commun.* **1996**, *225*, 209.

[17] R. Komori, Y. Amano, M. Ogawa-Ohnishi, Y. Matsubayashi, Identification of tyrosylprotein sulfotransferase in Arabidopsis, *Proc. Natl. Acad. Sci. U. S. A.* **2009**, *106*, 15067.

[18] K. Kobashi, Y. Fukaya, D. H. Kim, T. Akao, S. Takebe, A novel type of aryl sulfotransferase obtained from an anaerobic bacterium of human intestine, *Arch. Biochem. Biophys.* **1986**, *245*, 537.

[19] R. L. Blanchard, R. R. Freimuth, J. Buck, R. M. Weinshilboum, M. W. H. Coughtrie, A proposed nomenclature system for the cytosolic sulfotransferase (SULT) superfamily, *Pharmacogenet.* **2004**, *14*, 199.

[20] Y. Kakuta, L. G. Pedersen, L. C. Pedersen, M. Niegishi, Conserved structural motifs in the sulfotransferase family, *Trends Biochem. Sci.* **1998**, *23*, 129.

[21] E. Chapman, M. D. Best, S. R. Hanson, C. H. Wong, Sulfotransferases: Structure, mechanism, biological activity, inhibition, and synthetic utility, *Angew. Chem. Int. Ed.* **2004**, *43*, 3526.

[22] M. W. H. Coughtrie, S. Sharp, K. Maxwell, N. P. Innes, Biology and function of the reversible sulfation pathway catalysed by human sulfotransferases and sulfatases, *Chem.-Biol. Interact.* **1998**, *109*, 3.

[23] G. A. Johnson, K. J. Barsuhn, J. M. Mccall, Sulfation of minoxidil by liver sulfotransferase, *Biochem. Biopharmacol.* **1982**, *31*, 2949.

[24] E. Banoglu, Current status of the cytosolic sulfotransferases in the metabolic activation of promutagens and procarcinogens, *Curr. Drug. Metab.* **2000**, *1*, 1.

[25] C. N. Falany, Sulfation and sulfotransferases .3. Enzymology of human cytosolic sulfotransferases, *Faseb J.* **1997**, *11*, 206.

[26] S. R. Hanson, M. D. Best, C. H. Wong, Sulfatases: Structure, mechanism, biological activity, inhibition, and synthetic utility, *Angew. Chem. Int. Ed.* **2004**, *43*, 5736.

[27] J. R. Pasqualini, Estrogen Sulfotransferases in Breast and Endometrial Cancers, *Steroid Enzymes and Cancer* **2009**, *1155*, 88.

[28] S. J. Stanway, P. Delavault, A. Purohit, L. W. L. Woo, C. Thurieau, B. V. L. Potter, M. J. Reed, Steroid sulfatase: A new target for the endocrine therapy of breast cancer, *Oncologist* **2007**, *12*, 370.

[29] J. U. Baenziger, S. Kumar, R. M. Brodbeck, P. L. Smith, M. C. Beranek, Circulatory Half-Life but Not Interaction with the Lutropin Chorionic-Gonadotropin Receptor Is Modulated by Sulfation of Bovine Lutropin Oligosaccharides, *Proc. Natl. Acad. Sci. U. S. A.* **1992**, *89*, 334.

[30] U. Lindahl, M. Kusche-Gullberg, L. Kjellen, Regulated diversity of heparan sulfate, *J. Biol. Chem.* **1998**, *273*, 24979.

[31] M. Morimoto-Tomita, K. Uchimura, Z. Werb, S. Hemmerich, S. D. Rosen, Cloning and characterization of two extracellular heparin-degrading endosulfatases in mice and humans, *J. Biol. Chem.* **2002**, *277*, 49175.

[32] J. D. Esko, S. B. Selleck, Order out of chaos: assembly of ligand binding sites in heparan sulfate, *Annu. Rev. Biochem.* **2002**, *71*, 435.

[33] F. R. Bettelheim, Tyrosine-*O*-sulfate in a peptide from fibrinogen, *J. Am. Chem. Soc.* **1954**, *76*, 2838.

[34] H. Gregory, P. M. Hardy, D. S. Jones, G. W. Kenner, R. C. Sheppard, The antral hormone gastrin: structure of gastrin, *Nature* **1964**, *204*, 931.

[35] A. Anastasi, G. Bertaccini, V. Erspamer, Pharmacological data on phyllokinin (bradykinyl-isoleucyl-tyrosine *O*-sulphate) and bradykinyl-isoleucyl-tyrosine, *Br. J. Pharmacol.* **1966**, *27*, 479.

[36] V. Mutt, J. E. Jorpes, Structure of porcine cholecystokinin-pancreozymin, *Eur. J. Biochem.* **1968**, *6*, 156.

[37] A. Anastasi, V. Erspamer, R. Endean, Isolation and amino acid sequence of Caerulein, the active decapeptide of the skin of *Hyla caerulea*, *Arch. Biochem. Biophys.* **1968**, *125*, 57.

[38] C. D. Unsworth, J. Hughes, J. S. Morley, *O*-sulphated Leu-enkephalin in brain, *Nature* **1982**, *295*, 519.

[39] D. Bagdy, E. Barabas, L. Graf, T. E. Peterson, S. Magnusson, Hirudin, *Methods in enzymology* **1976**, *45*, 669.

[40] W. B. Huttner, Sulphation of tyrosine residues - a widespread modification of proteins, *Nature* **1982**, *299*, 273.

[41] A. Hille, P. Rosa, W. B. Huttner, Tyrosine sulfation: a post-translational modification of proteins destined for secretion?, *FEBS Lett* **1984**, *177*, 129.

[42] R. W. H. Lee, W. B. Huttner, Tyrosine-*O*-sulfated proteins of PC12 Pheochromocytoma cells and their sulfation by a tyrosylprotein sulfotransferase, *J. Biol. Chem.* **1983**, *258*, 11326.

[43] R. W. H. Lee, W. B. Huttner, (Glu62, Ala30, Tyr8)n serves as high-affinity substrate for tyrosylprotein sulfotransferase: A Golgi enzyme, *Proc. Natl. Acad. Sci. U. S. A.* **1985**, *82*, 6143.

[44] P. A. Baeuerle, W. B. Huttner, Tyrosine sulfation is a trans-Golgi-specific protein modification, *J. Cell Biol.* **1987**, *105*, 2655.

[45] Y. B. Ouyang, W. S. Lane, K. L. Moore, Tyrosylprotein sulfotransferase: Purification and molecular cloning of an enzyme that catalyzes tyrosine *O*-sulfation, a common posttranslational modification of eukaryotic proteins, *Proc. Natl. Acad. Sci. U. S. A.* **1998**, *95*, 2896.

[46] Y. B. Ouyang, K. L. Moore, Molecular cloning and expression of human and mouse tyrosylprotein sulfotransferase-2 and a tyrosylprotein sulfotransferase homologue in *Caenorhabditis elegans*, *J. Biol. Chem.* **1998**, *273*, 24770.

[47] R. Beisswanger, D. Corbeil, C. Vannier, C. Thiele, U. Dohrmann, R. Kellner, K. Ashman, C. Niehrs, W. B. Huttner, Existence of distinct tyrosylprotein sulfotransferase genes: Molecular characterization of tyrosylprotein sulfotransferase-2, *Proc. Natl. Acad. Sci. U. S. A.* **1998**, *95*, 11134.

[48] K. L. Moore, The biology and enzymology of protein tyrosine *O*-sulfation, *J. Biol. Chem.* **2003**, *278*, 24243.

[49] C. Seibert, M. Cadene, A. Sanfiz, B. T. Chait, T. P. Sakmar, Tyrosine sulfation of CCR5 N-terminal peptide by tyrosylprotein sulfotransferases 1 and 2 follows a discrete pattern and temporal sequence, *Proc. Natl. Acad. Sci. U. S. A.* **2002**, *99*, 11031.

[50] S. Goettsch, W. Goettsch, H. Morawietz, P. Bayer, Shear stress mediates tyrosylprotein sulfotransferase isoform shift in human endothelial cells, *Biochem. Biophys. Res. Commun.* **2002**, *294*, 541.

[51] Y. B. Ouyang, J. T. B. Crawley, C. E. Aston, K. L. Moore, Reduced body weight and increased postimplantation fetal death in tyrosylprotein sulfotransferase-1-deficient mice, *J. Biol. Chem.* **2002**, *277*, 23781.

[52] A. Borghei, Y. B. Ouyang, A. D. Westmuckett, M. R. Marcello, C. P. Landel, J. P. Evans, K. L. Moore, Targeted disruption of tyrosylprotein sulfotransferase-2, an enzyme that catalyzes post-translational protein tyrosine *O*-sulfation, causes male infertility, *J. Biol. Chem.* **2006**, *281*, 9423.

[53] A. D. Westmuckett, A. J. Hoffhines, A. Borghei, K. L. Moore, Early postnatal pulmonary failure and primary hypothyroidism in mice with combined TPST-1 and TPST-2 deficiency, *Gen. Comp. Endocrinol.* **2008**, *156*, 145.

[54] E. Mishiro, Y. Sakakibara, M. C. Liu, M. Suiko, Differential enzymatic characteristics and tissue-specific expression of human TPST-1 and TPST-2, *J. Biochem.* **2006**, *140*, 731.

[55] H. B. Nicholas, S. S. Chan, G. L. Rosenquist, Reevaluation of the determinants of tyrosine sulfation, *Endocrine* **1999**, *11*, 285.

[56] F. Monigatti, E. Gasteiger, A. Bairoch, E. Jung, The Sulfinator: predicting tyrosine sulfation sites in protein sequences, *Bioinformatics* **2002**, *18*, 769.

[57] F. Monigatti, B. Hekking, H. Steen, Protein sulfation analysis - A primer, *Biochim. Biophys. Acta, Proteins Proteomics* **2006**, *1764*, 1904.

[58] P. P. Wilkins, K. L. Moore, R. P. Mcever, R. D. Cummings, Tyrosine sulfation of P-selectin glycoprotein ligand-1 is required for high-affinity binding to P-selectin, *J. Biol. Chem.* **1995**, *270*, 22677.

[59] A. Leppanen, P. Mehta, Y. B. Ouyang, T. Z. Ju, J. Helin, K. L. Moore, I. van Die, W. M. Canfield, R. P. McEver, R. D. Cummings, A novel glycosulfopeptide binds to P-selectin and inhibits leukocyte adhesion to P-selectin, *J. Biol. Chem.* **1999**, *274*, 24838.

[60] A. Leppanen, S. P. White, J. Helin, R. P. McEver, R. D. Cummings, Binding of glycosulfopeptides to P-selectin requires stereospecific contributions of individual tyrosine sulfate and sugar residues, *J. Biol. Chem.* **2000**, *275*, 39569.

[61] W. S. Somers, J. Tang, G. D. Shaw, R. T. Camphausen, Insights into the molecular basis of leukocyte tethering and rolling revealed by structures of P- and E-selectin bound to SLe(X) and PSGL-1, *Cell* **2000**, *103*, 467.

[62] M. M. Lederman, A. Penn-Nicholson, M. Cho, D. Mosier, Biology of CCR5 and its role in HIV infection and treatment, *J. Am. Med. Assoc.* **2006**, *296*, 815.

[63] E. G. Cormier, M. Persuh, D. A. D. Thompson, S. W. Lin, T. P. Sakmar, W. C. Olson, T. Dragic, Specific interaction of CCR5 amino-terminal domain peptides containing sulfotyrosines with HIV-1 envelope glycoprotein gp120, *Proc. Natl. Acad. Sci. U. S. A.* **2000**, *97*, 5762.

[64] H. Choe, W. H. Li, P. L. Wright, N. Vasilieva, M. Venturi, C. C. Huang, C. Grundner, T. Dorfman, M. B. Zwick, L. P. Wang, E. S. Rosenberg, P. D. Kwong, D. R. Burton, J. E. Robinson, J. G. Sodroski, M. Farzan, Tyrosine sulfation of human antibodies contributes to recognition of the CCR5 binding region of HIV-1 gp120, *Cell* **2003**, *114*, 161.

[65] T. Yagami, K. Kitagawa, C. Aida, H. Fujiwara, S. Futaki, Stabilization of a tyrosine *O*-sulfate residue by a cationic functional group: formation of a conjugate acid-base pair, *J. Pept. Res.* **2000**, *56*, 239.

[66] W. B. Huttner, Determination and occurence of tyrosine *O*-sulfate in proteins, *Methods in enzymology* **1984**, *107*, 200.

[67] D. Balsved, J. R. Bundgaard, J. W. Sen, Stability of tyrosine sulfate in acidic solutions, *Anal. Biochem.* **2007**, *363*, 70.

[68] L. Moroder, L. Wilschowitz, M. Gemeiner, W. Gohring, S. Knof, R. Scharf, P. Thamm, J. D. Gardner, T. E. Solomon, E. Wunsch, Synthesis of cholecystokinin-pancreozymin. Synthesis of [28-threonine,31-norleucine]- and [28-threonine,31-leucine]cholecystokinin-pancreozymin-(25-33)-nonapeptide, *Hoppe-Seylers Z. Physiol. Chem.* **1981**, *362*, 929.

[69] H. H. Tallan, S. T. Bella, W. H. Stein, S. Moore, Tyrosine-*O*-sulfate as a constituent of normal human urine, *J. Biol. Chem.* **1955**, *217*, 703.

[70] J. G. Jones, K. S. Dodgson, G. M. Powell, F. A. Rose, Studies on L-tyrosine *O*-sulphate, *Biochem. J.* **1963**, *87*, 548.

[71] K. S. Dodgson, G. M. Powell, F. A. Rose, N. Tudball, Observations on the metabolism of tyrosine *O*-[35S]-sulphate in the rat, *Biochem. J.* **1961**, *79*, 209.

[72] R. A. John, F. A. Rose, F. S. Wusteman, K. S. Dodgson, Detection and determination of L-tyrosine *O*-sulphate in rabbit and other mammalian urine, *Biochem. J.* **1966**, *100*, 278.

[73] J. G. S. Ranasinghe, Y. Sakakibara, M. Harada, K. Nishiyama, M. C. Liu, M. Suiko, Structural identification of sulfated tyrosine in human urine, *Biosci. Biotechnol. Biochem.* **1999**, *63*, 229.

[74] K. S. Dodgson, F. A. Rose, N. Tudball, Studies on sulphatases, *Biochem. J.* **1959**, *71*, 10.

[75] A. L. Fluharty, R. L. Stevens, E. B. Goldstein, H. Kihara, The activity of arylsulfatase A and B on tyrosine *O*-sulfates, *Biochim. Biophys. Acta* **1979**, *566*, 321.

[76] C. P. Dietrich, H. B. Nader, V. Buonassisi, P. Colburn, Inhibition of synthesis of heparan sulfate by selenate: possible dependence on sulfation for chain polymerization, *Faseb J.* **1988**, *2*, 56.

[77] P. A. Baeuerle, W. B. Huttner, Chlorate - a potent inhibitor of protein sulfation in intact cells, *Biochem. Biophys. Res. Commun.* **1986**, *141*, 870.

[78] D. E. Humphries, J. E. Silbert, Chlorate: a reversible inhibitor of proteoglycan sulfation, *Biochem. Biophys. Res. Commun.* **1988**, *154*, 365.

[79] J. W. Kehoe, N. Velappan, M. Walbolt, J. Rasmussen, D. King, J. Lou, K. Knopp, P. Pavlik, J. D. Marks, C. R. Bertozzi, R. M. Bradbury, Using phage display to select antibodies recognizing post-translational modifications independently of sequence context, *Mol. Cell. Proteomics* **2006**, *5*, 2350.

[80] A. J. Hoffhines, E. Damoc, K. G. Bridges, J. A. Leary, K. L. Moore, Detection and purification of tyrosine-sulfated proteins using a novel anti-sulfotyrosine monoclonal antibody, *J. Biol. Chem.* **2006**, *281*, 37877.

[81] J. L. Wolfender, F. X. Chu, H. Ball, F. Wolfender, M. Fainzilber, M. A. Baldwin, A. L. Burlingame, Identification of tyrosine sulfation in *Conus pennaceus* conotoxins alpha-PnIA and alpha-PnIB: Further investigation of labile sulfo- and phosphopeptides by electrospray, matrix-assisted laser desorption/ionization (MALDI) and atmospheric pressure MALDI mass spectrometry, *J. Mass Spectrom.* **1999**, *34*, 447.

[82] C. Seibert, T. P. Sakmar, Toward a framework for sulfoproteomics: Synthesis and characterization of sulfotyrosine-containing peptides, *Biopolymers* **2008**, *90*, 459.

[83] J. Zaia, R. Boynton, D. Heinegard, F. Barry, Posttranslational modifications to human bone sialoprotein determined by mass spectrometry, *Biochemistry* **2001**, *40*, 12983.

[84] J. F. Nemeth-Cawley, S. Karnik, J. C. Rouse, Analysis of sulfated peptides using positive electrospray ionization tandem mass spectrometry, *J. Mass Spectrom.* **2001**, *36*, 1301.

[85] M. Salek, S. Costagliola, W. D. Lehmann, Protein tyrosine-*O*-sulfation snalysis by exhaustive product ion scanning with minimum collision offset in a nanoESI Q-TOF tandem mass spectrometer, *Anal. Chem.* **2004**, *76*, 5136.

[86] R. A. Zubarev, N. L. Kelleher, F. W. McLafferty, Electron capture dissociation of multiply charged protein cations. A nonergodic process, *J. Am. Chem. Soc.* **1998**, *120*, 3265.

[87] B. A. Budnik, K. F. Haselmann, R. A. Zubarev, Electron detachment dissociation of peptide di-anions: an electron-hole recombination phenomenon, *Chem. Phys. Lett.* **2001**, *342*, 299.

[88] L. M. Mikesh, B. Ueberheide, A. Chi, J. J. Coon, J. E. Syka, J. Shabanowitz, D. F. Hunt, The utility of ETD mass spectrometry in proteomic analysis, *Biochim. Biophys. Acta* **2006**, *1764*, 1811.

[89] K. F. Haselmann, B. A. Budnik, J. V. Olsen, M. L. Nielsen, C. A. Reis, H. Clausen, A. H. Johnsen, R. A. Zubarev, Advantages of external accumulation for electron capture dissociation in fourier transform mass spectrometry, *Anal. Chem.* **2001**, *73*, 2998.

[90] Y. Yu, A. J. Hoffhines, K. L. Moore, J. A. Leary, Determination of the sites of tyrosine *O*-sulfation in peptides and proteins, *Nat. Methods* **2007**, *4*, 583.

[91] H. C. Reitz, R. E. Ferrel, H. Fraenkel-Conrat, H. S. Olcott, Action of sulfating agents on proteins and model substances. I Concentrated sulfuric acid, *J. Am. Chem. Soc.* **1946**, *68*, 1024.

[92] M. A. Ondetti, J. Pluscec, E. F. Sabo, J. T. Sheehan, N. Williams, Synthesis of Cholecystokinin-pancreozymin .1. C-terminal dodecapeptide, *J. Am. Chem. Soc.* **1970**, *92*, 195.

[93] B. Penke, F. Hajnal, J. Lonovics, G. Holzinger, T. Kadar, G. Telegdy, J. Rivier, Synthesis of potent heptapeptide analogues of cholecystokinin, *J. Med. Chem.* **1984**, *27*, 845.

[94] N. Fujii, S. Futaki, S. Funakoshi, K. Akaji, H. Morimoto, R. Doi, K. Inoue, M. Kogire, S. Sumi, M. Yun, T. Tobe, M. Aono, M. Matsuda, H. Narusawa, M. Moriga, H. Yajima, Studies on peptides .160. Synthesis of a 33-residue peptide corresponding to the entire amino-acid sequence of human cholecystokinin (Hcck-33), *Chem. Pharm. Bull.* **1988**, *36*, 3281.

[95] S. Futaki, T. Taike, T. Yagami, T. Ogawa, T. Akita, K. Kitagawa, Use of dimethylformamide sulfur-trioxide complex as a sulfating agent of tyrosine, *J. Chem. Soc. Perk. T. 1* **1990**, 1739.

[96] K. M. Koeller, M. E. B. Smith, C. H. Wong, Chemoenzymatic synthesis of PSGL-1 glycopeptides: Sulfation on tyrosine affects glycosyltransferase-catalyzed synthesis of the O-glycan, *Bioorg. Med. Chem.* **2000**, *8*, 1017.

[97] T. Young, L. L. Kiessling, A strategy for the synthesis of sulfated peptides, *Angew. Chem. Int. Ed.* **2002**, *41*, 3449.

[98] S. Futaki, T. Taike, T. Akita, K. Kitagawa, A new approach for the synthesis of tyrosine sulphate containing peptides: Use of the p-(methylsulphinyl)benzyl group as a key protecting group of serine, *J. Chem. Soc. Chem. Commun.* **1990**, 523.

[99] K. Kitagawa, S. Futaki, T. Yagami, S. Sumi, K. Inoue, Solid-phase synthesis of cionin, a protochordate-derived octapeptide related to the gastrin/cholecystokinin family of peptides, and its mono-tyrosine-sulfate-containing derivatives, *Int. J. Pept. Prot. Res* **1994**, *43*, 190.

[100] B. Loubinoux, S. Tabbache, P. Gerardin, J. Miazimbakana, Protection of phenols via the azidomethylene group - Application in the synthesis of unstable phenolic-compounds, *Tetrahedron* **1988**, *44*, 6055.

[101] L. Moroder, L. Wilschowitz, E. Jaeger, S. Knof, P. Thamm, E. Wunsch, Synthesis of tyrosin *O*-sulfate-containing peptides, *Hoppe-Seyler's Z. Physiol. Chem.* **1979**, *360*, 787.

[102] T. Yagami, S. Shiwa, S. Futaki, K. Kitagawa, Evaluation of the final deprotection system for the solid-phase synthesis of Tyr(SO3h)-containing peptides with 9-fluorenylmethyloxycarbonyl (Fmoc)-strategy and its application to the synthesis of Cholecystokinin (Cck)-12, *Chem. Pharm. Bull.* **1993**, *41*, 376.

[103] K. Kitagawa, C. Aida, H. Fujiwara, T. Yagami, S. Futaki, Efficient solid-phase synthesis of sulfated tyrosine-containing peptides using 2-chlorotrityl resin: Facile synthesis of gastrin/cholecystokinin peptides, *Tetrahedron Lett.* **1997**, *38*, 599.

[104] K. Kitagawa, C. Aida, H. Fujiwara, T. Yagami, S. Futaki, M. Kogire, J. Ida, K. Inoue, Facile solid-phase synthesis of sulfated tyrosine-containing peptides: Total synthesis of human big gastrin-II and cholecystokinin (CCK)-39(1,2), *J. Org. Chem.* **2001**, *66*, 1.

[105] L. Duma, D. Haussinger, M. Rogowski, P. Lusso, S. Grzesiek, Recognition of RANTES by extracellular parts of the CCR5 receptor, *J. Mol. Biol.* **2007**, *365*, 1063.

[106] Y. Liu, I. F. F. Lien, S. Ruttgaizer, P. Dove, S. D. Taylor, Synthesis and protection of aryl sulfates using the 2,2,2-trichloroethyl moiety, *Org. Lett.* **2004**, *6*, 209.

[107] L. J. Ingram, S. D. Taylor, Introduction of 2,2,2-trichloroethyl-protected sulfates into monosaccharides with a sulfuryl imidazolium salt and application to the synthesis of sulfated carbohydrates, *Angew. Chem. Int. Ed.* **2006**, *45*, 3503.

[108] A. Bunschoten, J. A. W. Kruijtzer, J. H. Ippel, C. J. C. de Haas, J. A. G. van Strijp, J. Kemmink, R. M. J. Liskamp, A general sequence independent solid phase method for the site specific synthesis of multiple sulfated-tyrosine containing peptides, *Chem. Commun.* **2009**, 2999.

[109] A. M. Ali, S. D. Taylor, Efficient Solid-phase synthesis of sulfotyrosine peptides using a sulfate protecting-group strategy, *Angew. Chem. Int. Ed.* **2009**, *48*, 2024.

[110] A. M. Ali, S. D. Taylor, Synthesis of disulfated peptides corresponding to the N-terminus of chemokines receptors CXCR6 (CXCR61–20) andDARC (DARC8–42) using a sulfate-protecting group strategy, *J. Pept. Sci.* **2010**, *16*, 190.

[111] L. S. Simpson, T. S. Widlanski, A comprehensive approach to the synthesis of sulfate esters, *J. Am. Chem. Soc.* **2006**, *128*, 1605.

[112] L. S. Simpson, J. Z. Zhu, T. S. Widlanski, M. J. Stone, Regulation of chemokine recognition by site-specific tyrosine sulfation of receptor peptides, *Chem. Biol.* **2009**, *16*, 153.

[113] I. Marseigne, P. Roy, A. Dor, C. Durieux, D. Pelaprat, M. Reibaud, J. C. Blanchard, B. P. Roques, Full agonists of CCK8 containing a nonhydrolyzable sulfated tyrosine residue, *J. Med. Chem.* **1989**, *32*, 445.

[114] R. Gonzalez-muniz, F. Cornille, F. Bergeron, D. Ficheux, J. Pothier, C. Durieux, B. P. Roques, Solid phase synthesis of a fully active analogue of cholecystokinin using the acid-stable Boc-Phe (p-CH2) SO3H as a substitute for Boc-Tyr(S03H) in CCK8, *Int. J. Pep. Prot. Res.* **1991**, *37*, 331.

[115] S. Roosenburg, P. Laverman, L. Joosten, A. Eek, W. J. G. Oyen, M. de Jong, F. P. J. T. Rutjes, F. L. van Delft, O. C. Boerman, Stabilized 111In-labeled sCCK8 analogues for targeting CCK2-receptor positive tumors: Synthesis and evaluation, *Bioconjugate Chem.* **2010**, DOI: 10.1021/bc900465y.

[116] S. N. Lam, P. Acharya, R. Wyatt, P. D. Kwong, C. A. Bewley, Tyrosine-sulfate isosteres of CCR5 N-terminus as tools for studying HIV-1 entry, *Bioorg. Med. Chem.* **2008**, *16*, 10113.

[117] C. Niehrs, M. Kraft, R. W. H. Lee, W. B. Huttner, Analysis of the substrate-specificity of tyrosylprotein sulfotransferase using synthetic peptides, *J. Biol. Chem.* **1990**, *265*, 8525.

[118] C. T. Veldkamp, C. Seibert, F. C. Peterson, T. P. Sakmar, B. F. Volkman, Recognition of a CXCR4 sulfotyrosine by the chemokine stromal cell-derived factor-1α (SDF-1α/CXCL12), *J. Mol. Biol.* **2006**, *359*, 1400.

[119] C. H. Jen, K. L. Moore, J. A. Leary, Pattern and temporal sequence of sulfation of CCR5 N-terminal peptides by tyrosylprotein sulfotransferase-2: An assessment of the effects of N-terminal residues, *Biochemistry* **2009**, *48*, 5332.

[120] K. Kobashi, D. H. Kim, T. Morikawa, A Novel Type of Arylsulfotransferase, *J. Prot. Chem.* **1987**, *6*, 237.

[121] B. Delhom, G. Alvaro, G. Caminal, J. L. Torres, P. Clapes, Synthesis of sulfated bioactive peptides using immobilized arylsulfotransferase from *Eubacterium sp.*, *Biotech. Lett.* **1996**, *18*, 609.

[122] B. Kim, Y. J. Hyun, K. S. Lee, K. Kobashi, D. H. Kim, Cloning, expression and purification of arylsulfate sulfotransferase from *Eubacterium A-44*, *Biol. Pharm. Bull.* **2007**, *30*, 11.

[123] M. Farzan, C. E. Schnitzler, N. Vasilieva, D. Leung, J. Kuhn, C. Gerard, N. P. Gerard, H. Choe, Sulfated tyrosines contribute to the formation of the C5a docking site of the human C5a anaphylatoxin receptor, *J. Exp. Med.* **2001**, *193*, 1059.

[124] B. P. Morgan, K. J. Marchbank, M. P. Longhi, C. L. Harris, A. M. Gallimore, Complement: central to innate immunity and bridging to adaptive responses, *Immunol. Lett.* **2005**, *97*, 171.

[125] M. J. Walport, Complement, *The New Eng. J. Med.* **2001**, *344*, 1058.

[126] M. K. Pangburn, R. D. Schreiber, H. J. Muller-Eberhard, Formation of the initial C3 convertase of the alternative complement pathway, *J. Exp. Med.* **1981**, *154*, 856.

[127] D. Ricklin, J. D. Lambris, Complement-targeted therapeutics, *Nature Biotech.* **2007**, *25*, 1265.

[128] M. U. Ehrengruber, T. Geiser, D. A. Deranleau, Activation of human neutrophils by C3a and C5a: Comparison of the effects on shape changes, chemotaxis, secretion, and respiratory burst, *FEBS Lett.* **1994**, *346*, 181.

[129] V. A. Bokisch, H. J. Muller-Eberhard, Anaphylatoxin inactivator of human plasma. Its isolation and characterization as a carboxypeptidase, *J. Clin. Invest.* **1970**, *49*, 2427.

[130] S. R. Marder, D. E. Chenoweth, I. M. Goldstein, H. D. Perez, Chemotactic Responses of Human Peripheral-Blood Monocytes to the Complement-Derived Peptides C5a and C5a Des Arg, *J. Immunol.* **1985**, *134*, 3325.

[131] T. Peng, L. M. Hao, J. A. Madri, X. Su, J. A. Elias, G. L. Stahl, S. Squinto, Y. Wang, Role of C5 in the development of airway inflammation, airway hyperresponsiveness, and ongoing airway response, *J. Clin. Invest.* **2005**, *115*, 1590.

[132] H. M. Zhang, G. J. Qin, G. Liang, J. N. Li, R. A. Barrington, D. X. Liu, C5aR-mediated myocardial ischemia/reperfusion injury, *Biochem. Biophys. Res. Commun.* **2007**, *357*, 446.

[133] Reprinted by permission from Macmillan Publishers Ltd: Nature Biotechnology, Vol. 25, Issue 11, p. 1265, copyright (2007).

[134] P. N. Monk, A. Scola, P. K. Madala, D. P. Fairlie, Function, structure and therapeutic potential of complement C5a receptors, *Br. J. Pharmacol.* **2007**, *152*, 429.

[135] F. Boulay, L. Mery, M. Tardif, L. Brouchon, P. Vignais, Expression cloning of a receptor for C5a anaphylatoxin on differentiated Hl-60 cells, *Biochemistry* **1991**, *30*, 2993.

[136] N. P. Gerard, C. Gerard, The chemotactic receptor for human-C5a anaphylatoxin, *Nature* **1991**, *349*, 614.

[137] M. Ohno, T. Hirata, M. Enomoto, T. Araki, H. Ishimaru, T. A. Takahashi, A putative chemoattractant receptor, C5L2, is expressed in granulocyte and immature dendritic cells, but not in mature dendritic cells, *Mol. Immunol.* **2000**, *37*, 407.

[138] S. Okinaga, D. Slattery, A. Humbles, Z. Zsengeller, O. Morteau, M. B. Kinrade, R. M. Brodbeck, J. E. Krause, H. R. Choe, N. P. Gerard, C. Gerard, C5L2, a nonsignaling C5A binding protein, *Biochemistry* **2003**, *42*, 9406.

[139] L. H. C. van Lith, J. Oosterom, A. van Elsas, G. J. R. Zaman, C5a-stimulated recruitment of beta-Arresting to the nonsignaling 7-transmembrane decoy receptor C5L2, *J. Biomol. Screen.* **2009**, *14*, 1067.

[140] N. P. Gerard, B. Lu, P. X. Liu, S. Craig, Y. Fujiwara, S. Okinaga, C. Gerard, An anti-inflammatory function for the complement anaphylatoxin C5a-binding protein, C5L2, *J. Biol. Chem.* **2005**, *280*, 39677.

[141] N. J. Chen, C. Mirtsos, D. Suh, Y. C. Lu, W. J. Lin, C. McKerlie, T. Lee, H. Baribault, H. Tian, W. C. Yeh, C5L2 is critical for the biological activities of the anaphylatoxins C5a and C3a, *Nature* **2007**, *446*, 203.

[142] A. M. Scola, K. O. Johswich, B. P. Morgan, A. Klos, P. N. Monk, The human complement fragment receptor, C5L2, is a recycling decoy receptor, *Mol. Immunol.* **2009**, *46*, 1149.

[143] M. Allegretti, A. Moriconi, A. R. Beccari, R. Di Bitondo, C. Bizzarri, R. Bertini, F. Colotta, Targeting C5a: Recent advances in drug discovery, *Curr. Med. Chem.* **2005**, *12*, 217.

[144] S. J. Siciliano, T. E. Rollins, J. Demartino, Z. Konteatis, L. Malkowitz, G. Vanriper, S. Bondy, H. Rosen, M. S. Springer, 2-Site Binding of C5a by Its Receptor - an Alternative Binding Paradigm for G-Protein-Coupled Receptors, *Proc. Natl. Acad. Sci. U. S. A.* **1994**, *91*, 1214.

[145] J. A. Smith, Neutrophils, host defense, and inflammation: a double-edged sword, *J. Leukocyte Biol.* **1994**, *56*, 672.

[146] N. M. Bless, R. L. Warner, V. A. Padgaonkar, A. B. Lentsch, B. J. Czermak, H. Schmal, H. P. Friedl, P. A. Ward, Roles for C-X-C chemokines and C5a in lung injury after hindlimb ischemia-reperfusion, *Am. J. Phys.* **1999**, *276*, L57.

[147] J. Elmgreen, Subnormal activation of phagocytes by complement in chronic inflammatory bowel-disease - neutrophil chemotaxis to complement split product C5a, *Gut* **1984**, *25*, 737.

[148] T. M. Woodruff, T. V. Arumugam, I. A. Shiels, R. C. Reid, D. P. Fairlie, S. M. Taylor, A potent human C5a receptor antagonist protects against disease pathology in a rat model of inflammatory bowel disease, *J. Immunol.* **2003**, *171*, 5514.

[149] J. Elmgreen, T. M. Hansen, Subnormal sensitivity of neutrophils to complement split product C5a in rheumatoid-arthritis - Relation to complement catabolism and disease extent, *Ann. Rheumatic Dis.* **1985**, *44*, 514.

[150] P. J. Jose, I. K. Moss, R. N. Maini, T. J. Williams, Measurement of the chemotactic complement fragment C5a in rheumatoid synovial-fluids by radioimmunoassay - Role of C5a in the acute inflammatory phase, *Ann. Rheumatic Dis.* **1990**, *49*, 747.

[151] F. Fischetti, P. Durigutto, P. Macor, R. Marzari, R. Carretta, F. Tedesco, Selective therapeutic control of C5a and the terminal complement complex by anti-C5 single-chain Fv in an experimental model of antigen-induced arthritis in rats, *Arthritis and Rheumatism* **2007**, *56*, 1187.

[152] A. M. Finch, A. K. Wong, N. J. Paczkowski, S. K. Wadi, D. J. Craik, D. P. Fairlie, S. M. Taylor, Low-molecular-weight peptidic and cyclic antagonists of the receptor for the complement factor C5a, *J. Med. Chem.* **1999**, *42*, 1965.

[153] H. Sumichika, K. Sakata, N. Sato, S. Takeshita, S. Ishibuchi, M. Nakamura, T. Kamahori, S. Ehara, K. Itoh, T. Ohtsuka, T. Ohbora, T. Mishina, H. Komatsu, Y. Naka, Identification of a potent and orally active non-peptide C5a receptor antagonist, *J. Biol. Chem.* **2002**, *277*, 49403.

[154] R. M. Brodbeck, D. N. Cortright, A. P. Kieltyka, J. Y. Yu, C. O. Baltazar, M. E. Buck, R. Meade, G. D. Maynard, A. Thurkauf, D. S. Chien, A. J. Hutchison, J. E. Krause, Identification and characterization of NDT 9513727 [N,N-bis(1,3-Benzodioxol-5-ylmethyl)-1-butyl-2,4-diphenyl-1H-imidazole-5-methanamine], a novel, orally bioavailable C5a receptor inverse agonist, *J. Pharm. Exp. Ther.* **2008**, *327*, 898.

[155] Y. Gong, J. K. Barbay, M. Buntinx, J. Li, J. Van Wauweb, C. Claes, G. Van Lommen, P. J. Hornby, W. He, Design and optimization of aniline-substituted tetrahydroquinoline C5a receptor antagonists, *Bioorg. Med. Chem. Lett.* **2008**, *18*, 3852.

[156] J. J. Chen, D. C. Cole, G. Ciszewski, K. Crouse, J. W. Ellingboe, P. Nowak, G. J. Tawa, G. Berstein, W. Li, Identification of a new class of small molecule C5a receptor antagonists, *Bioorg. Med. Chem. Lett.* **2010**, *20*, 662.

[157] J. Koehl, Drug evaluation: The C5a receptor antagonist PMX-53, *Curr. Opin. Mol. Ther.* **2006**, *8*, 529.

[158] Arana Therapeutics, http://www.arana.com/inflammation_franchise_pmx.htm, 26-3-2010.

[159] T. M. Woodruff, S. Pollitt, L. M. Proctor, S. Z. Stocks, H. D. Manthey, H. M. Williams, I. B. Mahadevan, I. A. Shiels, S. M. Taylor, Increased potency of a novel complement factor 5a receptor antagonist in a rat model of inflammatory bowel disease, *J. Pharm. Exp. Ther.* **2005**, *314*, 811.

[160] G2 Therapeutics and Novo Nordisk
http://www.g2therapies.com.au/pdf/G2%20Media%20Release%20221008.pdf, 26-3-2010.

[161] C. J. C. de Haas, K. E. Veldkamp, A. Peschel, F. Weerkamp, W. J. B. Van Wamel, E. C. J. M. Heezius, M. J. J. G. Poppelier, K. P. M. Van Kessel, J. A. G. van Strijp, Chemotaxis inhibitory protein of *Staphylococcus aureus*, a bacterial antiinflammatory agent, *J. Exp. Med.* **2004**, *199*, 687.

[162] J. D. Lambris, D. Ricklin, B. V. Geisbrecht, Complement evasion by human pathogens, *Nat. Rev. Micriobiol.* **2008**, *6*, 132.

[163] F. D. Lowy, Medical progress - *Staphylococcus aureus* infections, *N. Engl. J. Med.* **1998**, *339*, 520.

[164] K. E. Veldkamp, H. C. J. M. Heezius, J. Verhoef, J. A. G. van Strijp, K. P. M. van Kessel, Modulation of neutrophil chemokine receptors by *Staphylococcus aureus* supernate, *Infect. Immun.* **2000**, *68*, 5908.

[165] B. Postma, M. J. Poppelier, J. C. van Galen, E. R. Prossnitz, J. A. G. van Strijp, C. J. C. de Haas, K. P. M. van Kessel, Chemotaxis inhibitory protein of *Staphylococcus aureus* binds specifically to the C5a and formylated peptide receptor, *J. Immunol.* **2004**, *172*, 6994.

[166] P. J. Haas, *Staphylococcal* drug discovery, PhD thesis, Utrecht University (Utrecht), **2006**, 73.

[167] A. J. Wright, A. Higginbottom, D. Philippe, A. Upadhyay, S. Bagby, R. C. Read, P. N. Monk, L. J. Partridge, Characterisation of receptor binding by the chemotaxis inhibitory protein of *Staphylococcus aureus* and the effects of the host immune response, *Mol. Immunol.* **2007**, *44*, 2507.

[168] P. J. Haas, C. J. C. de Haas, W. Kleibeuker, M. J. J. G. Poppelier, K. P. M. van Kessel, J. A. W. Kruijtzer, R. M. J. Liskamp, J. A. G. van Strijp, N-terminal residues of the chemotaxis inhibitory protein of *Staphylococcus aureus* are essential for blocking formylated peptide receptor but not C5a receptor, *J. Immunol.* **2004**, *173*, 5704.

[169] P. J. Haas, C. J. C. de Haas, M. J. J. C. Poppelier, K. P. M. van Kessel, J. A. G. van Strijp, K. Dijkstra, R. M. Scheek, H. Fan, J. A. W. Kruijtzer, R. M. J. Liskamp, J. Kemmink, The structure of the C5a receptor-blocking domain of chemotaxis inhibitory protein of *Staphylococcus aureus* is related to a group of immune evasive molecules, *J. Mol. Biol.* **2005**, *353*, 859.

[170] E. Gustafsson, Molecular evolution of a C5aR antagonist against inflammatory disease, PhD thesis, Lund University (Lund), **2009**,

[171] E. Gustafsson, P. J. Haas, B. Walse, M. Hijnen, C. Furebring, M. Ohlin, J. A. G. van Strijp, K. P. M. van Kessel, Identification of conformational epitopes for human IgG on Chemotaxis inhibitory protein of *Staphylococcus aureus*, *Bmc Immunol.* **2009**, *10*, 13.

[172] E. Gustafsson, A. Rosen, K. Barchan, K. P. M. van Kessel, K. Haraldsson, S. Lindman, C. Forsberg, L. Ljung, K. Bryder, B. Walse, P. J. Haas, J. A. G. van Strijp, C. Furebring, Directed evolution of chemotaxis inhibitory protein of *Staphylococcus aureus* generates biologically functional variants with reduced interaction with human antibodies, *Protein Eng., Des. Sel.* **2010**, *23*, 91.

Chapter 2

A general sequence independent solid phase method for the site-specific synthesis of multiple sulfated-tyrosine containing peptides

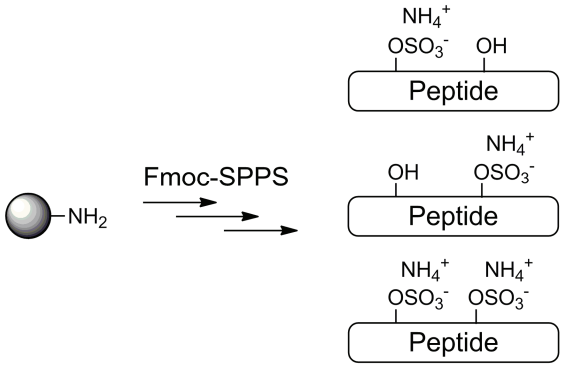

Parts of this chapter have been published:
A. Bunschoten, J. A. W. Kruijtzer, J. H. Ippel, C. J. C. de Haas, J. A. G. van Strijp, J. Kemmink, R. M. J. Liskamp, *Chemical Communications*, **2009**, 2999-3001.

2

2.1 Introduction

Although much less well-known than protein phosphorylation, the significance of protein sulfation is rapidly gaining momentum.[1-8] Based upon the analysis of tyrosine sulfation in *Drosophila Melanogaster*, it is estimated that as much as 1% of all tyrosine residues occurring in proteins can be sulfated, making it, together with phosphorylation, the most frequently occurring post-translational modification of tyrosine.[9]

Studies towards the role and importance of sulfation, of for example GPCR proteins, as a key modulator of extracellular protein-protein interactions, require the availability of reliable and convenient methods for the preparation of crucial sulfated peptides. However, so far no reliable general sequence-independent method is available for the site-specific incorporation of especially multiply sulfated tyrosines. Clearly, the absence of these methods reflects the relative instability of sulfated tyrosine residues towards acids as compared to phosphorylated tyrosine residues in peptides and proteins.[10, 11] A proposed mechanism of the acid-catalyzed hydrolysis of aryl sulfate esters is depicted in (Fig. 2.1).[12]

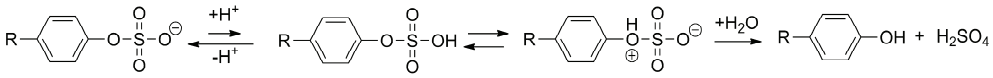

Figure 2.1 Proposed mechanism for the acid hydrolysis of aryl sulfate esters.[12]

As was described in the general introduction, we are interested in the inhibitory interactions of the Chemotaxis Inhibitory Protein of *Staphylococcus aureus* (CHIPS) with the G protein-coupled receptor C5aR. Knowledge about these interactions might be used to develop new anti-inflammatory compounds. In order to circumvent studies of ligands with the entire transmembrane C5a-receptor, we required sulfated N-terminal peptides as representative mimics of this part of the C5a-receptor, which contains two sulfated tyrosine residues in vivo.[13] This N-terminal part of the C5aR is crucial for the binding of its natural ligand C5a and it has been shown that CHIPS binds also to this part of the receptor.[13-15]

However, upon evaluation of the relatively scarce literature on the synthesis of multiply sulfated peptides available at the start of the research described in this chapter,[16-19] we concluded that (i) a solid phase synthesis according to the Boc-strategy is unfit in view of the acid lability of sulfated tyrosine residues, (ii) evidently, global sulfation using e.g. sulfurtrioxide does not lead to sulfation of specific tyrosine residues when more tyrosine, threonine and serine residues are present, (iii) so far, TFA-stable sulfated tyrosine building blocks for use in solid phase peptide synthesis (SPPS) are unavailable and (iv) no general and convenient sequence independent SPPS strategy is available for the synthesis of highly functionalized and multiply sulfated peptides using conventional Fmoc/*t*Bu SPPS.

Therefore, we describe in this chapter a new sequence independent synthetic route for the site-specific incorporation of multiply sulfated tyrosine residues into peptides by solid phase methods. Within this chapter the possibilities of this new method are explored in the synthesis of a small collection of sulfated C5a-receptor mimics.

In the same time-frame in which our research was performed, two others methods for the synthesis of sulfated peptides have been described in the literature. Ali and Taylor described the use of a sulfated

tyrosine building block protected with a dichlorovinyl (DCV) group (Fmoc-Tyr(SO_3DCV)-OH) (Fig. 2.2) in Fmoc/*t*Bu SPPS.[20] To prevent the degradation of this protecting group they had to use 2-methylpiperidine instead of piperidine for the deprotection of the Fmoc group. The DCV group is removed by hydrogenolysis using Pd/C and H_2. This deprotection will be hampered by catalyst poisoning by the sulfur-containing amino acids cysteine and methionine, when present. In addition, reduction of the indole ring in tryptophan may occur. Recently these authors described an adapted deprotection method in which they removed the DCV group by hydrogenolysis in the presence of triethylamine to prevent reduction of tryptophan and catalyst poisoning by methionine.[21-23] However, catalyst poisoning by cysteine and disulfide formation may still occur.

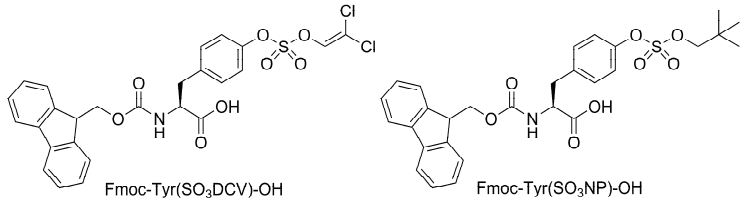

Figure 2.2 Two tyrosine building blocks containing a protected sulfate suitable for Fmoc/*t*Bu-SPPS.

The other method was described by Simpson et al., who used a neopentyl-protected sulfated tyrosine building block (Fmoc-Tyr(SO_3NP)-OH) (Fig. 2.2). Surprisingly, in contrast to earlier described harsh deprotection conditions involving strong nucleophiles (NaN_3), long reaction times and elevated temperatures (overnight 70 °C in DMF),[24] they were able to remove the neopentyl protecting group by incubating the peptide with protected sulfate in an aqueous solution of ammonium acetate at 37 °C for 6-12 hr.[25] In contrast to what was reported by the authors, the building block and the peptides containing this protected sulfated tyrosine residue were not stable against the standard deprotection and cleavage conditions used (TFA/TIS/H_2O; 95/2.5/2.5, 2 h, rt). This treatment resulted in an estimated 50 % loss of the desired peptide with protected sulfate groups (Fig. 2.3).

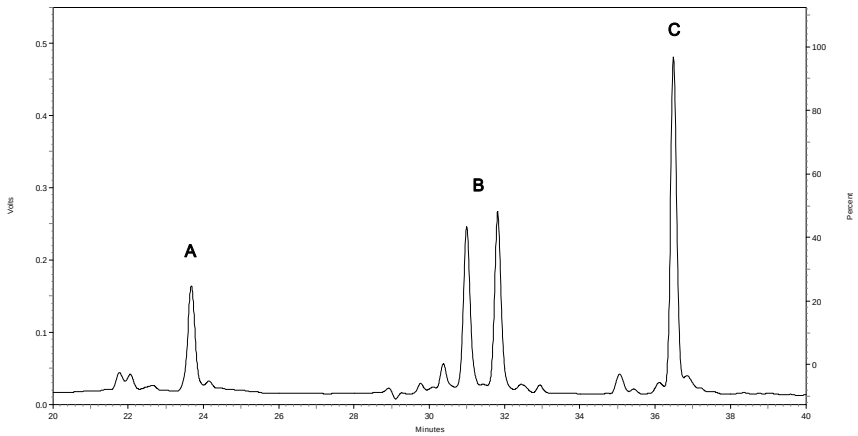

Figure 2.3 HPLC chromatogram (absorption at 214 nm) of crude $C5aR_{7\text{-}28}S_2$ synthesized with Fmoc-Tyr(SO_3NP)-OH after deprotection and cleavage of the resin (TFA/TIS/H_2O; 95/2.5/2.5, 2h, rt). The mixture contains $C5aR_{7\text{-}28}$ (A 15%), peptides containing one -SO_3NP group (B (35%) and the desired peptide containing two –SO_3NP groups (C 50%).

2.2 Results

In order to synthesize our multiply sulfated target peptides, we have developed a general sequence independent solid phase method by which a peptide was synthesized according to the Fmoc/*t*Bu-strategy, followed by selective deprotection of the tyrosine residues to be sulfated and introduction of a 2,2,2-trichloroethyl-protected sulfate group. Upon completion of the synthesis of the sulfated peptide, it was cleaved from the resin by acidolysis and protecting groups were removed with the exception of the sulfate protecting group, thereby preventing undesired acid-induced removal of the sulfate group(s) during this step. Finally, the sulfate protecting groups were removed in a slightly acidic (pH 6.4) reductive step, without affecting the sulfate groups.

Synthesis of the sulfating reagents

The reagent 2,2,2-trichloroethyl chlorosulfate (**1**), used to introduce a protected sulfate group onto free tyrosine residues, has been described by Taylor and co-workers. They applied this reagent, synthesized according to a procedure described by Hedayatullah (Fig. 2.4),[26, 27] in the synthesis of sulfated steroid hormones.[28] Although 2,2,2-trichloroethyl chlorosulfate (**1**) is a very useful reagent, as will be described in this chapter, it is a liquid that has to be stored at anhydrous conditions and low temperatures to prevent degradation. In 2006, Ingram et al. described the synthesis and application of a sulfuryl imidazolium salt, which was successfully applied in the synthesis of *O*-sulfated carbohydrates.[29] Later derivatives of this salt were also used to synthesize difficult *O*- and *N*-sulfated carbohydrates.[30] These sulfuryl imidazolium salts are crystalline compounds which can be stored at room temperature and do not release a nucleophilic chloride ion upon reaction with the nucleophile that has to be sulfated. This nucleophilic chloride ion has been shown to cause side-reactions during the sulfation of carbohydrates.[29]

To explore the possibilities of sulfuryl imidazolium salts, a derivative of 2,2,2-trichloroethyl chlorosulfate (**3**) was synthesized via the introduction of imidazole and the formation of the salt by methylating the free amine by Meerweins reagent. The synthesized reagent **3** proved to be at least as reactive as 2,2,2-trichloroethyl chlorosulfate (**1**) towards an unprotected tyrosine in our test peptide Ac-FYH(Dmbz)F-NH_2 and showed no degradation upon 9 months of storage at room temperature. Although reagent **1** was used in the research described in this thesis, sulfuryl imidazolium salt **3**, and derivatives of it, will probably replace 2,2,2-trichloroethyl chlorosulfate as a more convenient and stable sulfating reagent.

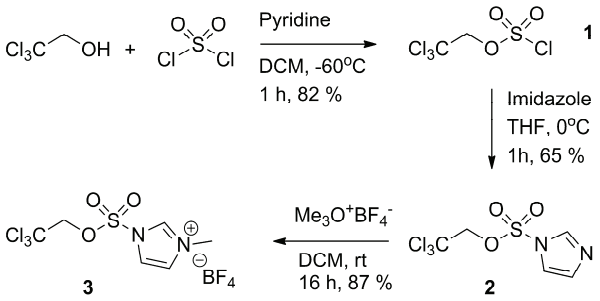

Figure 2.4 Synthesis of 2,2,2-trichloroethyl chlorosulfate (**1**) and its imidazolium salt (**3**).

Synthesis of sulfated peptides

Sulfation of tyrosine is not limited to proteins, but also occurs on bioactive peptides such as neuropeptides and peptide hormones. For evaluation of our synthesis strategy, the synthesis of sulfated Leu-enkephaline (**9**) was attempted (Fig. 2.5).[31] In this strategy the phenolic hydroxyl functionality of tyrosine was protected with a 2-Cl Trt-group (**5**), which was removed with 1% TFA. The released phenolic hydroxyl functionality was sulfated with 2,2,2-trichloroethyl chlorosulfate **1** leading to **7**. By treatment with 95% TFA, Leu-enkephaline **8** containing the protected sulfate ester was cleaved from the resin. These harsh acidic conditions did not affect the 2,2,2-trichloroethyl sulfate ester, which was successfully removed in the next step by a reductive beta-elimination reaction using zinc-dust and ammonium formate.[28] The sulfated Leu-enkephaline **9** was obtained pure, in a good yield of 63% (after HPLC purification).

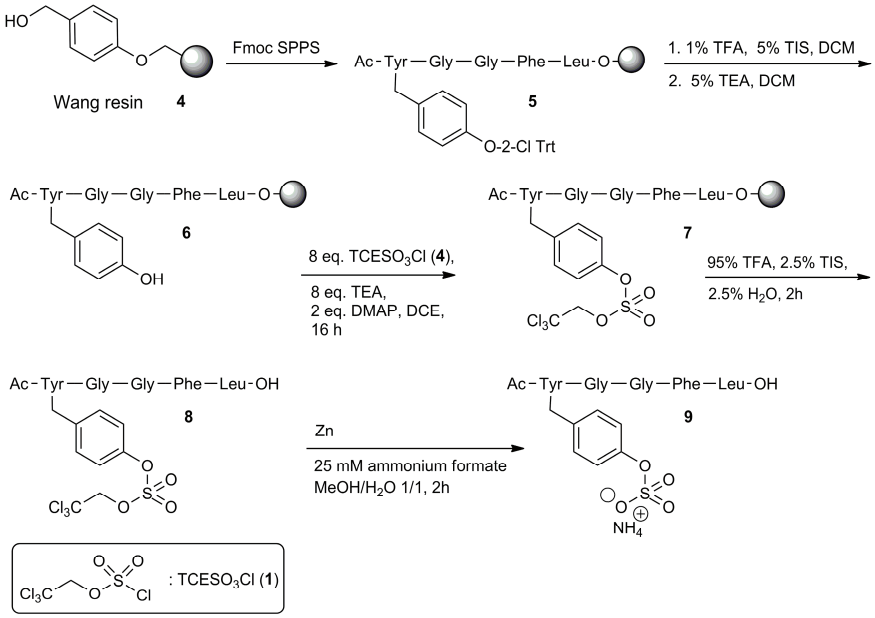

Figure 2.5 Solid phase synthesis of sulfated Leu-enkephalin **9**.

Encouraged by these results, we embarked on our actual target, the synthesis of multiply sulfated fragments of the N-terminal part of the C5a-receptor (C5aR).[13] The above described strategy was used for these significantly more complex peptides, containing 70-90% of amino acid residues with a functional side chain requiring protection (Fig. 2.6).[32] Standard protecting groups were used for the side chains, which were considered to be all compatible with the strategy exemplified by the synthesis of sulfated Leu-enkephaline **9** (Fig. 2.5).

Our goal was to synthesize a small collection of N-terminal fragments of the C5aR: fragment 10-18, which is the binding site for CHIPS according to Postma et al.[14]; fragment 10-24, based on preliminary NMR experiments of CHIPS binding to C5aR fragments; fragment 7-28; and fragment 1-35, which is the complete extra-cellular N-terminus. Applying the same strategy used for the Leu-enkephaline (**9**), three sulfated peptides were successfully synthesized: sulfated fragment 10-18 ($C5aR_{10\text{-}18}S_2$) (**14**) (Figure 2.6), sulfated fragment 10-24 ($C5aR_{10\text{-}24}S_2$) (**15**) and sulfated fragment 1-35 ($C5aR_{1\text{-}35}S_2$) (**16**). To study the influences of the two sulfated tyrosines, the unsulfated fragment 10-18 ($C5aR_{10\text{-}18}$) (**17**) was also synthesized.

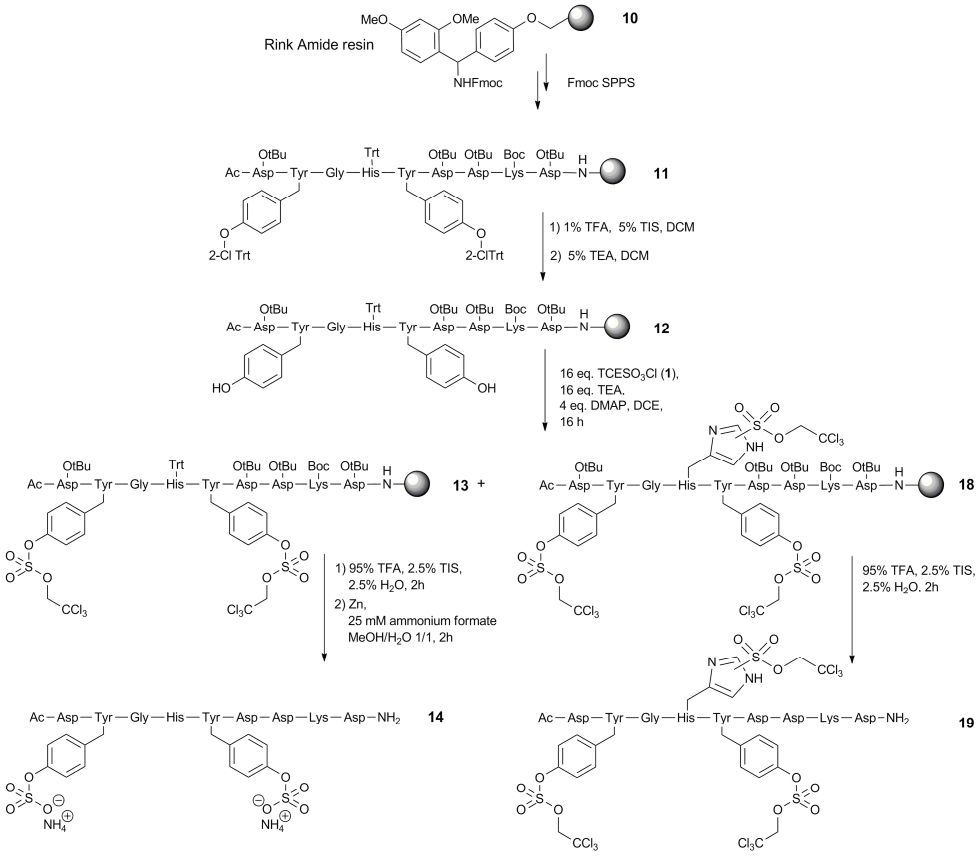

Figure 2.6 Synthesis of a disulfated $C5aR_{10\text{-}18}$ peptide ($C5aR_{10\text{-}18}$ S_2)(**14**) and the formation of side product (**19**)

Protection of histidine

During the synthesis of these sulfated peptides, each time a major side-product (30-50%) with a mass corresponding to a tri-sulfated peptide was observed. MS/MS-analysis (Fig. 2.7) of the isolated and purified side-product obtained during the synthesis of $C5aR_{10\text{-}18}(SO_3TCE)_2$ (**13**) showed that also the histidine had reacted with the 2,2,2-trichloroethyl chlorosulfate resulting in peptide **19** (Fig. 2.6). Tests on a small resin-bound model peptide, Ac-Phe-Tyr(2-Cl-Trt)-His(Trt)-Phe-NH-resin, showed that the trityl-protected histidine was also being sulfated to some extent by 2,2,2-trichloroethyl chlorosulfate (**1**) or by the imidazole reagent (**3**). The formation of tri-sulfated peptide **19** probably happened by a combination of premature deprotection of the histidine by treatment with 1% TFA and by reaction of the unprotected π-nitrogen of the histidine with 2,2,2-trichloroethyl chlorosulfate (**1**). The trityl protecting group, attached to the τ-nitrogen of the histidine side chain, provides mainly steric hindrance to prevent undesired reactions with the imidazole moiety. In certain reactions this steric hindrance might not be enough. It is, for example, known that Trt-protected histidine can still be methylated on the unprotected nitrogen.[33] During the reaction of the protected peptide with 2,2,2-trichloroethyl chlorosulfate, it appeared that steric hindrance was also not sufficient in this reaction.

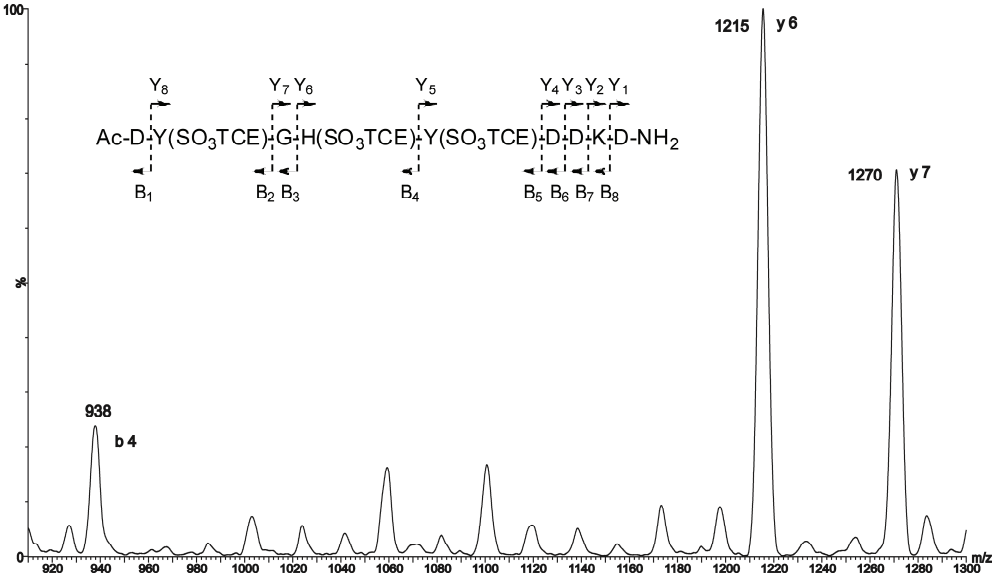

Figure 2.7 MS/MS spectrum of Ac-DY(SO_3TCE)GH(SO_3TCE)Y(SO_3TCE)DDKD-NH_2 (**19**). All b- and y-ions were accounted for. The m/z values of the b4- and y6-ions reveal the presence of the -SO_3TCE on the histidine residue.

The only way to prevent this unwanted reaction of the histidine side chain with 2,2,2-trichloroetyl chlorosulfate was to use a histidine residue with a different protecting group on its side chain, which would not only provide steric hindrance, but would also diminish the reactivity of the imidazole

nitrogens. Next to this, the protecting group should be stable during the Fmoc/tBu SPPS and should be stable during the selective acidolysis of the 2-chlorotrityl protecting group used to deprotect the tyrosine residues, but should also be removable without harming the sulfated tyrosine residues.

Fortuitously, the base-labile 2,6-dimethoxybenzoyl (Dmbz) group, described by Zaramella et al., on the τ-nitrogen of histidine turned out to be a suitable replacement of the Trt-group.[34] This protecting group should prevent the reaction of the π-nitrogen of histidine with 2,2,2-trichloroethyl chlorosulfate and can be removed by 7 M ammonia in methanol. These conditions did not affect the sulfate group on a tyrosine residue. The building block necessary for the SPPS, Fmoc-His(Dmbz)-OH (**20**) was synthesized as described in literature, starting from Fmoc-His(Trt)-OH, in a yield of 81% (Fig. 2.8A).[34] Because of the importance of the position of the protecting group described by Zaramella et al., we measured an HMBC spectrum of compound **20**. Within the HMBC spectrum of compound **20** (Fig. 2.8B) cross peaks can be observed between the two nitrogen atoms and the two protons of the histidine side-chain. Next to these signals also a cross peak can be observed between the π-nitrogen and the β-protons of histidine. Because the τ-nitrogen is one bond further away, this one is less likely to be observed. The cross peak between the π-nitrogen and the β-protons was indeed observed in the HMBC spectrum of compound **20** and coincided with the nitrogen resonating at the higher chemical shift value. This higher chemical shift value for the imidazole nitrogen corresponds to a ´pyridine-type´ nitrogen, the substituted ´pyrrole-type´ nitrogen resonates at a lower chemical shift value. The Dmbz group is attached to the ´pyrrole-type´ nitrogen and the measured HMBC spectrum for compound **20** (Fig. 2.8B) is compatible with the Dmbz attached to the τ-nitrogen as described in the literature.[35]

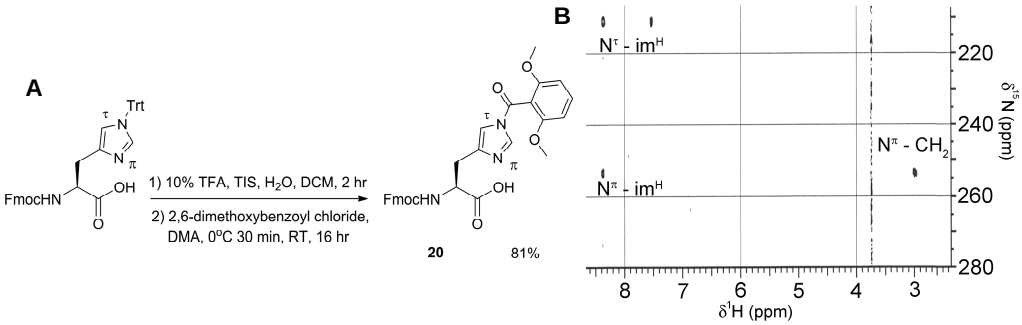

Figure 2.8 A) Synthesis of Fmoc-His(Dmbz)-OH (**20**); B) HMBC spectrum of Fmoc-His(Dmbz)-OH (**20**).

The introduction of a TCE-protected sulfate by 2,2,2-trichloroethyl chlorosulfate (**1**) or its imidazolium salt (**3**) has been tested on a small test peptide (Ac-Phe-Tyr-His(Dmbz)-Phe-NH_2)(**34**) resulting in a sulfated tyrosine residue without sulfation of the histidine side chain. Deprotection of the Dmbz protecting group, by 7 M NH_3 in MeOH, has also been tested in the presence of a sulfated

tyrosine residue on this same test peptide, which resulted in a deprotected histidine without removal of the sulfate group from the tyrosine side chain (Fig. 2.9).

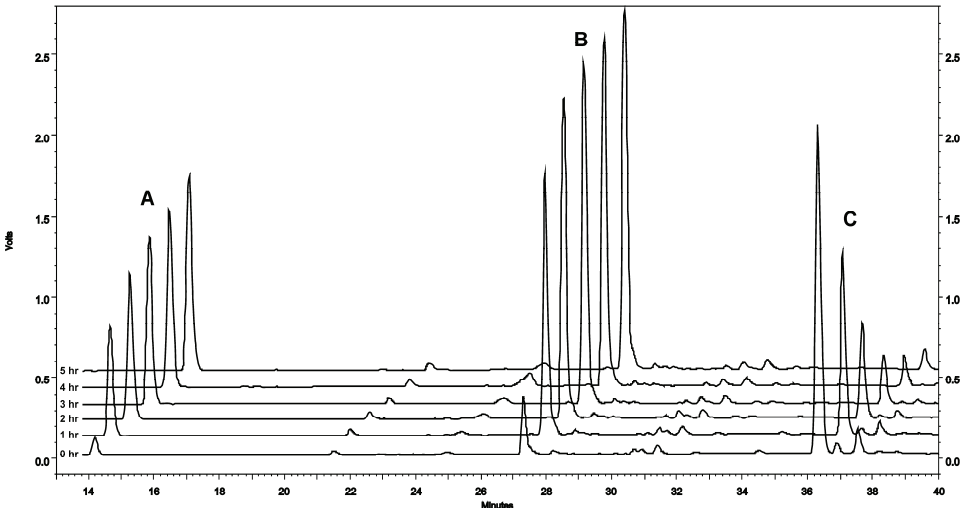

Figure 2.9 Deprotection of His(Dmbz) in the peptide Ac-Phe-Tyr($SO_3^-NH_4^+$)-His(Dmbz)-Phe-NH_2 (**34**) by 7 M NH_3 in MeOH followed in time by HPLC. Peak **A** is the protecting group removed from the histidine residue: 2,6-dimethoxybenzamide (**36**); peak **B** is Ac-Phe-Tyr($SO_3^-NH_4^+$)-His-Phe-NH_2 (**35**) and peak **C** is Ac-Phe-Tyr($SO_3^-NH_4^+$)-His(Dmbz)-Phe-NH_2 (**34**).

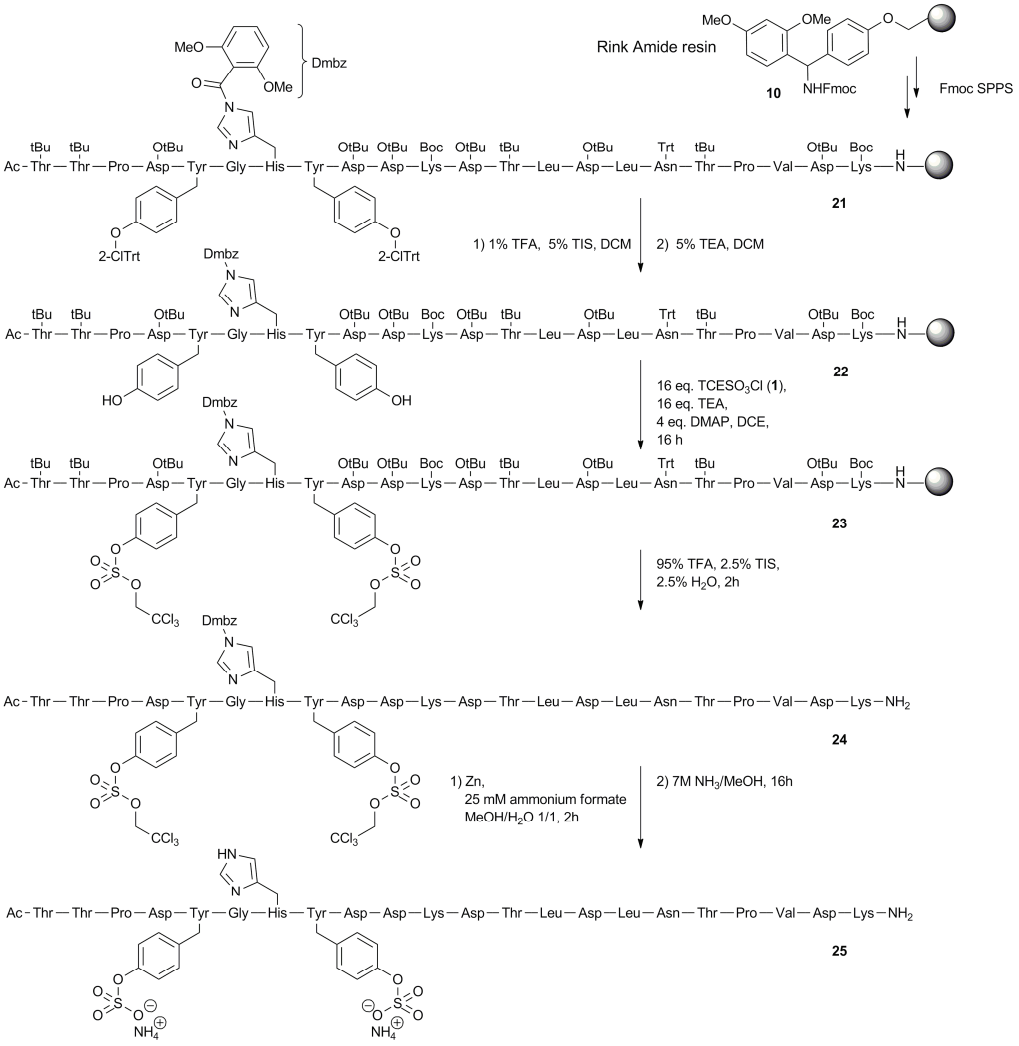

Figure 2.10 Synthesis of $C5aR_{7\text{-}28}S_2$ (**25**)

With the selection of a suitable protecting group for histidine, the three sulfated forms of $C5aR_{7\text{-}28}$ (**25-27**) could be synthesized without the occurrence of the earlier observed side-product (Fig. 2.10 and Table 2.1). Instead of Fmoc-His(Trt)-OH, now Fmoc-His(Dmbz)-OH (**20**) was introduced in the peptide sequence. After solid phase synthesis of **21** the tyrosine residues were selectively deprotected leading to peptide **22.** Sulfation of the deprotected tyrosines afforded **23**, which was deprotected -with the exception of the sulfated tyrosine residues and the histidine residue- and cleaved from the resin to yield **24.** After the removal of the 2,2,2,-trichloroethyl ester and then the removal of the Dmbz group, sulfated peptide **25** was successfully obtained. The same protocol in combination with standard *t*Bu protected tyrosine residues was applied for the site-specific sulfation of tyrosine residues. In this way

mono-tyrosine sulfated peptides **26** and **27** were synthesized in addition to the disulfated tyrosine peptide **25**. For comparison, the unsulfated C5aR$_{7\text{-}28}$ (**28**) was also synthesized. The resulting peptides were characterized by mass spectrometry and NMR spectroscopy.

Table 2.1 Synthesized C5a-receptor mimics.

Peptide	Fragment	Sequence
14	C5aR$_{10\text{-}18}$S$_2$	Ac-DY($SO_3^-NH_4^+$)GHY($SO_3^-NH_4^+$)DDKD-NH_2
17	C5aR$_{10\text{-}18}$	Ac-DYGHYDDKD-NH_2
15	C5aR $_{10\text{-}24}$S$_2$	Ac-DY($SO_3^-NH_4^+$)GHY($SO_3^-NH_4^+$)DDKDTLDLNT-NH_2
25	C5aR $_{7\text{-}28}$S$_2$	Ac-TTPDY($SO_3^-NH_4^+$)GHY($SO_3^-NH_4^+$)DDKDTLDLNTPVDK-NH_2
26	C5aR$_{7\text{-}28}$S^{11}	Ac-TTPDY($SO_3^-NH_4^+$)GHYDDKDTLDLNTPVDK-NH_2
27	C5aR$_{7\text{-}28}$S^{14}	Ac-TTPDYGHY($SO_3^-NH_4^+$)DDKDTLDLNTPVDK-NH_2
28	C5aR $_{7\text{-}28}$	Ac-TTPDYGHYDDKDTLDLNTPVDK-NH_2
29	C5aR $_{7\text{-}28}$S$_2$-βAGC	Ac-TTPDY($SO_3^-NH_4^+$)GHY($SO_3^-NH_4^+$)DDKDTLDLNTPVDKβAGC-NH_2
16	C5aR $_{1\text{-}35}$S$_2$	Ac-MNSFNYTTPDY($SO_3^-NH_4^+$)GHY($SO_3^-NH_4^+$)DDKDTLDLNTPVDKTSNTLRV-NH_2

Synthesis of cysteine-containing sulfated peptides

Next to these peptides, which will be used for studying the binding of CHIPS to the C5a-receptor (Chapter 3), a cysteine-containing fragment was synthesized (C5aR$_{7\text{-}28}$S$_2$-βAGC, **29**). Incorporation of a cysteine residue in a peptide sequence allows functionalization with e.g. fluorescent labels, radiolabels and selective attachment to (SPR)surfaces via a thiol maleimide reaction.

To test if our sulfating strategy was compatible with cysteine residues, the C5aR$_{7\text{-}28}$S$_2$ (**25**) sequence was elongated on the C-terminus with a β-alanine (NH-CH_2-CH_2-C(O)), a glycine and a trityl side-chain protected cysteine residue. The trityl protection of the cysteine residue was expected to be stable against the deprotection conditions used for the removal of the 2-Cl trityl protection of the tyrosine residues.[36] The same procedure was used as described above for the C5aR$_{7\text{-}28}$S$_2$ (**25**), but after the final deprotection of the TCE and Dmbz protecting groups several peaks appeared in the HPLC chromatogram (Fig. 2.11 A). Because these peaks only appeared in this cysteine containing peptide, we hypothesized that these additional peaks were caused by complications originating from cysteine. First of all cysteine can form disulfides under oxygen-rich or basic conditions such as used for the deprotection of the Dmbz group. Secondly, thiols are known to form complexes with metal ions such as zinc, which is used for the removal of the TCE group. To reduce the disulfide bonds we incubated the peptide prior to HPLC purification with DTT. This resulted in a reduction of the number of peaks but resulted also in a very broad main peak. (Fig. 2.11 B). When the peptide was incubated not only with DTT but also with EDTA to complex the zinc present from deprotecting the TCE group, the desired product (**29**) could be isolated (Fig. 2.11 C). To our knowledge, this is the first example of a cysteine-containing sulfated peptide, successfully synthesized by applying the 2,2,2-trichloroethyl chlorosulfate reagent.

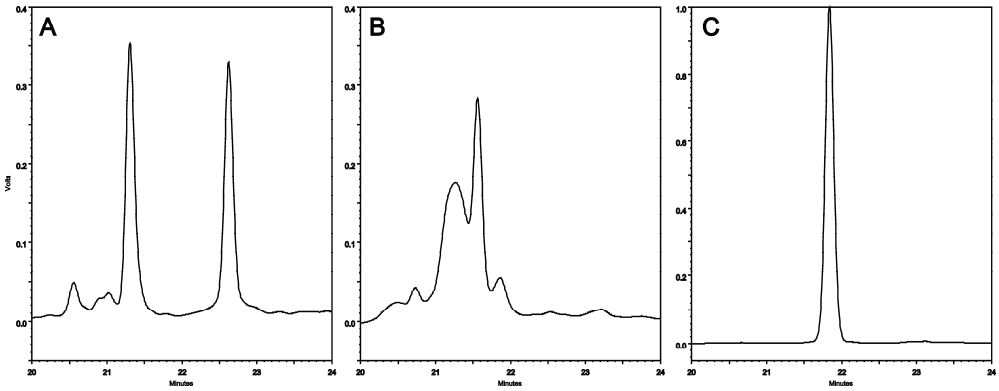

Figure 2.11 HPLC chromatogram (absorption at 214 nm) of C5aR$_{7\text{-}28}$S$_2$–βAGC-NH$_2$ (**29**) after standard deprotection (A), after incubation with 5 eq. of DTT (B) and after incubation with 5 eq. of DTT and EDTA (C).

2.3 Discussion

A new general method for the synthesis of sulfated peptides was described in this chapter. This method allows for the introduction of sulfate groups onto multiple tyrosine residues within highly functional and complex peptides. The sulfate groups were introduced in a protected form so they were completely stable to acidic conditions, making it possible to follow normal Fmoc/*t*Bu SPPS and purification protocols. The method was successfully tested by the synthesis of sulfated Leu-enkephalin **9**. The strategy used in that synthesis was then applied on the actual target peptides: N-terminal fragments of the C5a-receptor, which were required for studying the binding of CHIPS to the C5a-receptor (chapter 3).[15, 37] For the construction of this small library of C5aR mimics, the strategy here described was used for the synthesis of disulfated C5a-receptor mimics **14, 15** and **16**. For elucidating the influence of the sulfate groups also the unsulfated C5aR mimics (**17** and **28**) were synthesized. During the synthesis of the sulfated peptides a major side-product was identified and appeared to be a peptide containing three protected sulfates, with the third protected sulfate on the histidine residue (Fig. 2.6). To prevent the formation of this side product a 2,6-dimethoxybenzoyl side-chain protection was introduced for the histidine residue within the C5aR mimics **25**, **26** and **27**. This histidine Fmoc-building block was successfully synthesized from Fmoc-His(Trt)-OH and the Dmbz group could be removed from the sulfated peptide with 7 M NH_3 in MeOH without harming the sulfated tyrosine residues. With the synthesis of the two monosulfated C5aR mimics (**26** and **27**) as well as with the synthesis of the entire N-terminal part of the C5aR (**16**) we demonstrated that site specific incorporation of sulfated tyrosine residues is possible with this strategy. Since these C5aR mimics contain sulfated tyrosine residues next to unsulfated tyrosine residues.

The compatibility, of this new strategy for the synthesis of sulfated peptides, with cysteine was evaluated by the synthesis of a C5aR mimic elongated with a small spacer and a cysteine residue (**29**). This first example of the synthesis of a cysteine-containing multiply sulfated peptide is suitable for site-selective labeling or attachment to surfaces. The purification of this mimic needed some small

changes: DTT and EDTA were added just before HPLC purification to reduce disulfides and to remove all zinc originating from the deprotection of the TCE protecting group from the sulfate groups.

In conclusion, a new strategy for the site-selective incorporation of multiply sulfated tyrosine residues into highly functionalized peptides was described here. Standard Fmoc/tBu SPPS protocols and HPLC purifications can be applied without harming the protected sulfate introduced on tyrosine. The described strategy is compatible with all standard Fmoc-building blocks used in this chapter, except for trityl-protected histidine which can be replaced by the Dmbz-protected histidine. Cysteine-containing peptides can be synthesized via this new strategy with little adjustments before HPLC purification. For methionine and tryptophan residues no complications are expected when standard Fmoc-building blocks are used.

2.4 Experimental

General

Peptide grade DIPEA, DCM, NMP, TFA, and HPLC grade solvents were purchased from Biosolve B. V. (Valkenswaard, The Netherlands). The Fmoc-protected amino acids were purchased from GL Biochem Ltd. (Shanghai, China) and Fmoc-Tyr(2Cl-Trt)-OH was purchased from EMD/Novabiochem (Gibbstown, USA). The side chain protecting groups were chosen as: Boc for lysine; *t*Bu for aspartic acid, serine, threonine and tyrosine; Trt for asparagine and histidine; Pbf for arginine. TentaGel™ S RAM resin functionalized with a modified Rink Amide linker, (low crosslinked polystyrene grafted with polyethylene glycol, 0.20-0.27 mmol.g^{-1} and a particle size of 90 μm) was purchased from Rapp Polymere GmbH (Tübingen, Germany). ArgoGel™ Wang resin (0.40 mmol/g, particle size 194 μm) was purchased from Argonaut Technologies (Muttenz, Switzerland). Zinc dust (<10μm) was activated before use by washing with 2% HCl, washing with ethanol and ether and dried under vacuum according to a literature procedure.[38] Sulfuryl chloride was distilled under atmospheric pressure before use. Pyridine was distilled from CaH_2. TEA was subsequently distilled from ninhydrine and KOH. THF was freshly distilled from $LiAlH_4$. Unless stated otherwise, chemicals were obtained from commercial sources and used without further purification. Analytical thin layer chromatography (TLC) was performed on Merck pre-coated silica gel 60 F_{254} (0.25mm) plates. Spots were visualized with UV light, ninhydrine, or Cl_2-TDM.[39] Column chromatography was performed using Silicycle SiliaFlash P60 (40-63 μm) from Screening Devices (Amersfoort, The Netherlands). ^{1}H NMR, ^{13}C NMR and two dimensional spectra were obtained on a Varian 300 MHz and a Varian 500 MHz spectrometer. Chemical shifts are given in ppm with respect to internal standard TMS for ^{1}H NMR. ^{13}C NMR spectra were recorded using the attached proton test (APT) pulse sequence.

Analytical HPLC was performed using an automatic HPLC system (Shimadzu) with an analytical reversed-phase column and a UV detector operating at 214 nm with a flow rate of 1 mL/min. A

Phenomenex Luna C8 column (100 Å, 5 µm, 250×4.60 mm), a Phenomenex Gemini C18 (110 Å**,** 5 µm, 250 x 4.6 mm), an Alltech Adsorbosphere C8 (90 Å, 5 µm, 250 x 4.6 mm) or an Alltech Alltima C8 (100 Å, 5 µm, 250 x 4.6 mm) was used. Either TFA buffers (buffer A: H_2O:CH_3CN, 95:5, v:v; buffer B: CH_3CN:H_2O:, 60:40, v:v, both containing 0.1% TFA) or NH_4OAc buffers (buffer A: H_2O:CH_3CN, 95:5, v:v; buffer B: CH_3CN:H_2O, 60:40, v:v, both containing 10 mM of NH_4OAc) were used. Elution was effected with a linear gradient from 100% A to 100% B over 48 min.

Preparative HPLC was performed using an automatic HPLC system (Applied Biosystems) or a Prep LCMS-QP8000α HPLC system (Shimadzu) with a preparative reversed-phase column and an UV detector operating at 214 nm with a flow rate of 12.5 mL/min. A Phenomenex Jupiter C4 (300 Å**,** 10 µm, 250 x 21.2 mm), a Phenomenex Gemini C18 (110 Å**,** 10 µm, 250 x 21.2 mm), an Alltech Adsorbosphere C8 (90 Å, 10 µm, 250 x 22 mm) or an Alltech Alltima C8 (100 Å, 10 µm, 250 x 22mm) was used. Either TFA buffers (buffer A: H_2O:CH_3CN, 95:5, v:v; buffer B: CH_3CN:H_2O, 60:40, v:v, both containing 0.1% TFA) or NH_4OAc buffers (buffer A: H_2O:CH_3CN, 95:5, v:v; buffer B: CH_3CN:H_2O, 60:40, v:v, both containing 10 mM of NH_4OAc) were used. Elution was effected with a linear gradient from 100% A to 100% B over 100 min.

The peptides were characterized using electrospray mass spectrometry (ESI-MS) and was performed on a Thermo Finnigan LCQ DECA XP MAX ion trap mass spectrometer, a Shimadzu LCMS-QP8000 single quadrupole bench-top mass spectrometer or a Waters LCT Time of Flight mass spectrometer (ESI-TOF) (high resolution), all operating in positive or negative ionization mode.

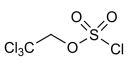

2,2,2-trichloroethyl chlorosulfate 1:

2,2,2-trichloroethyl chlorosulfate (**1)** was synthesized as described by Hedayatullah et al.[26, 27] 2,2,2-trichloroethanol (28.8 mL, 0.3 mol) was, together with pyridine (24.5 mL, 0.3 mol), dissolved in dry DCM (400 mL) and cooled to –60 °C (N_2/acetone). Sulfuryl chloride (25.5 mL, 0.315 mol) was added dropwise to the reaction mixture. Stirring was continued for 2 hours at –60 °C and another hour at rt. The reaction mixture was washed with water (2 times 250 mL), 2M HCl (250 mL) and dried (Na_2SO_4). Concentration *in vacuo* yielded a pale yellow liquid. After distillation under reduced pressure (4 mbar, 60 °C) the product (61.1 g, 82%) was obtained as a clear colourless liquid. R_f (Hex/EtOAc, 4:1, v/v): 0.73. ^{1}H NMR (300 MHz) ($CDCl_3$): δ [ppm]: 4.92 (s, 2H); ^{13}C NMR (75 MHz) ($CDCl_3$): δ [ppm]: 81.2 (O-CH_2), 91.3 (CCl_3).

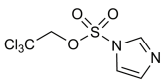

2,2,2-trichloroethyl imidazolesulfate 2:

2,2,2-trichloroethyl chlorosulfate (**1)** (24.8 g, 100 mmol) was dissolved in freshly distilled THF (100 mL) and added dropwise to a cooled solution (ice/water) of imidazole (24.6 g, 360 mmol) in THF (170 mL) under nitrogen atmosphere. After addition, the reaction mixture was allowed to reach room temperature. After 1 hour, the reaction mixture was filtrated and concentrated *in vacuo*. The residue was dissolved in DCM (200 mL) and washed with

water (2 times 100 mL), brine (75 mL) and dried (Na_2SO_4). The resulting crude product was purified by column chromatography with EtOAc/Hexanes (1:4) as eluens yielding the product (20.5 g, 65 %) as a white solid. R_f (Hex/EtOAc, 4:1, v/v): 0.21.
^{1}H NMR (300 MHz) ($CDCl_3$): δ [ppm]: 4.67 (s, 2H, CH_2), 7.22 (s 1H, N-CH=C*H*-N), 7.40 (s 1H, N-C*H*=CH-N), 8.04 (s, 1H, N-CH=N); ^{13}C NMR (75 MHz) ($CDCl_3$): δ [ppm]: 80.1 (CH_2), 91.6 (CCl_3), 118.0 (N-*C*H=CH-N), 131.8 (N-CH=*C*H-N), 137.0 (N-*C*H=N).

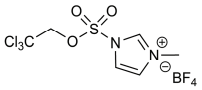

2,2,2-trichloroethyl methylimidazoliumsulfate tetrafluoroborate salt 3: Meerweins reagent (6.6 g, 45 mmol) was added to a solution of **2** (14.2 g, 45 mmol) in dry DCM (100 mL). The resulting suspension was stirred for 16 hours after which it was concentrated *in vacuo*. The residue was triturated in cold THF (30 mL) and the filtrate was dried under vacuum, which yielded the product (16.3 g, 87 %) as a white solid. R_f (MeOH/DCM, 1:9, v/v): 0.41. ^{1}H NMR (300 MHz) (DMSO): δ [ppm]: 3.94 (s, 3H, CH_3), 5.57 (s, 2H, CH_2), 8.06 (s 1H, N-CH=C*H*-N), 8.51 (s 1H, N-C*H*=CH-N), 10.11 (s, 1H, N-CH=N); ^{13}C NMR (75 MHz) (DMSO): δ [ppm]: 37.4 (CH_3), 82.2 (CH_2), 92.3 (CCl_3), 121, 126 (N-CH=CH-N), 140 (N-CH=N).

Sulfated Leu-enkephalin (9):

Fmoc-Leu-OH was attached to the ArgoGel™ Wang resin (0.40 mmol/g) (**4**) using the procedure of Sieber yielding Fmoc-Leu-ArgoGel Wang resin with a loading of 0.31 mmol/g.[40] The immobilized peptide **5** was assembled on an automatic ABI 433A Peptide Synthesizer using the ABI FastMoc 0.25 mmol protocols, except that the coupling time was 45 min. instead of 20 min.[41, 42] The synthesis was carried out on 0.81 g Fmoc-Leu preloaded resin. After cleavage of the Fmoc-group by means of a 20% piperidine solution in NMP (3 min. and 7.6 min.), the resin was washed with NMP (5 times 10 mL). Subsequently, 1 mmol of the appropriate amino acid was dissolved in NMP (2 mL), and HBTU/HOBt (1 mmol, 2.78 mL of 0.36 M in NMP) was added. To this mixture DIPEA (1 mL, 2 M in NMP) was added and the activated amino acid was then transferred to the reaction vessel. After 45 min the reaction vessel was drained and the resin was washed with NMP (3 times 10 mL) followed by acetylation of any remaining free amino groups with acetic anhydride capping solution (0.5 M Ac_2O, 0.125 M DIPEA, and 0.015 M HOBt in NMP) for 15 min. The deprotection and coupling reactions were followed by monitoring the dibenzofulvene-piperidine adduct at 301 nm.[42] An additional deprotection cycle and a double coupling of the next amino acid were carried out when the deprotection was not complete. The last coupling cycle was monitored by removal of the Fmoc-group by a 20% piperidine solution, washing the resin with NMP, and acetylation of the N-terminus by treatment with acetic anhydride capping solution for 15 min. Finally, the resin was washed with NMP (5 times 10 mL) and DCM (6 times 10 mL), removed from the reaction vessel, washed with ether, and dried *in vacuo* over P_2O_5.

Next, selective cleavage of the 2Cl-Trt protecting group from **5** was carried out by treatment of the resin 10 times 2 min. with a mixture of DCM/TFA/TIS (94/1/5, 20 mL), followed by washing of the resin with 5% TEA in DCM (two times, 20 mL) to remove all the TFA from the resin.
The thus obtained resin **6** was swollen in 8 mL of DCE and TEA (280 µL, 2 mmol) and DMAP (61 mg, 0.5 mmol) were added and shaken until complete dissolution, then 2,2,2-trichloroethyl chlorosulfate **1** (265 µL, 2 mmol) was added. After shaking overnight, the resin was washed with DCE (3 times 10 mL), and ether (3 times 10 mL), and dried *in vacuo* over P_2O_5.
The anchored peptide **8** thus obtained was deprotected and cleaved from the solid support by treatment with TFA/H_2O/TIS (95/2.5/2.5, 25 mL) for 2 h at room temperature. The mixture was then filtered and the residue washed thoroughly with TFA (2 times 10 mL). The reaction mixture was concentrated *in vacuo* to a volume of approximately 10 mL and was added dropwise to 90 mL MTBE/n-hexane (1/1, v/v) solution. The precipitate was collected by centrifugation (2000 rpm, 10 min.), the supernatant was decanted, and the pellet was resuspended in MTBE/n-hexane (1/1, v/v, 100 mL) and centrifuged again. This was repeated twice, after which the pellets were dissolved in CH_3CN/water (1/1, v/v, ca. 60 mL) and lyophilized to give 182 mg of the crude peptide **8** as a white fluffy solid.
The crude peptide **8** (70 mg) was dissolved in 4 mL buffer A, 4 mL buffer B and 2 mL TFA and purified by preparative HPLC (Jupiter C4, TFA buffers) in two runs. Fractions containing the pure product were pooled and lyophilized to give 58 mg of pure peptide **8**. The purity of peptide **8** was established by analytical HPLC (Luna C8, TFA buffers, Rt = 48.51 min., Purity >99%) and characterization was carried out by ESI-MS (monoisotopic mass $[M-H]^-$ calcd for $C_{32}H_{39}Cl_3N_5O_{11}S$, 806.14; found, 806.45).
Next 50 mg of peptide **8** was dissolved in 50 mL MeOH and 50 mL 50 mM ammonium formate, 100 mg activated zinc dust was added and the mixture was shaken for 2 h under nitrogen atmosphere. The reaction mixture was filtered, the residue was washed with MeOH and the filtrate concentrated *in vacuo* to remove MeOH, followed by lyophilization of the remaining aqueous solution to yield crude peptide **9**.
Crude peptide **9** (45 mg) was dissolved in 4 mL buffer A and purified by preparative HPLC (Jupiter C4, NH_4OAc buffers). Fractions containing the pure product were pooled and lyophilized to give 38 mg (63%) of pure peptide **9**. The purity of peptide **9** was established by analytical HPLC (Luna C8, TFA buffers, Rt = 29.99 min., Purity >99%) and characterization was carried out by high resolution ESI-TOF (monoisotopic mass $[M+H]^+$ calcd for $C_{30}H_{40}N_5O_{11}S$, 678.2445; found, 678.2456).

$C5aR_{10\text{-}18}S_2$ (14):
Disulfated peptide **14** was synthesized on Tentagel™ S RAM resin (**10**) (0.23 mmol/g) following the same procedure as described for peptide **9** on a 0.25 mmol scale (1.09 g resin). The resin with the protected peptide attached (**11**) was treated 4 times 2 min. with a mixture of DCM/TFA/TIS (94/1/5, 20 mL) to remove the 2-Cl Trt groups, followed by washing of the resin with 5% TEA in DCM (2 times, 20 mL).

The thus obtained resin (**12**) was swollen in 8 mL of DCE, TEA (346 µL, 2.5 mmol) and DMAP (61 mg, 0.5 mmol) were added and shaken until complete dissolution, then 2,2,2-trichloroethyl chlorosulfate **1** (333 µL, 2.5 mmol) was added. After shaking overnight, the resin was washed with DCE (3 times 10 mL), and ether (3 times 10 mL), and dried *in vacuo* over P_2O_5. The peptide thus obtained was deprotected and cleaved from the solid support as described for peptide **9**, which resulted in 336 mg crude peptide.

Crude peptide (150 mg) was dissolved in 10 mL buffer A and 5 mL buffer B and purified by preparative HPLC (Adsorbosphere C8, TFA buffers) in three runs. Fractions containing the pure product were pooled and lyophilized to give 22 mg of pure peptide **13**. The purity of peptide **13** was established by analytical HPLC (adsorbosphere C8, TFA buffers, Rt = 29.3 min., Purity >99%) and characterization was carried out by ESI-MS (monoisotopic mass $[M+2H]^{2+}$ calcd for $C_{54}H_{67}Cl_6N_{13}O_{26}S_2$: 794.60; found: 794.65).

Next, 21.4 mg of peptide **13** was dissolved in MeOH (15 mL) and 50 mM ammonium formate (15 mL), 100 mg activated zinc dust was added and the mixture was stirred for 3 h under nitrogen atmosphere. The reaction mixture was filtered, the residue was washed with MeOH and the filtrate concentrated *in vacuo* to remove MeOH, followed by lyophilization of the remaining aqueous solution to yield crude peptide **14**. Crude peptide **14** was dissolved in 4 mL buffer A and purified by preparative HPLC (Adsorbosphere C8, NH_4OAc buffers). Fractions containing the pure product were pooled and lyophilized to give 6 mg (4%) of pure peptide **14**. The purity of peptide **14** was established by analytical HPLC (Gemini C18, TFA buffers, Rt = 14.58 min., Purity >99%) and characterization was carried out by ESI-TOF (monoisotopic mass $[M+2H]^{2+}$ calcd for $C_{50}H_{65}N_{13}O_{26}S_2$: 664.68; found: 664.72).

C5aR$_{10\text{-}24}$S$_2$ (15):

Disulfated peptide **15** was synthesized on Tentagel™ S RAM resin (**10**) (0.26 mmol/g) following the same procedure as described for peptide **9** on a 0.25 mmol scale (1.01 g resin). The resin with the protected peptide attached was treated 4 times 2 min. with a mixture of DCM/TFA/TIS (94/1/5, 20 mL) to remove the 2-Cl Trt group, followed by washing of the resin with 5% TEA in DCM (2 times, 20 mL) to remove all the TFA from the resin. The thus obtained resin was swollen in 8 mL of DCM, TEA (570 µL, 4 mmol) and DMAP (122 mg, 1 mmol) were added and shaken until complete dissolution, then 2,2,2-trichloroethyl chlorosulfate **1** (533 µL, 4 mmol) was added. After shaking overnight, the resin was washed with DCM (3 times 10 mL), and ether (3 times 10 mL), and dried *in vacuo* over P_2O_5. The peptide thus obtained was deprotected and cleaved from the solid support as described for peptide **9**, which resulted in 491 mg crude peptide.

Crude peptide (400 mg) was dissolved in 20 mL buffer A and 15 mL buffer B and purified by preparative HPLC (Alltima C8, TFA buffers) in seven runs. Fractions containing the pure product were pooled and lyophilized to give 147 mg of pure peptide. The purity of this peptide was established by analytical HPLC (adsorbosphere C8, TFA buffers, Rt = 39.75 min., Purity >99%) and

characterization was carried out by ESI-MS (monoisotopic mass $[M+2H]^{2+}$ calcd for $C_{82}H_{114}Cl_6N_{20}O_{37}S_2$: 1123.26; found: 1123.20).
Next, 30 mg of this peptide was dissolved in MeOH (25 mL) and 50 mM ammonium formate (25 mL), 100 mg activated zinc dust was added and the mixture was stirred for 2 h under nitrogen atmosphere. The reaction mixture was filtered, the residue was washed with MeOH and the filtrate concentrated *in vacuo* to remove MeOH, followed by lyophilization of the remaining aqueous solution to yield crude peptide **15**.
Crude peptide **15** was dissolved in 4 mL buffer A and purified by preparative HPLC (Adsorbosphere C8, NH_4OAc buffers). Fractions containing the pure product were pooled and lyophilized to give 9 mg (11%) of pure peptide **15**. The purity of peptide **15** was established by analytical HPLC (Gemini C18, TFA buffers, Rt = 21.35 min., Purity >99%) and characterization was carried out by ESI-TOF (monoisotopic mass $[M+2H]^{2+}$ calcd for $C_{78}H_{112}N_{20}O_{37}S_2$: 993.35; found: 993.35).

C5aR$_{1\text{-}35}$S$_2$ (16):
Disulfated peptide **16** was synthesized on Tentagel™ S RAM resin (**10**) (0.26 mmol/g) following the same procedure as described for peptide **9** on a 0.25 mmol scale (1.01 g resin). The resin with the protected peptide attached was treated 4 times 2 min. with a mixture of DCM/TFA/TIS (94/1/5, 20 mL) to remove the 2-Cl Trt group, followed by washing of the resin with 5% TEA in DCM (2 times, 20 mL) to remove all the TFA from the resin.
The thus obtained resin was swollen in 8 mL of DCM, TEA (570 µL, 4 mmol) and DMAP (122 mg, 1 mmol) were added and shaken until complete dissolution, then 2,2,2-trichloroethyl chlorosulfate **1** (533 µL, 4 mmol) was added. After shaking overnight, the resin was washed with DCM (3 times 10 mL), and ether (3 times 10 mL), and dried *in vacuo* over P_2O_5. The peptide thus obtained was deprotected and cleaved from the solid support as described for peptide **9**, which resulted in 876 mg crude peptide. Crude peptide (400 mg) was dissolved in 20 mL buffer A and 15 mL buffer B and purified by preparative HPLC (Alltima C8, TFA buffers) in seven runs. Fractions containing the pure product were pooled and lyophilized to give 150 mg of pure peptide. The purity of this peptide was established by analytical HPLC (Adsorbosphere C8, TFA buffers, Rt = 38.75 min., Purity >95%) and characterization was carried out by ESI-MS (most abundant mass $[M+3H]^{3+}$ calcd for $C_{181}H_{269}Cl_6N_{47}O_{69}S_3$: 1506.21; found: 1505.85).
Next, 35 mg of this peptide was dissolved in MeOH (25 mL) and 50 mM ammonium formate (25 mL), 100 mg activated zinc dust was added and the mixture was stirred for 2 h under nitrogen atmosphere. The reaction mixture was filtered, the residue was washed with MeOH and the filtrate concentrated *in vacuo* to remove MeOH, followed by lyophilization of the remaining aqueous solution to yield crude peptide **16**. The crude peptide **16** was dissolved in 4 mL buffer A and purified by preparative HPLC (Adsorbosphere C8, NH_4OAc buffers). Fractions containing the pure product were pooled and lyophilized to give 8 mg (7%) of pure peptide **16**. The purity of peptide **16** was established by analytical HPLC (Gemini C18, TFA buffers, Rt = 25.86 min., Purity >99%) and

characterization was carried out by ESI-TOF (average mass $[M+2H]^{2+}$ calcd for $C_{177}H_{267}N_{47}O_{69}S_3$: 2127.78; found: 2127.74).

C5aR$_{10-18}$ (17):

Peptide **17** was synthesized on Tentagel™ S RAM resin (**10**) (0.23 mmol/g) following the same procedure as described for peptide **9** on a 0.25 mmol scale (1.11 g resin). After the automated synthesis the peptide was deprotected and cleaved from the solid support by treatment with TFA/H_2O/TIS (95/2.5/2.5, 25 mL), for 2 h at room temperature resulting in 256 mg crude peptide **17**. The crude peptide (250 mg) was dissolved in 30 mL buffer A and purified by preparative HPLC (Adsorbosphere C8, TFA buffers) in six runs. Fractions containing the pure product were pooled and lyophilized to give 178 mg (62%) of pure peptide **17**. The purity of peptide **17** was established by analytical HPLC (Adsorbosphere C8, TFA buffers, Rt = 15.47 min., Purity >99%) and characterization was carried out by ESI-MS (monoisotopic mass $[M+2H]^{2+}$ calcd for $C_{50}H_{65}N_{13}O_{20}$: 584.73; found: 584.86).

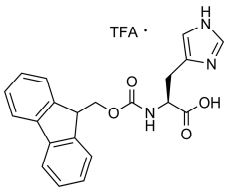

Fmoc-His-OH . TFA

Fmoc-His(Trt)-OH (12.4 g, 20mmol) was dissolved in DCM (400 mL) containing 10% TFA (40 mL), TIS (4.1 mL, 20 mmol) and H_2O (0.36 mL, 20 mmol). The mixture was stirred at rt for 2 hours after which it was concentrated *in vacuo*. The residue was triturated by hot EtOAc yielding the product as a white solid. Yield: 8.74 g (89%) ^{1}H NMR (300 MHz) (DMSO): δ [ppm]: 2.97-3.05 (m, 1H, $C_\beta H$), 3.13-3.20 (m, 1H, $C_\beta H$), 4.18-4.38 (m, 4H, $C_\alpha H$, CH-CH_2(Fmoc)), 7.29-7.45 (m, 5H, Fmoc, im.-H), 7.65 (d, J = 7.4 Hz, 2H, Fmoc), 7.84 (d, J = 8.3 Hz, 1H, Fmoc-NH), 7.90 (d, J = 7.4, 2H, Fmoc), 8.98 (s, 1H, im.-H); ^{13}C NMR (75 MHz) ($CDCl_3$): δ [ppm]: 26.1 (Cβ), 46.5 (CH-Fmoc), 52.9 (Cα), 65.6 (CH_2-Fmoc), 120.1, 125.1, 127.0, 127.6 (Ar-Fmoc), 128.3, 129.0 (CH-im), 129.7 (C-im), 140.6, 143.7 (C-Fmoc), 155.9 (C(O)NH), 172.2 (C(O)OH).

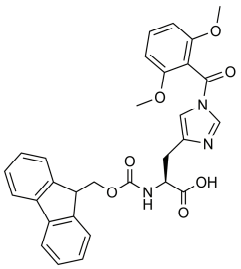

Fmoc-His(Dmbz)-OH (20)

Fmoc-His(Dmbz)-OH was synthesized following a slightly modified procedure as was described by Zaramella et al.[34] Fmoc-His-OH.TFA (4.91 g, 10 mmol) was dissolved in DMA (75 mL), cooled to 0 °C (ice/water) and DIPEA (4.96 mL, 30 mmol) was added. 2,6-Dimethoxybenzoylchloride was dissolved in DMA (30 mL) and the solution was added dropwise to the cooled reaction mixture. The mixture was stirred for 30 min. at 0 °C and overnight at rt. Then, the reaction mixture was concentrated in vacuo, the residue was dissolved in EtOAc (200 mL), the organic layer was washed with 1N $KHSO_4$ (200 mL), water (200 mL), brine (200 mL), dried with Na_2SO_4 and concentrated *in vacuo*. The resulting crude product was purified by column chromatography with 1%

AcOH in EtOAc as eluent yielding compound **20** as a white solid. Yield: 4.91 g (91%). ^{1}H NMR (300 MHz) (DMSO): δ [ppm]: 2.96 (dd, J´ = 14.8 Hz, J´´ = 10.3 Hz) 1H, $C_{\beta}H$), 3.06-3.09 (m, 1H, $C_{\beta}H$), 3.71 (s, 6H, OMe), 4.21-4.39 (m, 4H, $C_{\alpha}H$, CH-CH_2(Fmoc)), 6,82 (d, J = 8.5 Hz, 2H, Ar-H), 7.30-7.34 (m, 2H, Ar-Fmoc), 7.41 (m, 2H, Ar-Fmoc), 7.50-7.54 (m, 2H, Ar-H + im.-H), 7.68-7.69 (m, 2H, Ar-Fmoc), 7.76 (d, J = 8.0 Hz, 1H, im.-H), 7.88 (d, J = 7.4 Hz, 2H, Ar-Fmoc); ^{13}C NMR (75 MHz) ($CDCl_3$): δ [ppm]: 29.6 (Cβ), 46.6 (CH-Fmoc), 53.4 (Cα), 56.1 (O-CH_3), 65.7 (CH_2-Fmoc), 104.5 (CH-dmbz), 111.0 (C(O)-C), 120.1, 125.3, 127.1, 127.7 (Ar-Fmoc), 133.0 (CH-dmbz), 140.4 (C-im), 140.7, 143.8 (C-Fmoc), 156.0 (C(O)NH), 157.1 (*C*-O-CH_3), 162.7 (C(O)N), 173.3 (C(O)OH).

Sulfated Ac-FYHF-NH_2 (35):

Ac-FY($SO_3^-NH_4^+$)HF-NH_2 (**35**) was synthesized by manual SPPS on Tentagel™ S RAM resin (**10)** (0,24 mmol/g) on a 0.5 mmol scale (Fig 2.12). The tyrosine residue was introduced using Fmoc-Tyr(2Cl-Trt)-OH, the histidine residue was introduced using Fmoc-His(Dmbz)-OH (**20**). Mixing was performed by bubbling with nitrogen gas. After cleavage of the Fmoc-group by means of a 20% piperidine solution in NMP (3 times 8 min., 10 mL), the resin was washed with NMP (3 times 10 mL), diethyl ether (2 times 10 mL) and DCM (3 times 10 mL) after which a Kaisertest was performed to confirm the deprotection.[43] Next the resin was washed with NMP (3 times 10 mL) and a solution of 2 mmol of the appropriate amino acid, HBTU, HOBt and 4 mmol of DIPEA in 8 mL of NMP was added and mixed for 90 min. Next, the resin was washed and subjected to the kaisertest to confirm complete coupling. The last coupling cycle was followed by removal of the Fmoc-group by 20 % piperidine in NMP, washing the resin with NMP, and acetylation of the N-terminus by treatment with an acetic anhydride capping solution (0.5 M Ac_2O, 0.125 M DIPEA, and 0.015 M HOBt in 10 mL NMP) for 30 min. Finally, resin **30** was washed with NMP (5 times 10 mL) and DCM (6 times 10 mL), removed from the reaction vessel, washed with ether, and dried *in vacuo*.

Resin **30** (400 mg) was subjected to selective deprotection of the tyrosine residues by treatment with with 10 mL of a mixture of DCM/TFA/TIS (94/1/5) 10 times 2 min. and twice washing with 5 % TEA in 10 mL DCM. The thus obtained resin **31** was swollen in 8 mL of DCE, TEA (222 µL, 1.6 mmol) and DMAP (49 mg, 0.4 mmol) were added and shaken until complete dissolution, then 2,2,2-trichloroethyl chlorosulfate **1** (213 µL, 1.6 mmol) was added. After shaking for 16h, resin **32** was washed with DCE (3 times 10 mL), and ether (3 times 10 mL), and dried *in vacuo*. Deprotection and cleavage of peptide **33** from the solid support was performed as described for peptide **9** and yielded 74 mg peptide. After lyophilization, the purity of peptide **33** was established by analytical HPLC (Adsorbosphere C8, TFA buffers, Rt = 48.73 min., purity >90%) and characterization was carried out by ESI-MS (monoisotopic mass $[M+H]^+$ calcd for $C_{46}H_{48}N_7O_{12}S$, 1028.21; found, 1028.10).

25 mg of peptide **33** was dissolved in 5 mL MeOH and 5 mL 50 mM ammonium formate, 25 mg activated zinc power was added and the mixture was stirred for 2 h under nitrogen atmosphere. The reaction mixture was filtered, the residue was washed with MeOH/H_2O (1/1, v/v) and the filtrate

concentrated *in vacuo* to remove MeOH, followed by lyophilization of the remaining aqueous solution to give crude peptide **34**.

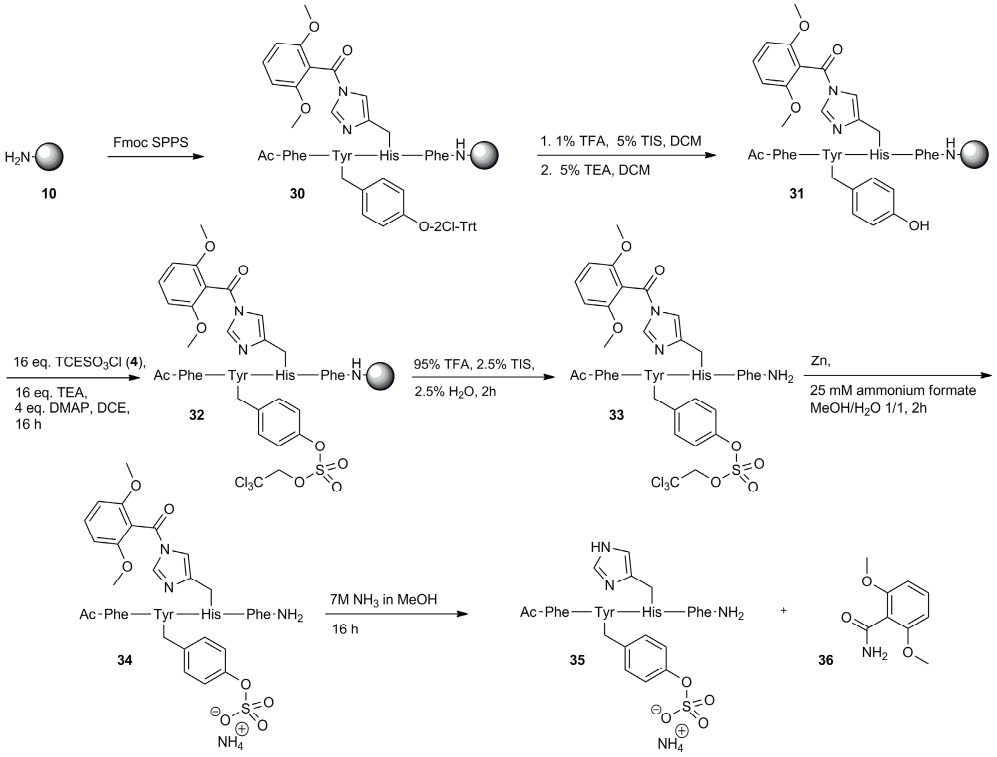

Scheme 2.12 Solid phase synthesis of sulfated testpeptide Ac-FYHF-NH_2 (**35**).

Crude peptide **34** (25 mg) was dissolved in 4 mL buffer A and purified by preparative HPLC (Adsorbosphere C8, NH_4OAc buffers). Fractions containing the pure product were pooled and lyophilized to give 21 mg of pure peptide **34**. The purity of peptide **34** was established by analytical HPLC (Adsorbosphere C8, TFA buffers, Rt = 32.27 min., Purity >95%).

4 mg of peptide **34** was dissolved in 10 mL 7 M NH_3 in MeOH and mixed for 16 hours. After concentration *in vacuo* the peptide was dissolved in 4 mL CH_3CN/H_2O (1/1, v/v) and lyophilized to give 4 mg (82%) of the crude peptide **35** as a white fluffy solid. The purity of peptide **35** was established by analytical HPLC (Adsorbosphere C8, TFA buffers, Rt = 24.87 min., Purity >75%) and characterization was carried out by ESI-MS (monoisotopic mass $[M+H]^+$ calcd for $C_{35}H_{39}N_7O_9S$, 734.25; found, 734.36). The peak at Rt = 10.48 min. was characterized with ESI-MS (monoisotopic mass $[M+H]^+$ calcd for $C_9H_{11}O_3$, 182.07; found 182.05) and appeared to be the removed protecting group 2,6-dimethoxybenzoyl amide **36** (Fig. 2.9)

C5aR$_{7\text{-}28}$S$_2$ (25):

Disulfated peptide **25** was assembled on an automatic ABI 433A Peptide Synthesizer on Tentagel™ S RAM resin (0,25 mmol/g) (**10)** on a 0.25 mmol scale as described for peptide **9**. Tyrosine residues 11 and 14 were introduced using Fmoc-Tyr(2Cl-Trt)-OH, histidine 13 was introduced using Fmoc-His(Dmbz)-OH (**20**).

After selective cleavage of the 2Cl-Trt protecting groups, as was described earlier, the resin was swollen in 8 mL DCE. TEA (554 µL, 4 mmol) and DMAP (122 mg, 1 mmol) were added and shaken until complete dissolution, then 2,2,2-trichloroethyl chlorosulfate **1** (533 µL, 4 mmol) was added. After shaking overnight, the resin was washed with DCM (3 times 10 mL), and ether (3 times 10 mL), and dried *in vacuo.* Deprotection and cleavage of the peptide from the solid support **23**, was performed as described above. After lyophilization crude peptide **24** (680 mg) was obtained as a white fluffy solid. The crude peptide (300 mg) was dissolved in 12 mL buffer A, 12 mL buffer B and 6 mL TFA and purified by preparative HPLC (Alltima C8, TFA buffers) in six runs. Fractions containing the pure product were pooled and lyophilized to give 85 mg of pure peptide **24**. The purity of peptide **24** was established by analytical HPLC (Gemini C18, TFA buffers, Rt = 39.58 min., Purity >95%) and characterization was carried out by ESI-TOF (monoisotopic mass $[M+2H]^{2+}$ calcd for $C_{124}H_{176}Cl_6N_{28}O_{51}S_2$, 1574.48; found, 1574.78).

Next 80 mg of peptide **24** was dissolved in 40 mL MeOH and 40 mL 50 mM ammonium formate, 160 mg activated zinc dust was added and the mixture was stirred for 2 h under nitrogen atmosphere. Next the reaction mixture was filtered, the residue washed with MeOH/H_2O (1/1, v/v), the filtrate concentrated *in vacuo* to remove MeOH and the remaining aqueous solution was lyophilized to give the crude peptide. This peptide was dissolved in 40 mL 7 M NH_3 in MeOH and stirred for 16 hours. After concentration *in vacuo* the residue was dissolved in 30 mL CH_3CN/H_2O (1/1, v/v) and lyophilized. The thus obtained peptide was dissolved in 5 mL buffer A and purified by preparative HPLC (Gemini C18, NH_4OAc buffers). Fractions containing the pure product were pooled and lyophilized to give 13 mg (5%) of pure peptide **25**. The purity of peptide **25** was established by analytical HPLC (Gemini C18, TFA buffers, Rt = 21.52 min., Purity >98%) and characterization was carried out by ESI-TOF (monoisotopic mass $[M+2H]^{2+}$ calcd for $C_{111}H_{166}N_{28}O_{48}S_2$, 1362.5504; found, 1362.4146).

C5aR$_{7\text{-}28}$S^{11} (26):

Sulfated peptide **26** was assembled on an automatic ABI 433A Peptide Synthesizer on Tentagel® S RAM resin (0,25 mmol/g) **10** on a 0.25 mmol scale as was described for peptide **9**. Tyrosine residue 11 was introduced using Fmoc-Tyr(2Cl-Trt)-OH, histidine residue 13 was introduced usings Fmoc-His(Dmbz)-OH (**20**).

After selective cleavage of the 2Cl-Trt protecting group, as was described earlier, the resin was swollen in 8 mL DCE. TEA (285 µL, 2 mmol) and DMAP (61 mg, 0.5 mmol) were added and shaken until complete dissolution, then 2,2,2-trichloroethyl chlorosulfate **1** (267 µL, 2 mmol) was added. After shaking overnight, the resin was washed with DCM (3 times 10 mL), and ether (3 times 10

mL), and dried *in vacuo*. Deprotection and cleavage of the peptide from the solid support was performed as described for peptide **9**. After lyophilization crude peptide (667 mg) was obtained as a white fluffy solid. The crude peptide (450 mg) was dissolved in 27 mL buffer A, 9 mL buffer B and 9 mL TFA and purified by preparative HPLC (Alltima C8, TFA buffers) in nine runs. Fractions containing the pure product were pooled and lyophilized to give 150 mg of pure peptide. The purity of this peptide was established by analytical HPLC (Gemini C18, TFA buffers, Rt = 33.87 min., Purity >98%) and characterization was carried out by ESI-TOF (monoisotopic mass $[M+2H]^{2+}$ calcd for $C_{122}H_{175}Cl_3N_{28}O_{48}S$, 1469.55; found, 1469.84).

Next, 145 mg of this protected peptide was dissolved in 50 mL MeOH and 50 mL of 50 mM ammonium formate, 200 mg of activated zinc dust was added and the mixture was stirred for 2h under nitrogen atmosphere. Next the reaction mixture was filtered, the residue washed with MeOH/H_2O (1/1, v/v), the filtrate concentrated *in vacuo* to remove MeOH and the remaining aqueous solution was lyophilized to obtain the crude peptide. This crude peptide was dissolved in 40 mL 7 M NH_3 in MeOH and stirred for 16 hours. After concentration *in vacuo* the residue was dissolved in 40 mL CH_3CN/H_2O (1/1, v/v) and lyophilized. The thus obtained peptide was dissolved in 15 mL buffer A and purified by preparative HPLC (Gemini C18, NH_4OAc buffers). Fractions containing the pure product were pooled and lyophilized to give 83 mg (19%) of pure peptide **26**. The purity of peptide **26** was established by analytical HPLC (Gemini C18, TFA buffers, Rt = 21.66 min., Purity >99%)) and characterization was carried out by ESI-TOF (monoisotopic mass $[M+2H]^{2+}$ calcd for $C_{111}H_{166}N_{28}O_{45}S$, 1322.565; found, 1322.679).

$C5aR_{7\text{-}28}S^{14}$ (27):

Sulfated peptide **27** was assembled on an automatic ABI 433A Peptide Synthesizer on Tentagel™ S RAM resin (0.25 mmol/g) **10** on a 0.25 mmol scale as described for peptide **9.** Tyrosine residue 14 was introduced using Fmoc-Tyr(2Cl-Trt)-OH, histidine residue 13 was introduced using Fmoc-His(Dmbz)-OH (**20**).

After selective cleavage of the 2Cl-Trt protecting group, as was described earlier, the resin was swollen in 8 mL DCE. TEA (285 µL, 2 mmol) and DMAP (61 mg, 0.5 mmol) were added and shaken until complete dissolution, then 2,2,2-trichloroethyl chlorosulfate **1** (267 µL, 2 mmol) was added. After shaking overnight, the resin was washed with DCM (3 times 10 mL), and ether (3 times 10 mL), and dried *in vacuo*. Deprotection and cleavage of the peptide from the solid support, was performed as described above. After lyophilization crude peptide (659 mg) was obtained as a white fluffy solid. Part of the crude peptide (100 mg) was dissolved in 6 mL buffer A, 2 mL buffer B and 2 mL TFA and purified by preparative HPLC (Alltima C8, TFA buffers) in two runs. Fractions containing the pure product were pooled and lyophilized to give 32 mg of pure peptide. The purity of this peptide was established by analytical HPLC (Gemini C18, TFA buffers, Rt = 33.28 min., Purity >95%)) and characterization was carried out by ESI-TOF (monoisotopic mass $[M+2H]^{2+}$ calcd for $C_{122}H_{175}Cl_3N_{28}O_{48}S$, 1469.55; found, 1469.81).

Next, the protected peptide was dissolved in 20 mL MeOH and 20 mL of 50 mM ammonium formate, 50 mg of activated zinc dust was added and the mixture was stirred for 2h under nitrogen atmosphere. Then, the reaction mixture was filtered, the residue was washed with MeOH/H_2O (1/1, v/v) and the filtrate was concentrated *in vacuo* to remove MeOH, followed by lyophilization of the remaining aqueous solution to give the crude peptide. This crude peptide was dissolved in 20 mL 7 M NH_3 in MeOH and stirred for 16 hours. After concentration *in vacuo* the residue was dissolved in 20 mL CH_3CN/H_2O (1/1, v/v) and lyophilized. The thus obtained peptide was dissolved in 5 mL buffer A and purified by preparative HPLC (Gemini C18, NH_4OAc buffers). Fractions containing the pure product were pooled and lyophilized to give 13 mg (13%) of pure peptide **27**. The purity of peptide **27** was established by analytical HPLC (Gemini C18, TFA buffers, Rt = 22.04 min., Purity >95%)) and characterization was carried out by ESI-TOF (monoisotopic mass $[M+3H]^{3+}$ calcd for $C_{111}H_{166}N_{28}O_{45}S$, 882.04; found, 882.18).

C5aR$_{7\text{-}28}$ (28):

Peptide **28** was assembled on an automatic ABI 433A Peptide Synthesizer on Tentagel™ S RAM resin (0.25 mmol/g) (**10**) on a 0.25 mmol scale as was described for peptide **9**. The last coupling cycle was followed by removal of the Fmoc-group by a 20 % piperidine solution, washing the resin with NMP, and acetylation of the N-terminus by treatment with an acetic anhydride capping solution (0.5 M Ac_2O, 0.125 M DIPEA, and 0.015 M HOBt in NMP) for 30 min. Finally, the resin was washed with NMP (5 times 10 mL) and DCM (6 times 10 mL), removed from the reaction vessel, washed with ether, and dried *in vacuo*. The anchored peptide was cleaved and deprotected as described for peptide **9** yielding 550 mg of the crude peptide. Crude peptide (150 mg) was dissolved in 15 mL buffer A and purified by preparative HPLC (Alltima C8, TFA buffers) in three runs. Fractions containing the pure product were pooled and lyophilized to yield 74 mg (42%) pure C5aR$_{7\text{-}28}$ **28**. The purity of peptide **28** was established by analytical HPLC (Gemini C18, TFA buffers, Rt = 21.38 min., Purity >99%) and characterization was carried out by ESI-TOF (monoisotopic mass $[M+2H]^{2+}$ calcd for $C_{111}H_{166}N_{28}O_{42}$, 1282.59; found, 1282.50).

C5aR$_{7\text{-}28}$S$_2$-βAGC-NH$_2$ (29):

Disulfated peptide **29** was assembled on an automatic ABI 433A Peptide Synthesizer on Tentagel™ S RAM resin (0.25 mmol/g) **10** on a 0.25 mmol scale as was described for peptide **9.** Tyrosine residue 11 and 14 were introduced using Fmoc-Tyr(2Cl-Trt)-OH, histidine residue 13 was introduced using Fmoc-His(Dmbz)-OH (**20**).

After selective cleavage of the 2Cl-Trt protecting group, as was described earlier, the resin was swollen in 8 mL DCE. TEA (570 µL, 4 mmol) and DMAP (122 mg, 1 mmol) were added and shaken until complete dissolution, then 2,2,2-trichloroethyl chlorosulfate **1** (533 µL, 4 mmol) was added. After shaking overnight, the resin was washed with DCM (3 times 10 mL), and ether (3 times 10 mL), and dried *in vacuo.* Deprotection and cleavage of the peptide from the solid support, was performed as was described above. After lyophilization crude peptide (660 mg) was obtained as a

white fluffy solid. The crude peptide (300 mg) was dissolved in 25 mL buffer A and 5 mL buffer B and purified by preparative HPLC (Gemini C18, TFA buffers) in six runs. Fractions containing the pure product were pooled and lyophilized to give 64 mg of pure peptide.

Next, this protected peptide was dissolved in 25 mL MeOH and 25 mL of 50 mM ammonium formate, 150 mg of activated zinc dust was added and the mixture was stirred for 2h under nitrogen atmosphere. Next the reaction mixture was filtered, the residue washed with MeOH/H_2O (1/1, v/v), the filtrate concentrated *in vacuo* to remove MeOH and the remaining aqueous solution was lyophilized to give the crude peptide. This crude peptide was dissolved in 25 mL 7 M NH_3 in MeOH and stirred for 16 hours. After concentration *in vacuo* the residue was dissolved in 5 mL CH_3CN/H_2O (1/1, v/v) and lyophilized. The thus obtained peptide was dissolved in 5 mL 25 mM NH_4OAc containing DTT (12.8 mg, 5 eq.) and EDTA (24.4 mg, 5 eq.) brought to pH 8.5 and flushed with nitrogen. After 2 hours the peptide was purified by preparative HPLC (Gemini C18, NH_4OAc buffers). Fractions containing the pure product were pooled and lyophilized to give 13 mg (4%) of pure peptide **29**. The purity of peptide **29** was established by analytical HPLC (Gemini C18, NH_4OAc buffers, Rt = 21.84 min., Purity >95%)) and characterization was carried out by ESI-TOF (monoisotopic mass $[M+3H]^{3+}$ calcd for $C_{119}H_{179}N_{31}O_{51}S_3$, 985.72; found, 985.91).

NMR assignments of the receptor mimics 25-28.

NMR samples of the receptor mimics were prepared in 9/1 (v/v) H_2O/D_2O sodium phosphate buffers (20 mM, pH 6.2 or 6.5) to peptide concentrations of 1 mM. Sequential ^1H NMR assignments were performed following standard 2D NMR strategies, using a combination of 2D NOESY and 2D TOCSY spectra.[44] All spectra were recorded on a Varian Inova 500 spectrometer at 6 ^oC. Mixing times were set to 60 ms for TOCSY spectra and 400 ms for NOESY spectra. Additional ^{13}C assignments were derived from gradient enhanced ^{13}C-^1H HSQC heteronuclear correlation spectra, using known proton assignments of amino acids.[45, 46]

2.5 References

[1] W. B. Huttner, Sulphation of tyrosine residues - a widespread modification of proteins, *Nature* **1982**, *299*, 273.

[2] W. B. Huttner, Protein tyrosine sulfation, *Trends Biochem. Sci.* **1987**, *12*, 361.

[3] W. B. Huttner, Tyrosine sulfation and the secretory pathway, *Annu. Rev. Physiol.* **1988**, *50*, 363.

[4] J. W. Kehoe, C. R. Bertozzi, Tyrosine sulfation: a modulator of extracellular protein-protein interactions, *Chem. Biol.* **2000**, *7*, R57.

[5] K. L. Moore, The biology and enzymology of protein tyrosine *O*-sulfation, *J. Biol. Chem.* **2003**, *278*, 24243.

[6] A. S. Woods, H. Y. J. Wang, S. N. Jackson, Sulfation, the up-and-coming post-translational modification: Its role and mechanism in protein-protein interaction, *J. Proteome Res.* **2007**, *6*, 1176.

[7] C. Seibert, T. P. Sakmar, Toward a framework for sulfoproteomics: Synthesis and characterization of sulfotyrosine-containing peptides, *Biopolymers* **2008**, *90*, 459.

[8] M. J. Stone, S. Chuang, X. Hou, M. Shoham, J. Z. Zhu, Tyrosine sulfation: an increasingly recognised post-translational modification of secreted proteins, *New. Biotech.* **2009**, *25*, 299.

[9] P. A. Baeuerle, W. B. Huttner, Tyrosine sulfation of yolk proteins 1, 2, and 3 in *Drosophila melanogaster*, *J. Biol. Chem.* **1985**, *260*, 6434.

[10] J. L. Kice, J. M. Anderson, The mechanism of the acid hydrolysis of sodium aryl sulfates, *J. Am. Chem. Soc.* **1966**, *88*, 5242.

[11] D. Balsved, J. R. Bundgaard, J. W. Sen, Stability of tyrosine sulfate in acidic solutions, *Anal. Biochem.* **2007**, *363*, 70.

[12] T. Yagami, K. Kitagawa, C. Aida, H. Fujiwara, S. Futaki, Stabilization of a tyrosine *O*-sulfate residue by a cationic functional group: formation of a conjugate acid-base pair, *J. Pept. Res.* **2000**, *56*, 239.

[13] M. Farzan, C. E. Schnitzler, N. Vasilieva, D. Leung, J. Kuhn, C. Gerard, N. P. Gerard, H. Choe, Sulfated tyrosines contribute to the formation of the C5a docking site of the human C5a anaphylatoxin receptor, *J. Exp. Med.* **2001**, *193*, 1059.

[14] B. Postma, W. Kleibeuker, M. J. J. G. Poppelier, M. Boonstra, K. P. M. Van Kessel, J. A. G. Van Strijp, C. J. C. de Haas, Residues 10-18 within the C5a receptor N-terminus compose a binding domain for chemotaxis inhibitory protein of *Staphylococcus aureus*, *J. Biol. Chem.* **2005**, *280*, 2020.

[15] J. H. Ippel, C. J. C. De Haas, A. Bunschoten, J. A. G. van Strijp, J. A. W. Kruijtzer, R. M. J. Liskamp, J. Kemmink, Structure of the tyrosine-sulfated C5a-receptor N-terminus in complex with chemotaxis inhibitory protein of Staphylococcus aureus, *J. Biol. Chem.* **2009**, *284*, 12363.

[16] H. J. Musiol, A. Escherich, L. Moroder, in *Methods of Organic Chemistry, Vol. E22b* (Eds.: M. Goodman, F. A., L. Moroder, C. Toniolo), Houben-Weyl, **2003**, pp. 425.

[17] T. Young, L. L. Kiessling, A strategy for the synthesis of sulfated peptides, *Angew. Chem. Int. Ed.* **2002**, *41*, 3449.

[18] K. Kitagawa, C. Aida, H. Fujiwara, T. Yagami, S. Futaki, M. Kogire, J. Ida, K. Inoue, Facile solid-phase synthesis of sulfated tyrosine-containing peptides: Total synthesis of human big gastrin-II and cholecystokinin (CCK)-39(1,2), *J. Org. Chem.* **2001**, *66*, 1.

[19] M. Ueki, S. Watanabe, R. Yamanaka, M. Ohta, O. Okunaka, in *Japanese Peptide Symposium, Vol. 36*, Japanese Peptide Society, **1999**, pp. 117.

[20] A. M. Ali, S. D. Taylor, Efficient Solid-phase synthesis of sulfotyrosine peptides using a sulfate protecting-group strategy, *Angew. Chem. Int. Ed.* **2009**, *48*, 2024.

[21] K. F. Medzihradszky, H. Medzihradszky-Schweiger, Ueber die katalytische hydrierung schwefelhaltiger peptidderivate, *Acta Chim. Hung. Tomus* **1965**, *44*, 15.

[22] H. Medzihradszky-Schweiger, Promoted hydrogenolysis of carbobenzoxyamino acids in the presence of organic bases, *Acta Chim. Hung. Tomus* **1973**, *76*, 437.

[23] A. M. Ali, S. D. Taylor, Synthesis of disulfated peptides corresponding to the N-terminus of chemokines receptors CXCR6 (CXCR61–20) andDARC (DARC8–42) using a sulfate-protecting group strategy, *J. Pept. Sci.* **2010**, *16*, 190.

[24] L. S. Simpson, T. S. Widlanski, A comprehensive approach to the synthesis of sulfate esters, *J. Am. Chem. Soc.* **2006**, *128*, 1605.

[25] L. S. Simpson, J. Z. Zhu, T. S. Widlanski, M. J. Stone, Regulation of chemokine recognition by site-specific tyrosine sulfation of receptor peptides, *Chem. Biol.* **2009**, *16*, 153.

[26] M. Hedayatullah, J. C. Leveque, L. Denivelle, Action of sulfuryl chloride on some phenols and alcohols, *C. R. Acad. Sc. Paris* **1971**, *273*, 1444.

[27] M. Hedayatullah, J. C. Leveque, L. Denivelle, Aryl and alkyl chlorosulfates and neutral sulfates. Action of sulfuryl chloride on alcohols, *C. R. Acad. Sc. Paris* **1972**, *274*, 1937.

[28] Y. Liu, I. F. F. Lien, S. Ruttgaizer, P. Dove, S. D. Taylor, Synthesis and protection of aryl sulfates using the 2,2,2-trichloroethyl moiety, *Org. Lett.* **2004**, *6*, 209.

[29] L. J. Ingram, S. D. Taylor, Introduction of 2,2,2-trichloroethyl-protected sulfates into monosaccharides with a sulfuryl imidazolium salt and application to the synthesis of sulfated carbohydrates, *Angew. Chem. Int. Ed.* **2006**, *45*, 3503.

[30] L. J. Ingram, A. Desoky, A. M. Ali, S. D. Taylor, O- and N-Sulfations of Carbohydrates Using Sulfuryl Imidazolium Salts, *J. Org. Chem.* **2009**, *74*, 6479.

[31] C. D. Unsworth, J. Hughes, J. S. Morley, *O*-sulphated Leu-enkephalin in brain, *Nature* **1982**, *295*, 519.

[32] Ranging from 16 out of 22 amino acids in $C5aR_{7\text{-}28}$ (73%) up to 8 out of 9 amino acids in $C5aR_{10\text{-}18}$ (89%).

[33] J. H. Jones, D. L. Rathbone, P. B. Wyatt, The regiospecific alkylation of histidine side chains, *Synthesis* **1987**, 1110.

[34] S. Zaramella, R. Stromberg, E. Yeheskiely, Acyl groups as prospective protection for imidazole, II. Application of N-im-2,6-dimethoxybenzoyl histidine in solid-phase peptide synthesis, *Eur. J. Org. Chem.* **2003**, 2454.

[35] S. Zaramella, P. Heinonen, E. Yeheskiely, R. Stromberg, Facile determination of the protecting group location of N-im-protected histidine derivatives by (1)-N-15 hteronuclear correlation NMR, *J. Org. Chem.* **2003**, *68*, 7521.

[36] K. Barlos, D. Gatos, O. Hatzi, N. Koch, S. Koutsogianni, Synthesis of the very acid-sensitive Fmoc-Cys(Mmt)-OH and its application in solid-phase peptide synthesis, *Int. J. Pept. Prot. Res.* **1996**, *47*, 148.

[37] A. Bunschoten, J. A. W. Kruijtzer, J. H. Ippel, C. J. C. de Haas, J. A. G. van Strijp, J. Kemmink, R. M. J. Liskamp, A general sequence independent solid phase method for the site specific synthesis of multiple sulfated-tyrosine containing peptides, *Chem. Commun.* **2009**, 2999.

[38] D. D. Perrin, W. L. F. Armarego, in *Purification of laboratory chemicals*, 3e ed., Pergamon Press, Oxford, **1988**, p. 360.

[39] E. von Arx, M. Faupel, M. Brugger, Das 4,4´-tetramethyldiamino-diphenylmethan reagens (TDM). Eine modifikation der chlor-o-tolidin farbereaktion fur die dunnschichtchromatographie, *J. Chromatogr., A* **1976**, *120*, 224.

[40] P. Sieber, An improved method for anchoring of 9-fluorenylmethoxycarbonyl-amino acids to 4-alkoxybenzyl alcohol resins, *Tetrahedron Lett.* **1987**, *28*, 6147.

[41] A. Biosystems, *Applied Biosystems Model 433A Peptide Synthesizer User´s Manual* **June 1993**, version 1.0.

[42] A. Biosystems, *Applied Biosystems Research News* **June 1993**, Model 433A Peptide Synthesizer.

[43] E. Kaiser, R. L. Colescott, C. D. Bossinger, P. I. Cook, Color test for detection of free terminal amino groups in the solid-phase synthesis of peptides, *Anal. Biochem.* **1970**, *34*, 595.

[44] G. Wagner, K. Wuthrich, Sequential Resonance Assignments in Protein lH Nuclear Magnetic Resonance Spectra Basic Pancreatic Trypsin Inhibitor, *J. Mol. Biol.* **1982**, *155*, 347.

[45] A. Bax, M. F. Summers, ´H and 13C Assignments from sensitivity-enhanced detection of heteronuclear multiple-bond connectivity by 2D multiple quantum NMR, *J. Am. Chem. Soc.* **1986**, *108*, 2093.

[46] L. E. Kay, P. Keifer, T. Saarinen, Pure absorption gradient enhanced heteronuclear single quantum correlation spectroscopy with improved sensitivity, *J. Am. Chem. Soc.* **1992**, *114*, 10663.

Chapter 3

Structure of the Tyrosine-Sulfated C5a-Receptor N-terminus in Complex with Chemotaxis Inhibitory Protein of *Staphylococcus aureus*

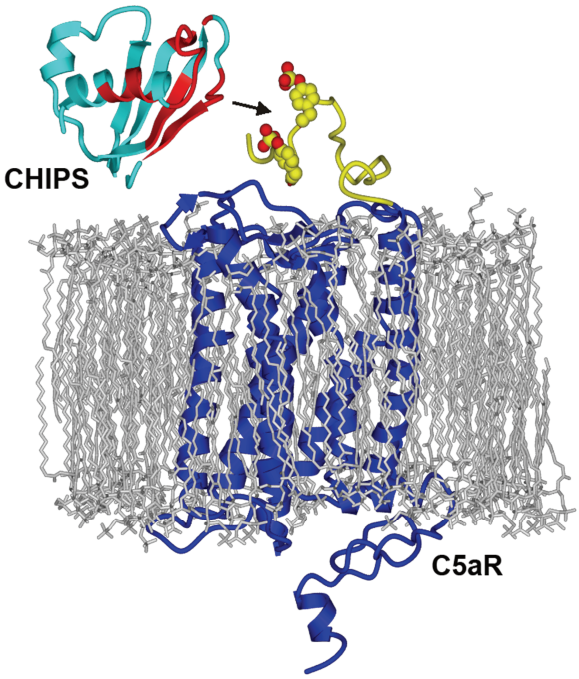

Parts of this chapter have been published:

J. H. Ippel*, C. J. C. de Haas*, A. Bunschoten*, J. A. G. van Strijp, J. A. W. Kruijtzer, R. M. J. Liskamp, J. Kemmink, *Journal of Biological Chemistry*, **2009**, *248*, 12363-12372

*) These authors contributed equally to this work

3

3.1 Introduction

The human complement system is a key component of the innate host defense directed against invading pathogens. Complement component C5a is a 74-residue glycoprotein generated via complement activation by cleavage of the α-chain of its precursor C5. C5a is a strong chemoattractant involved in the recruitment of neutrophils and monocytes, activation of phagocytes, release of granule-based enzymes, and generation of oxidants.[1, 2] C5a exerts its effect by activating the C5a-receptor (C5aR). Although the complement system is highly efficient, excessive or erroneous activation of the C5aR can have deleterious effects on host tissues. C5a has been implicated in the pathogenesis of many inflammatory and immunological diseases, including sepsis, rheumatoid arthritis, inflammatory bowel disease, immune complex disease, and reperfusion injury.[1, 3-5] Consequently, there is an active ongoing search for compounds that suppress C5a-mediated inflammatory responses.[6-8]

Chemotaxis inhibitory protein of *Staphylococcus aureus* (CHIPS) is a 121-residue protein excreted by *S. aureus*, which efficiently inhibits the activation of neutrophils and monocytes by formylated peptides and C5a.[9, 10] CHIPS specifically binds to the formylated peptide receptor (FPR) and the C5aR with nanomolar affinity (K_d = 35.4±7.7 nM and 1.1±0.2 nM, respectively), thereby suppressing the inflammatory response of the host.[11] A CHIPS fragment lacking residues 1-30* (designated $CHIPS_{31-121}$) has the same activity in blocking the C5aR compared to wild type CHIPS.[12] $CHIPS_{31-121}$ is a compact protein comprising an α-helix packed onto a four-stranded anti-parallel β-sheet.[12] C5a has an entirely different fold (PDB ID code 1KJS) and is comprised of an anti-parallel bundle of four α-helices stabilized by three disulphide bonds.[13, 14] Preliminary experiments indicated that CHIPS binds exclusively to the extracellular N-terminal portion of the C5aR.[15] In contrast, the binding of C5a by its receptor involves two separate binding sites: C5a residues located in the region between 12-46 bind to a primary binding site partly coinciding with the binding site of CHIPS,[7, 16] while the C-terminus of C5a (residues 69-74) binds to the activation domain of the C5aR located in the receptor core.[17, 18] Due to their dissimilarity in sequence and structure, the binding sites of CHIPS and C5a are not identical.[16] The present working model is that CHIPS interferes with the primary binding site of C5a located at the N-terminus of the C5aR, thereby preventing the C-terminal tail of C5a from contacting the activation domain of the C5aR and blocking downstream signaling. Currently, the development of C5aR inhibitors has been focused primarily on mimicking C5a in order to directly interrupt C5a-mediated C5aR signaling.[4, 5, 19] Understanding the interactions between CHIPS and the C5aR may provide valuable insights towards the development of a new class of C5aR antagonists.

Postma et al. proposed that residues involved in CHIPS binding are located between residues *10-18** of the C5aR.[15] Specifically, the acidic residues *D10*, *D15*, and *D18* and glycine residue *G12* appear to be critical for binding. High-affinity binding was observed between ^{125}I-labeled CHIPS and the N-terminal portion of the C5aR (residues *1-38*) expressed on the cell surface of HEK293 cells (K_d = 29.7±4.4 nM). In contrast, very moderate affinity between CHIPS and a synthetic C5aR N-terminal peptide (residues *1-37*; K_d = 40±19 μM), measured by isothermal titration calorimetry (ITC), was recently reported by Wright et al..[20] The discrepancy in the magnitude of these dissociation constants may be explained by the presence of two sulfate groups on tyrosine *11* and *14* of the C5aR N-terminus expressed on the cell surface of HEK293 cells which are absent in the synthetic C5aR peptide utilized by Wright and coworkers.[20] Farzan et al. stressed the critical role of these sulfate groups in activation of the C5aR by C5a.[21] Previous mutational studies employing FITC-labeled CHIPS, however, suggested that the sulfate groups had only a limited effect on the binding affinity.[15]

In order to resolve these discrepancies, we set out to chemically synthesize sulfated and non-sulfated peptide mimics of the N-terminus of the human C5aR (chapter 2). We have measured the binding affinities of these peptides to $CHIPS_{31-121}$ by ITC and used the C5aR mimic with the highest affinity to determine the structure of the complex between $CHIPS_{31-121}$ and the C5aR N-terminus by NMR spectroscopy.

*) Residue numbers of CHIPS are shown in regular fonts, residue numbers of the C5a-are shown in italics fonts.

Figure 3.1 Amino acid sequence of residues *1-35* of the human C5aR (numbering according to Swiss-Prot entry **P21730**). The positions of the sulfated tyrosine residues *11* and *14* are in black.

3.2 Results

Affinity of CHIPS for C5aR mimics determined by ITC

In total eight sulfated and non-sulfated peptides, serving as mimics of the N-terminus of the human C5aR (Fig. 3.1), were synthesized (Chapter 2) and their affinity to $CHIPS_{31-121}$ was measured by ITC (Table 1 and 2). The sequences of these peptides were selected based upon previous studies and preliminary NMR experiments.[15] The influence of the two sulfate groups at positions *11* and *14* was tested by comparing the non-sulfated peptides $C5aR_{10-18}$ and $C5aR_{7-28}$ with their sulfated counterparts $C5aR_{10-18}S_2$ and $C5aR_{7-28}S_2$. Clearly, the sulfate groups have a substantial influence on the binding affinity. Peptide $C5aR_{10-18}$ did not show any detectable binding, while affinity in the micromolar range was observed for sulfated peptide $C5aR_{10-18}S_2$ (K_d = 15.9±1.4 μM). Sulfation of peptide $C5aR_{7-28}$ enhanced the affinity to CHIPS even more than two orders of magnitude (Table 3.1).

Table 3.1. Thermodynamic binding parameters of $CHIPS_{31-121}$:C5aR peptide complexes determined by ITC

Peptide	K_d **(nM)**	ΔG **(kJ mol^{-1})**	ΔH **(kJ mol^{-1})**	ΔS **(J K^{-1}mol^{-1})**
$C5aR_{10-18}$	-[a]	-	-	-
$C5aR_{10-18}S_2$	(15.9±1.4)x10^3	-27.4±0.2	-41.9±3.1	-49±10
$C5aR_{10-24}S_2$[b]	24.7±0.4	-43.4±0.1	-85.4±0.3	-141±1
$C5aR_{7-28}$	(3.2±0.1)x10^3	-31.3±0.1	-78.0±2.5	-157±8
$C5aR_{7-28}S_2$	8.4±1.1	-46.1±0.3	-94.5±2.2	-162±7
$C5aR_{1-35}S_2$	27.8±5.0	-43.1±0.4	-93.8±2.2	-170±7

The data are averages from at least three independent experiments unless indicated otherwise (mean ±SEM). The errors in the thermodynamic parameters were estimated by Monte Carlo simulations using the standard deviations of the individual experiments. The average stoichiometric value n = 1.13±0.04 (the error bound represents ±SEM; n = 14). [a]No detectable binding observed in two independent experiments. [b]Data from one experiment. Error bounds represent ±SD.

The minimal sequence required for high affinity binding was further investigated by comparing the affinities of sulfated sequences *10-18*, *10-24*, *7-28*, and *1-35*, respectively (Table 3.1). Extension of peptide C5aR$_{10\text{-}18}$S$_2$ with six additional amino acids at the C-terminal side, peptide C5aR$_{10\text{-}24}$S$_2$, resulted in nanomolar binding to CHIPS (K_d = 24.7±0.4 nM). Even stronger binding was observed for peptide C5aR$_{7\text{-}28}$S$_2$ (K_d = 8.4±1.1 nM). A small decrease in affinity was observed for the peptide representing the entire extra-cellular N-terminus (C5aR$_{1\text{-}35}$S$_2$).

The relative importance of the two sulfated tyrosine residues was compared by measuring the binding affinity of both monosulfated C5aR$_{7\text{-}28}$ peptides (Table 3.2). The observed binding affinities showed that the sulfate group of tyrosine *14* contributed substantially more to the binding affinity with CHIPS than the sulfate group on tyrosine *11*.

Table 3.2 Thermodynamic binding parameters of CHIPS$_{31\text{-}121}$:C5aR peptide complexes determined by ITC

Peptide	K_d **(nM)**	ΔG **(kJ mol^{-1})**	ΔH **(kJ mol^{-1})**	ΔS **(J K^{-1}mol^{-1})**
C5aR$_{7\text{-}28}$S^{11}	458±33	-36.2±0.2	-100±2	-215±5
C5aR$_{7\text{-}28}$S^{14}	35.2±6.0	-42.5±0.4	-97.4±5.6	-184.1±19

The data are averages from at least three independent experiments unless indicated otherwise (mean ±SEM). The errors in the thermodynamic parameters were estimated by Monte Carlo simulations using the standard deviations of the individual experiments.

The thermodynamic binding parameters of the various C5aR mimics (Fig. 3.2) revealed a clear trend. Extending the sequence of the sulfated C5aR mimics from residues *10-18* to *7-28* resulted in a continuous increase of the enthalpy (Fig. 3.2A). This gain in enthalpy for these peptides compensated generously the extra loss of entropy and resulted in an increased binding affinity. The additional residues present in peptide C5aR$_{1\text{-}35}$S$_2$ compared to peptide C5aR$_{7\text{-}28}$S$_2$ did not contribute to the enthalpy of binding, but did cause an additional loss of entropy upon binding. This resulted in an overall lower binding affinity of C5aR$_{1\text{-}35}$S$_2$ compared to peptide C5aR$_{7\text{-}28}$S$_2$. The favorable binding affinity of monosulfated peptide C5aR$_{7\text{-}28}$S^{14} compared to C5aR$_{7\text{-}28}$S^{11} appeared to be entropy-driven. While the enthalpy stayed the same, the entropy penalty was decreased going from C5aR$_{7\text{-}28}$S^{11} to C5aR$_{7\text{-}28}$S^{14} to C5aR$_{7\text{-}28}$S$_2$, which resulted in a lower binding affinity.

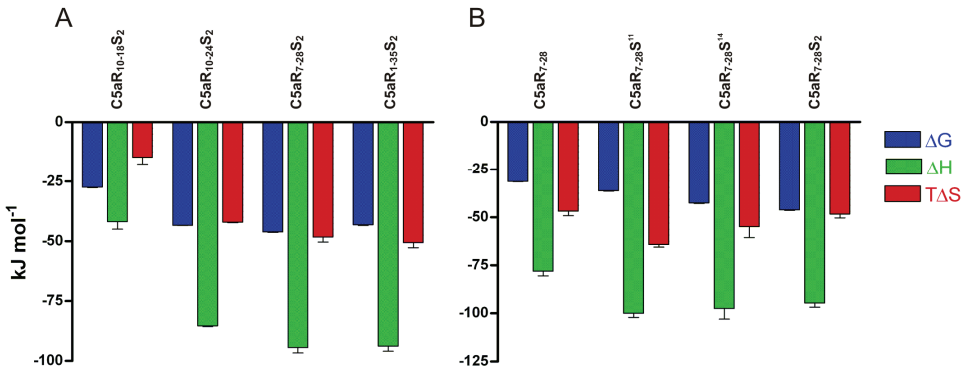

Figure 3.2 Comparison of the thermodynamic profile of binding between CHIPS and the C5a-Receptor mimics. A) comparison of the different sequences of our C5aR mimics. B) comparison of the position of the sulfate groups on the C5aR mimics.

In summary, the ITC data generated for the various peptides revealed that tight binding to CHIPS required at least residues *10-24* of the C5aR as well as the presence of both *O*-sulfated tyrosine residues. The doubly sulfated peptide $C5aR_{7\text{-}28}S_2$ comprises all residues involved in CHIPS-binding and showed the highest binding affinity.

Inhibitory potency of the C5aR mimics

The role of the sulfate groups on the bioactivity was investigated by comparing the model peptides $C5aR_{7\text{-}28}$, $C5aR_{7\text{-}28}S^{11}$, $C5aR_{7\text{-}28}S^{14}$ and $C5aR_{7\text{-}28}S_2$ for their ability to compete with the C5aR for binding either CHIPS or C5a. C5a-induced calcium mobilization in a U937/C5aR cell-line, stably expressing the C5aR, was used as a functional C5a-dependent activation assay. Fluo-3 AM was used as a probe sensitive to free calcium, increasing levels of fluorescence upon calcium release were detected by flow cytometry.

First, the potency of the $C5aR_{7\text{-}28}$ peptides to compete with the binding between CHIPS and the native C5aR was tested. In this experiment 10 nM of $CHIPS_{31\text{-}121}$ was added to the activation assay representing the minimal amount of CHIPS required to completely suppress C5aR activation by C5a. Subsequently, either peptide $C5aR_{7\text{-}28}$, $C5aR_{7\text{-}28}S^{11}$, $C5aR_{7\text{-}28}S^{14}$ or $C5aR_{7\text{-}28}S_2$ was added in order to interfere with CHIPS inhibition, as is schematically represented in Fig. 3.3*A*. In Fig. 3.3*B* it is shown that at concentrations >30 nM, peptide $C5aR_{7\text{-}28}S_2$ competed with the native C5aR in binding CHIPS, releasing the C5aR for C5a-induced activation. Peptide $C5aR_{7\text{-}28}S^{14}$ was also capable of competing with the native C5aR at concentrations >100 nM. $C5aR_{7\text{-}28}S^{11}$ and $C5aR_{7\text{-}28}$ showed no competition with C5aR up to 30 µM.

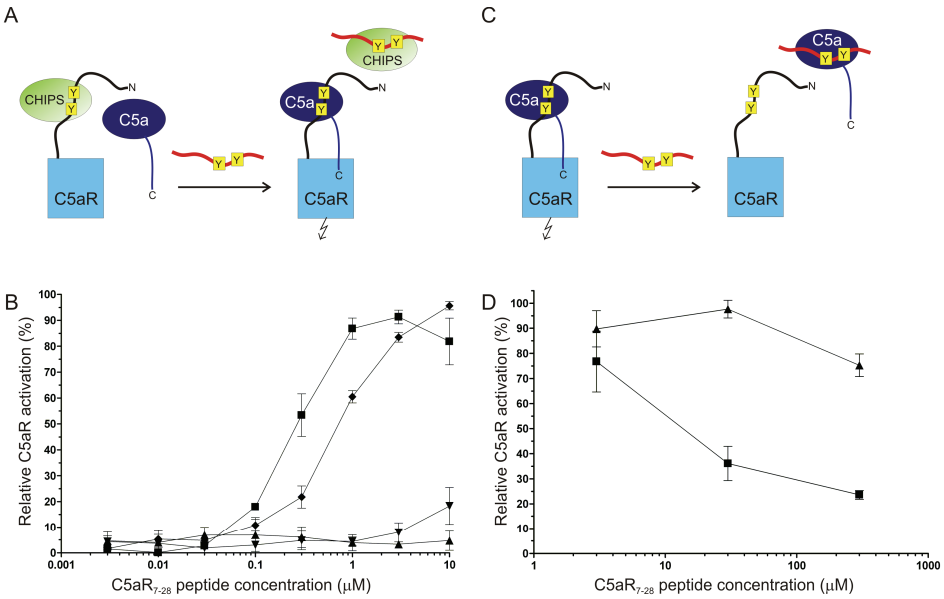

Figure 3.3 Inhibition of the C5a-induced calcium mobilization within a U937 cell-line stably expressing the C5a-receptor. A) Schematic representation of the C5a/C5aR$_{7\text{-}28}$S$_2$ inhibition experiment in the presence of CHIPS. B) The C5a inhibition experiment in the presence of CHIPS. U937/C5aR cells were preincubated with increasing concentrations of C5aR$_{7\text{-}28}$ (▲),C5aR$_{7\text{-}28}$S^{11} (▼), C5aR$_{7\text{-}28}$S^{14} (♦) or C5aR$_{7\text{-}28}$S$_2$ (■). C) Schematic representation of the C5a/C5aR$_{7\text{-}28}$S$_2$ inhibition experiment in absence of CHIPS. D) The C5a inhibition experiment in the absence of CHIPS. U937/C5aR cells were preincubated with increasing concentrations of C5aR$_{7\text{-}28}$ (▲) or C5aR$_{7\text{-}28}$S$_2$ (■).

Next, the inhibitory potency of the C5aR peptides towards C5a was tested, as is schematically represented in Fig. 3.3*C*. In Fig. 3.3*D* it is shown that >10 μM of peptide C5aR$_{7\text{-}28}$S$_2$ was needed to inhibit the C5a-induced calcium mobilization. It is important to note that peptide C5aR$_{7\text{-}28}$S$_2$ does not completely recapitulate the dual binding mode of C5a to its receptor. As a result, the affinity of C5a for C5aR$_{7\text{-}28}$S$_2$ was four orders of magnitude lower compared to its affinity for the native C5aR (K_d = 1 nM).[21, 22] The decrease in relative C5aR-activation at C5aR$_{7\text{-}28}$S$_2$ concentrations > 1 μM, observed in the experiment in the presence of CHIPS (Fig. 3.3*B*), is due to C5a:C5aR$_{7\text{-}28}$S$_2$ complex formation, in a similar way as observed in the experiment without CHIPS (Fig. 3.3*D*). In both experiments, the unsulfated C5aR$_{7\text{-}28}$ peptide was inactive (Fig. 3.3, *B* and *D*). These experiments clearly demonstrated the crucial role of the sulfate moieties in inhibition of the C5aR by CHIPS.

NMR titration studies of the CHIPS$_{31\text{-}121}$/C5aR$_{7\text{-}28}$ complexes

Residue specific information concerning the interactions between the C5aR and CHIPS was derived from NMR experiments. Titration of the unlabeled model peptide C5aR$_{7\text{-}28}$S$_2$, which is unstructured free in solution, to ^{15}N-labeled CHIPS$_{31\text{-}121}$ resulted in perturbation of numerous peaks in the ^{15}N

heteronuclear single quantum correlation (HSQC) NMR spectrum of $CHIPS_{31\text{-}121}$. Increasing concentrations of $C5aR_{7\text{-}28}S_2$ resulted in the disappearance of free $CHIPS_{31\text{-}121}$ peaks and the concomitant appearance of $CHIPS_{31\text{-}121}$:$C5aR_{7\text{-}28}S_2$ peaks, compatible with a slow-exchange binding regime (Fig. 3.4*A*).[23] The NMR spectra of $^{13}C/^{15}N$-labeled $CHIPS_{31\text{-}121}$ in complex with unlabeled $C5aR_{7\text{-}28}S_2$ were reassigned and the protein amide ^{15}N-^{1}H and $^{13}C\alpha/\beta$ chemical shifts were compared with those of free $CHIPS_{31\text{-}121}$. A weighted sum of these chemical shift changes was plotted *vs.* residue number (Fig. 3.4*B*). Two regions showed a relatively large perturbation in backbone and $C\alpha/\beta$ chemical shifts upon binding: (*i*) Residues 43-61, which include part of the α-helix and subsequent loop 52-59 and (*ii*) residues 95-111, which include strands β_3 and β_4 (Fig. 3.4*C*). Previously we concluded from backbone ^{15}N relaxation measurements that residues residing in the 52-59 loop region of free $CHIPS_{31\text{-}121}$ were less ordered compared to the rest of the protein backbone (without considering the N- and C-termini).[12] In the $CHIPS_{31\text{-}121}$:$C5aR_{7\text{-}28}S_2$ complex, this loop adopted an ordered conformation as can be concluded from backbone ^{15}N relaxation data (Fig. 3.5).

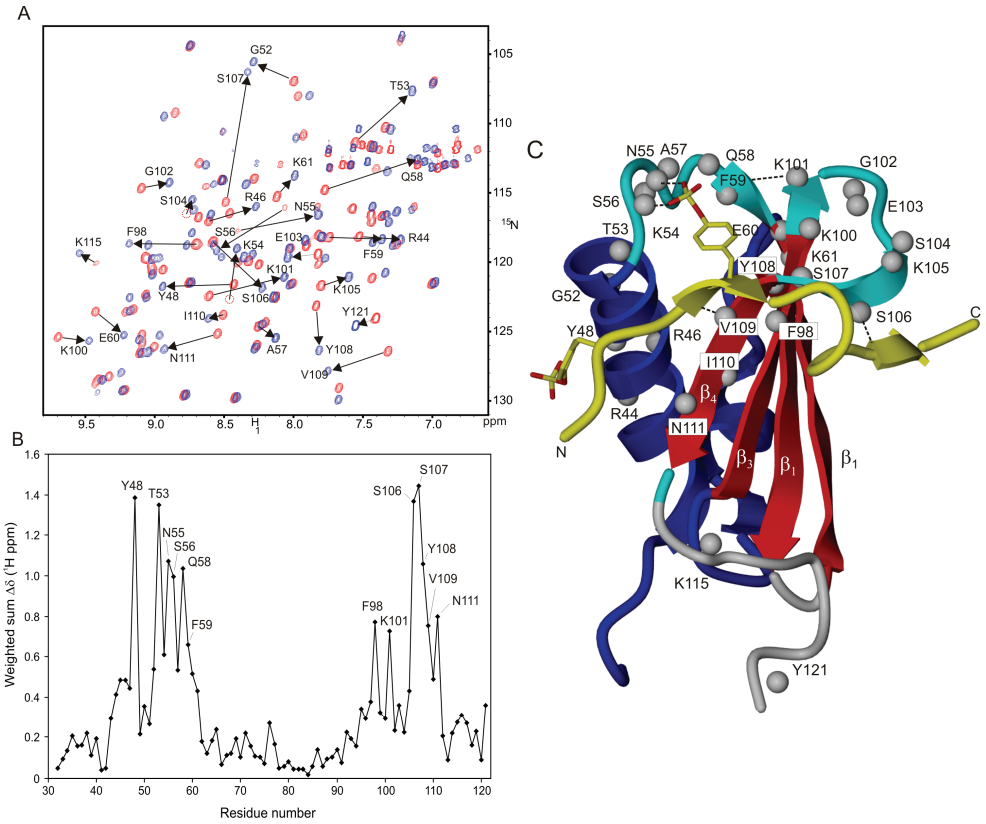

Figure 3.4 Chemical shift perturbations of $CHIPS_{31\text{-}121}$ upon complex formation with the C5aR peptide $C5aR_{7\text{-}28}S_2$. A) Overlay of the ^{15}N-^{1}H HSQC spectrum of free uniformly ^{15}N-labeled $CHIPS_{31\text{-}121}$ (red) and of the titrated stoichiometric ^{15}N-$CHIPS_{31\text{-}121}$:$C5aR_{7\text{-}28}S_2$ complex (blue). B) Weighted sum of CHIPS amide ^{15}N-^{1}H and $^{13}C\alpha/\beta$

chemical shift changes, $\Delta\delta(^1H\ ppm) = [(\Delta\delta_{NH})^2 + (0.25\Delta\delta_{C\alpha})^2 + (0.25\Delta\delta_{C\beta})^2 + (0.1\Delta\delta_N)^2]^{1/2}$, upon binding the C5aR$_{7\text{-}28}S_2$ peptide, plotted *vs.* residue number. C) Cartoon representation of mapped positions within the CHIPS$_{31\text{-}121}$ structure that display perturbed chemical shifts after formation of the CHIPS$_{31\text{-}121}$:C5aR$_{7\text{-}28}$S$_2$ complex. Amide protons that have a large chemical shift perturbation are indicated by gray balls. Broken lines indicate newly formed amide hydrogen-bonds.

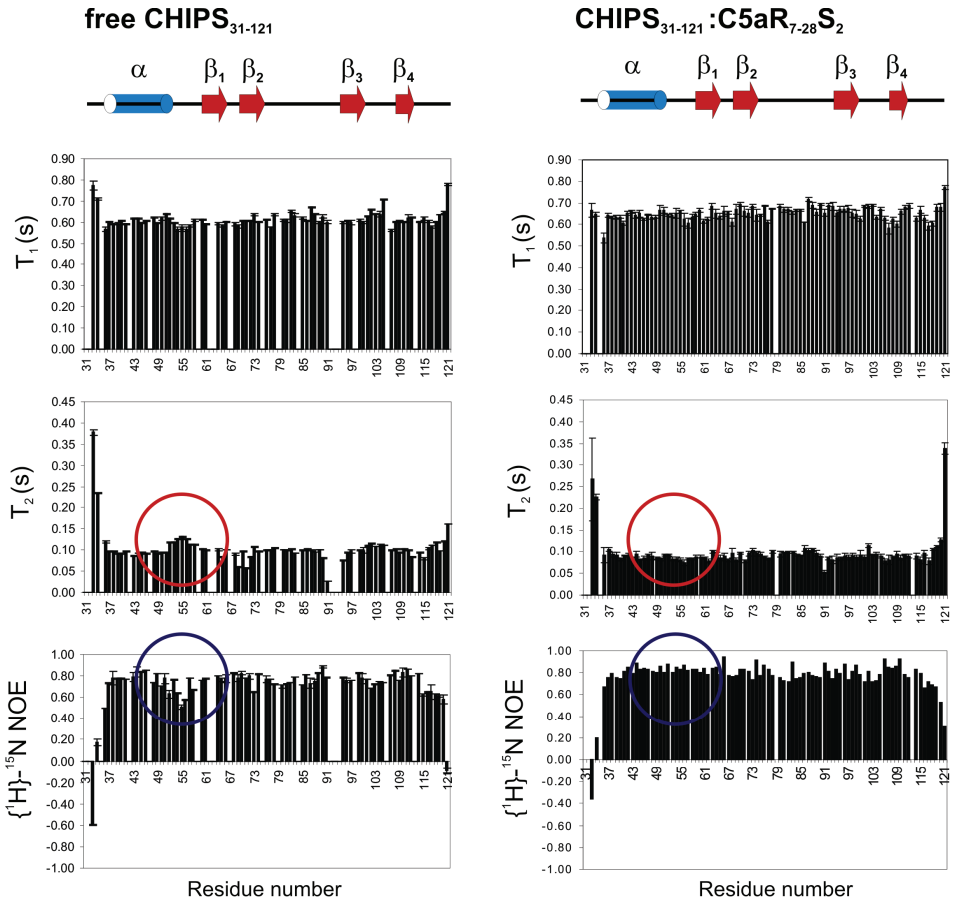

Figure 3.5 Backbone ^{15}N relaxation parameters T_1, T_2, and heteronuclear [^{1}H]-^{15}N-NOE of free CHIPS$_{31\text{-}121}$ (left) and of the CHIPS$_{31\text{-}121}$:C5aR$_{7\text{-}28}$S$_2$ complex (right) plotted against the residue numbers. The location of the secondary structure elements was derived from the structure of free CHIPS$_{31\text{-}121}$, and is shown at the top of the graph. The data points of T_2 and heteronuclear [^{1}H]-^{15}N-NOE concerning the loop between the helix and strand β_1 (residues 52-59) are indicated by circles.

The structure of the stoichiometric complex of $^{13}C/^{15}N$-labeled CHIPS$_{31\text{-}121}$ and unlabeled C5aR$_{7\text{-}28}$S$_2$ has been determined by NMR. An overlay of 25 selected low-energy structures of the CHIPS$_{31\text{-}}$

$_{121}$:C5aR$_{7\text{-}28}$S$_2$ complex is presented in Fig. 3.6A. The structure of CHIPS$_{31\text{-}121}$ in the complex is largely similar to free CHIPS$_{31\text{-}121}$ (Fig. 3.7). Subtle changes in the structure of CHIPS upon binding include ordering of the helix-strand loop between residues 52-59 and the appearance of a small β-strand between residues 103-107. The C5aR$_{7\text{-}28}$S$_2$ peptide is wrapped around a large portion of CHIPS$_{31\text{-}121}$ covering a substantial part of its solvent accessible surface area (buried ~18 nm^2 *vs.* total ~92 nm^2). The C5aR$_{7\text{-}28}$S$_2$ peptide, which is a random coil free in solution, clearly adopts a well-defined conformation upon binding pre-organized CHIPS. Essentially, two amino acid stretches of equal size define the binding interface with CHIPS: Residues *10-14* and *19-24* of C5aR$_{7\text{-}28}$S$_2$ form two short β-strands (labeled I and II in Fig. 3.6A) running in an anti-parallel fashion with respect to strand β$_4$ and residues 104-107 of CHIPS$_{31\text{-}121}$. These two stretches are connected by a single turn comprised of residues *15-18*. Residues *25-28* of C5aR$_{7\text{-}28}$S$_2$ are disordered in the structural ensemble (Fig. 3.6A) and do not interact with CHIPS$_{31\text{-}121}$. Residues *7-9* are less well defined compared to the *10-24* core region, probably due to increased conformational freedom.

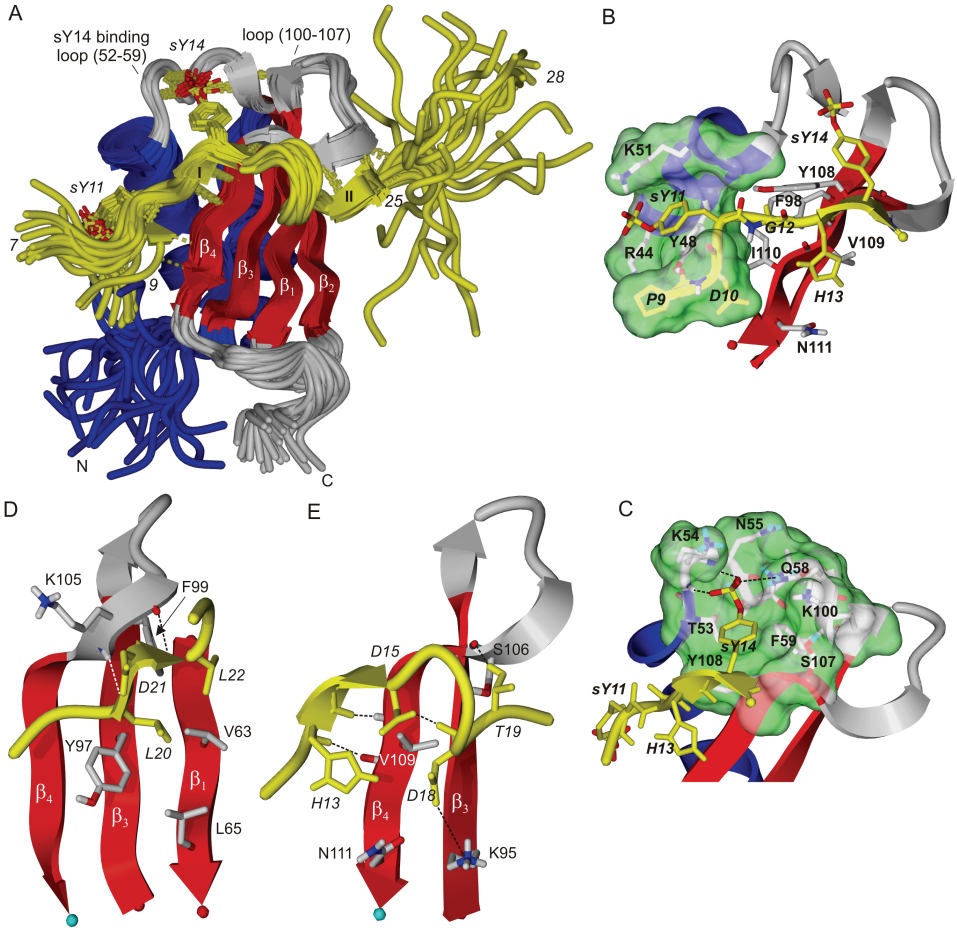

Figure 3.6 Structure of the $CHIPS_{31-121}$:$C5aR_{7-28}S_2$ complex. A) Overlay of the 25 selected low-energy NMR structures determined of the complex between $CHIPS_{31-121}$ and $C5aR_{7-28}S_2$. Newly formed beta strands in the peptide are labeled I and II. B) Binding pocket of *sY11*. Residues lining the pocket are labeled. C) Binding pocket of *sY14*. D) View of the binding strand II and the hydrophobic interactions of peptide residues *L20* and *L22*, positioned towards the β sheet surface of CHIPS. E) View of the binding strand I and turn-motif of the complex. Residues *D16* and *K17* of the peptide stick out into solution and are omitted from the plot for clarity. Intermolecular interactions are indicated by broken lines. Coloring scheme: $C5aR_{7-28}S_2$ in yellow; the side-chains of *sY11* and *sY14* in yellow sticks and the sulfate oxygens in red; the $CHIPS_{31-121}$ β strands in red; the $CHIPS_{31-121}$ binding loops, the β_1-β_2 loop, and the C-terminus (113-121) in gray; the $CHIPS_{31-121}$ β-helix and remaining backbone in blue. The solvent-accessible surface surrounding the sulfated tyrosine is colored green.

Details concerning specific interactions between $C5aR_{7-28}S_2$ and $CHIPS_{31-121}$ are presented in Fig. 3.6B-E. The first stretch of $C5aR_{7-28}S_2$ involved in CHIPS binding includes the two sulfated tyrosine residues *Y11* and *Y14* (subsequently referred to as *sY11* and *sY14*). *sY11* is stacked on top of Y48, with the sulfate group of *sY11* neutralized by the positive charge of residues R44 and K51 located in the CHIPS helix (Fig. 3.6B). *sY14* is bound by the loop region 52-59 of CHIPS, while residues Y108 and K100 surround the binding pocket (Fig. 3.6C). The oxygen atoms of the sulfate group of *sY14* are primarily coordinated to the backbone amide protons of K54 and N55 and the side-chain amide of Q58. Surprisingly, the positively charged side-chains of K54 and K100 are only partially positioned within the coordination sphere of the sulfate group of *sY14*. Instead, these side-chains are mostly involved in cationic-π stacking with the aromatic ring of *sY14* or in long-range electrostatic interactions.

The second stretch of $C5aR_{7-28}S_2$ (residues *19-24*) involved in binding is located on the opposite face of the CHIPS molecule near residues 104-107 between strand β_3 and β_4. This short β-strand is stabilized by backbone hydrogen bonds between residues *L20* and *L22* of $C5aR_{7-28}S_2$ and S104 and S106 of $CHIPS_{31-121}$. The side-chains of *L20* and *L22* are in contact with the hydrophobic β-sheet surface of CHIPS (Fig. 3.6D). Finally, oppositely charged residues *D21* and K105 are in close proximity to each other while the side-chains of *T19* and S106 are within hydrogen-bonding distance (Figure 3.6E). Experimentally, we observed the hydroxyl proton of *T19* in the NMR spectra, implying it is protected from solvent exchange.

The turn-motif comprising residues *15-18* of $C5aR_{7-28}S_2$ is stabilized by intra-molecular interactions between the negatively charged carboxyl group of *D15* and the backbone amide protons of *D16*, *K17* and *D18* comprising the turn (Fig. 3.6E). The side-chains of *D16* and *K17* are on average not in close contact to CHIPS. Finally, a salt-bridge between the side-chains of *D18* and K95 of $CHIPS_{31-121}$ provides additional stability (Fig. 3.6E).

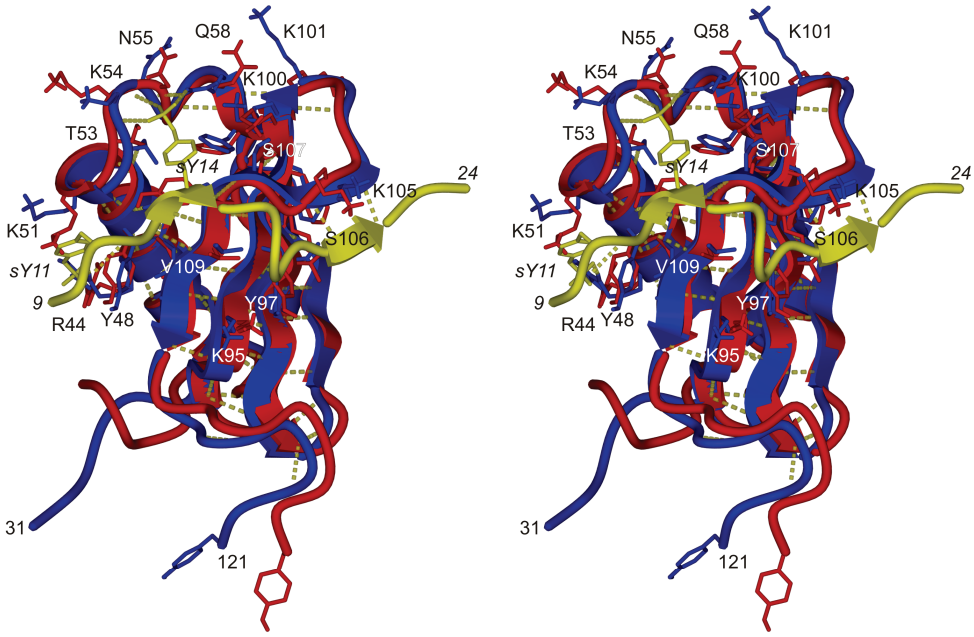

Figure 3.7 Side-by-side stereo plot displaying the difference between a representative structure of free $CHIPS_{31-121}$ (red) (PDB ID code 1XEE) and the corresponding structure of the $CHIPS_{31-121}$ protein as part of the $CHIPS_{31-121}$:$C5aR_{7-28}S_2$ complex (blue). Amino acid side-chains of $CHIPS_{31-121}$ that are important for binding $C5aR_{7-28}S_2$ in the core region between residues *9-24*, and that have different orientations in the free and unbound form, are displayed in stick representation. The backbone trace of residues *9-24* of $C5aR_{7-28}S_2$ is displayed in yellow with residues *sY11* and *sY14* in stick representation. The two models mutually overlay with an rms deviation of 0.089 nm for the well-defined backbone atoms between residues 36-113. The ensemble average backbone rms deviation is 0.13±0.02 nm.

Mutation studies

In order to assess the role of specific molecular interactions in the $CHIPS_{31-121}$:$C5aR_{7-28}S_2$ complex, several mutants of $CHIPS_{31-121}$ were prepared to verify their inhibitory propensities in a biological assay with intact C5aR. This was quantified as the concentration of C5a needed to achieve 50% activation of the C5aR (AC_{50}) in the presence of 100 nM wild type $CHIPS_{31-121}$ or mutant. We selected a number of mutants based upon their position in the structure (Fig. 3.8A). Only mutants Y97A and S106A, next to the already described K95A,[12] showed substantial decreased AC_{50} values.

CD spectroscopy was used to check the structural integrity of the four least active CHIPS mutants (Fig. 3.8B). No significant differences in secondary structure were observed between wild type CHIPS, and mutants Y97A and S106A. The same holds for mutants R44A and K95A studied

previously.[12] This indicates that the loss of inhibitory potency of these mutants is not caused by loss of structural integrity, but by altered specific binding.

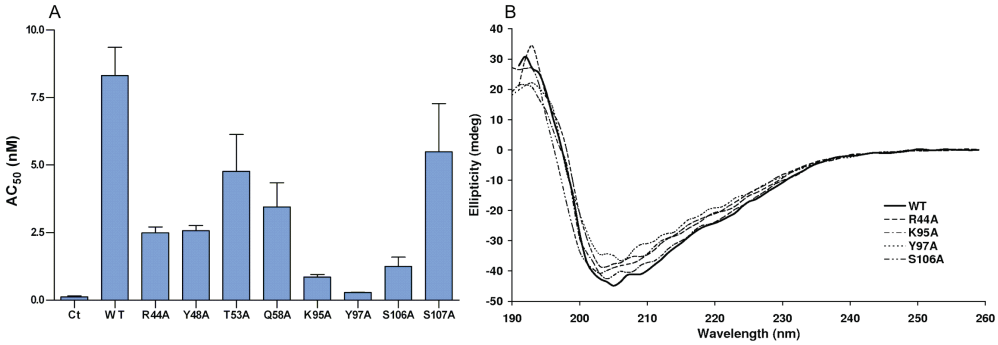

Figure 3.8 A) Activity assay of CHIPS mutants. AC_{50} values represent the concentration of C5a necessary to regain 50% activity after inhibition with 100nM CHIPS or CHIPS mutants. CT = control, WT = wild type CHIPS; B) CD spectra of the four least active CHIPS mutants. The similarity between the spectra demonstrates that their structural integrity is not compromised.

3.3 Discussion

The important role of *O*-sulfated tyrosine residues in a wide range of biological processes is becoming increasingly recognized.[24] Several G protein-coupled receptors, including the C5aR, have been demonstrated to contain *O*-sulfated tyrosine residues within their N-termini. This posttranslational modification is required for proper ligand binding and receptor activation.[21, 25-28]

Here, we assessed the role of the *O*-sulfated tyrosine residues in the interaction of the C5aR with the immune evasion protein CHIPS. The data obtained demonstrated that the *O*-sulfated tyrosine residues *11* and *14* of the C5aR are essential for tight binding to CHIPS. However, residues beyond the smallest C5aR fragment we have investigated (residues *10-18*) also add substantially to the binding affinity (Table 3.1). Among the fragments measured by ITC, peptide $C5aR_{7\text{-}28}S_2$ exhibited the highest affinity for CHIPS (K_d = 8.4±1.1 nM). The observed K_d value is comparable to the K_d values of ^{125}I-labeled CHIPS for the naturally sulfated intact C5aR (K_d = 1.1±0.2 nM) and C5aR N-terminus (residues 1-38; K_d = 29.7±4.4 nM), as previously reported by Postma et al.[11, 15] Peptide $C5aR_{7\text{-}28}S_2$ competed with the C5aR N-terminus in binding $CHIPS_{31\text{-}121}$ in a calcium mobilization assay at concentrations >10 nM (Fig. 3.3). In this bioactivity assay, the unsulfated peptide $C5aR_{7\text{-}28}$ did not show any effect. We conclude that peptide $C5aR_{7\text{-}28}S_2$ comprises all moieties of the C5aR essential for tight binding to the CHIPS protein and is therefore a representative model of the N-terminal portion of the human C5aR.

The two sulfate groups present in $C5aR_{7\text{-}28}S_2$ show different influences on the binding of this peptide to $CHIPS_{31\text{-}121}$. Both show an increase in binding affinity, but the contribution of *sY14* is significantly

larger than the contribution of *sY11*. This difference appears to be caused more by a smaller entropy penalty than by an increase in enthalpy but it is more complex to interpret. These species cannot be directly compared to the doubly sulfated peptides. Differences in structural properties and solvent behavior are likely to be responsible for the differences in the observed thermodynamic profiles. The difference in binding affinity, determined by ITC, is also observed in a calcium mobilization assay. $C5aR_{7\text{-}28}S^{14}$ is capable to recover the C5a activity at a significant lower concentration than $C5aR_{7\text{-}28}S^{11}$, but both sulfate groups are necessary to show competition with the native C5aR at low nanomolar concentration.

The structure of the $CHIPS_{31\text{-}121}$:$C5aR_{7\text{-}28}S_2$ complex defines residues *10-24* as the core region of the C5aR N-terminus interacting with CHIPS. The binding motif is comprised of two short β-strands interconnected by a turn. These two strands, labeled I and II in Figure 3.6*A*, are hydrogen bonded in an anti-parallel fashion to strand β_4 and residues 104-107 of CHIPS, respectively. The sulfated tyrosine residues *sY11* and *sY14* indeed play a key role in stabilization of the complex. Sulfated tyrosine *sY11* is located near the α-helix of CHIPS and interacts primarily with the aromatic ring of tyrosine Y48, and with the end-groups of R44 and K51 closely placed around the negatively charged sulfate group. *sY14* is tightly bound by residues of the loop region 52-59 of CHIPS. The charged sulfate group of *sY14* is coordinated by the backbone amide protons of K54 and N55, and by the side-chain amide protons of Q58. Unexpectedly, the positively charged side-chains of nearby lysine residues K54 and K100 are not involved in specific interactions with the sulfate group of *sY14* (Fig. 3.6C). The slightly higher affinity to CHIPS of peptide $C5aR_{7\text{-}28}S_2$ compared to peptide $C5aR_{10\text{-}24}S_2$ (Table 3.1) indicates that residues outside the core region *10-24* of C5aR also contribute to binding. This contribution is assumed to involve non-specific interactions of the residues at the N-terminal side of $C5aR_{7\text{-}28}S_2$ (*T7-P9*).

Postma et al. did not observe major differences in the binding of CHIPS-FITC to a sulfated or non-sulfated C5aR N-terminus (residues *1-38*) expressed on HEK293 cells.[15] The FITC label, which was employed to detect binding by means of fluorescence flow cytometry, was introduced covalently at random positions to surface-exposed side-chains of lysine residues. The structure of the $CHIPS_{31\text{-}121}$:$C5aR_{7\text{-}28}S_2$ complex reveals that lysine K51 is near tyrosine *sY11* while K54 and K100 are in close proximity to tyrosine *sY14*. It is likely that modification of these particular lysine residues in CHIPS by the large FITC group interferes with the binding of C5aR and decreases the overall affinity for steric reasons.

The activity of 16 lysine and arginine to alanine single-point mutants of full length $CHIPS_{1\text{-}121}$ with respect to activation of the C5aR and FPR was reported by Haas et al.[12] Of these mutants, R44A, R46A and K95A were most affected. With the structure of the $CHIPS_{31\text{-}121}$:$C5aR_{7\text{-}28}S_2$ complex, described in this chapter, the structural reasons for these diminished affinities can be rationalized. Although the side-chain of R44 is not well-defined in the NMR ensemble, the guanidinium group of

R44 is on average in close proximity to the sulfated tyrosine *sY11* of $C5aR_{7\text{-}28}S_2$. The role of mutant R46A is related to the structural integrity of CHIPS as was accounted for previously.[12] Residue K95 is located at the start of strand β_3 of CHIPS and its side-chain is in direct contact with the side-chain of residue *D18* of $C5aR_{7\text{-}28}S_2$ (Fig. 3.6E). This interaction is evidently important for maintaining the turn-motif, which places the two short β-strands of $C5aR_{7\text{-}28}S_2$ in an optimal position to interact with CHIPS (Fig. 3.6A).

Among the CHIPS mutants other than the previously described lysine and arginine mutants,[12] Y97A and S106A have the lowest inhibitory potency with respect to C5a-mediated C5aR activation. The aromatic ring of Y97 supports the backbone of *D18* and *T19* and is in contact with residue *L20* of $C5aR_{7\text{-}28}S_2$ (Fig. 3.6D). The sensitivity of the S106A mutant is explained by the fact that the hydroxyl group of S106 is involved in a hydrogen-bond network together with *T19* of $C5aR_{7\text{-}28}S_2$.

Previous mutational studies showed that residues *D10*, *G12*, *D15* and *D18* of the C5aR are essential for binding of CHIPS.[15] The structure of the complex suggests that *D15* and *D18* are important for maintaining the turn motif between the two short β-strands of $C5aR_{7\text{-}28}S_2$. The side-chain carboxyl group of residue *D10* is within hydrogen-bond distance with residues residing in beta strand β_4 of CHIPS. Finally, residue *G12* is favored in the complex, because the side-chain of any other L-amino acid would lead to clashes with the adjacent strand β_4 of CHIPS. The side-chains of residues *D16* and *K17* are not involved in key interactions with CHIPS and are therefore not critical for binding.

In conclusion, all moieties of the C5aR required for high affinity binding to the immune evasion protein CHIPS are present in the synthetic peptide $C5aR_{7\text{-}28}S_2$. In particular, two O-sulfated tyrosine residues at positions *11* and *14* of the C5aR are crucial for tight binding to CHIPS. The key C5aR binding element of CHIPS is the loop located between the α-helix and strand β_1 (residues 52-59). This loop accommodates sulfated tyrosine *sY14* and represents a potential lead sequence for the development of novel C5aR antagonists.

3.4 Experimental procedures

Synthesis of C5aR-peptides

The C5aR peptides were synthesized on an ABI 433A peptide synthesizer (Applied Biosystems) applying Fmoc/*t*Bu chemistry according to a method described in chapter 2 of this thesis. The final peptides were checked for purity (>98%) and composition by HPLC and mass spectrometry. Peptide concentrations were determined by weight.

Biosynthesis of CHIPS and CHIPS-mutants

Wild type $CHIPS_{31\text{-}121}$ and mutants were cloned and expressed as described before.[12] Inclusion bodies were isolated using CelLytic B Bacterial Cell Lysis/Extraction Reagent (Sigma-Aldrich) and

lysozyme, according to the manufacturer´s description. Inclusion bodies were intensively washed with 0.5% N,N-dimethyldodecylamine *N*-oxide (Sigma-Aldrich) in 20 mM sodium phosphate buffer with 0.5 M NaCl, pH 7.8, pelleted and solubilized in 50 mM Tris, pH 8.0, containing 6 M guanidine. After dialysis in 20 mM sodium phosphate buffer, pH 8.0 the protein was loaded on a HiTrap SP XL cation exchange column (GE Healthcare Bio-Sciences) and eluted with a 1 M NaCl gradient. Protein containing fractions were pooled, analyzed on SDS-PAGE for purity, and dialyzed in PBS. Protein concentrations were determined by measuring the absorbance at 280 nm in the presence of 8 M urea and using the extinction coefficients obtained from the ExPASy ProtParam tool.[29]

Calcium mobilization assay

Calcium mobilization studies were performed in Fluo-3-AM labeled U937/C5aR cells as described.[12] The potency of the C5aR mimics $C5aR_{7\text{-}28}$, $C5aR_{7\text{-}28}S^{11}$, $C5aR_{7\text{-}28}S^{14}$ and $C5aR_{7\text{-}28}S_2$ to block the CHIPS-inhibiting effect on the C5a-induced calcium mobilization was investigated. Therefore, 10 nM $CHIPS_{31\text{-}121}$ was pre-incubated with increasing concentrations of each C5aR mimic (3 nM to 10 µM) for 30 min at room temperature. Next, the CHIPS/peptide mixture was added to Fluo-3-AM labeled U937/C5aR cells for 30 s before 4 nM C5a was used as a stimulus for intracellular calcium mobilization. An increase in fluorescence was measured with a FACSCalibur flow cytometer (Becton Dickinson). The AC_{50} values in the calcium mobilization assay were determined using non-linear curve-fitting and were statistically analyzed by means of the GraphPad Prism (La Jolla, CA, USA) software package.

ITC experiments

The ITC measurements of the unsulfated and doubly sulfated C5aR mimics and $CHIPS_{31\text{-}121}$ were performed at 298 K on a MCS Isothermal Titration Calorimeter (MicroCal). The measuring cell was filled with 1.345 mL of a 26 µM solution of $CHIPS_{31\text{-}121}$ in a 20 mM sodium phosphate buffer at pH 6.5. The syringe was loaded with 250 µL of a 0.5 mM solution of one of the peptides in the same buffer. After each addition of 7.5-15 µL of peptide solution, the heat change due to binding of the added peptide was measured. $C5aR_{7\text{-}28}S^{11}$ and $C5aR_{7\text{-}28}S^{14}$ were measured on an ITC_{200} Microcalorimeter (MicroCal). The measuring cell was filled with 208 µL of a 26 µM solution of $CHIPS_{31\text{-}121}$ in a 20 mM sodium phosphate buffer at pH 6.5. The syringe was loaded with 30 µL of a 0.5 mM solution of one of the peptides in the same buffer. After each addition of 1 µL of peptide solution, the heat change due to binding of the added peptide was measured. The data were analyzed using Microcal Origin software and fitted by non-linear regression analysis. The errors were estimated by performing a Monte Carlo simulation.

CD measurements

CD spectra (190-260 nm) were recorded on an Olis RSM1000 spectrophotometer operating at 0.3 nm spectral resolution (slit size 0.2 mm). Samples of wild-type $CHIPS_{31\text{-}121}$ (47 µM) and mutants (46-51 µM) in 20 mM sodium phosphate buffer (pH 7.4) were measured at 298 K using a 0.5 mm cuvette. To

gain sufficient S/N ratios multiple scans were summed, with data points averaged by three-point triangular smoothing.

NMR spectroscopy

NMR samples of the various peptides were prepared in 9/1 (v/v) H_2O/D_2O sodium phosphate buffers (20 mM, pH 6.2 or 6.5), having peptide concentrations that vary between 0.5 mM ($C5aR_{1\text{-}35}S_2$) and 2 mM ($C5aR_{10\text{-}18}$ and $C5aR_{10\text{-}18}S_2$). Sequential ^{1}H NMR assignments of the free C5aR peptides $C5aR_{10\text{-}18}$, $C5aR_{10\text{-}18}S_2$, $C5aR_{10\text{-}24}S_2$, $C5aR_{7\text{-}28}$, $C5aR_{7\text{-}28}S_2$, $C5aR_{7\text{-}28}S^{11}$, $C5aR_{7\text{-}28}S^{14}$, and $C5aR_{1\text{-}35}S_2$ were performed following standard 2D-NMR strategies, using a combination of 2D NOESY and 2D TOCSY spectra.[30] Spectrometers used were a Varian Inova 500, a Varian Inova 600, and a Bruker Avance 900 spectrometer.

Sequential resonance assignment of the CHIPS protein in a stoichiometric complex between peptide $C5aR_{7\text{-}28}S_2$ and uniformly $^{13}C/^{15}N$-labeled $CHIPS_{31\text{-}121}$ was carried out by means of triple resonance spectroscopy recorded on Varian Inova 500 and 600 MHz spectrometers. NMR samples of the complex remained stable up to several months at 298 K, with no obvious degradation of the acid-labile sulfated tyrosine residues. In order to filter out and sequentially assign the proton resonances of the unlabeled peptide in the complex, 2D ^{13}C-^{15}N-filtered TOCSY and 2D ^{13}C-^{15}N-filtered NOESY spectra (500, 600 and 900 MHz) were recorded on a sample containing a 1:1 complex of peptide $C5aR_{7\text{-}28}S_2$ and uniformly $^{13}C/^{15}N$-labeled $CHIPS_{31\text{-}121}$.[31, 32]

Final NOE analysis and resonance assignment of the bound $C5aR_{7\text{-}28}S_2$ peptide was performed on the isotope filtered 2D NOESY 900 MHz dataset recorded at 298 K and a mixing time of 200 ms. In order to assign intermolecular NOEs between bound, unlabeled $C5aR_{7\text{-}28}S_2$ and uniformly $^{13}C/^{15}N$-labeled $CHIPS_{31\text{-}121}$, a 900 MHz ^{13}C-edited-ω3-filtered 3D-NOESY spectrum was recorded on the sample of the 1:1 complex.[23, 33] The data were processed and analyzed using NMRPipe and Sparky (Goddard TD and Kneller DG, SPARKY 3, University of California, San Francisco).[34]

Structure determination of the $CHIPS_{31\text{-}121}$:$C5aR_{7\text{-}28}S_2$ complex

A standard Aria1.2/CNS1.1 simulated annealing protocol has been applied to solve the NMR structure separately for both the $CHIPS_{31\text{-}121}$ protein and the approximate $C5aR_{7\text{-}28}S_2$ peptide, when bound in the complex.[35] 160 structures of $CHIPS_{31\text{-}121}$ and 160 structures of $C5aR_{7\text{-}28}$ peptide were calculated. Sixty of the lowest-energy structures of the protein were initially selected. Coordinates of these 60 protein structures are subsequently fitted and averaged over the ensemble (the backbone RMS deviation to mean is 0.028 nm for residues 36-113), with side chains regularized by simulated annealing energy-minimization. This average structure is used as a reference for subsequent docking with the three lowest energy conformers of the $C5aR_{7\text{-}28}$ peptide. The three low-energy peptide structures were taken directly from the Aria generated ensemble calculated based on peptide-peptide NOEs from the 900 MHz ^{13}C-^{15}N-filtered 2D NOESY. Hydrogen-bond restraints and dihedral

restraints derived from TALOS were taken into account in the structure calculations.[36] TALOS phi/psi restraints for CHIPS residues 52-59 were removed in the structure calculation, because these residues have carbon chemical shifts that are influenced to a large extent by the presence of the *sY14* ring when bound in the 52-59 loop pocket.

Distance restraint-docking between the experimentally derived peptide structures and the averaged CHIPS protein structure were performed using the Yasara Structure/WhatIF 8.3.3 Twinset software (Nijmegen, The Netherlands, www.yasara.org). Using the Yasara program, the two tyrosines, *Y11* and *Y14*, in the peptide chain (as calculated by Aria 1.2) were patched with sulfate groups and the peptide was capped with acetyl and NH_2 end blocking groups. Force field (Amber 99) parameters of the modified groups were calculated by the self-parameterizing option of Yasara, in combination with quantum-mechanically derived AM1 geometry optimization.

In the docking procedure, the sulfated peptide $C5aR_{7\text{-}28}S_2$ and CHIPS protein were manually placed side-by-side at a distance between 2.5-3.0 nm from each other. First, random starting conformations of the peptide were generated by a Molecular Dynamics (MD) run at elevated temperature (750-900 K). In the final docking, the intramolecular distance restraints (combined from the Aria1.2 runs of both the individual peptide and protein), dihedral restraints, together with the intermolecular restraints were introduced in a controlled stepwise manner during a 100 ps MD docking procedure, performed at 300 K. 130 Selected generated structures of the docked complex were refined in explicit solvent for another 20 ps using all experimental restraints, and including a full electrostatic description of the system. Parameters used: Amber99 force field,[37] periodic boundary (PB) conditions, pre-equilibrated cube of water with dimensions scaled to accommodate a 0.8 nm shell around the solute, counterions for charge neutralization of the PB box, 0.786 nm non-bonded cutoff, 1 fs time step, update non-bonded interactions every 2 fs, Ewald summation, constant pressure (1.0 g/cm^3), and a simulation temperature of 300 K.

From this ensemble of 130 calculated structures, 25 final structures were selected, based on the criteria of a combination of lowest restraint violation energy and best predicted back-calculated chemical shifts for protons at the peptide-protein binding interface. Shiftcalc 2004 was used to calculate proton chemical shifts in the complexes.[38] The selected 25 structures were refined in explicit solvent for an additional 100 ps of restrained MD, in order to search for structural water molecules important for binding. After stripping off the water molecules, the coordinates of the protein-peptide complex are combined into a single ensemble for deposition to the Protein Data Bank (www.rcsb.org PDB ID code 2K3U). All structural calculations were done on a Dual-Quad Xeon 5135 Linux workstation. Structural data analysis was carried out with Procheck NMR and Yasara/WhatIf. Surface calculations were done using PISA v1.14.[39, 40]

Table 3.3 Structural statistics of the $CHIPS_{31-121}$:$C5aR_{7-28}S_2$ complex

Total NOE restraints	3824[a]
Intramolecular restraints (both protein and peptide part)[b]	
Unambiguous NOE restraints	
Intra-residue	1248
Sequential	754
Medium (|i-j| >1 and (|i-j| < 4)	358
Long-range (|i-j| > 3)	851
Ambiguous NOE restraints	45
Intermolecular NOE restraints	568[c]
Dihedral angle restraints	113[d]
Hydrogen bond restraints	26 (13 H-bonds)
Average violations of experimental restraints per structure	
Number of distance restraints (>0.05 nm)	35.2 ± 3.3[e]
Average violation distance restraints (nm)	0.00167
Number of dihedral angle restraints (>10 deg)	0.9 ± 1.1
Average violation dihedral restraints (deg)	0.43
Average potential energies (kJ/mol)[f]	
Total	-20590.4 + 117.6
Bonds	272.9 ± 6.5
Angles	1097.4 ± 29.5
Planarity	49.8 ± 3.9
Dihedrals	26635.2 ± 103.0
Coulomb	-45026.0 ± 153.4
vdWaals	-3619.6 ± 46.5
NOE restraints	1388.7 ± 100.3
Dihedral restraints	2.9 ± 5.1
Average RMS deviations from ideal covalent geometry[g]	
Bonds	0.00553 ± 0.00005 nm
Angles	1.90 ± 0.03 deg
Impropers	1.30 ± 0.05 deg
Ramachandran statistics (non-glycine residues of ordered regions: protein 36-113 and peptide 10-23)[h]	
Residues in most favored regions (%)	84.1
Residues in additional allowed regions (%)	15.4
Residues in generously allowed regions (%)	0.4
Residues in disallowed regions (%)	0.1
Ensemble RMSD distance from the mean structure (nm) (residues of ordered regions: protein 36-113 and peptide 10-23)[i]	
Backbone atoms (C, Cα, N, O)	0.058 ± 0.012
All heavy atoms	0.089 ± 0.009

[a]Symmetrical cross-peaks and redundant NOEs observed in different spectra reflecting the same ^{1}H-^{1}H pair are only counted once. [b]Number of ambiguous and unambiguous NOEs for both peptide and protein as calculated by Aria1.2. [c]Semi-quantitative (upper limit) unambiguous distance restraints between peptide and protein, derived from different spectra and weighted by occurrence. [d]TALOS restraints for phi/psi angles were introduced from the assigned carbon chemical shifts, but were only applied to amino acids that were statistically predicted by the program to fall within a well-defined Ramachandran area. Phi/psi restraints for CHIPS residues (52-59) were removed in the structure calculation, due to the strong influence of ring current of *sY14* on nearby carbon chemical shifs of amino acids in the *sY14* binding loop. [e]Mostly upper limit distance violations of the intermolecular distance restraints. [f]Potential energies (Amber99 force field) of the solvated complex, but excluding solvated water energy contributions. [g]WHATIF data analysis referenced to ideal covalent geometries for amino acids. Z-scores for bond lengths, angles, impropers and planarity all fall in the expected range between 0.67 and 2.0. [h]Analysis according to Procheck NMR. [i]Average pairwise RMSD and standard deviation for the ordered region of CHIPS (36-113) and $C5aR_{7\text{-}28}S_2$ (10-23): Backbone atoms (C, Cα, N, O) = 0.081 ± 0.009 nm, and all heavy atoms = 0.122 ± 0.007 nm.

3.4 References

[1] R. F. Guo, P. A. Ward, Role of C5A in inflammatory responses, *Annu. Rev. Immunol.* **2005**, *23*, 821.

[2] P. J. Haas, J. A. G. van Strijp, Anaphylatoxins: their role in bacterial infection and inflammation, *Immunol. Res.* **2007**, *37*, 161.

[3] N. C. Riedemann, R. F. Guo, P. A. Ward, A key role of C5a/C5aR activation for the development of sepsis, *J. Leukocyte Biol.* **2003**, *74*, 966.

[4] T. Heller, M. Hennecke, U. Baumann, J. E. Gessner, A. M. zu Vilsendorf, M. Baensch, F. Boulay, A. Kola, A. Klos, W. Bautsch, J. Kohl, Selection of a C5a Receptor antagonist from phage libraries attenuating the inflammatory response in immune complex disease and ischemia/reperfusion injury, *J. Immunol* **1999**, *163*, 985.

[5] A. J. Strachan, T. M. Woodruff, G. Haaima, D. P. Fairlie, S. M. Taylor, A new small molecule C5a receptor antagonist inhibits the reverse-passive arthus reaction and endotoxic shock in rats, *J. Immunol.* **2000**, *164*, 6560.

[6] A. J. Hutchison, J. E. Krause, The discovery of small molecule C5a antagonists, *Annu. Rep. Med. Chem.* **2004**, *39*, 139.

[7] P. N. Monk, A. Scola, P. K. Madala, D. P. Fairlie, Function, structure and therapeutic potential of complement C5a receptors, *Br. J. Pharmacol.* **2007**, *152*, 429.

[8] L. M. Proctor, T. M. Woodruff, S. M. Taylor, Recent developments in C5/C5a inhibitors, *Expert Opin. Ther. Pat.* **2006**, *16*, 445.

[9] K. E. Veldkamp, H. C. J. M. Heezius, J. Verhoef, J. A. G. van Strijp, K. P. M. van Kessel, Modulation of neutrophil chemokine receptors by *Staphylococcus aureus* supernate, *Infect. Immun.* **2000**, *68*, 5908.

[10] C. J. C. de Haas, K. E. Veldkamp, A. Peschel, F. Weerkamp, W. J. B. Van Wamel, E. C. J. M. Heezius, M. J. J. G. Poppelier, K. P. M. Van Kessel, J. A. G. van Strijp, Chemotaxis inhibitory protein of *Staphylococcus aureus*, a bacterial antiinflammatory agent, *J. Exp. Med.* **2004**, *199*, 687.

[11] B. Postma, M. J. Poppelier, J. C. van Galen, E. R. Prossnitz, J. A. G. van Strijp, C. J. C. de Haas, K. P. M. van Kessel, Chemotaxis inhibitory protein of *Staphylococcus aureus* binds specifically to the C5a and formylated peptide receptor, *J. Immunol.* **2004**, *172*, 6994.

[12] P. J. Haas, C. J. C. de Haas, M. J. J. C. Poppelier, K. P. M. van Kessel, J. A. G. van Strijp, K. Dijkstra, R. M. Scheek, H. Fan, J. A. W. Kruijtzer, R. M. J. Liskamp, J. Kemmink, The structure of the C5a receptor-blocking domain of chemotaxis inhibitory protein of *Staphylococcus aureus* is related to a group of immune evasive molecules, *J. Mol. Biol.* **2005**, *353*, 859.

[13] E. R. P. Zuiderweg, D. G. Nettesheim, K. W. Mollisson, G. W. Carter, Tertiary structure of human complement component C5a in solution from nuclear magnetic resonance data, *Biochemistry* **1989**, *28*, 859.

[14] X. Zhang, W. Boyar, M. J. Toth, L. P. Wennogle, N. C. Gonella, Structural definition of the C5a C-terminus by two-dimensional nuclear magnetic resonance spectroscopy, *Proteins* **1997**, *28*, 261.

[15] B. Postma, W. Kleibeuker, M. J. J. G. Poppelier, M. Boonstra, K. P. M. Van Kessel, J. A. G. Van Strijp, C. J. C. de Haas, Residues 10-18 within the C5a receptor N-terminus compose a binding domain for chemotaxis inhibitory protein of *Staphylococcus aureus*, *J. Biol. Chem.* **2005**, *280*, 2020.

[16] Z. G. Chen, X. L. Zhang, N. C. Gonnella, T. C. Pellas, W. C. Boyar, F. Ni, Residues 21-30 within the extracellular N-terminal region of the C5a receptor represent a binding domain for the C5a anaphylatoxin, *J. Biol. Chem.* **1998**, *273*, 10411.

[17] C. Gerard, N. P. Gerard, C5a anaphylatoxin and Its 7 transmembrane-segment receptor, *Annu. Rev. Immunol.* **1994**, *12*, 775.

[18] B. O. Gerber, E. C. Meng, V. Dotsch, T. J. Baranski, H. R. Bourne, An activation switch in the ligand binding pocket of the C5a receptor, *J. Biol. Chem.* **2001**, *276*, 3394.

[19] D. R. March, L. M. Proctor, M. J. Stoermer, R. Sbaglia, G. Abbenante, R. C. Reid, T. M. Woodruff, K. Wadi, N. Paczkowski, J. D. A. Tyndall, S. M. Taylor, D. P. Fairlie, Potent cyclic antagonists of the complement C5a receptor on human polymorphonuclear leukocytes. Relationships between structures and activity, *Mol. Pharmacol.* **2004**, *65*, 868.

[20] A. J. Wright, A. Higginbottom, D. Philippe, A. Upadhyay, S. Bagby, R. C. Read, P. N. Monk, L. J. Partridge, Characterisation of receptor binding by the chemotaxis inhibitory protein of *Staphylococcus aureus* and the effects of the host immune response, *Mol. Immunol.* **2007**, *44*, 2507.

[21] M. Farzan, C. E. Schnitzler, N. Vasilieva, D. Leung, J. Kuhn, C. Gerard, N. P. Gerard, H. Choe, Sulfated tyrosines contribute to the formation of the C5a docking site of the human C5a anaphylatoxin receptor, *J. Exp. Med.* **2001**, *193*, 1059.

[22] D. E. van Epps, S. J. Simpson, R. Johnson, Relationship of C5a Receptor modulation to the functional responsiveness of human polymorphonuclear leukocytes to C5a, *J. Immunol.* **1993**, *150*, 246.

[23] J. Cavanagh, W. J. Fairbrother, A. G. Palmer, M. Rance, N. J. Skelton, *Protein NMR Spectroscopy: Principles and Practice (second edition)*, Elsevier Academic Press, San Diego, **2007**.

[24] K. L. Moore, The biology and enzymology of protein tyrosine *O*-sulfation, *J. Biol. Chem.* **2003**, *278*, 24243.

[25] N. Bannert, S. Craig, M. Farzan, D. Sogah, N. V. Santo, H. Choe, J. Sodroski, Sialylated O-Glycans and sulfated tyrosines in the NH2-terminal domain of CC chemokine receptor 5 contribute to high affinity binding of chemokines, *J. Exp. Med.* **2001**, *194*, 1661.

[26] R. A. Colvin, G. S. V. Campanella, L. A. Manice, A. D. Luster, CXCR3 requires tyrosine sulfation for ligand binding and a second extracellular loop arginine residue for ligand-induced chemotaxis, *Mol. Cell. Biol.* **2006**, *26*, 5838.

[27] C. T. Veldkamp, C. Seibert, F. C. Peterson, T. P. Sakmar, B. F. Volkman, Recognition of a CXCR4 sulfotyrosine by the chemokine stromal cell-derived factor-1α (SDF-1α/CXCL12), *J. Mol. Biol.* **2006**, *359*, 1400.

[28] J. Liu, S. Louie, W. Hsu, K. M. Yu, H. B. Nicholas, G. L. Rosenquist, Tyrosine sulfation is prevalent in human chemokine receptors important in lung disease, *Am. J. Resp. Cell Mol. Biol.* **2008**, *38*, 738.

[29] Swiss Institute of Bioinformatics, http://www.expasy.ch/tools/protparam.html, 13-05-2010.

[30] G. Wagner, K. Wuthrich, Sequential Resonance Assignments in Protein lH Nuclear Magnetic Resonance Spectra Basic Pancreatic Trypsin Inhibitor, *J. Mol. Biol.* **1982**, *155*, 347.

[31] M. Ikura, A. Bax, Isotope-filtered 2d NMR of a protein peptide complex - Study of a skeletal-muscle Myosin light chain kinase fragment bound to Calmodulin, *J. Am. Chem. Soc.* **1992**, *114*, 2433.

[32] G. Otting, K. Wuthrich, Heteronuclear filters in 2-dimensional [H-1, H-1] NMR-spectroscopy - Combined use with isotope labeling for studies of macromolecular conformation and intermolecular interactions, *Quat. Rev. Biophys.* **1990**, *23*, 39.

[33] A. L. Breeze, Isotope-filtered NMR methods for the study of biomolecular structure and interactions, *Prog. Nucl. Magn. Reson. Spectrosc.* **2000**, *36*, 323.

[34] F. Delaglio, S. Grzesiek, G. W. Vuister, G. Zhu, J. Pfeifer, A. Bax, Nmrpipe - a Multidimensional Spectral Processing System Based on Unix Pipes, *J. Biomol. NMR* **1995**, *6*, 277.

[35] J. P. Linge, M. Habeck, W. Rieping, M. Nilges, ARIA: automated NOE assignment and NMR structure calculation, *Bioinformatics* **2003**, *19*, 315.

[36] G. Cornilescu, F. Delaglio, A. Bax, Protein backbone angle restraints from searching a database for chemical shift and sequence homology, *J. Biomol. NMR* **1999**, *13*, 289.

[37] J. W. Ponder, D. A. Case, Force fields for protein simulations, *Adv. Protein Chem.* **2003**, *66*, 27.

[38] M. P. Williamson, J. Kikuchi, T. Asakura, Application of H-1-NMR chemical-shifts to measure the quality of protein structures, *J. Mol. Biol.* **1995**, *247*, 541.

[39] R. A. Laskowski, J. A. C. Rullmann, M. W. MacArthur, R. Kaptein, J. M. Thornton, AQUA and PROCHECK-NMR: Programs for checking the quality of protein structures solved by NMR, *J. Biomol. NMR* **1996**, *8*, 477.

[40] E. Krissinel, K. Henrick, Inference of macromolecular assemblies from crystalline state, *J. Mol. Biol.* **2007**, *372*, 774.

Chapter 4

CHIPS binds to the Phosphorylated N-terminus of the C5a-Receptor

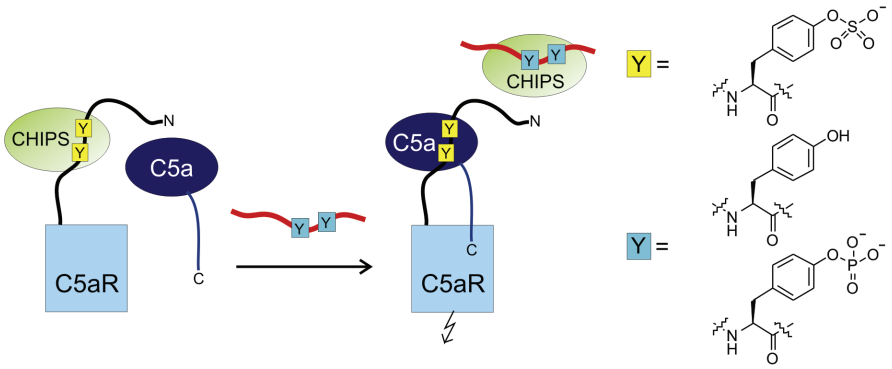

Parts of this chapter have been published:

A. Bunschoten, L. J. Feitsma, C. J. C. de Haas, J. A. W. Kruijtzer, R. M. J. Liskamp, J. Kemmink, *Bioorganic & Medicinal Chemistry Letters*, **2010,** *20*, 3338-3340.

4

4.1 Introduction

Post-translational modifications (PTM´s) are widely used in nature to regulate the structure and function of proteins.[1] PTM´s can be structurally very different, ranging from e.g., glycosylation and acetylation to methylation of arginine or lysine side-chains. On the other hand, seemingly very similar PTM´s, like phosphorylation and sulfation, exist. The introduced phosphate and sulfate moieties have roughly the same size, are both negatively charged and both can be present on the side-chain of tyrosine residues (Fig. 4.1). Despite their similarity, sulfated and phosphorylated tyrosine residues are believed to have very different biological functions and localization. Phosphorylation is mainly found intracellular and is involved in signal transduction pathways, while sulfation is believed to be an irreversible extracellular enhancement mechanism for protein-protein interactions.[2]

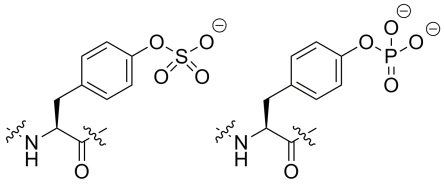

Figure 4.1 Structures of sulfotyrosine and phosphotyrosine.

In the literature several cases have been described in which sulfated tyrosine residues were replaced by their phosphorylated counterparts. Beiler and Martin showed already in 1948 that both the sulfated and phosphorylated flavanone glycoside hesperidin are potent inhibitors of hyaluronidase.[3] Baldwin et al. were the first to suggest that the sequence-requirements for phosphorylation and sulfation might be similar: They showed that gastrin, which is mainly sulfated in vivo, could be phosphorylated by EGF-stimulated tyrosine kinase of A431 cells.[4] Hofsteenge et al. showed that the blood anticoagulant hirudin, which contains a sulfated tyrosine at position 63 *in vivo*, could act as a substrate for tyrosine protein kinase III. Both the sulfated and phosphorylated hirudin showed a ten-fold increase in affinity for α-thrombin.[5] Rat progastrin, sulfated *in vivo*, can also be phosphorylated by three different tyrosine protein kinases.[6] Otvos et al. demonstrated that both sulfated and phophorylated rabies virus 31D peptides were capable of stimulating T-helper cells.[7] Sulfation and phosphorylation can even occur simultaneously. Waheed and Etten showed in 1985 that the glycoprotein aylsulfatase A contained both phosphate and sulfate groups. They could, however, not determine whether these groups were attached to the peptide or carbohydrate part of this enzyme.[8] Taylor et al. showed that the neuroendocrine peptide chrombacin contained both a sulfotyrosine and a phosphoserine.[9] Recently Dave et al. reported the presence of two sulfated serines next to a phosphorylated serine in the murine dioxin receptor.[10]

In contrast to these results, which suggest that there is little difference between sulfation and phosphorylation, several recent reports indicate the opposite view. Hoffhines et al. developed an anti-sulfotyrosine monoclonal antibody (PSG2), which shows a 13-fold higher affinity for a sulfated tyrosine over a phosphorylated tyrosine. In a peptide containing a sulfated tyrosine the affinity was even a 10^3-fold higher compared to the same peptide with the tyrosine phosphorylated.[11] Knight et al. remodelled a protease to cleave peptides containing a phosphorylated tyrosine residue. The catalytic efficiency of this enzyme for a peptide substrate containing a phosphorylated tyrosine appeared to be 5-fold higher compared to peptides containing an unmodified tyrosine and 2-fold higher compared to peptides containing a sulfated tyrosine.[12] The sulfated N-terminus of the CCR5 receptor plays a crucial role in HIV-1 infection by forming a binding site for the gp120:CD4 complex and in this way facilitating viral entry.[13] Lam et al. showed that a phosphorylated CCR5 peptide did not compete with native sulfated CCR5 peptide for binding to the CD4-activated gp120 complex.[14] Varadarajan et al. adapted a protease to specifically recognize sulfotyrosine-containing peptides. They were able to obtain a 200-fold increase in selectivity compared to phosphotyrosine-containing peptides.[15]

Figure 4.2 Amino acid sequence of residues 7-28 of the human C5aR (numbering according to Swiss-Prot entry **P21730**). The positions of the phosphorylated tyrosine residues *11* and *14* are in black. This peptide will be referred to as $C5aR_{7\text{-}28}$ with the addition of P_2 for the doubly phosphorylated peptide and P^{11} or P^{14} for the two mono-phosphorylated peptides.

The extracellular N-terminus of the C5a-receptor (C5aR) contains *in vivo* two sulfated tyrosine residues at position *11* and *14* (Fig. 4.2). These two sulfated tyrosine residues are essential for activation of this receptor by its endogenous ligand C5a.[16] Activation of the C5aR triggers recruitment of specific white blood cells to potential sites of infection.[17] This process can be inhibited by the Chemotaxis Inhibitory Protein of *Staphylococcus aureus* (CHIPS), which binds with high-affinity exclusively to the sulfated N-terminus of the C5aR.[18-20] A truncated version of CHIPS missing 30 residues at the N-terminus and designated $CHIPS_{31\text{-}121}$ appeared to have the same inhibitory potency compared to native CHIPS.[21] Peptides representing the N-terminal portion of the C5aR are valuable models for studying the interactions of CHIPS with the C5aR. In chapter 3 we described a 380-fold increase in affinity of $CHIPS_{31\text{-}121}$ for a peptide comprised of residues 7-28 of the C5a-receptor upon sulfation of tyrosine *11* and *14* as compared to the unsulfated C5aR peptide.

In this chapter the synthesis of phosphorylated $C5aR_{7\text{-}28}$ peptides will be described. The interactions of these phosphorylated peptides with $CHIPS_{31\text{-}121}$ were studied with ITC, NMR and in a biological assay and the effects of replacing the sulfate groups by phosphates are compared with the results obtained with the sulfated C5aR peptides described in chapter 3. In this way we gained more insight in the molecular interactions of CHIPS with the C5aR and into the biological significance of both PTM´s.

4.2 Results

Synthesis of phosphorylated C5aR mimics

Two C5aR mimics were synthesized by solid phase peptide synthesis, containing a single phosphorylated tyrosine at either position *11* ($C5aR_{7\text{-}28}P^{11}$) or *14* ($C5aR_{7\text{-}28}P^{14}$) as well as one C5aR mimic with both positions *11* and *14* phosphorylated ($C5aR_{7\text{-}28}P_2$). The phosphorylated tyrosine residue were introduced as the commercially available Fmoc-Tyr(PO(OBzl)OH)-OH building block and were coupled using an adapted coupling scheme. This procedure included using one additional equivalent of base during coupling of the phosphorylated building block and an additional ionic washing step (1.1M DIPEA, 1M TFA in NMP) after each Fmoc deprotection during the remaining coupling cycles to exchange the piperidinium counterions by tertiary ammonium ions.[22, 23]

ITC

The affinity of CHIPS for these three phosphorylated C5aR mimics was measured using Isothermal Titration Calorimetry (ITC). The dissociation constants (K_d) revealed that the phosphate groups had a significant influence on the binding affinity with CHIPS. Introduction of a phosphate group at position *11* resulted in a 13-fold increase in binding affinity as compared to the unphosphorylated peptide C5a$R_{7\text{-}28}$ (Table 4.1). Clearly, the phosphate group at position *14* was involved in even stronger interactions since this phosphate group increased the binding affinity 70-fold. Finally, a 100-fold higher affinity compared to its unphosphorylated version was determined for the doubly phosphorylated peptide C5a$R_{7\text{-}28}P_2$ (K_d = 29.4 nM). A similar trend has been observed for sulfated C5aR mimics in chapter 3.

Table 4.1 Thermodynamic binding parameters of $CHIPS_{31\text{-}121}$:C5aR phosphopeptide complexes determined by ITC

Peptide	K_d (nM)	ΔG (kJ mol^{-1})	ΔH (kJ mol^{-1})	ΔS (J $K^{-1}mol^{-1}$)
C5a$R_{7\text{-}28}$	(3.2±0.1)x10^3	-31.3±0.1	-78.0±2.5	-157±8
C5a$R_{7\text{-}28}P^{11}$	244±35	-37.1±0.4	-59.8±0.3	-78±2
C5a$R_{7\text{-}28}P^{14}$	47.5±3.1	-41.1±0.2	-67.7±0.4	-91±1
C5a$R_{7\text{-}28}P_2$	29.4±4.3	-42.3±0.4	-61.3±0.4	-65±2

The thermodynamic binding parameters revealed a small change of the binding enthalpy upon Phosphorylation and a more substantial change of the binding entropy resulting in a more negative ΔG and thus a higher affinity as compared to the unphosphorylated C5a$R_{7\text{-}28}$. Comparison of the three phosphorylated peptides showed that the difference in binding affinity was caused by both the enthalpy and the entropy penalty.

NMR experiments with the CHIPS:C5a$R_{7\text{-}28}P_2$ complex

In order to obtain more information about the mode of binding of CHIPS to phosphorylated C5aR mimics a ^{15}N-HSQC spectrum of ^{15}N-labelled CHIPS was recorded before and after addition of an excess of doubly phosphorylated receptor mimic C5a$R_{7\text{-}28}P_2$. Based upon previous assignments the chemical shift changes of the backbone amides of CHIPS were determined by titration with C5a$R_{7\text{-}28}P_2$.[19] A comparison of the amide ^{1}H-^{15}N chemical shift perturbations upon binding of either peptide C5a$R_{7\text{-}28}S_2$ or C5a$R_{7\text{-}28}P_2$ is presented in Fig. 4.3. The data of residues 31-36, 54-56, and 93 were omitted from the perturbation plot of the CHIPS:C5a$R_{7\text{-}28}P_2$ complex as these residues could not be assigned unambiguously on the bases of previous spectra.

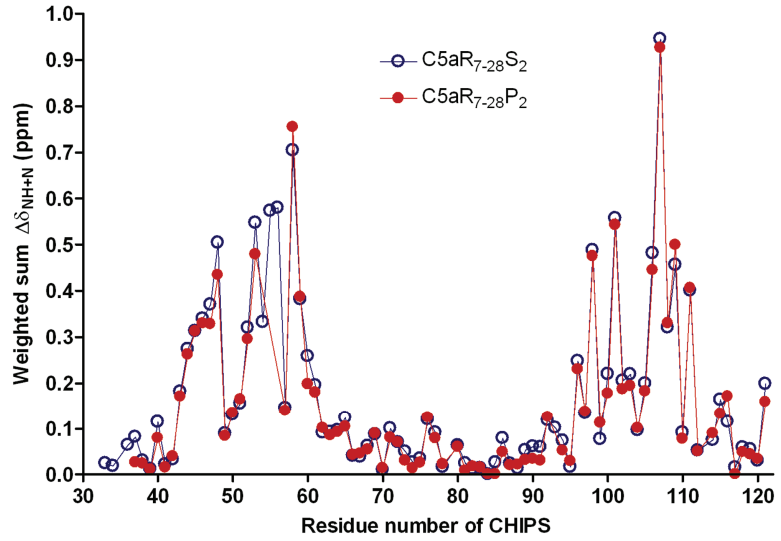

Figure 4.3 Weighted sum of CHIPS amide ^{15}N-^{1}H chemical shift changes ($\Delta\delta$(ppm) = $[(\Delta\delta_{NH})^2 + (0.1\Delta\delta_N)^2]^{1/2}$) upon binding of $C5aR_{7\text{-}28}S_2$ (O) or the $C5aR_{7\text{-}28}P_2$ (●). Data are plotted *vs.* residue number.

Biological activity of phosphorylated C5aR mimics

The phosphorylated C5aR mimics were also evaluated in a calcium mobilization assay to determine if they could compete with the native sulfated C5aR N-terminus. Activation of the C5aR by C5a was monitored in this assay by measuring the fluorescence of a U937/C5aR cell line loaded with a calcium sensitive Fluo-3 AM probe. Inhibition of the activation of the C5a-receptor by CHIPS can be prevented by the addition of C5aR mimics, restoring receptor activation by C5a.[19] At concentrations > 1 μM the phosphorylated peptides $C5aR_{7\text{-}28}P^{14}$ and $C5aR_{7\text{-}28}P_2$ competed with the native C5aR N-terminus present on the surface of the U937/C5aR cells. Peptide $C5aR_{7\text{-}28}P^{11}$ competed with the native C5aR N-terminus at concentrations > 10 μM (Fig. 4.4A). The previously obtained results with sulfated C5aR mimics (Fig. 4.4B) were described in chapter 3.

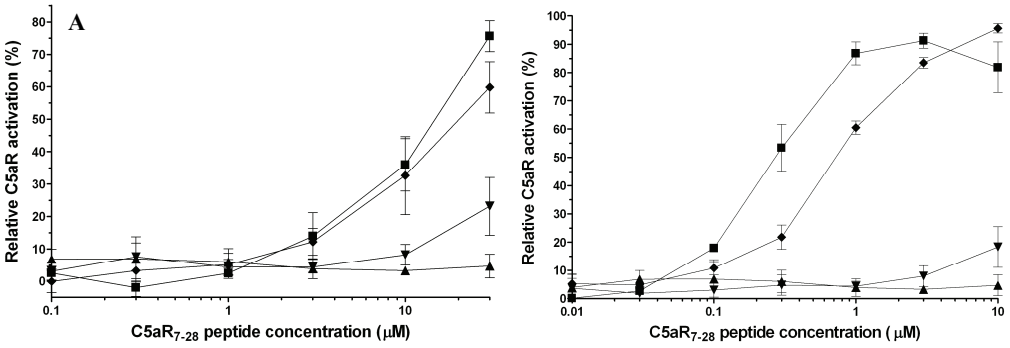

Figure 4.4 Calcium mobilization experiments: A) U937/C5aR cells were activated by 4 nM C5a in the presence of 10 nM CHIPS and increasing concentrations of $C5aR_{7-28}$ (▲),$C5aR_{7-28}P^{11}$ (▼), $C5aR_{7-28}P^{14}$ (♦) or $C5aR_{7-28}P_2$ (■). B) U937/C5aR cells were activated by 4 nM C5a in the presence of 10 nM CHIPS and increasing concentrations of $C5aR_{7-28}$ (▲), $C5aR_{7-28}S^{11}$ (▼), $C5aR_{7-28}S^{14}$ (♦) or $C5aR_{7-28}S_2$ (■) (Chapter 3).

4.3 Discussion

Both the mono phosphorylated and the doubly phosphorylated C5aR mimics, $C5aR_{7-28}P^{11}$, $C5aR_{7-28}P^{14}$, and $C5aR_{7-28}P_2$, were successfully synthesized by applying conventional Fmoc SPPS. The phosphorylated tyrosines were conveniently incorporated using an Fmoc-protected tyrosine building block with a monobenzylated phosphate group. ITC experiments with these peptides and $CHIPS_{31-121}$ revealed that the presence of phosphate groups resulted in significant higher affinities compared to the unphosphorylated C5aR mimics. The K_ds varied between 244 nM for $C5aR_{7-28}P^{11}$ to 29.4 nM for doubly phosphorylated $C5aR_{7-28}P_2$. The latter peptide bound 100-fold times stronger to $CHIPS_{31-121}$ than unphosphorylated $C5aR_{7-28}$ (K_d = 3.2 μM).[19]

Comparison of the phosphorylated peptides described here with the previously measured sulfated peptides (Chapter 3) revealed that phosphorylation of the C5aR N-terminus resulted in similar binding affinities as sulfation.[19, 24] Simultaneous modification of both tyrosine residues *11* and *14* led to the highest affinity for CHIPS. The difference in contribution of tyrosine residues *11* and *14* to the overall affinity showed a similar trend. In case of sulfation it was previously concluded that tyrosine *14* of the C5aR contributes most to the affinity with CHIPS. This can be rationalized from numerous interactions between sulfated tyrosine *14* and the CHIPS 52-59 binding loop (Chapter 3). The same structural features also seemed to be present in case of phosphorylated tyrosine residue *14*. The difference between the two functionalized tyrosine residues was, however, larger for the sulfated form: $C5aR_{7-28}P^{11}$ bound stronger to CHIPS than its sulfated version $C5aR_{7-28}S^{11}$.[24] Similar behaviour of the functionalized C5aR mimics suggests that CHIPS binds to sulfated and phosphorylated C5aR mimics in the same way.

Similarity in structure between phosphorylated *versus* sulfated C5a-receptor mimics in complex with $CHIPS_{31-121}$ was further supported by NMR spectroscopy. An almost identical pattern of chemical shift perturbations was observed in ^{15}N-HSQC spectra of $CHIPS_{31-121}$ upon addition of $C5aR_{7-28}S_2$ or $C5aR_{7-28}P_2$. This is a strong indication for the presence of similar structural features in both cases.

Surprisingly, the phosphorylated peptides were less active in the calcium mobilization assay as compared to sulfated peptides (Fig. 4.4). Approximately 30-fold higher concentrations of $C5aR_{7-28}P_2$ were needed to compete with the native C5aR N-terminus.[19] This observation was in apparent contradiction with the results obtained from ITC and NMR experiments which revealed similar affinities and modes of binding for either phosphorylated or sulfated C5aR mimics. Several factors may account for this different behaviour. Doubly charged cations (Mg^{2+}, Ca^{2+}) and high

concentrations of Human Serum Albumin (HSA) in the growth medium of the U937/C5aR cells can form a complex with the phosphorylated peptides. Also the presence of fast-acting phosphatases in the cell medium or a higher affinity of other membrane bound proteins for phosphorylated peptides might interfere with the ability of the phosphorylated C5aR mimics to compete with the native receptor.

In conclusion, sulfated and phosphorylated peptide mimics comprising residues *7-28* of the C5aR had comparable affinity for the Chemotaxis Inhibitory Protein of *Staphylococcus aureus* (CHIPS). The affinity of $CHIPS_{31\text{-}121}$ for the doubly phosphorylated/sulfated peptides $C5aR_{7\text{-}28}P_2$ and $C5aR_{7\text{-}28}S_2$ is at least two orders of magnitude higher compared to the bare $C5aR_{7\text{-}28}$ peptide. NMR spectroscopic studies indicated that the complexes of either sulfated or phosphorylated peptides with CHIPS include very similar structural features. Thus, the phosphorylated C5aR peptide mimic is an attractive alternative compared to its sulfated version in *in vitro* studies because of its convenient chemical synthesis and improved stability. Replacement of sulfated C5aR mimics by phosphorylated mimics in *in vivo* experiments is less evident as the biological activity of the phosphorylated peptides was significantly less than the sulfated peptides. Apparently other extracellular constituents or mechanisms present in such assays or in *vivo* may interfere with binding or the activity of phosphorylated constructs.

4.4 Experimental

General

Peptide grade DIPEA, DCM, NMP, TFA, and HPLC grade solvents were purchased from Biosolve B. V. (Valkenswaard, The Netherlands). The Fmoc-protected amino acids were purchased from GL Biochem Ltd (Shanghai, China). The side chain protecting groups were chosen as: Boc for lysine; *t*Bu for aspartic acid, threonine and tyrosine; Trt for asparagine and histidine. Fmoc-Tyr(PO(OBzl)OH)-OH was purchased from EMD/Novabiochem (gibbstown, USA). Unless stated otherwise, chemicals were obtained from commercial sources and used without further purification. ^{1}H NMR, ^{13}C NMR and two dimensional spectra were obtained on a Varian 500 MHz spectrometer. Chemical shifts are given in ppm with respect to internal standard TMS for ^{1}H NMR.

Analytical HPLC was performed using an automatic HPLC system (Shimadzu) with an analytical reversed-phase column, a UV detector operating at 214 nm with a flow rate of 0.75 mL/min. A Phenomenex Gemini C18 (110 Å**,** 5 µm, 250 x 4.6 mm) column was used. Either TFA buffers (buffer A: H_2O:MeOH, 80:20, v:v; buffer B: MeOH:H_2O:, 95:5, v:v, both containing 0.1% TFA) or TEAP buffers (buffer A: H_2O:CH_3CN, 95:5, v:v; buffer B: CH_3CN:H_2O:, 60:40, v:v both containing 25 mM triethylamine with the pH adjusted to 4.5 by addition of phosphoric acid) were used. Elution was effected with a linear gradient from 100% A to 100% B over 48 min.

Preparative HPLC was performed using an automatic Prep LCMS-QP8000α HPLC system (Shimadzu) with a preparative reversed-phase column, a UV detector operating at 214 nm with a flow rate of 12.5 mL/min. A Phenomenex Gemini C18 (110 Å, 10 μm, 250 x 21.2 mm) column was used. Either TFA buffers (buffer A: H_2O:MeOH, 80:20, v:v; buffer B: MeOH:H_2O:, 95:5, v:v, both containing 0.1% TFA) or TEAP buffers (buffer A: H_2O:CH_3CN, 95:5, v:v; buffer B: CH_3CN:H_2O, 60:40, v:v both containing 25 mM triethylamine with the pH adjusted to 4.5 by addition of phosphoric acid) were used. Elution was effected with a linear gradient from 100% A to 100% B over 100 min.

The peptides were characterized using electrospray mass spectrometry (ESI-MS) and this was performed on a Thermo Finnigan LCQ DECA XP MAX ion trap mass spectrometer or a Shimadzu LCMS-QP8000 single quadrupole bench-top mass spectrometer.

C5aR$_{7\text{-}28}$P$_2$:

Diphosphorylated peptide C5aR$_{7\text{-}28}$P$_2$ was synthesized on a Tentagel™ S RAM resin (0.24 mmol/g) (Rapp Polymere GmbH, Germany) on a 0.25 mmol scale. The peptide was assembled on an automatic ABI 433A Peptide Synthesizer using the ABI FastMoc 0.25 mmol protocols, except for the coupling of the Fmoc-Tyr(PO(OBzl)OH)-OH and for the couplings following the coupling of the phosphorylated building block.[25, 26] The synthesis was carried out on 1.04 g resin. The resin was washed with DCM and NMP (5 times, 10 mL). After cleavage of the Fmoc-group by means of a 20% piperidine solution in NMP (3 min. and 7.6 min.), 1 mmol of the appropriate amino acid was dissolved in NMP (2 mL), and HBTU/HOBt (1 mmol, 2.78 mL of 0.36 M in NMP) was added. To this mixture DIPEA (1 mL, 2 M in NMP) was added, and the activated amino acid was then transferred to the reaction vessel. After 45 min, the reaction vessel was drained and the resin was washed with NMP (3 times, 10 mL). Next acetylation of any remaining free amino groups with an acetic anhydride capping solution (0.5 M Ac_2O, 0.125 M DIPEA, and 0.015 M HOBt in NMP) was performed for 15 min. After capping the Fmoc group was removed by treatment with 20% piperidine solution in NMP (3 min. and 7.6 min.). Deprotection and coupling reactions were followed by monitoring the dibenzofulvene-piperidine adduct at 301 nm.[26]

During the coupling of Fmoc-Tyr(PO(OBzl)OH)-OH one additional equivalent of DIPEA was added (1.5 mL, 2M in NMP).[22] For the remaining coupling steps after the introduction of a phosphorylated building block an additional washing cycle with an ion exchange solution (1.1M DIPEA, 1M TFA in NMP, 2 times 5 min., 10 mL) was included after each deprotection of the Fmoc group after coupling of the phosphorylated building block to exchange the piperidinium counterion for a tertiary ammonium ion.[23] Standard coupling procedures can be used for the remaining residues after this ion exchange. The last coupling cycle was followed by removal of the Fmoc-group by a 20% piperidine solution, washing the resin with NMP, and acetylation of the N-terminus by treatment with acetic anhydride capping solution (0.5 M Ac_2O, 0.125 M DIPEA, and 0.015 M HOBt in NMP) for 15 min.

Finally, the resin was washed with NMP (5 times 10 mL) and DCM (6 times 10 mL), removed from the reaction vessel, washed with ether, and dried *in vacuo* over P_2O_5.
The anchored peptide thus obtained was deprotected and cleaved from the solid support by treatment with TFA/H_2O/TIS (95/2.5/2.5, 25 mL), for 2 h at room temperature. The mixture was then filtered and the residue washed thoroughly with TFA (2 times 10 mL). The reaction mixture was concentrated *in vacuo* to a volume of approximately 10 mL and added drop wise to 90 mL MTBE/n-hexane (1/1, v/v) solution. The precipitate was collected by centrifugation (3000 rpm, 10 min.). The supernatant was decanted, the pellets were resuspended in MTBE/n-hexane (1/1, v/v, 100 mL) and centrifuged again. This was repeated twice. After this, the pellets were dissolved in CH_3CN/H_2O (1/1, v/v, ca. 60 mL) and lyophilized to give 635 mg of the crude peptide as a white fluffy solid.
Part of the crude peptide (80 mg) was dissolved in 8 mL buffer A, 2 mL buffer B and purified by preparitive HPLC (Gemini C18, 25 mM TEAP buffers pH 4.5) in two runs. Fractions containing the pure product were pooled and lyophilized. To remove the salts of the buffers used during purification, the product was purified again by preparative HPLC (Prosphere C4, 10mM Ammonium acetate buffers) to give 16 mg (19%) of pure $C5aR_{7\text{-}28}P_2$.
The purity of $C5aR_{7\text{-}28}P_2$ was established by analytical HPLC (Gemini C18, TFA buffers, Rt = 25.3 min., purity>98%) and characterization was carried out by ESI-MS (monoisotopic mass $[M+2H]^{2+}$ calcd for $C_{111}H_{168}N_{28}O_{48}P_2$, 1362.55; found, 1362.88).

$C5aR_{7\text{-}28}P^{11}$:

Monophosphorylated peptide $C5aR_{7\text{-}28}P^{11}$ was synthesized on Tentagel™ S RAM resin (0.24 mmol/g) following the same procedure as described for $C5aR_{7\text{-}28}P_2$ at 0.25 mmol scale (1.07 g resin). The thus obtained peptide was deprotected and cleaved from the resin as was described for $C5aR_{7\text{-}28}P_2$, which resulted in 560 mg crude peptide.
Half of the crude peptide (250 mg) was dissolved in 25 mL buffer A and purified by preparative HPLC (Gemini C18, TFA buffers) in five runs. Fractions containing the pure product were pooled and lyophilized to give 75 mg (23%) of pure peptide. The purity of $C5aR_{7\text{-}28}P^{11}$ was established by analytical HPLC (Gemini C18, TFA buffers, Rt = 25.6 min., purity>90%) and characterization was carried out by ESI-MS (monoisotopic mass $[M+2H]^{2+}$ calcd for $C_{111}H_{167}N_{28}O_{45}P$: 1322.57; found: 1322.97).

$C5aR_{7\text{-}28}P^{14}$:

Monophosphorylated peptide $C5aR_{7\text{-}28}P^{14}$ was synthesized on Tentagel™ S RAM resin (0.24 mmol/g) following the same procedure as described for $C5aR_{7\text{-}28}P_2$ at 0.25 mmol scale (1.05 g resin). The peptide thus obtained was deprotected and cleaved from the resin as described for $C5aR_{7\text{-}28}P_2$, which resulted in 532 mg crude peptide.
Half of the crude peptide (300 mg) was dissolved in 30 mL buffer A and purified by preparative HPLC (Gemini C18, TFA buffers) in six runs. Fractions containing the pure product were pooled and lyophilized to give 69 mg (17%) of pure peptide. The purity of $C5aR_{7\text{-}28}P^{14}$ was established by

analytical HPLC (Gemini C18, TFA buffers, Rt = 26.1 min., purity>90%) and characterization was carried out by ESI-MS (monoisotopic mass $[M+2H]^{2+}$ calcd for $C_{111}H_{167}N_{28}O_{45}P$: 1322.57; found: 1323.08).

ITC experiments

The ITC measurements of the unphosphorylated, diphosphorylated and both mono-phosphorylated peptides ($C5aR_{7\text{-}28}$, $C5aR_{7\text{-}28}P^{11}$, $C5aR_{7}\text{-}28P^{14}$ and $C5aR_{7\text{-}28}P_2$) were performed at 293 K on an ITC_{200} Microcalorimeter (MicroCal / GE Healthcare). The measuring cell was filled with 208 µL of a 26 µM solution of $CHIPS_{31\text{-}121}$ in a 20 mM sodium phosphate buffer at pH 6.5. The syringe was loaded with 30 µL of a 0.5 mM solution of one of the peptides in the same buffer. After each addition of 1 µL of peptide solution, the heat change due to binding of the added peptide was measured. The data were analyzed using Microcal Origin software and fitted by non-linear regression analysis. The errors were estimated by performing a Monte Carlo simulation.

NMR experiments

The ^{15}N-HSQC spectra of $CHIPS_{31\text{-}121}$ and of $CHIPS_{31\text{-}121}$ in complex with $C5aR_{7\text{-}28}P_2$ were recorded on a Varian Inova 500 at room temperature. CHIPS was dissolved in 15/1 (v/v) H_2O/D_2O sodium phosphate buffers (20 mM, pH 6.5) at a concentration of 1.4 mM. 25 µL of a solution of $C5aR_{7\text{-}28}P_2$ (85 mM) was added until saturation of binding to CHIPS was accomplished. Chemical shift changes of the backbone amides of CHIPS are followed upon binding with $C5aR_{7\text{-}28}P_2$ and the chemical shift changes are summed ($\Delta\delta$ (ppm) = $[(\Delta\delta_{NH})^2 + (0.1\Delta\delta_N)^2]^{1/2}$ and plotted against the residues of CHIPS.

Biological assay

Calcium mobilization studies were performed in Fluo-3-labeled U937/C5aR cells as was described earlier.[19, 21] The potency of the peptides $C5aR_{7\text{-}28}$, $C5aR_{7\text{-}28}P^{11}$, $C5aR_{7\text{-}28}P^{14}$ and $C5aR_{7\text{-}28}P_2$ to block the inhibiting effect of CHIPS on the C5a-induced calcium mobilization was investigated. Therefore, 10 nM $CHIPS_{31\text{-}121}$ was pre-incubated with peptides $C5aR_{7\text{-}28}$ $C5aR_{7\text{-}28}P^{11}$, $C5aR_{7\text{-}28}P^{14}$ and $C5aR_{7\text{-}28}P_2$ (10 nM to 30 µM) for 30 min at room temperature. Next, the CHIPS/peptide mixture was added to Fluo-3-labeled U937/C5aR cells for 30 s before 4 nM C5a was used as a stimulus for calcium mobilization. The increase in fluorescent signals was measured with a FACSCalibur flow cytometer (Becton Dickinson).

4.5 References

[1] C. T. Walsh, S. Garneau-Tsodikova, G. J. Gatto, Protein posttranslational modifications: The chemistry of proteome diversifications, *Angew. Chem. Int. Ed.* **2005**, *44*, 7342.

[2] C. Seibert, T. P. Sakmar, Toward a framework for sulfoproteomics: Synthesis and characterization of sulfotyrosine-containing peptides, *Biopolymers* **2008**, *90*, 459.

[3] J. M. Beiler, G. J. Martin, Inhibition of hyaluronidase action by derivatives of hesperidin, *J. Biol. Chem.* **1948**, *174*, 31.

[4] G. S. Baldwin, J. Knesel, J. M. Monckton, Phosphorylation of gastrin-17 by epidermal growth factor-stimulated tyrosine kinase, *Nature* **1983**, *301*, 435.

[5] J. Hofsteenge, S. R. Stone, A. Donelladeana, L. A. Pinna, The effect of substituting phosphotyrosine for sulphotyrosine on the activity of Hirudin, *Eur. J. Biochem.* **1990**, *188*, 55.

[6] A. Donelladeana, A. Varro, G. J. Dockray, L. A. Pinna, Substitution of phosphotyrosine for sulphotyrosine in biologically-active peptides - enzymatic phosphorylation of a progastrin peptide confers immunoreactivity reminiscent of the sulfated derivative, *Biochim. Biophys. Acta* **1991**, *1095*, 75.

[7] L. Otvos, B. Cappelletto, I. Varga, J. D. Wade, Z. Q. Xiang, K. Kaiser, L. J. Stephens, H. C. J. Ertl, The effects of post-translational side-chain modifications on the stimulatory activity, serum stability and conformation of synthetic peptides carrying T helper cell epitopes, *Biochim. Biophys. Acta, Mol. Cell Res.* **1996**, *1313*, 11.

[8] A. Waheed, R. L. Etten, Phosphorylation and sulfation of arylsulfatase A accompanies biosynthesis of the enzyme in normal and carcinoma cell lines, *Biochim. Biophys. Acta* **1985**, *847*, 53.

[9] S. W. Taylor, C. Z. Sun, A. Hsieh, N. L. Andon, S. S. Ghosh, A sulfated, phosphorylated 7 kDa secreted peptide characterized by direct analysis of cell culture media, *J. Proteome Res.* **2008**, *7*, 795.

[10] K. A. Dave, F. Whelan, C. Bindloss, S. G. B. Furness, A. Chapman-Smith, M. L. Whitelaw, J. J. Gorman, Sulfonation and phosphorylation of regions of the dioxin receptor susceptible to methionine modifications, *Mol. Cell. Proteomics* **2009**, *8*, 706.

[11] A. J. Hoffhines, E. Damoc, K. G. Bridges, J. A. Leary, K. L. Moore, Detection and purification of tyrosine-sulfated proteins using a novel anti-sulfotyrosine monoclonal antibody, *J. Biol. Chem.* **2006**, *281*, 37877.

[12] Z. A. Knight, J. L. Garrison, K. Chan, D. S. King, K. M. Shokat, A remodelled protease that cleaves phosphotyrosine substrates, *J. Am. Chem. Soc.* **2007**, *129*, 11672.

[13] M. Farzan, T. Mirzabekov, P. Kolchinsky, R. Wyatt, M. Cayabyab, N. P. Gerard, C. Gerard, J. Sodroski, H. Choe, Tyrosine sulfation of the amino terminus of CCR5 facilitates HIV-1 entry, *Cell* **1999**, *96*, 667.

[14] S. N. Lam, P. Acharya, R. Wyatt, P. D. Kwong, C. A. Bewley, Tyrosine-sulfate isosteres of CCR5 N-terminus as tools for studying HIV-1 entry, *Bioorg. Med. Chem.* **2008**, *16*, 10113.

[15] N. Varadarajan, G. Georgiou, B. L. Iverson, An engineered protease that cleaves specifically after sulfated tyrosine, *Angew. Chem. Int. Ed.* **2008**, *47*, 7861.

[16] M. Farzan, C. E. Schnitzler, N. Vasilieva, D. Leung, J. Kuhn, C. Gerard, N. P. Gerard, H. Choe, Sulfated tyrosines contribute to the formation of the C5a docking site of the human C5a anaphylatoxin receptor, *J. Exp. Med.* **2001**, *193*, 1059.

[17] R. F. Guo, P. A. Ward, Role of C5A in inflammatory responses, *Annu. Rev. Immunol.* **2005**, *23*, 821.

[18] B. Postma, M. J. Poppelier, J. C. van Galen, E. R. Prossnitz, J. A. G. van Strijp, C. J. C. de Haas, K. P. M. van Kessel, Chemotaxis inhibitory protein of *Staphylococcus aureus* binds specifically to the C5a and formylated peptide receptor, *J. Immunol.* **2004**, *172*, 6994.

[19] J. H. Ippel, C. J. C. De Haas, A. Bunschoten, J. A. G. van Strijp, J. A. W. Kruijtzer, R. M. J. Liskamp, J. Kemmink, Structure of the tyrosine-sulfated C5a Receptor N-terminus in complex with chemotaxis inhibitory protein of Staphylococcus aureus, *J. Biol. Chem.* **2009**, *284*, 12363.

[20] B. Postma, W. Kleibeuker, M. J. J. G. Poppelier, M. Boonstra, K. P. M. Van Kessel, J. A. G. Van Strijp, C. J. C. de Haas, Residues 10-18 within the C5a receptor N terminus compose a binding domain for chemotaxis inhibitory protein of *Staphylococcus aureus*, *J. Biol. Chem.* **2005**, *280*, 2020.

[21] P. J. Haas, C. J. C. de Haas, M. J. J. C. Poppelier, K. P. M. van Kessel, J. A. G. van Strijp, K. Dijkstra, R. M. Scheek, H. Fan, J. A. W. Kruijtzer, R. M. J. Liskamp, J. Kemmink, The structure of the C5a receptor-blocking domain of chemotaxis inhibitory protein of *Staphylococcus aureus* is related to a group of immune evasive molecules, *J. Mol. Biol.* **2005**, *353*, 859.

[22] P. White, Optimization of coupling methods for the introduction of mono-benzyl phosphate esters of fmoc protected phosphoamino acids, Abstract of the 17th American Peptide Symposium, San Diego, USA, **2001**, 97.

[23] R. Pascal, P. O. Schmit, C. Mendre, M. N. Dufour, G. Guillon, Use of diisopropylcarbodiimide in the solid-phase synthesis of phosphorylated peptides by the preformed phosphoamino acid building block approach, Abstract of the 26th European Peptide Symposium, Montpellier, France, **2000**, 263.

[24] A. Bunschoten, J. A. W. Kruijtzer, J. H. Ippel, C. J. C. de Haas, J. A. G. van Strijp, J. Kemmink, R. M. J. Liskamp, A general sequence independent solid phase method for the site specific synthesis of multiple sulfated-tyrosine containing peptides, *Chem. Commun.* **2009**, 2999.

[25] A. Biosystems, *Applied Biosystems Model 433A Peptide Synthesizer User´s Manual* **June 1993**, version 1.0.

[26] A. Biosystems, *Applied Biosystems Research News* **June 1993**, Model 433A Peptide Synthesizer.

Chapter 5

A Peptide Mimic of the Chemotaxis Inhibitory Protein of *Staphylococcus aureus*: Towards the Development of novel Anti-Inflammatory Compounds

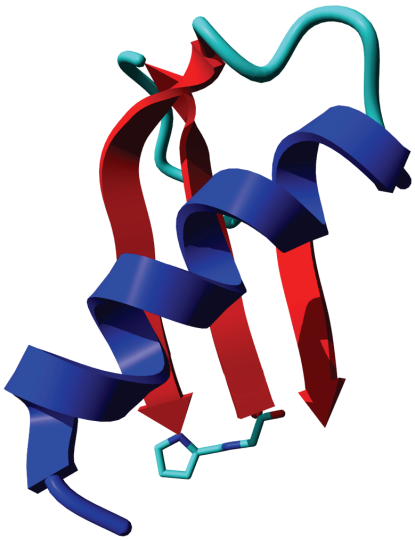

Parts of this chapter have been accepted for publication:

A. Bunschoten, J. H. Ippel, J. A. W. Kruijtzer, L. J. Feitsma, C. J. C. de Haas, R. M. J. Liskamp, J. Kemmink, *Amino* Acids, 2010.

5

5.1 Introduction

As part of the host defense system, the human complement cascade initiates inflammatory responses directed against invading infectious microorganisms, injury and other threatening conditions.[1] Complement factor C5a is the most powerful pro-inflammatory agent generated during complement activation. C5a interacts with the membrane-associated G-protein coupled C5a-receptor (C5aR) resulting in chemotaxis of specific white blood cells, activation of phagocytes, release of granule-based enzymes, and the generation of oxidants.[2] C5a is a 74-residue glycoprotein comprised of a bundle of four anti-parallel α-helices stabilized by three disulfide bonds (PDB ID code: 1KJS).

Binding and activation of the C5a-receptor by C5a is considered a two-step process, in which residues in the region between 12-46 of C5a bind to a primary binding site located in the extracellular N-terminus of the C5aR. Subsequently the C-terminal portion of C5a (residues 69-74) binds to the C5aR activation domain located inside the receptor core.[3, 4] Together these two binding sites provide the complex of C5a and the C5aR sub-nanomolar affinity ($K_d \approx 0.60$ nM).[5] Although under normal circumstances C5a-mediated C5aR activation is highly favorable, excessive levels of C5a can be deleterious to the host and have been related to numerous inflammatory and autoimmune diseases (e.g. rheumatoid arthritis, inflammatory bowel disease, reperfusion injury). Specific inhibition of C5aR activation is considered a promising strategy to treat such conditions.[6] So far, the design and development of novel anti-inflammatory agents was primarily focused on small organic compounds and short C5a peptide analogs, which bind with high affinity to the C5aR activation site.[6, 7] An alternative approach to inhibit C5aR activation was inspired by the discovery of the Chemotaxis Inhibitory Protein of *Staphylococcus aureus* abbreviated as CHIPS.[8] CHIPS is a 121-residue immune evasive protein excreted by the *Staphylococcus aureus* bacteria in order to prevent host inflammatory responses triggered by formylated peptides and C5a. CHIPS binds to the formylated peptide receptor (FPR) and the C5aR with high affinity ($K_d = 35.4 \pm 7.7$ nM and $K_d = 1.1 \pm 0.2$ nM, respectively).[9] Mutational studies revealed that the C5aR blocking activity of CHIPS is entirely conserved in a protein fragment lacking the first 30 residues. This truncated protein was designated $CHIPS_{31\text{-}121}$ and its structure was solved by us.[10] $CHIPS_{31\text{-}121}$ has an entirely different folding topology compared to C5a and is composed of a single α-helix packed onto a four-stranded anti-parallel β-sheet. This particular topology is present in several other *S. aureus* proteins with immune modulating properties.[10]

In contrast to C5a, CHIPS binds exclusively to the C5aR N-terminus.[11] This part of the receptor is post-translationally modified by introduction of two sulfate groups on tyrosine residues at positions *11* and *14*.[12] Sulfation of these tyrosines appeared to be crucial for tight binding to $CHIPS_{31\text{-}121}$ as was concluded from ITC binding studies using several sulfated and unsulfated mimics of the C5aR N-terminus (Chapter 3).[13, 14] The highest affinity for $CHIPS_{31\text{-}121}$ ($K_d = 8.4 \pm 1.1$ nM) was observed for a peptide composed of residues *7-28* of the C5aR with both tyrosine residues sulfated (designated $C5aR_{7\text{-}28}S_2$).[13] This peptide binds almost as strong to CHIPS as the native C5aR. This implies that all moieties essential for the interactions between CHIPS and the C5aR are present within this peptide mimic. The free N-terminus of the C5aR is virtually unstructured, which is also the case for the short receptor mimics. Upon binding to CHIPS residues *10* to *24* of these C5aR mimics adopt a well-defined conformation (PDB ID code: 2K3U).[13] In the complex, residues *10-14* and *19-24* of $C5aR_{7\text{-}28}S_2$ form two short stretches of β-strand, which are hydrogen bonded in an anti-parallel fashion to strand β_4 and residues 104-107 of $CHIPS_{31\text{-}121}$, respectively. These two stretches are interconnected by a single turn comprised of residues *15-18*. Sulfated tyrosine *11* interacts mainly with residues in the α-helix of $CHIPS_{31\text{-}121}$, while sulfated tyrosine *14* is primarily accommodated by residues in the loop between the α-helix and the first β-strand (residues 52-59; Fig. 5.1). The sequence between

residues T66 and Y94 of $CHIPS_{31\text{-}121}$ does not contribute to interactions with the receptor, but are essential for its native structure.[13]

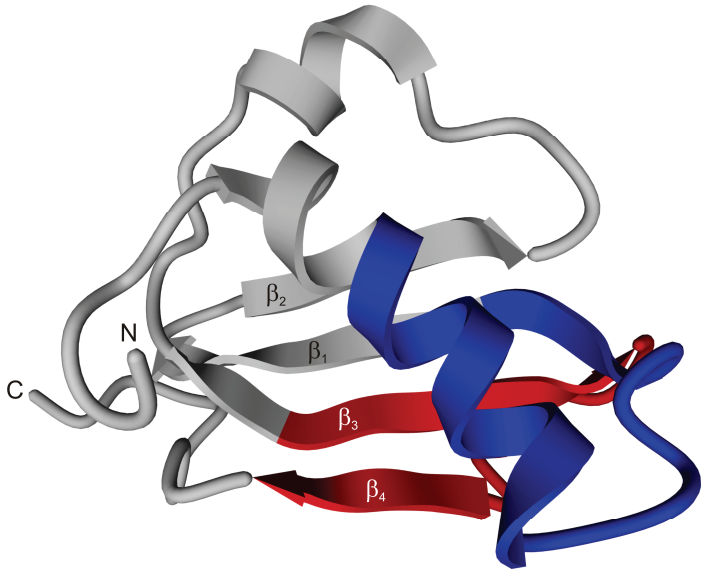

Figure 5.1 Cartoon representation of one of the NMR structures of $CHIPS_{31\text{-}121}$ (PDB ID code: 1XEE). The two regions interacting with the C5aR are indicated: Residues 43-61 in blue and residues 95-111 in red. The remainder of the protein is shown in gray. The N- and C-termini as well as the numbering of the β-strands are indicated.

Despite its strong C5aR inhibitory potency, intact CHIPS itself is not amenable for use as an anti-inflammatory agent. Several immunogenic surface epitopes have been identified by Gustafsson et al.[15] Recent studies showed the presence of anti-CHIPS antibodies in numerous serum samples of human donors.[16, 17] Therefore, administration of intact CHIPS protein can potentially lead to adverse immunogenic responses. Here, we describe the design, chemical synthesis, and analysis of a protein construct in which specific segments of CHIPS crucial for interactions with the C5aR have been incorporated while a number of non-interacting segments were omitted. We denote this protein construct with the acronym CHOPS, which stands for ´CHemotaxis inhibitory cOnstruct Protein of *Staphylococcus aureus*´. The ultimate goal is to obtain a CHOPS molecule, which is non-immunogenic, but has a high inhibitory potency for the C5aR.

5.2 Results

Design of CHOPS

The *Staphylococcal* protein CHIPS is one of the most potent inhibitors of C5a-induced inflammatory responses presently known. In contrast to the numerous agents developed to interact directly with the C5aR activation site located inside the receptor core,[18, 19] CHIPS blocks activation by C5a by binding with high affinity to the flexible extracellular N-terminal portion of the C5aR.[11] The interaction

surface of $CHIPS_{31-121}$ with the C5aR comprises ~20% of its solvent accessible surface and is not confined to a limited region of the protein. The interactions between CHIPS and the C5aR involve a substantial number of non-sequential amino acids optimally positioned in the inhibitory protein to provide tight binding. A successful mimic of CHIPS should not only include the amino acid residues (or mimics of these) crucial for C5aR binding, but also the amino acids responsible for the proper spatial arrangement dictated by the CHIPS folding topology. Our first approach to build such a structure was to leave out a limited number of residues which do not interact directly with the C5aR, but with the intention to leave the structural integrity of $CHIPS_{31-121}$ intact. NMR titration studies revealed that two regions of $CHIPS_{31-121}$ show relatively large perturbations in the backbone and Cβ chemical shifts:[13] The first region includes residues 43-61, which comprises part of the α-helix and the subsequent loop connecting strand β_1 (Fig. 5.1). The second region is composed of residues 95-111 and comprises strands β_3 and β_4 of $CHIPS_{31-121}$. The non-interacting portion of $CHIPS_{31-121}$ comprises strand β_2 and the long loop connecting β_2 with β_3 (Fig. 5.1). This portion could potentially be left out by directly connecting strand β_1 with β_3 via a tight turn.

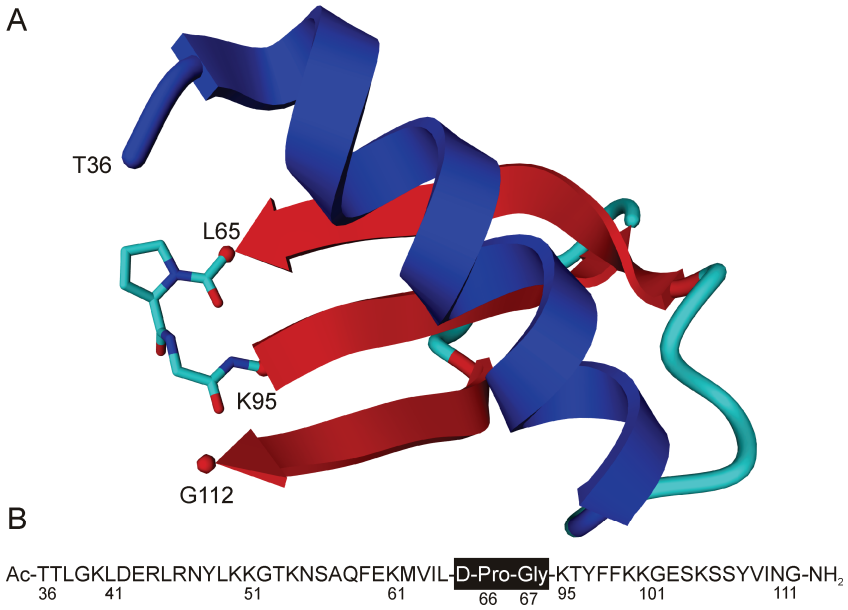

Figure 5.2 Characteristics of the CHOPS construct. A) Cartoon representation of CHOPS based on the structure of $CHIPS_{31-121}$. The D-Pro-Gly linker is shown in stick representation. The α-helix is colored blue, the β-sheets red. The numbering of terminal residues and of the residues flanking the linker is indicated. B) The amino acid sequence of CHOPS. The numbering is according to Swiss-Prot entry A6QIG7 without the signal peptide. The position of the D-Pro-Gly linker sequence is indicated in black.

Inspection of the NMR structural models of $CHIPS_{31-121}$ revealed that residue L65 at the end of strand β_1 and residue K95 at the start of strand β_3 are proximal and offered an excellent opportunity to link the two fragments interacting with the C5aR together to form one short, contiguous sequence. Several β-hairpin inducing–sequences have been described and reviewed in the literature.[20, 21] One of the smallest peptide fragments, which induces a β-turn and facilitates the formation of an anti parallel β-sheet, is the dipeptide D-Pro-Gly.[22] This fragment was chosen to link the N- and C-terminal segments of CHIPS, which interact with the C5aR, together. These segments were chosen to comprise the complete elements of secondary structure as present in native CHIPS (i.e. the α-helix and β-strands β_1, β_3, and β_4) in order to pursue structural integrity. The resulting construct consisted of the CHIPS amino acid sequences T36-L65 and K95-G112 interconnect by D-Pro-Gly (Fig. 5.2). A number of residues suggested to be part of discontinuous immunogenic epitopes by Gustafsson et al. are not present in this construct (designated CHOPS).[15] A model representation of CHOPS based on the structure of native $CHIPS_{31-121}$ is presented in Fig. 5.2A.

Affinity of CHOPS for the C5aR N-terminus

The affinity of the CHOPS fragment for the C5aR was determined by using isothermal titration calorimetry (ITC). We synthesized two peptide mimics of the C5aR N-terminus: Unsulfated peptide $C5aR_{7-28}$ representing residues *7-28* of the C5aR and peptide $C5aR_{7-28}S_2$, the same sequence with tyrosine residues *11* and *14* *O*-sulfated (Chapter 2). We titrated a solution of CHOPS with these peptides and recorded the subsequent heat exchange upon formation of the complex. Two typical ITC experiments are shown in Fig. 5.3. Clearly, titration of the doubly sulfated peptide $C5aR_{7-28}S_2$ to CHOPS resulted in a substantial exothermic effect (Fig. 5.3A) while no significant response was detected in the ITC experiment with the unsulfated peptide $C5aR_{7-28}$ (Fig. 5.3B). Gratifyingly, the affinity of CHOPS for $C5aR_{7-28}S_2$ was in the micromolar range (K_d = 3.6 ± 0.2 μM; n = 3). The thermodynamic analysis of these ITC data plus the comparison with previous ITC studies of $CHIPS_{31-121}$ and C5a peptide mimics is compiled in table 5.1.

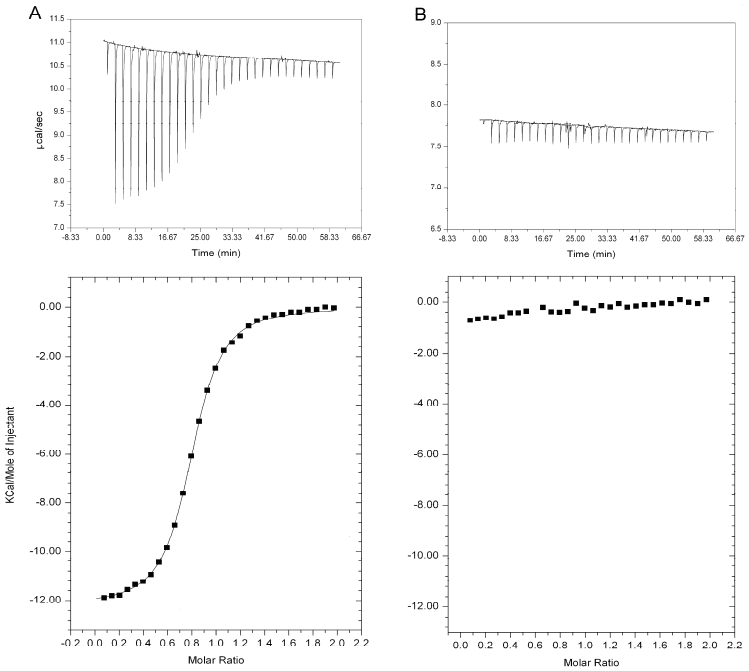

Figure 5.3 ITC titration experiments monitored at 283K. A) Titration of sulfated C5aR mimic $C5aR_{7\text{-}28}S_2$ to CHOPS. B) Titration of unsulfated $C5aR_{7\text{-}28}$ to CHOPS. The results of two typical binding experiments are shown in which 1 µL aliquots of 2.5 mM solutions of either C5aR mimic were titrated into a 0.19 mM solution of CHOPS. The upper two graphs are the raw data obtained from the titration experiments, the lower two graphs represent the integrated data-points and in case of A) the fitted binding curve.

Table 5.1 Thermodynamic binding parameters of $C5aR_{7\text{-}28}$ peptide complexes determined by ITC measured.

Complex[a]	**K_d (µM)**	**ΔG (kJ mol^{-1})**	**ΔH (kJ mol^{-1})**	**ΔS (J K^{-1} mol^{-1})**
$C5aR_{7\text{-}28}$:A[b]	3.2 ± 0.1	-31.3 ± 0.1	-78.0 ± 2.5	-157 ± 8
$C5aR_{7\text{-}28}$:B	-[c]	-	-	-
$C5aR_{7\text{-}28}S_2$:A[b]	(8.4 ± 1.1) x 10^{-3}	-46.1 ± 0.3	-94.5 ± 2.2	-162 ± 7
$C5aR_{7\text{-}28}S_2$:B	3.6 ± 0.2	-29.5 ± 0.2	-50.2 ± 0.7	-73 ± 3

[a]C5aR peptides are numbered according to Swiss-Prot entry P21730. The presence of sulfate groups on tyrosine residues *11* and *14* is indicated by S_2. A refers to the complex with $CHIPS_{31\text{-}121}$ while B refers to CHOPS. The data are averages from at least three independent experiments (mean ±SEM). The errors in the thermodynamic parameters were estimated by Monte Carlo simulations using the standard deviations of the individual experiments. [b]Data taken from Chapter 3. [c]No detectable binding observed.

NMR spectroscopy

Previous NMR studies revealed that the synthetic peptides $C5aR_{7\text{-}28}$ and $C5aR_{7\text{-}28}S_2$, which mimic the N-terminal portion of the C5aR, were very flexible in solution and did not have detectable propensity

for any preferred secondary structure. Although there is no detailed structure available of the intact C5aR, it is expected that its free extracellular N-terminus (residues 1-35) is unstructured as well. The protein $CHIPS_{31-121}$ does adopt a well-defined conformation with flexible regions at the termini and some disorder in the loop region between the α-helix and strand β_1.[10] As could be inferred from ^{15}N relaxation studies this particular loop region adopts an ordered conformation in the complex with $C5aR_{7-28}S_2$ (Chapter 3).[13] NMR spectra of the free CHOPS construct appear to be typical for a largely unstructured polypeptide chain (Fig. 5.4A). 2D NOE spectra of free CHOPS contain predominantly sequential NOE´s, but a few long-range contacts could be identified. These non-sequential cross-peaks are indicative for an anti-parallel orientation of strands β_1 and β_3, which are bridged by the β-hairpin inducing D-Pro-Gly sequence (Fig. 5.5).

Titration of CHOPS with the unsulfated receptor mimic $C5aR_{7-28}$ did not result in any changes in the ^1H-spectrum of the latter. In contrast, titration of CHOPS with the sulfated receptor mimic $C5aR_{7-28}S_2$ resulted in increased dispersion of resonance lines, which is characteristic for non-random coil behavior (Fig. 5.4B). The complex between CHOPS and $C5aR_{7-28}S_2$ is still flexible and the ^1H-spectra show a high degree of overlap. Nevertheless, some of the NMR signals could be assigned as indicated in Fig. 5.4B. These new signals are at comparable positions as in spectra of the complex between $CHIPS_{31-121}$ and $C5aR_{7-28}S_2$, and are indicative for the formation of native-like structure. Similar features were observed in ^1H-^{13}C HSQC spectra upon titration of $C5aR_{7-28}S_2$ to CHOPS (Fig. 5.6).

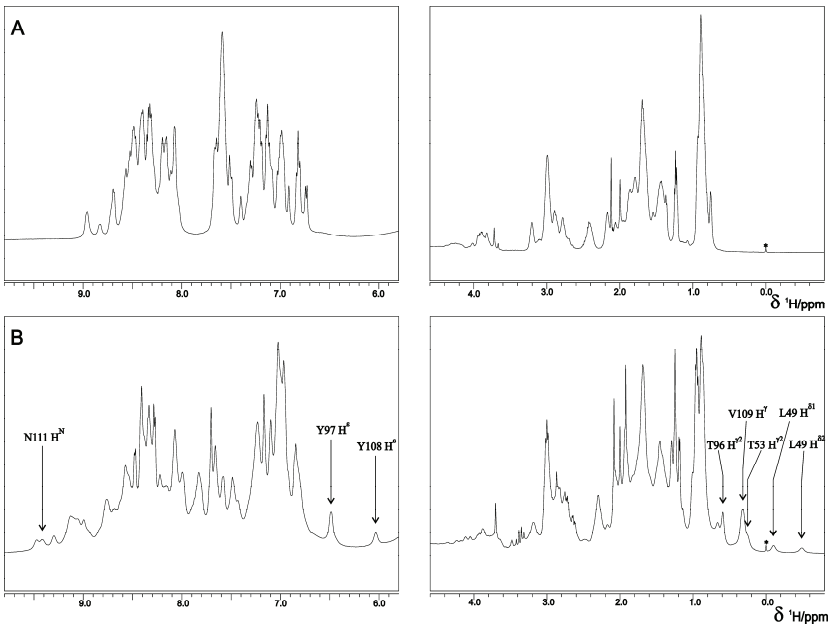

Figure 5.4 1D ^1H-NMR spectra of CHOPS. A) Spectrum of free CHOPS. B) Spectrum of CHOPS in a 1:1 complex with receptor mimic $C5aR_{7-28}S_2$. Several signals, which could be assigned based on 2D-experiments are labeled in the spectra. The chemical shift reference compound is indicated by an asterisk.

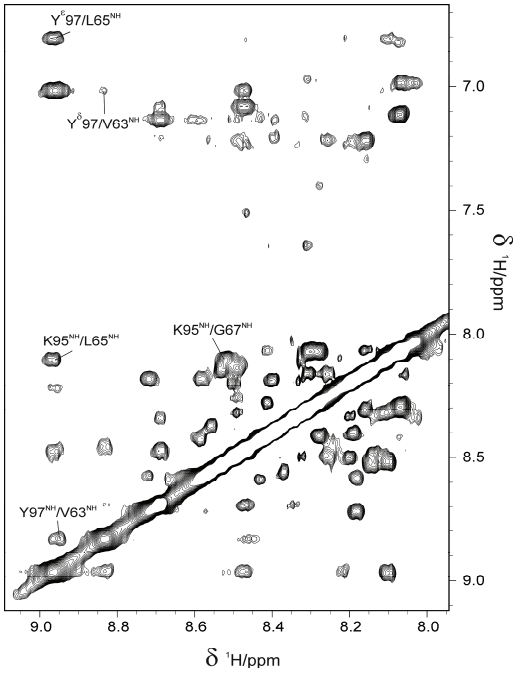

Figure 5.5 Section of the NOESY spectrum of free CHOPS in solution. Several non-sequential cross peak assignments are shown indicative for the presence of a β-hairpin comprising strands β_1 and β_3.

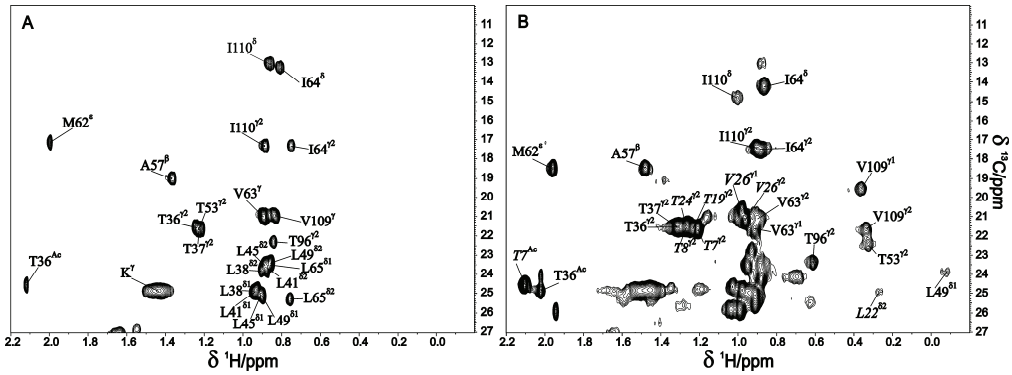

Figure 5.6 ^{1}H-^{13}C HSQC spectra of CHOPS. A) Methyl group region of the ^{1}H-^{13}C HSQC spectrum free CHOPS. B) Similar spectrum of CHOPS in complex with receptor mimic C5a$R_{7\text{-}28}S_2$. The assignments are indicated. Peaks originating from C5a$R_{7\text{-}28}S_2$ are shown in italic font.

The NOESY spectra of the CHOPS:C5a$R_{7\text{-}28}S_2$ complex suffered from severe overlap, but still a limited number of long-range intramolecular and intermolecular NOE cross-peaks could be assigned. Inter-molecular NOE´s were identified between the aromatic side-chain protons of sulfated tyrosine sY*14* of C5a$R_{7\text{-}28}S_2$ and the side-chains of T53 (Fig. 5.7A) and Y108 (Fig. 5.7C) of CHOPS. H*13* of

$C5aR_{7\text{-}28}S_2$ has an NOE contact with V109 of CHOPS (Fig. 5.7B). Intra-molecular NOE´s were identified between T53 and L49 and between Y97 and V109 (Fig. 5.7A). Similar peaks were observed in NOESY spectra of the complex between $CHIPS_{31\text{-}121}$ and $C5aR_{7\text{-}28}S_2$. The position of these residues in the NMR structure of the $CHIPS_{31\text{-}121}$:$C5aR_{7\text{-}28}S_2$ complex is indicated in Figs 5.7D and 5.7E.

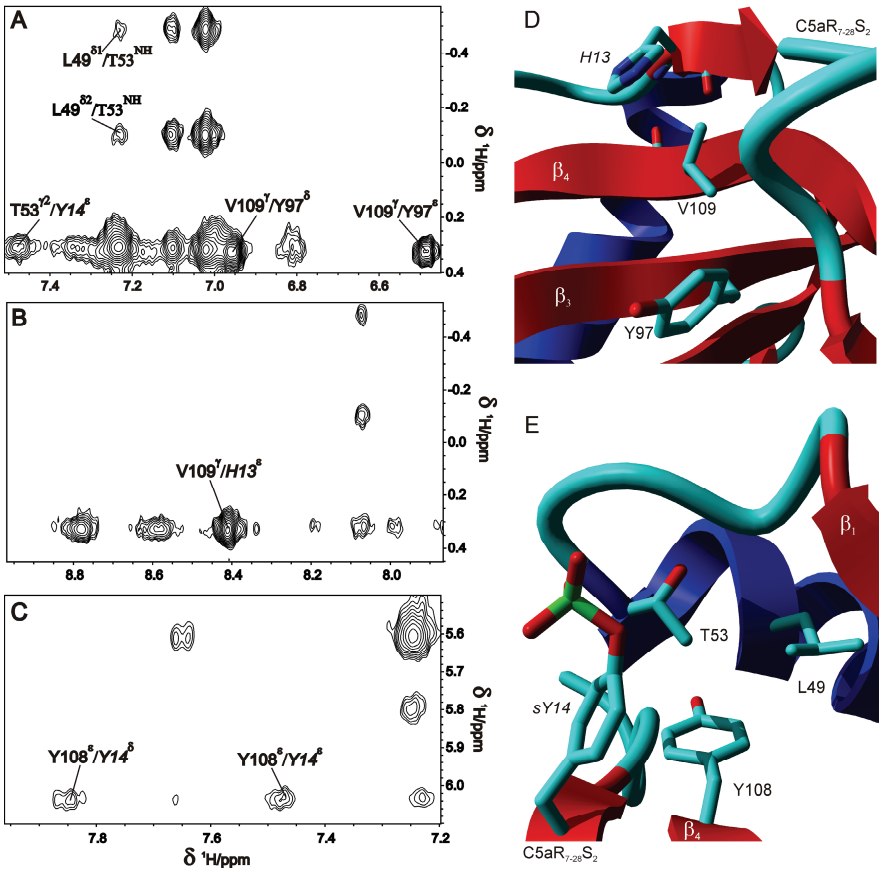

Figure 5.7 Observed cross-peaks in the NOESY spectrum of the CHOPS:$C5aR_{7\text{-}28}S_2$ complex in relation to structural features of the $CHIPS_{31\text{-}121}$:$C5aR_{7\text{-}28}S_2$ complex (PDB ID code: 2K3U). A-C) Different sections of the NOESY spectrum recorded at 288K of a 1:1 mixture of CHOPS and $C5aR_{7\text{-}28}S_2$. Identified long-range intra-molecular and inter-molecular NOE cross-peaks are indicated (normal fonts for residues belonging to CHOPS and italic fonts for residues belonging to $C5aR_{7\text{-}28}S_2$). D-E) Cartoon representation of the structure of the $CHIPS_{31\text{-}121}$:$C5aR_{7\text{-}28}S_2$ complex. The side-chains of the residues indentified in a-c are shown in stick representation (helices in blue, β-sheets in red).

CD spectroscopy

The presence of residual structure in the C5aR mimics and CHOPS was also monitored by circular dichroism spectroscopy (CD). The CD spectra of the C5a-receptor mimics, $C5aR_{7\text{-}28}$ and $C5aR_{7\text{-}28}S_2$, and CHOPS showed no structural features apart from a shallow minimum at 200 nm (Fig. 5.8). The CD spectrum of free $CHIPS_{31\text{-}121}$ is comprised of a large positive signal around 190 nm and a minimum around 205 nm (Fig. 5.8). This spectrum does not change significantly upon binding of $C5aR_{7\text{-}28}S_2$ (data not shown). Titration of CHOPS with a stoichiometric amount of unsulfated receptor mimic $C5aR_{7\text{-}28}$ resulted in an increase of the CD signal, although the shape of the spectrum did not change (Fig. 5.8A). Stoichiometric titration of CHOPS with sulfated receptor mimic $C5aR_{7\text{-}28}S_2$, on the other hand yielded a clear change of the CD spectrum: An increase in the signal around 190 nm and a shift of the minimum from 200 to 205 nm (Fig. 5.8B). These changes shift the appearance of the CD spectrum towards that of $CHIPS_{31\text{-}121}$ although at lower intensities.

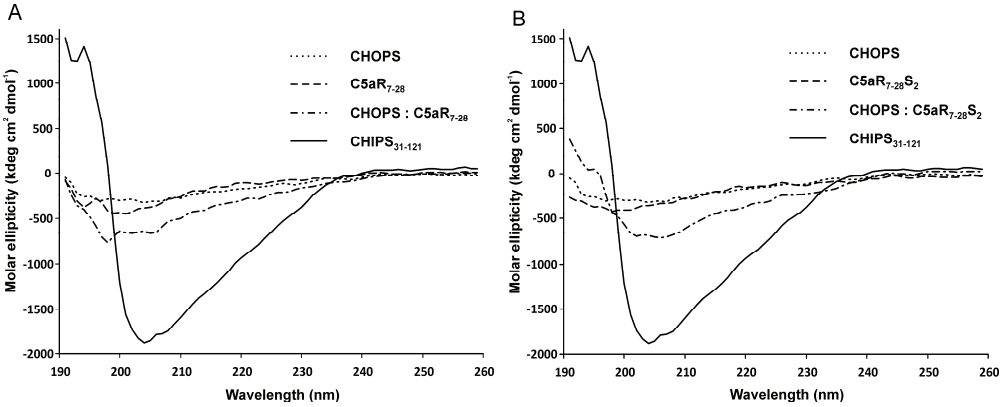

Figure 5.8 Circular dichroism spectra (CD) of CHOPS, $CHIPS_{31\text{-}121}$ and C5aR mimics. A) CD spectra of CHOPS, $C5aR_{7\text{-}28}$, CHOPS:$C5aR_{7\text{-}28}$, and $CHIPS_{31\text{-}121}$. B) CD spectra of CHOPS, $C5aR_{7\text{-}28}S_2$, CHOPS:$C5aR_{7\text{-}28}S_2$, and $CHIPS_{31\text{-}121}$.

5.3 Discussion and conclusions

In the research described in this chapter we aimed to create a shorter version of the immune evasive protein CHIPS based on the NMR structure of the complex between $CHIPS_{31\text{-}121}$ and $C5aR_{7\text{-}28}S_2$. The construct we designed (CHOPS) comprises all portions of $CHIPS_{31\text{-}121}$ important in the interaction with the C5aR. Portions outside the binding region including strand β_2 and the connecting loop between β_2 and β_3 were discarded. This was accomplished by coupling strand β_1 and β_3 together via a D-Pro-Gly linker segment. The resulting 50 residue peptide appeared to be largely unfolded apart from some residual structure around the β-hairpin inducing D-Pro-Gly linker sequence. ITC studies revealed that CHOPS binds to the doubly sulfated C5a-receptor mimic $C5aR_{7\text{-}28}S_2$ with micromolar affinity (K_d = 3.6 ± 0.2 μM). Although the affinity of $C5aR_{7\text{-}28}S_2$ to CHOPS is three orders of magnitude lower compared to binding to $CHIPS_{31\text{-}121}$ (K_d = 8.4 ± 1.2 nM),[13] this is a promising result

for a first lead compound. No detectable affinity of CHOPS was observed in the ITC measurements using the unsulfated mimic $C5aR_{7\text{-}28}$. This is consistent with previous measurements of $CHIPS_{31\text{-}121}$ and $C5aR_{7\text{-}28}$, which revealed that the absence of the two sulfate moieties results in an almost 400-fold decrease in affinity.

NMR spectroscopy confirmed the results obtained by ITC. Titration of CHOPS with unsulfated receptor mimic $C5aR_{7\text{-}28}$ resulted in the sum of its constituent ^{1}H-spectra, while titration of doubly sulfated peptide $C5aR_{7\text{-}28}S_2$ yielded a completely different ^{1}H-spectrum with signals shifted from their random coil position. The latter is indicative for the formation of defined structural elements. The NMR titration experiments using $C5aR_{7\text{-}28}S_2$ showed binding in a fast-exchange regime, compatible with the observed micromolar affinity by ITC.[23] Several characteristic features observed in spectra of the $CHIPS_{31\text{-}121}$:$C5aR_{7\text{-}28}S_2$ complex were also present in spectra of CHOPS:$C5aR_{7\text{-}28}S_2$. Specific resonances of residues L49, T53, T96, Y97, Y108, V109 and N111 have chemical shifts comparable with their counterparts in the $CHIPS_{31\text{-}121}$:$C5aR_{7\text{-}28}S_2$ complex. We also observed NOE cross-peaks between residues *sY14*, T53, L49, and Y108 and between residues *H13*, V109, and Y97 in NOESY spectra of CHOPS:$C5aR_{7\text{-}28}S_2$. These peaks are reminiscent of NOE contacts observed in spectra of the complex between $CHIPS_{31\text{-}121}$ and $C5aR_{7\text{-}28}S_2$ and reveal that CHOPS, in the presence of sulfated peptide $C5aR_{7\text{-}28}S_2$, adopts similar structures as native $CHIPS_{31\text{-}121}$.

The structural characteristics of CHOPS, either free in solution or in complex with the C5aR mimics, were also studied by CD spectroscopy. The spectra of the separate peptides (CHOPS, $C5aR_{7\text{-}28}$ or $C5aR_{7\text{-}28}S_2$) did not show any significant absorption apart from a shallow minimum around 200 nm. Titration of CHOPS with receptor mimic $C5aR_{7\text{-}28}$ increased the amount of absorption, but not the position of its minimum. Titration of CHOPS with the doubly sulfated receptor mimic $C5aR_{7\text{-}28}S_2$ caused an increase in absorption around 190 nm as well as a shift of the absorption minimum from 200 nm to 205 nm. Although the maximum and minimum intensities are smaller, the overall shape of the CD spectrum of the CHOPS:$C5aR_{7\text{-}28}S_2$ complex resembles that of native $CHIPS_{31\text{-}121}$.

In conclusion, we have designed and synthesized a significantly reduced-size mimic of the protein CHIPS, which we coined CHOPS. This construct has a binding affinity of 3.6 μM with respect to the sulfated receptor mimic $C5aR_{7\text{-}28}S_2$, but no affinity for the unsulfated receptor mimic $C5aR_{7\text{-}28}$. We conclude, based on NMR and CD studies, that CHOPS adopts structures comparable with native $CHIPS_{31\text{-}121}$ upon binding of $C5aR_{7\text{-}28}S_2$. The CHOPS:$C5aR_{7\text{-}28}S_2$ complex is, however, still flexible. We expect that improved affinity can be achieved by introduction of more rigid moieties, which will force this mimic more into the structure of native CHIPS.

5.4 Experimental

General

Peptide grade DIPEA, DCM, NMP, TFA, piperidine, and HPLC grade solvents were purchased from Biosolve B. V. (Valkenswaard, The Netherlands). Fmoc-protected amino acids were purchased from GL Biochem Ltd. (Shanghai, China). Side chain protecting groups were chosen as: Boc for lysine, *t*Bu for aspartic acid, glutamic acid, serine, threonine, and tyrosine, Trt for asparagine and glutamine, and Pbf for arginine. Unless stated otherwise, chemicals were obtained from commercial sources and used without further purification.

Analytical HPLC was performed using an automatic HPLC system (Shimadzu) with an analytical reversed-phase column and a UV detector operating at 214 nm with a flow rate of 0.75 mL/min. A Phenomenex Gemini C18 column (110 Å, 5 μm, 250×4.6 mm) was used. TFA buffers were used (buffer A: H_2O:MeOH, 80:20, v:v; buffer B: MeOH:H_2O:, 95:5, v:v, both containing 0.1% TFA). Elution was effected with a linear gradient from 100% A to 100% B over 48 min. Preparative HPLC was performed using an automatic Prep LCMS-QP8000α HPLC system (Shimadzu) with a preparative reversed-phase column and a UV detector operating at 214 nm with a flow rate of 12.5 mL/min. A Reprosil-Pur C18-AQ column (120 Å, 10 μm, 250 x 22mm) was used. TFA buffers were used (buffer A: H_2O:MeOH, 80:20, v:v; buffer B: MeOH:H_2O:, 95:5, v:v, both containing 0.1% TFA). Elution was effected with a linear gradient from 100% A to 100% B over 100 min. The peptides were characterized using electrospray mass spectrometry (ESI-MS), which was performed on a Thermo Finnigan LCQ DECA XP MAX ion trap mass spectrometer.

CHOPS:

CHOPS was synthesized on a Rink Amide PEG resin (0.52 mmol/g) (Matrix Innovation Inc., Montreal, Canada) on a 0.25 mmol scale. The peptide was assembled using an automatic ABI 433A Peptide Synthesizer, equipped with a UV-monitoring system, which was used to monitor the Fmoc removal step *i.e.* formation of the dibenzofulvene-piperidine adduct absorbing at 301 nm. ABI FastMoc 0.25 mmol protocols were applied, with the exception of a standard double coupling of 45 min.[24, 25] The synthesis was carried out on 0.48 g resin. The resin was washed with DCM and NMP (5 times). Subsequently, 1 mmol of the appropriate amino acid was dissolved in NMP (2 mL), and HBTU/HOBt (1 mmol, 2.78 mL of 0.36 M in NMP) was added. To this mixture DIPEA (1 mL, 2 M in NMP) was added, and the activated amino acid was then transferred to the reaction vessel. After 45 min, the reaction vessel was drained and the resin was washed with NMP (3 times) followed by addition of another batch of pre-activated amino acid, which was allowed to couple for another 45 min. Next, any of the remaining free amino groups were acetylated with an acetic anhydride capping solution (0.5 M Ac_2O, 0.125 M DIPEA, and 0.015 M HOBt in NMP) for 15 min. After capping the Fmoc protecting group was removed from the N-terminus by treatment with 20% piperidine solution in NMP twice (3 min and 7.6 min). The last coupling cycle was followed by removal of the Fmoc-group by a 20% piperidine solution, washing the resin with NMP, and acetylation of the N-terminus

by treatment with the acetic anhydride capping solution for 15 min. Finally, the resin was washed with NMP (5 times 10 mL) and DCM (6 times 10 mL), removed from the reaction vessel, washed with ether, and dried *in vacuo* over P_2O_5.

The anchored peptide obtained in this way was de-protected and cleaved from the solid support by treatment with TFA/H_2O/TIS (95/2.5/2.5, 25 mL) for 2 h at room temperature. The mixture was filtered and the residue washed thoroughly with TFA (2 times 10 mL). The reaction mixture was concentrated *in vacuo* to a volume of approximately 10 mL and added dropwise to 90 mL MTBE/n-hexane (1/1, v/v) solution. The precipitate was collected by centrifugation (3000 rpm, 10 min), the supernatant was decanted and the pellet was resuspended in MTBE/n-hexane (1/1, v/v) (100 mL) and centrifuged again. This procedure was repeated twice. Afterwards, the pellets were dissolved in CH_3CN/H_2O (1/1, v/v) (ca. 60 mL) and lyophilized to give 595 mg of the crude peptide as a white fluffy solid.

Crude peptide (400 mg) was dissolved in 30 mL buffer A, 10 mL buffer B and purified by preparative HPLC (Reprosil-Pur C18-AQ, TFA buffers) in eight runs. Fractions containing the pure product were pooled and lyophilized to give 29 mg of pure CHOPS. The purity of CHOPS was established by analytical HPLC (Gemini C18, TFA buffers, Rt = 36.4 min, Purity >98%) and characterization was carried out by ESI-MS (calculated average mass $[M+5H]^{5+}$ for $C_{261}H_{422}N_{70}O_{74}S$: 1152.34; found: 1152.30).

The C5a receptor mimic peptides $C5aR_{7\text{-}28}$ and $C5aR_{7\text{-}28}S_2$ were synthesized as has been described in chapter 2.

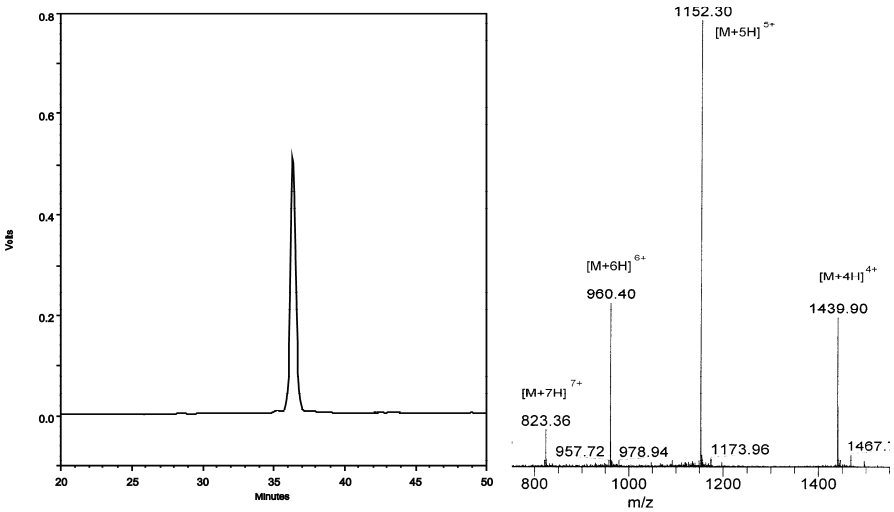

Figure 5.9 Analysis of CHOPS by HPLC (Reprosil-Pur C18-AQ, TFA buffers) and mass spectrometry.

ITC experiments

The binding affinities of the C5aR mimics $C5aR_{7-28}$ and $C5aR_{7-28}S_2$ with CHOPS were measured using an ITC_{200} Microcalorimeter (MicroCal) operating at 283 K. The measuring cell was filled with 208 µL of a 0.19 mM solution of CHOPS in a 20 mM sodium phosphate buffer at pH 6.5. The concentration of CHOPS was determined by OD_{280} measurements. The syringe was loaded with 30 µL of a 2.5 mM solution of one of the C5aR-mimics in the same buffer system. After each incremental addition of the solution in the syringe, the integrated heat change due to binding was measured. The data were analyzed using the Microcal Origin software and fitted by non-linear regression analysis. Three independent experiments were carried out. The experimental errors were estimated by Monte Carlo simulations using the standard deviations of the individual experiments.

NMR spectroscopy

NMR samples of $C5aR_{7-28}$, $C5aR_{7-28}S_2$ and CHOPS were at concentrations of 0.8-1 mM in 9/1 (v/v) H_2O/D_2O sodium phosphate buffers (20 mM, pH 6.5). Spectra were recorded at 288 K on a Varian INOVA 500 and a Bruker Avance 750 MHz spectrometer equipped with an HCN triple-resonance pulsed field gradient probe. Sequential ^1H NMR assignments of CHOPS were accomplished using a combination of NOESY, TOCSY, and ^{13}C-HSQC spectra.

CD measurements

CD spectra (190-260 nm) were recorded on an Olis RSM1000 spectrophotometer operating at 2 nm spectral resolution (slit size 1.24 mm). Samples of $CHIPS_{31-121}$ (43 µM) in 20 mM sodium phosphate buffer (pH 6.5), CHOPS (50 µM), $C5aR_{7-28}$ and $C5aR_{7-28}S_2$ (50 µM) in 10 mM sodium phosphate buffer (pH 7.4) were measured at 298 K using a 0.5 mm cuvette. To gain a satisfactory S/N ratio five scans were summed, with data points averaged by three-point triangular smoothing.

5.5 References

[1] H. Lee, P. L. Whitfeld, C. R. Mackay, Receptors for complement C5a. The importance of C5aR and the enigmatic role of C5L2, *Immunol. Cell Biol.* **2008**, *86*, 153.

[2] R. F. Guo, P. A. Ward, Role of C5A in inflammatory responses, *Annu. Rev. Immunol.* **2005**, *23*, 821.

[3] Z. G. Chen, X. L. Zhang, N. C. Gonnella, T. C. Pellas, W. C. Boyar, F. Ni, Residues 21-30 within the extracellular N-terminal region of the C5a receptor represent a binding domain for the C5a anaphylatoxin, *J. Biol. Chem.* **1998**, *273*, 10411.

[4] B. O. Gerber, E. C. Meng, V. Dotsch, T. J. Baranski, H. R. Bourne, An activation switch in the ligand binding pocket of the C5a receptor, *J. Biol. Chem.* **2001**, *276*, 3394.

[5] D. E. van Epps, S. J. Simpson, R. Johnson, Relationship of C5a Receptor modulation to the functional responsiveness of human polymorphonuclear leukocytes to C5a, *J. Immunol.* **1993**, *150*, 246.

[6] M. Allegretti, A. Moriconi, A. R. Beccari, R. Di Bitondo, C. Bizzarri, R. Bertini, F. Colotta, Targeting C5a: Recent advances in drug discovery, *Curr. Med. Chem.* **2005**, *12*, 217.

[7] P. N. Monk, A. Scola, P. K. Madala, D. P. Fairlie, Function, structure and therapeutic potential of complement C5a receptors, *Br. J. Pharmacol.* **2007**, *152*, 429.

[8] K. E. Veldkamp, H. C. J. M. Heezius, J. Verhoef, J. A. G. van Strijp, K. P. M. van Kessel, Modulation of neutrophil chemokine receptors by *Staphylococcus aureus* supernate, *Infect. Immun.* **2000**, *68*, 5908.

[9] B. Postma, M. J. Poppelier, J. C. van Galen, E. R. Prossnitz, J. A. G. van Strijp, C. J. C. de Haas, K. P. M. van Kessel, Chemotaxis inhibitory protein of *Staphylococcus aureus* binds specifically to the C5a and formylated peptide receptor, *J. Immunol.* **2004**, *172*, 6994.

[10] P. J. Haas, C. J. C. de Haas, M. J. J. C. Poppelier, K. P. M. van Kessel, J. A. G. van Strijp, K. Dijkstra, R. M. Scheek, H. Fan, J. A. W. Kruijtzer, R. M. J. Liskamp, J. Kemmink, The structure of the C5a receptor-blocking domain of chemotaxis inhibitory protein of *Staphylococcus aureus* is related to a group of immune evasive molecules, ***J. Mol. Biol.*** **2005**, *353*, 859.

[11] B. Postma, W. Kleibeuker, M. J. J. G. Poppelier, M. Boonstra, K. P. M. Van Kessel, J. A. G. Van Strijp, C. J. C. de Haas, Residues 10-18 within the C5a receptor N-terminus compose a binding domain for chemotaxis inhibitory protein of *Staphylococcus aureus*, ***J. Biol. Chem.*** **2005**, *280*, 2020.

[12] M. Farzan, C. E. Schnitzler, N. Vasilieva, D. Leung, J. Kuhn, C. Gerard, N. P. Gerard, H. Choe, Sulfated tyrosines contribute to the formation of the C5a docking site of the human C5a anaphylatoxin receptor, ***J. Exp. Med.*** **2001**, *193*, 1059.

[13] J. H. Ippel, C. J. C. De Haas, A. Bunschoten, J. A. G. van Strijp, J. A. W. Kruijtzer, R. M. J. Liskamp, J. Kemmink, Structure of the tyrosine-sulfated C5a-receptor N-terminus in complex with chemotaxis inhibitory protein of Staphylococcus aureus, ***J. Biol. Chem.*** **2009**, *284*, 12363.

[14] A. Bunschoten, J. A. W. Kruijtzer, J. H. Ippel, C. J. C. de Haas, J. A. G. van Strijp, J. Kemmink, R. M. J. Liskamp, A general sequence independent solid phase method for the site specific synthesis of multiple sulfated-tyrosine containing peptides, ***Chem. Commun.*** **2009**, 2999.

[15] E. Gustafsson, P. J. Haas, B. Walse, M. Hijnen, C. Furebring, M. Ohlin, J. A. G. van Strijp, K. P. M. van Kessel, Identification of conformational epitopes for human IgG on Chemotaxis inhibitory protein of *Staphylococcus aureus*, *Bmc Immunol.* **2009**, *10*, 13.

[16] P. J. Haas, *Staphylococcal* drug discovery, PhD thesis, Utrecht University (Utrecht), **2006**, 73.

[17] A. J. Wright, A. Higginbottom, D. Philippe, A. Upadhyay, S. Bagby, R. C. Read, P. N. Monk, L. J. Partridge, Characterisation of receptor binding by the chemotaxis inhibitory protein of *Staphylococcus aureus* and the effects of the host immune response, ***Mol. Immunol.*** **2007**, *44*, 2507.

[18] L. M. Proctor, T. M. Woodruff, S. M. Taylor, Recent developments in C5/C5a inhibitors, ***Expert Opin. Ther. Pat.*** **2006**, *16*, 445.

[19] J. J. Chen, D. C. Cole, G. Ciszewski, K. Crouse, J. W. Ellingboe, P. Nowak, G. J. Tawa, G. Berstein, W. Li, Identification of a new class of small molecule C5a receptor antagonists, ***Bioorg. Med. Chem. Lett.*** **2010**, *20*, 662.

[20] F. Blanco, M. Ramirez-Alvarado, L. Serrano, Formation and stability of beta-hairpin structures in polypeptides, ***Curr. Opin. Struc. Biol.*** **1998**, *8*, 107.

[21] C. E. Stotz, E. M. Topp, Applications of model beta-hairpin peptides, ***J. Pharm. Sci.*** **2004**, *93*, 2881.

[22] T. S. Haque, S. H. Gellman, Insights on beta-hairpin stability in aqueous solution from peptides with enforced type I´ and type II´ beta-turns, ***J. Am. Chem. Soc.*** **1997**, *119*, 2303.

[23] J. Cavanagh, W. J. Fairbrother, A. G. Palmer, M. Rance, N. J. Skelton, *Protein NMR Spectroscopy: Principles and Practice (second edition)*, Elsevier Academic Press, San Diego, **2007**.

[24] A. Biosystems, *Applied Biosystems Model 433A Peptide Synthesizer User´s Manual* **June 1993**, version 1.0.

[25] A. Biosystems, *Applied Biosystems Research News* **June 1993**, Model 433A Peptide Synthesizer.

Chapter 6

An approach to TAC-based mimics of Chemotaxis Inhibitory Protein of *Staphylococcus aureus*

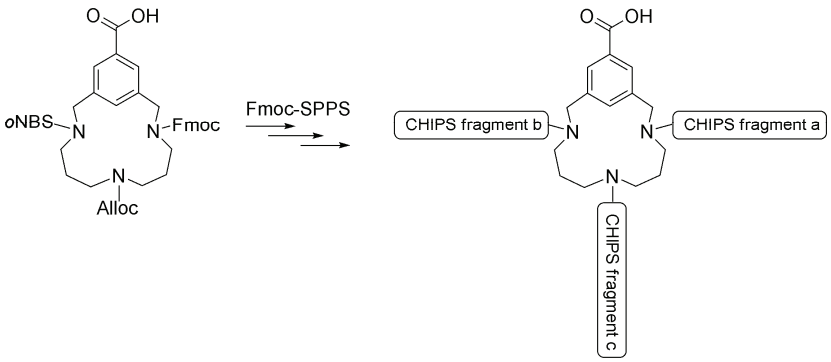

6

6.1 Introduction

Protein-protein interactions are notoriously difficult to target with small ligands, mainly because the interactions are, in most cases, spread over a large surface area of the proteins.[1] Small peptide fragments within the protein sequence, far removed from each other in the primary structure but close in the tertiary structure, can be identified to be involved in the interactions. Those fragments are referred to as ´hotspots´. Ideally one might be able to select these hotspots and arrange them in the appropriate position and they should be able to bind to the same targets as the native protein. Unfortunately, omitting large parts of a protein results in loss of the native structure of the protein and diminished activity. The non-interacting parts of a protein play a significant role in maintaining the core structure of the protein and presenting the interacting groups in the right three dimensional orientation. Attempts to replace these core parts of proteins by small synthetic scaffolds have led to the development of several active synthetic protein mimics.

Kemp´s triacid (Fig. 6.1A) has been used to mimic the triple-helical structure of collagen.[2] The regioselective addressable functionalized template (RAFT) scaffold, and similar scaffolds, of Mutter and coworkers (Fig. 6.1B) have been successfully used in creating artificial proteins such as synthetic vaccines,[3] multivalent protein ligands for the $\alpha_v\beta_3$-integrin receptor,[4] heme group-containing cytochrome b mimics and other metalloproteins, [5-7] ion channel mimics,[8-10] and the multimeric platelet adhesion von Willibrand factor A1.[11] Calixarene (Fig. 6.1C) has been applied as a cyclic peptide containing inhibitor for chymotrypsin.[12] Porphyrins (Fig. 6.1D) have been used as scaffolds to mimic cytochrome P-450,[13] ion channels,[14] and membrane proteins with electron transfer properties.[15] Cyclotriveratrylene (CTV) (Fig. 6.1E) has been applied in the synthesis of the triple helix structure of collagen.[16] A cholic acid-based scaffold with two orthogonal protecting groups was used to mimic serine proteases.[17] Later this scaffold (Fig. 6.1F) was equipped with three orthogonal protecting groups.[18] A pentaerythritol-based scaffold (Fig. 6.1G) was synthesized and used by Madder and coworkers to mimic serine proteases.[19, 20] The triazacyclophane scaffold (TAC) (Fig. 6.1H), developed by Liskamp and co-workers has been applied in developing peptide binders of D-Ala-D-Ala and D-Ala-D-Lac,[21] synthetic vaccines,[22] Cystatin B protein mimics,[23] and synthetic protein mimics with esterase activity.[24]

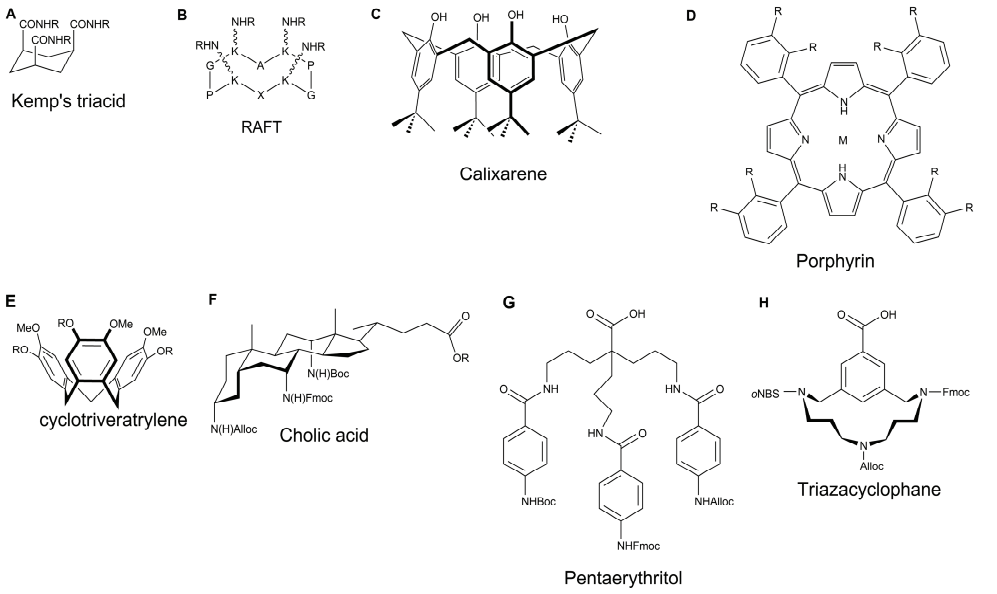

Figure 6.1 Overview of scaffold molecules used in the mimicry of proteins.

Chemotaxis Inhibitory Protein of *Staphylococcus aureus* (CHIPS) is a 121-residue protein excreted by the bacterium *S. aureus*, which is capable of inhibiting the activation of the formylated peptide receptor (FPR) and the C5a receptor (C5aR).[25] In doing so, CHIPS prevents the recruitment of neutrophils and monocytes to the site of infection. A truncated version of CHIPS (designated

$CHIPS_{31-121}$) has the same affinity for the C5aR compared to native CHIPS and its structure, a compact fold comprising an α-helix packed onto a four-stranded anti-parallel β-sheet, has been solved.[26] Unfortunately, CHIPS itself is highly immunogenic and will not make a suitable anti-inflammatory drug.[27, 28] The structure of CHIPS in complex with a C5a-receptor mimic has been solved, enabling the identification of ´hotspots´ in CHIPS (Chapter 3).[29] After the successful synthesis of CHOPS (Chapter 5), a 50-mer structural mimic of CHIPS with a 3.6 μM affinity for the C5a-receptor mimic $C5aR_{7-28}S_2$, we were interested to further reduce the size of new CHIPS mimics. The goal of the experiments described in this chapter was to investigate if the ´hotspots´ of CHIPS could be assembled on a scaffold and if these scaffolded CHIPS mimics had an affinity for the C5aR N-terminus mimics.

The triazacyclophane scaffold was selected for the synthesis of our CHIPS mimics because it encompasses several very useful features. The TAC-scaffold is a versatile scaffold with a fine balance between rigidity and flexibility. The scaffold has a rigid core structure, but the peptide arms connected to the core have a high degree of flexibility. The TAC-scaffold is compatible with (automated) solid phase peptide chemistry and the TAC-scaffold has three orthogonally protected secondary amines, which can be functionalized independently and in this way three different peptide sequences can be introduced on the scaffold. The robust chemistry for the synthesis of the TAC-scaffold and the methods for the application have been developed by Liskamp and co-workers, and the scaffold has been applied in several successful projects.[21-24, 30-34]

6.2 Results

Selection of hotspots on CHIPS

For the design of TAC-based CHIPS mimics, three fragments of CHIPS were selected to be attached to the orthogonal protected amines of TAC. This selection was based on the structure of the $CHIPS_{31-121}$:$C5aR_{7-28}S_2$ complex presented in Chapter 3. The fragments of CHIPS, which interact with the C5aR mimics, can be divided in three regions based on two separate approaches.

The first approach is to identify the two sulfate binding sites and the interactions with the other residues of the C5aR N-terminus (Fig. 6.2A). In these binding sites only the residues of $CHIPS_{31-121}$ that have an interaction with $C5aR_{7-28}S_2$ were selected for assembling on the TAC-scaffold (**12-14**).

The second approach was based on the secondary and tertiary structure of $CHIPS_{31-121}$, which could be divided in the α-helix connected to a small loop and two anti-parallel β-sheets (Fig. 6.2B). For the design of this TAC-based mimic of CHIPS (**15**) the complete native sequence of the selected fragments was used to stay as closely as possible to the tertiary structure of CHIPS. By preliminary modeling, the proposed mimic was built and checked if the proper orientation could be reached (Fig. 6.3C). It was decided to connect the three fragments to the TAC-scaffold via a glycine residue, which

was present in the native sequences of two of the three arms. Lysine 61 was replaced with a glycine residue in the third arm.

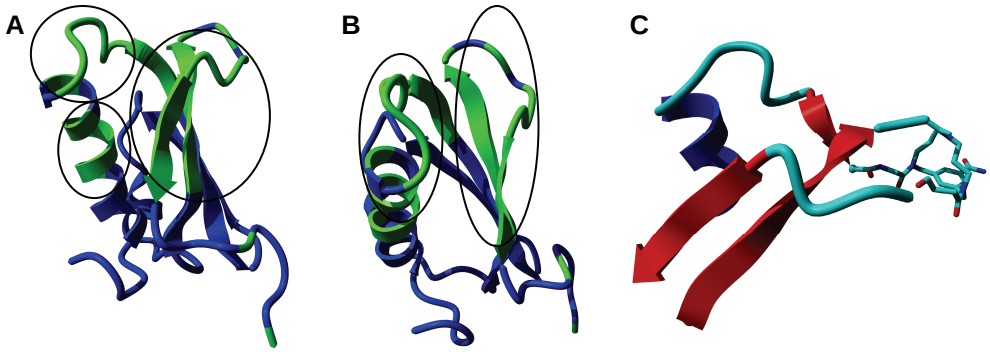

Figure 6.2 Structure of $CHIPS_{31\text{-}121}$ (1XEE) with the residues having a chemical perturbation >0.3 ppm in NMR titration experiments upon binding with the receptor mimic $C5aR_{7\text{-}28}S_2$ (figure 3.4B) depicted in green. Marked are the three different regions based on two separate selection methods: A) two *sY* binding motifs and the interaction site for the other residues of the C5aR N-terminus, B) α-helix and the two anti-parallel β-strands. C) Model of TAC-based mimic **15** with three native fragments of $CHIPS_{31\text{-}121}$ connected via glycines to the TAC-scaffold.

Synthesis of TAC

For the mimics based on the selection of the binding motifs (Figure 6.2A) it was decided to use the minimum sequences, preferably only the interacting residues of CHIPS and attach them directly to TAC (**9**). Three different designs were synthesized (figure 6.3): mimic **12** contained the residues involved in binding *sY11* on the Fmoc position of TAC, residues involved in binding *sY14* were placed at the *o*NBS position and the residues involved in formation of the small anti-parallel β-sheet between C5aR and CHIPS were incorporated at the Alloc position. Mimic **13** contained the same residues, but three glycines were added to correct for the side-chain orientation of the selected residues, compared to the orientation in native CHIPS. Glycine was chosen for its small size and because no additional steric hindrance or new functionalities would be introduced. Mimic **14** contains the same sequences compared to mimic **13** but two mutations were taken into account. These mutations, K100R and N111K were obtained from an active mutant of CHIPS developed by Gustafsson et al. to prevent recognition by the host immune system.[35]

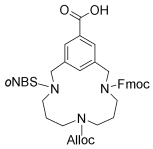

	12	**13**	**14**	**15**
-Fmoc	Ac-RYK-	Ac-RGYGK-	Ac-RGYGK-	-GESKSSYVIN-NH_2
-*o*NBS	Ac-KNQK-	Ac-KNQGK-	Ac-KNQGR-	Ac-YLKKGTKNSAQFEG-
-Alloc	Ac-SSYVIN-	Ac-SSYVIN-	Ac-SSYVIK-	Ac-KTYFFKKG-

Figure 6.3 Four TAC-based CHIPS mimics containing three different sequences of CHIPS connected to the TAC-scaffold.

For the construction of the designed mimics of CHIPS the TAC-scaffold was successfully synthesized following a literature procedure (Figure 6.4).[31] After coupling of this scaffold onto a rink amide resin the three protecting groups could be removed subsequently and the three different peptide sequences were attached by stepwise manual SPPS. After complete deprotection and cleavage from the solid support, these TAC-based CHIPS mimics (**12-14**) were successfully purified and characterized (Fig. 6.5).

The design of construct **15** contained an anti-parallel β-sheet of CHIPS. In order to form this structure on the TAC-scaffold one sequence had to be attached in the reverse order (N→C) instead of the standard order applied in SPPS, which is from C- to N-terminus. One approach previously used with TAC for attaching a peptide in the N→C order was the coupling of a complete peptide with a free N-terminus to resin-bound TAC with a carboxylic acid functionality coupled at the Fmoc position.[23] In our case this method would imply the synthesis and coupling of a completely protected peptide because of the side-chain functionalities present in this peptide sequence. The protected peptide proved to be very hard to handle because of solubility problems. Therefore another approach was developed which comprised the coupling of TAC containing a carboxylic acid functionality on the Fmoc position to a resin bound peptide with a free N-terminus, which results in the connection of a peptide in a ´reversed´ order to the scaffold. This approach demanded a differently functionalized TAC-scaffold (**11**) which was synthesized as shown in figure 6.3 by converting the acid functionality into an amide and creating a carboxylic acid functionality at the Fmoc position by reaction with succinic anhydride. After coupling of TAC to the resin bound peptide the other two peptide sequences were introduced via SPPS. After complete deprotection and cleavage from the solid support, this TAC-based CHIPS mimic was successfully purified and characterized (Fig. 6.5).

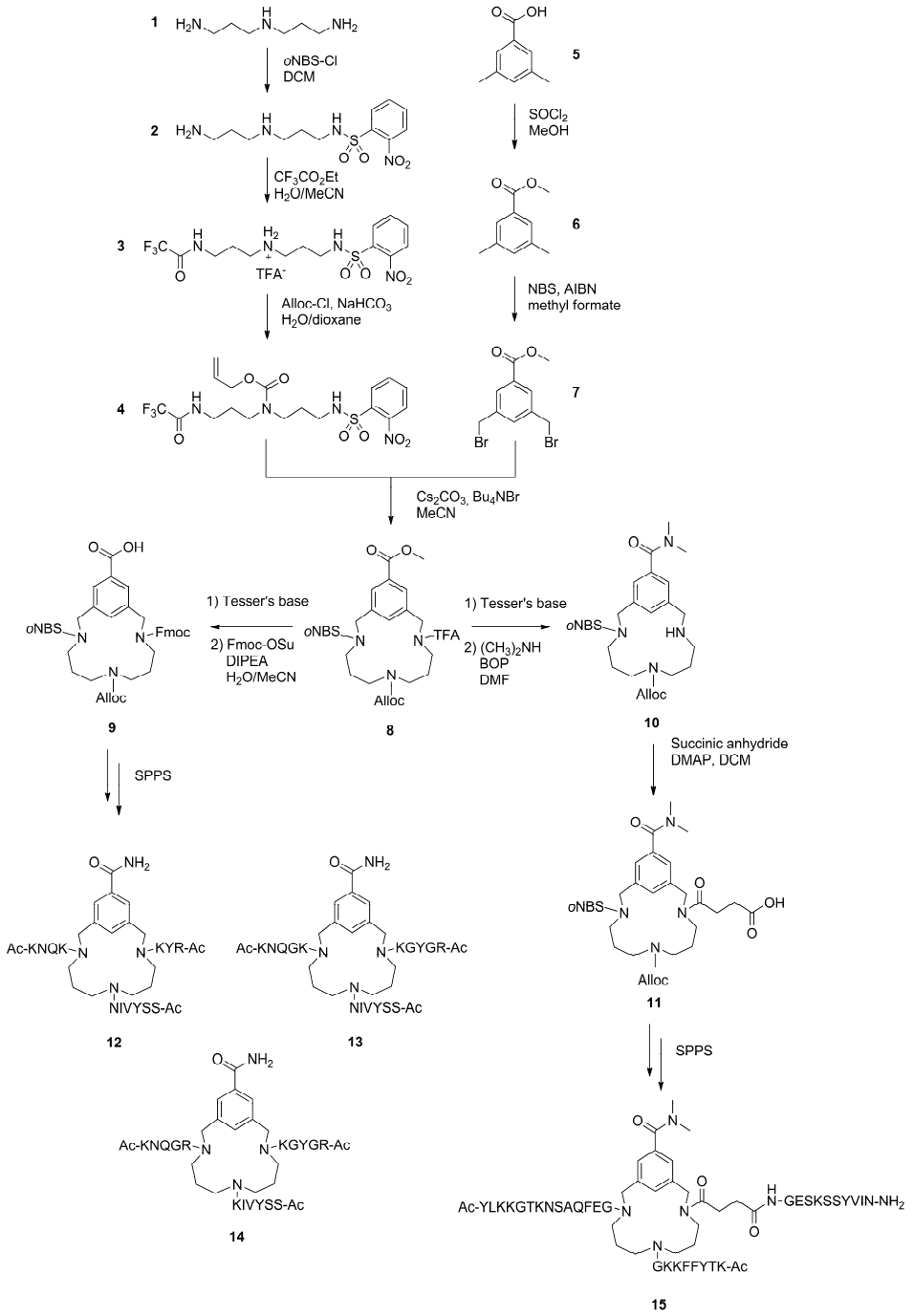

Figure 6.4 Synthesis of the TAC-based mimics of CHIPS (**12-15**).

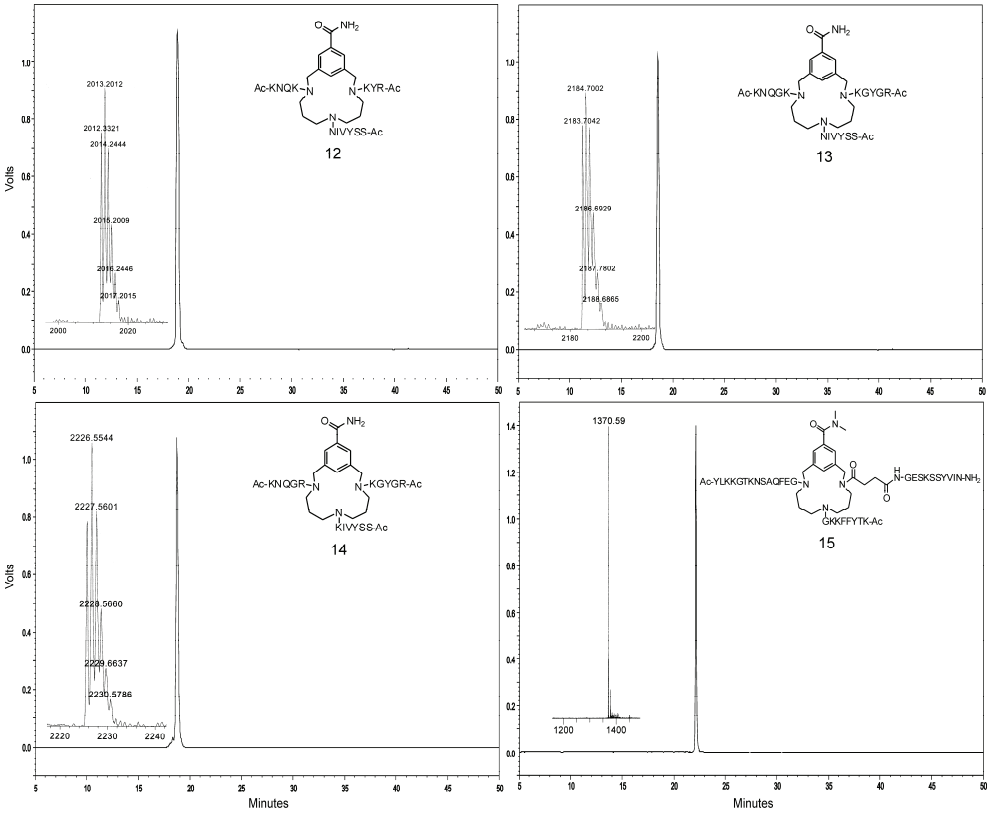

Figure 6.5 HPLC chromatograms (absorption at 220 nm) of **12-15** after preparative HPLC.

ITC

The four synthesized CHIPS mimics were tested for binding to the receptor mimic $C5aR_{7\text{-}28}S_2$ by Isothermal Titration Calorimetry (ITC) as was described in chapter 3.[29, 36] To a 30 μM solution of each CHIPS mimic (**12-15**) 0.5 mM of $C5aR_{7\text{-}28}S_2$ was titrated. None of the four constructs demonstrated any measurable effect indicative of binding.

Biological assay

In addition, the four synthesized CHIPS mimics were tested for inhibition of C5a-induced C5aR activation on U937/C5aR cells as was described in chapter 3.[29] None of the four constructs demonstrated inhibition up to a concentration of 300 μM.

6.3 Discussion and conclusion

Four TAC-scaffold-based CHIPS mimics were successfully synthesized by (automated) solid phase peptide chemistry. A new approach for the coupling of a peptide in ´reversed´ order to the TAC-scaffold was applied. In this approach the first peptide fragment was synthesized from the C- to the

N-terminus on the solid support after which the TAC-scaffold with a carboxylic acid moiety on the Fmoc-position was coupled to this peptide. After finishing the introduction of the other two fragments on the TAC-scaffold by solid phase peptide chemistry, the first arm was oriented from N- to C-terminus and the other two fragments were oriented from the C- to the N-terminus. This approach is especially useful for highly functionalized peptides.

In contrast to the successful synthesis of these constructs, the results of the binding studies were unsatisfactorily. None of the four constructs showed any detectable binding affinity towards the receptor mimic $C5aR_{7\text{-}28}S_2$ in the ITC experiments and for the native C5aR in the cell-based assays. Although mimic **15** contained most residues of CHIPS that showed interaction with our C5aR mimic, we have shown in previous chapters that the structure of CHIPS was very important for the right orientation of these residues. Based on the results described in this chapter we can conclude that the TAC-scaffold alone was not sufficient to induce a CHIPS-like conformation of the interacting residues. A second generation TAC-based CHIPS mimics will have to include some additional structure inducing elements like cyclic or interconnected peptide fragments to approach the CHIPS topology more closely.

6.4 Experimental

General

Peptide grade DIPEA, DCM, NMP, TFA, and HPLC grade solvents were purchased from Biosolve B.V. (Valkenswaard, The Netherlands). TentaGel™ S RAM resin functionalized with a Rink Amide linker, (low crosslinked polystyrene grafted with polyethylene glycol, 0.20-0.27 $mmol.g^{-1}$ and a particle size of 90 μm) was purchased from Rapp Polymere GmbH (Tübingen, Germany). The Fmoc-protected amino acids were purchased from GL Biochem Ltd. (Shanghai, China). The side-chain protecting groups were chosen as: Boc for lysine; *t*Bu for glutamic acid, serine, threonine and tyrosine; Trt for asparagine and glutamine; Pbf for arginine. Unless stated otherwise, chemicals were obtained from commercial sources and used without further purification. Analytical thin layer chromatography (TLC) was performed on Merck pre-coated silica gel 60 F_{254} (0.25mm) plates. Spots were visualized with UV light, ninhydrine, or Cl_2-TDM.[37] Column chromatography was performed using Silicycle SiliaFlash P60 (40-63 μm) from Screening Devices (Amersfoort, The Netherlands). ^1H NMR, ^{13}C NMR and two dimensional spectra were obtained on a Varian 300 MHz and a Varian 500 MHz spectrometer. Chemical shifts are given in ppm with respect to internal standard TMS for ^1H NMR. ^{13}C NMR spectra were recorded using the attached proton test (APT) pulse sequence. When necessary COSY, HSQC, TOCSY and ^1H spectra were recorded at elevated temperatures to obtain assignments. In the synthesis of TAC all NMR spectra were in accordance with previously published spectra.[31] Only ^1H-NMR spectra are mentioned here for previously published structures. The peptides were synthesized automatically on an Applied Biosystems 433A peptide synthesizer with a UV-monitoring system, which was used to monitor the Fmoc removal step *i.e.* formation of the dibenzofulvene-piperidine adduct absorbing at 301 nm.

Analytical HPLC was performed using an automatic HPLC system (Shimadzu) with an analytical reversed-phase column and a UV detector operating at 214 nm with a flow rate of 1 mL/min. An Alltech Alltima C8 (100 Å, 5 µm, 250 x 4.6 mm) or a Phenomex Gemini C18 (110 Å**,** 5 µm, 250 x 4.6 mm) column was used. The eluent were TFA buffers (buffer A: H_2O:CH_3CN, 95:5, v:v; buffer B: CH_3CN:H_2O, 60:40, v:v, both containing 0.1% TFA). Elution was effected with a linear gradient from 100% A to 100% B over 48 min.

Preparative HPLC was performed using an automatic Prep LCMS-QP8000α HPLC system (Shimadzu) with a preparative reversed-phase column and a UV detector operating at 214 nm with a flow rate of 12.5 mL/min. An Alltech Alltima C8 (100 Å, 10 µm, 250 x 22mm) or an Alltech Prosphere C18 (300 Å, 10 µm, 250 x 22mm) column was used. The eluent were TFA buffers (buffer A: H_2O:CH_3CN, 95:5, v:v; buffer B: CH_3CN:H_2O, 60:40, v:v, both containing 0.1% TFA). Elution was effected with a linear gradient from 100% A to 100% B over 100 min.

The peptides were characterized using electrospray ionisation mass spectrometry (ESI-MS), which were performed on a Thermo Finnigan LCQ DECA XP MAX ion trap mass spectrometer or a Shimadzu LCMS-QP8000 single quadrupole bench-top mass spectrometer.

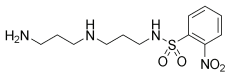

Mono-*o*NBS protected bis(3-aminopropyl)amine:

To a stirred, cooled solution (ice/water) of bis-(3-aminopropyl)-amine **1** (120 mL, 0.85 mol) in dry DCM (400 mL), *o*NBS-Cl (22.1 g, 100 mmol) in DCM (350 mL) was added dropwise. After addition, the reaction was stirred for one hour while reaching room temperature. The reaction mixture was washed with H_2O (400 mL). The aqueous layer was neutralized with conc. HCl and extracted twice with DCM (2 times 200 mL). After addition of NH_4Cl (75 g), the aqueous layer was again extracted twice with DCM (2 times 200 mL). The combined organic layers were dried on Na_2SO_4 and concentrated *in vacuo*. This afforded crude product **2** as a yellow oil (22 g, 69.5 mmol, 61%), which contained a small amount of di-substituted product and unreacted triamine. R_f (MeOH/DCM, 1:4, v/v): 0.43.
^{1}H NMR (300 MHz) ($CDCl_3$): δ [ppm] = 1.68 (m, br, 2x CH_2*CH_2*CH_2); 2.71 (m, 3x CH_2N); 3.19 (m, *CH_2*$NHSO_2Ar$); 7.70 (m, Ar-H); 7.83 (m, Ar-H); 8.11 (m, Ar-H).

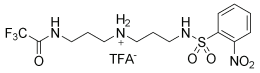

***o*NBS/TFAc-protected triamine 3:**

To a solution of crude mono-protected bis(3-aminoprotyl)amine **2** (22 g, 69.5 mmol) in CH_3CN (250 mL), ethyltrifluoroacetate (24.9 mL, 208 mmol) and H_2O (1.25 mL, 69.5 mmol) were added. The reaction mixture was refluxed with glass pearls for 16 hours. Then, the reaction mixture was filtrated and concentrated *in vacuo,* to give the crude product as yellow oil. Recrystallization from EtOAc/DCM resulted in product **3** as yellow crystals (25.1 g, 47.7 mmol, 58%). Also in this stage some product with two *o*NBS groups was

present. ^{1}H NMR (300 MHz) (DMSO): δ [ppm] = 1.76 (m, 2x $CH_2CH_2CH_2$); 2.89 (m, 3x CH_2N); 3.24 (m, CH_2NHSO_2Ar); 7.84-8.00 (m, Ar-H); 8.35 (NH); 9.53 (NH).

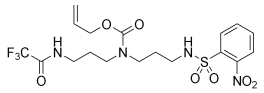

oNBS/Alloc/TFAc-protected triamine 4:

$NaHCO_3$ (15.2 g, 180 mmol) was dissolved in H_2O (150 mL) and added to a solution of crude oNBS/TFAc-protected triamine **3** (23.7 g, 45 mmol) in dioxane/H_2O (400 mL, 1/1, v/v). After cooling the reaction to 0°C (ice/water), a solution of Alloc-Cl (5.74 mL, 54 mmol) in dioxane (100 mL) was added dropwise under stirring. The reaction was allowed to reach room temperature and was stirred for 16 h. Afterwards, H_2O (400 mL) was added and the mixture was extracted twice with DCM (2 times 400mL), the combined organic layers were dried over Na_2SO_4. Concentration *in vacuo* afforded the crude product as yellow oil. Purification by silica gel chromatography (hexanes/EtOAc 1:1 (v/v)) afforded **4** as a yellow oil (16.2 g, 32.6 mmol, 73%). R_f (EtOAc/Hex, 1:1, v/v): 0.37.

^{1}H NMR (300 MHz) ($CDCl_3$): δ [ppm] = 1.78 (m, br, 4H, 2x $CH_2CH_2CH_2$); 3.13 (q, J=6.3 Hz, 2H, CH_2NHSO_2Ar); 3.33 (s, br, 6H 3x CH_2N); 4.61 (d, J=5.5 Hz, 2H, CH_2O); 5.28 (m, 2H, $CH=CH_2$); 5.42 (s, br, 0.5H, $NHSO_2$); 5.91 (m, 1H, $CH=CH_2$); 6.05 (s, br, 0.5H, $NHSO_2$); 6.61 (s, br, 0.5H, $NHCOCF_3$); 7.75 (m, 2H, Ar-H); 7.86 (m, 1H, Ar-H); 7.92 (s, br, 0.5H, $NHCOCF_3$); 8.12 (m, 1H, Ar-H).

Methyl 3,5-dimethyl benzoate 6:

Thionyl chloride (81.6 mL, 1.12 mol) was added dropwise to cooled (ice/water) methanol (600 mL) under stirring. After complete addition of the thionylchloride, 3,5-dimethylbenzoic acid (**5**) (37.5 g, 250 mmol) was added at once and the reaction mixture was stirred at room temperature for 16 h. After concentration of the reaction mixture *in vacuo*, the residue was dissolved in EtOAc (500mL) and washed with saturated $NaHCO_3$ (300 mL), brine (300 mL) and H_2O (300 mL). The organic layer was dried over Na_2SO_4 and concentration *in vacuo* afforded **6** as white crystals (40.25 g, 148 mmol, 98%). R_f (EtOAc/Hex, 1:1, v/v): 0.75.

^{1}H NMR (300 MHz) ($CDCl_3$): δ [ppm] = 2.35 (s, 6H, Ar-CH_3); 3.89 (s, 3H, OCH_3); 7.17 (s, 1H, Ar-H); 7.65 (s, 2H, Ar-H).

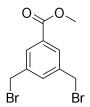

Methyl 3,5-bis(bromomethyl)benzoate 7:

To a solution of recrystallized NBS (94 g, 528 mmol) and methyl 3,5-dimethyl benzoate **6** (39.4 g, 240 mmol) in methyl formate (200 mL), AIBN (150 mg) was added. The reaction mixture was irradiated for four hours with a 100 Watt light bulb, which caused the reaction to reflux. Evaporation of methyl formate afforded a solid, which was resuspended in Et_2O (300 mL). After filtration, the filtrate was washed twice with $Na_2S_2O_5$ (10% w/w in H_2O) (2x 150mL) and twice with brine (2x 150 mL). The organic layer was dried over Na_2SO_4 and concentrated *in*

vacuo. The yellow solid was recrystallized from Et_2O, which afforded **7** as white crystals (44.7 g, 139 mmol, 58%). R_f (EtOAc/Hex, 1:3, v/v): 0.46.

^{1}H NMR (300 MHz) ($CDCl_3$): δ [ppm] = 3.93 (s, 3H, OCH_3); 4.50 (s, 4H, CH_2Br); 7.62 (t, J=1.65 Hz, 1H, Ar-H); 8.00 (d, J=1.65 Hz, 2H, Ar-H).

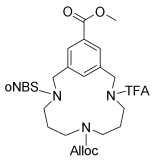

TAC(*o*NBS/Alloc/TFAc)-methylester 8:

To a solution of *o*NBS/Alloc/TFAc-protected triamine **4** (16 g, 32 mmol) in refluxing dry CH_3CN (2L), bisbromide **7** (10.4 g, 32 mmol), TBAB (10.4 g, 32 mmol) and Cs_2CO_3 (42 g, 128 mmol) were added. The reaction mixture was stirred under reflux for 1 hour, followed by concentration *in vacuo*. The residue was dissolved in DCM (500 mL) and washed with 0.2M $KHSO_4$ (500 mL), H_2O (300 mL) and brine (300 mL). Drying over Na_2SO_4 and concentration *in vacuo* afforded the crude product as yellow oil. Purification by silica gel chromatography (DCM/EtOAc 9:1 (v/v)) afforded **8** as yellowish foam (12 g, 18.2 mmol, 57 %). R_f (DCM/EtOAc, 7:1, v/v): 0.29.

^{1}H NMR (300 MHz) ($CDCl_3$): δ [ppm] = 1.35 (m, 2.5H, $CH_2CH_2CH_2$); 1.62 (m, 1.5H, $CH_2CH_2CH_2$); 2.92-3.11 (m, 4H, CH_2N); 3.23-3.45 (m, 4H, CH_2N); 3.93, 3.95 (2s, J=6.3 Hz, 3H, OCH_3); 4.45-4.51 (m, 4H, benzyl-CH_2 + OCH_2), 4.66 (s, 1H, benzyl-CH_2); 4.77 (s, 1H, benzyl-CH_2); 5.15-5.24 (m, 2H, CH=CH_2) 5.85 (m, 1H, *CH*=CH_2) 7.66-8.07 (m, 7H, *Ar*-H).

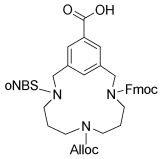

TAC(*o*NBS/Alloc/Fmoc)-carboxylic acid 9:

To a suspension of ester **8** (12 g, 18 mmol) in a mixture of dioxane (440 mL) and MeOH (158 mL), a 4N NaOH solution (31.5 mL) was added and the reaction mixture was stirred at room temperature for 4 h. The solution was neutralized by addition of 1N HCl, concentrated *in vacuo* and resuspended in 500 mL CH_3CN/H_2O (1:1, (v/v)). DIPEA was added to the reaction mixture until it turned clear and the pH was 10.5. A solution of Fmoc-OSu (6.7 g, 19.8 mmol) in CH_3CN (50 mL) was added, which caused the pH to decrease to 8.5. The reaction mixture was stirred at room temperature and the pH was kept at 8.5 by dropwise addition of DIPEA for 2 h. After acidification to pH 2 by addition of 2N HCl, the reaction mixture was extracted twice with EtOAc (2x 300 mL). The organic layers were combined, dried over Na_2SO_4 and concentrated *in vacuo*. The crude product was purified by silica gel chromatography (n-hexanes/EtOAc 1:2 (v/v), 0.5 vol % acetic acid), which afforded **9** as a white powder (10 g, 13 mmol, 72%). R_f (EtOAc/Hex/AcOH, 2:1:0.02, v/v): 0.18.

^{1}H NMR (300 MHz) ($CDCl_3$): δ [ppm] = 0.8-1.2, 1.3-1.6 (m, br, 4H, $CH_2CH_2CH_2$); 2.3-2.5, 2.7-3.1, 3.2-3.4 (m, 8H, CH_2N); 4.2-4.5, 4.6-4.8 (m, 9H, CH_2CH-Fmoc + Benzyl-CH_2 + Alloc-OCH_2); 5.17-5.23 (m, br, 2H, CH=CH_2)) 5.85 (m, 1H, *CH*=CH_2) 7.14-7.40, 7.54-7.80, 7.86-8.10 (m, 15H, *Ar*-H).

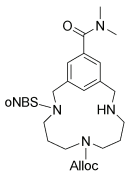

TAC(*o*NBS/Alloc)-amide 10:

To a solution of ester **8** (3.63 g, 5.6 mmol) in dioxane/MeOH (140mL/48.5mL), 4N NaOH (9.7mL) was added. The reaction was stirred at room temperature for 3 hours. After completion, the reaction was neutralized with 1N HCl (25mL), concentrated *in vacuo*, three times co-evaporated with toluene and dried over P_2O_5. The crude product was dissolved in DMF (200 mL) under nitrogen atmosphere and a solution of dimethylamine in THF (2M, 20 eq., 58 mL) was added dropwise. Afterwards, BOP (2.72 g, 6.16 mmol) was added and the reaction was stirred for 4 hours at room temperature. After completion, the reaction mixture was concentrated *in vacuo* and dissolved in EtOAc. After washing with 1M NaOH (250 mL), H_2O (250 mL) and brine, the organic layer was dried over Na_2SO_4 and concentrated *in vacuo*. The crude product was purified by silica gel chromatography (10% MeOH in DCM), which afforded **10** as yellowish foam (2.15 gr, 3.75 mmol, 67%). R_f (MeOH/DCM, 1:9, v/v): 0.30.

^{1}H NMR (300 MHz) ($CDCl_3$): δ [ppm] = 1.53 (m, 2H, *CH*$_2$CH$_2$NH); 1.6-1.8 (br m, 2H, *CH*$_2$CH$_2$N); 2.50 (t, J=6.3 Hz, 2H, *CH*$_2$NH); 2.90 (m, 2H, *CH*$_2$NS(O)$_2$); 2.96 (s, 3H, NCH$_3$); 3.10 (s, 3H, NCH$_3$); 3.16-3.28 (m, 4H, *CH*$_2$NC(O)); 3.86 (s, 2H, NH*CH*$_2$Ar); 4.42 (s, 2H, Ar-CH$_2$N), 4.47 (d, J= 5.5 Hz, 2H, *CH*$_2$CH=CH$_2$); 5.12-5.22 (m, 2H, CH=*CH*$_2$); 5.80-5.91 (m, 1H, *CH*=CH$_2$) 7.20-7-28 (m, 2H, Ar-H); 7.64-7.8 (m, 4H, Ar-H); 8.00-8.06 (m, 1H, Ar-H);

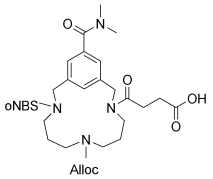

TAC(*o*NBS/Alloc/carboxylic acid)-amide 11:

To a solution of TAC-amide **10** (2.15 gr, 3.75 mmol) in DCM (50mL) under N_2 atmosphere, succinic anhydride (412 mg, 4.12 mmol) and DMAP (catalytic) were added under stirring. After 5 hours the reaction mixture was washed with 1M $KHSO_4$, H_2O and brine. The organic layer was dried over Na_2SO_4 and concentrated *in vacuo*. The crude product was purified by silica gel chromatography (8% MeOH in DCM), which afforded **11** as a yellow foam (2.2 gr, 3.3 mmol, 88%). R_f (MeOH/DCM, 1:9, v/v): 0.40.

^{1}H NMR (300 MHz) (CD_3OD): δ [ppm] = 1.27-1.55 (m, br, 4, CH$_2$*CH*$_2$CH$_2$); 2.64 (m, br, 4H, C(O)CH$_2$CH$_2$C(O)); 2.80-3.04 (m, br, 10H, N(CH$_3$)$_2$ + Alloc-N(CH$_2$)$_2$); 3.23-3.28, 3.36-3.49 (m, br, 4H, S(O)$_2$NCH$_2$ + CH$_2$C(O)N*CH*$_2$); 4.39-4.46 (m, 4H, benzyl-CH$_2$ + *CH*$_2$CH=CH$_2$); 4.64-4.66 (m, 2H, benzyl-CH$_2$); 5.06-5.21 (m, 2H, CH=*CH*$_2$); 5.76-5.87 (m, 1H, *CH*=CH$_2$); 7.33-7.40 (m, 2H, Ar-H); 7.54 (s, 0.5 H, Ar-H); 7.73-7.83 (m, 3.5H, Ar-H + *o*NBS-Ar-H); 8.00-8.04 (m, 1H, *o*NBS-Ar-H).

^{13}C NMR (75 MHZ) ($CDCl_3$): δ [ppm] = 29.3, 29.6, 30.4 (2x CH$_2$*C*H$_2$CH$_2$ + C(O)*C*H$_2$*C*H$_2$C(O)); 35.9, 40.3 (N(*C*H$_3$)$_2$); 47.0 and underneath CD_3OD residual solvent peaks (oNBS-N-*C*H$_2$-CH$_2$-*C*H$_2$-N(Alloc)-*C*H$_2$-CH$_2$-*C*H$_2$-N-C(O)); 52.0, 54.5 (2x benzyl-*C*H$_2$); 67.3(*C*H$_2$CH=CH$_2$); 118.0 (CH=*C*H$_2$); 125.8 (*o*NBS-Ar); 128.3 (Ar); 131.2, 131.7 (Ar + *o*NBS-Ar); 133.1 (*Ar*-C(O)); 133.6 (*o*NBS-Ar); 134.4 (*C*H=CH$_2$); 135.8 (*o*NBS-Ar); 138.9, 139.7, 140.3, 140.8, 142.1(Ar + oNBS-Ar-S(O)$_2$); 150.0 (Ar-NO$_2$); 157.5 (N*C*(O)O-CH$_2$); 172.7, 172.9, 174.4, 174.7, 176.5, 176.7 (N*C*(O)CH$_2$CH$_2$*C*(O)OH + *C*(O)N(CH$_3$)$_2$)

Both the ^{1}H- and ^{13}C-spectra demonstrated a high degree of splitting and overlap of signals, due to different conformations of the compound in solution. ^{1}H-spectra recorded in DMSO at 115ºC showed coalescence of the signals.

^{1}H NMR (500 MHz) (DMSO, 115ºC): δ [ppm] = 1.40 (m, br, 4, $CH_2CH_2CH_2$); 2.57 (m, br, 2H, $C(O)CH_2CH_2C(O)$); 2.68 (m, br, 2H, $C(O)CH_2CH_2C(O)$); 2.93 (m, br, 10H, $N(CH_3)_2$ + Alloc-$N(CH_2)_2$); 3.25 (m, br, 2H, $S(O)_2NCH_2$ or $CH_2C(O)NCH_2$); 3.36 (m, br, 2H, $S(O)_2NCH_2$ or $CH_2C(O)NCH_2$); 4.43 (m, 2H, $CH_2CH{=}CH_2$); 4.48 (s, 2H, benzyl-CH_2); 4.62 (s, 2H, benzyl-CH_2); 5.12-5.21 (m, 2H, $CH{=}CH_2$); 5.71-5.90 (m, 1H, $CH{=}CH_2$); 7.31 (s, 1H, Ar-H); 7.34 (s, 1H, Ar-H); 7.56 (s, 1H, Ar-H); 7.84-7.92 (m, 3H, *o*NBS-Ar-H); 8.06-8.08 (m, 1H, *o*NBS-Ar-H).

ESI-MS (monoisotopic mass $[M+H]^+$ calcd for $C_{31}H_{39}N_5O_{10}S$, 674.24; found, 674.20).

CHIPS mimic 12:

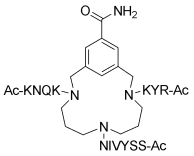

TentaGel S RAM (0.24 mmol/g, 1.04 g) was first deprotected by treatment with 20% piperidine/NMP (10mL, 3 times 8 min.), next the resin was loaded with TAC by coupling of TAC-carboxylic acid **9** (384 mg, 0.50 mmol) for 16 hr in the presence of BOP (221 mg, 0.5 mmol) and DIPEA (165 µL, 1.0 mmol) in NMP. The loading was tested by determining the Fmoc content of the resin, which was 0.21 mmol/g. The peptides were built up by manual solid phase peptide synthesis. A coupling cycle started by removal of the Fmoc group by 20% piperidine/NMP (10 mL, 3x 8 min.). After washing of the resin with NMP (2 times 10 mL) and DCM (2 times 10 mL) a Kaiser or chloranil test was performed to see if deprotection had occurred (chloranil for secondary amines).[38, 39] Each amino acid derivative was preactivated by mixing the amino acid (1 mmol) with HBTU (379 mg, 1 mmol), HOBt. H_2O (153 mg, 1 mmol) and DIPEA (330 µL, 2 mmol) in 10 mL NMP, this mixture was added to the deprotected resin for 1.5 hr. After washing with NMP (2 times 10 mL) and DCM (2 times 10 mL) the coupling was monitored with a Kaiser test. After complete coupling the resin was treated with capping solution (0.5 M Ac_2O, 0.125 M DIPEA, 15 mM HOBt.H_2O in NMP, 10 mL, 20 min.) to block any remaining unreacted amines. After washing with NMP (2 times 10 mL) and DCM (2 times 10 mL) the next deprotection-coupling cycle could start. After coupling of the last amino acid the Fmoc-group was removed and the N-terminus was acetylated by reaction with the capping solution (10 mL, 20 min.).

After completing the synthesis of the first peptide connected to TAC, the *o*NBS group was removed by treatment with DBU (187 µL, 1.25 mmol) and 2-mercaptoethanol (175 µL, 2.5 mmol) in 10 mL DMF (2 times 30 min.) The same protocol, as described for the first peptide, was followed for the synthesis of the second peptide.

After completion of the synthesis of the second peptide, the Alloc group was removed by treatment with anilinium *p*-toluensulfinate (1.25 g, 5 mmol) in NMP under argon bubbling for 10 min. after which freshly prepared $Pd(Ph_3P)_4$ (87 mg, 30 mol%)[40] was added and bubbling was continued for another hour. The resin was washed with NMP (3 times 10 mL), sodium diethyldithiocarbamate trihydrate (0.1 % in NMP, 10 mL), DIPEA (20% in NMP, 10 mL) and NMP (3 x 10 mL).

Then, the third peptide was assembled according to the same procedure. The complete construct thus obtained was deprotected and cleaved from the solid support by treatment with TFA/H_2O/TIS (95/2.5/2.5, 50 mL), for 2 h at room temperature. The mixture was filtered and the residue washed thoroughly with TFA (2 times 10 mL). The filtrate was concentrated *in vacuo* to a volume of approximately 10 mL and the residue was added dropwise to 90 mL MTBE/n-hexane (1/1, v/v) solution. The precipitate was collected by centrifugation (3000 rpm, 5 min.), the supernatant was decanted, and the pellet was resuspended in MTBE/n-hexane (1/1, v/v) (100 mL) and centrifuged again. This was repeated twice. After this, the pellets were dissolved in CH_3CN/H_2O (1/1, v/v) (ca. 60 mL) and lyophilized to give 409 mg of the crude peptide as a white fluffy solid.

Crude construct (210 mg) was dissolved in 15 mL buffer A, 5 mL buffer B and purified by preparative HPLC (Alltima C8, TFA buffers) in four runs. Fractions containing the pure product were pooled and lyophilized to give 83 mg (32%) of pure construct. **12**. The purity of **12** was established by analytical HPLC (Alltima C8, TFA buffers, Rt = 18.92 min., Purity >98%) and characterization was carried out by Maldi-TOF (monoisotopic mass $[M+H]^+$ calcd for $C_{93}H_{146}N_{26}O_{24}$, 2012.1; found, 2012.3).

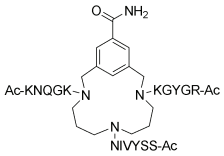

CHIPS mimic 13:

This construct was synthesized following the same procedure as described for mimic **12**, with a loading of TAC-carboxylic acid **9** on the resin of 0.24 mmol/g, yielding 487 mg of the crude compound as a white fluffy solid. The crude construct (210 mg) was dissolved in 15 mL buffer A, 5 mL buffer B and purified by preparative HPLC (Alltima C8, TFA buffers) in four runs. Fractions containing the pure product were pooled and lyophilized to give 68 mg (29%) of pure construct.

The purity of **13** was established by analytical HPLC (Alltima C8, TFA buffers, Rt = 18.53 min., Purity >99%) and characterization was carried out by Maldi-TOF (monoisotopic mass $[M+H]^+$ calcd for $C_{99}H_{155}N_{29}O_{27}$, 2183.2; found, 2183.7).

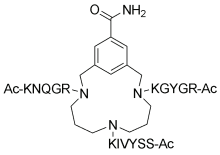

CHIPS mimic 14:

This construct was synthesized following the same procedure as described for mimic **12**, with a loading of TAC-carboxylic acid **9** on the resin of 0.21 mmol/g, yielding 423 mg of the crude compound as a white fluffy solid. The crude construct (210 mg) was dissolved in 15 mL buffer A, 5 mL buffer B and purified by preparative HPLC (Alltima C8, TFA buffers) in four runs. Fractions containing the pure product were pooled and lyophilized to give 92 mg (33%) of pure construct.

The purity of **14** was established by analytical HPLC (Alltima C8, TFA buffers, Rt = 18.73 min., Purity >98%) and characterization was carried out by Maldi-TOF (monoisotopic mass $[M+H]^+$ calcd for $C_{101}H_{161}N_{31}O_{26}$, 2225.2; found, 2225.6).

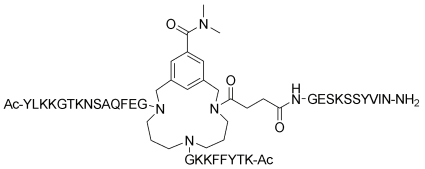

CHIPS mimic 15:

Construct **14** was synthesized on Tentagel S RAM resin (0.24 mmol/g) on a 0.25 mmol scale by standard SPPS on an automatic ABI 433A Peptide Synthesizer using the ABI FastMoc 0.25 mmol protocols, except that the coupling time was 45 min. instead of 20 min. [41, 42] After coupling of the first peptide sequence to the resin TAC-amide **11** (337 mg, 0.5 mmol) was coupled with BOP (221 mg, 0.5 mmol) and DIPEA (166 µL, 1 mmol) in DCM (10 mL). Then, the *o*NBS group was removed by treating the resin with DBU (187 µL, 1.25 mmol) and 2-mercaptoethanol (175 µL, 2.5 mmol) in 10 mL DMF (2 times 30 min.), deprotection was monitored by the chloranil test.[38] Coupling of the first glycine residue of the second peptide was performed by manual SPPS (2 times 90 min.). After capping the Fmoc loading was determined to be 0.18 mmol/g. The remainder of the peptide arm was synthesized using the ABI 433A Peptide Synthesizer. After this, the Alloc group was removed by treatment with anilinium *p*-toluensulfinate (1.25 g, 5 mmol) in NMP under argon bubbling for 10 min. Freshly prepared $Pd^0(Ph_3P)_4$ (87 mg, 30 mol%)[40] was added and bubbling was continued for another hour. Finally, after treatment with sodium diethyldithiocarbamate trihydrate (0.1 % in NMP, 10 mL, 5 min.) and DIPEA (20% in NMP, 10 mL) coupling of the first glycine of the third peptide was performed by manual SPPS (2 times 90 min.). After capping the Fmoc loading was determined to be 0.12 mmol/g. The remainder of the third peptide was synthesized using the ABI 433A Peptide Synthesizer.

Upon completion of the third peptide arm the complete construct thus obtained was deprotected and cleaved from the solid support by treatment with TFA/H_2O/TIS (95/2.5/2.5, 50 mL), for 2 hr at room temperature. The mixture was filtered and the residue washed thoroughly with TFA (2 times 10 mL). The reaction mixture was concentrated *in vacuo* to a volume of approximately 10 mL and the residue was added dropwise to 90 mL MTBE/n-hexane (1/1, v/v) solution. The precipitate was collected by centrifugation (3000 rpm, 5 min.), the supernatant was decanted, and the pellet was resuspended in MTBE/n-hexane (1/1, v/v) (100 mL) followed by centrifugation. This was repeated twice. The pellets were dissolved in CH_3CN/H_2O (1/1, v/v) (ca. 60 mL) and lyophilized to give 453 mg of the crude peptide as a white fluffy solid.

The crude construct (180 mg) was dissolved in 30 mL buffer A and purified by preparative HPLC (Prosphere C18, TFA buffers) in six runs. Fractions containing the pure product were pooled and lyophilized to give 7 mg (1.7 %) of pure construct. **15**. The purity of **15** was established by analytical HPLC (Gemini C18, TFA buffers, Rt = 22.15 min., Purity >98%) and characterization was carried out by Maldi-TOF (average mass $[M+3H]^{3+}$ calcd for $C_{192}H_{291}N_{47}O_{53}$, 1369.6; found, 1370.6).

6.5 References

[1] J. A. Robinson, S. DeMarco, F. Gombert, K. Moehle, D. Obrecht, The design, structures and therapeutic potential of protein epitope mimetics, *Drug Disc. Today* **2008**, *13*, 944.

[2] M. Goodman, Y. Feng, G. Melacini, J. P. Taulane, A template-induced incipient collagen-like triple-helical structure, *J. Am. Chem. Soc.* **1996**, *118*, 5156.

[3] K. Rose, W. G. Zeng, L. E. Brown, D. C. Jackson, A synthetic peptide-based polyoxime vaccine construct of high purity and activity, *Mol. Immunol.* **1995**, *32*, 1031.

[4] D. Boturyn, J. L. Coll, E. Garanger, M. C. Favrot, P. Dumy, Template assembled cyclopeptides as multimeric system for integrin targeting and endocytosis, *J. Am. Chem. Soc.* **2004**, *126*, 5730.

[5] H. K. Rau, W. Haehnel, Design, synthesis, and properties of a novel cytochrome b model, *J. Am. Chem. Soc.* **1998**, *120*, 468.

[6] H. K. Rau, N. DeJonge, W. Haehnel, Modular synthesis of de novo designed metalloproteins for light-induced electron transfer, *Proc. Natl. Acad. Sci. U. S. A.* **1998**, *95*, 11526.

[7] H. K. Rau, H. Snigula, A. Struck, B. Robert, H. Scheer, W. Haehnel, Design, synthesis and properties of synthetic chlorophyll proteins, *Eur. J. Biochem.* **2001**, *268*, 3284.

[8] M. Pawlak, U. Meseth, B. Dhanapal, M. Mutter, H. Vogel, Template-assembled melittin - Structural and functional-characterization of a designed, synthetic channel-forming protein, *Protein Sci.* **1994**, *3*, 1788.

[9] S. Futaki, M. Aoki, M. Fukuda, F. Kondo, M. Niwa, K. Kitagawa, Y. Nakaya, Assembling of the four individual helices corresponding to the transmembrane segments (S4 in repeat I-IV) of the sodium channel, *Tetrahedron Lett.* **1997**, *38*, 7071.

[10] S. Futaki, K. Sogawa, J. Maruyama, T. Asahara, M. Niwa, H. Hojo, Preparation of peptide thioesters using Fmoc-solid-phase peptide synthesis and its application to the construction of a template-assembled synthetic protein (TASP), *Tetrahedron Lett.* **1997**, *38*, 6237.

[11] J. Hauert, J. Fernandez-Carneado, O. Michielin, S. Mathieu, D. Grell, M. Schapira, O. Spertini, M. Mutter, G. Tuchscherer, T. Kovacsovics, A template-assembled synthetic protein surface mimetic of the von Willebrand factor A1 domain inhibits botrocetin-induced platelet aggregation, *Chembiochem* **2004**, *5*, 856.

[12] H. S. Park, Q. Lin, A. D. Hamilton, Protein surface recognition by synthetic receptors: A route to novel submicromolar inhibitors for alpha-chymotrypsin, *J. Am. Chem. Soc.* **1999**, *121*, 8.

[13] T. Sasaki, E. T. Kaiser, Helichrome - Synthesis and enzymatic-activity of a designed hemeprotein, *J. Am. Chem. Soc.* **1989**, *111*, 380.

[14] K. S. Akerfeldt, R. M. Kim, D. Camac, J. T. Groves, J. D. Lear, W. F. Degrado, Tetraphilin - a 4-Helix Proton Channel Built on a Tetraphenylporphyrin Framework, *J. Am. Chem. Soc.* **1992**, *114*, 9656.

[15] H. Mihara, K. Tomizaki, T. Fujimoto, S. Sakamoto, H. Aoyagi, N. Nishino, Artificial membrane protein functionalized with electron transfer system, *Chem. Lett.* **1996**, 187.

[16] E. T. Rump, D. T. S. Rijkers, H. W. Hilbers, P. G. de Groot, R. M. J. Liskamp, Cyclotriveratrylene (CTV) as a new chiral triacid scaffold capable of inducing triple helix formation of collagen peptides containing either a native sequence or Pro-Hyp-Gly repeats, *Chem. Eur. J.* **2002**, *8*, 4613.

[17] H. de Muynck, A. Madder, N. Farcy, P. J. de Clercq, M. N. Perez-Payan, L. M. Ohberg, A. P. Davis, Application of combinatorial procedures in the search for serine-protease-like activity with focus on the acyl transfer step, *Angew. Chem. Int. Ed.* **2000**, *39*, 145.

[18] X. T. Zhou, A. U. Rehman, C. Li, P. B. Savage, Preparation of a protected triamino analogue of cholic acid and sequential incorporation of amino acids in solution and on a solid support, *Org. Lett.* **2000**, *2*, 3015.

[19] N. Farcy, H. De Muynck, A. Madder, N. Hosten, P. J. De Clercq, A pentaerythritol-based molecular scaffold for solid-phase combinatorial chemistry, *Org. Lett.* **2001**, *3*, 4299.

[20] A. Gea, N. Farcy, N. R. I. Rossell, J. C. Martins, P. J. De Clercq, A. Madder, Solid-supported synthesis of highly functionalized tripodal peptides with flexible but preorganized geometry: Towards potential serine protease mimics, *Eur. J. Org. Chem.* **2006**, 4135.

[21] C. Chamorro, J. W. Hofman, R. M. J. Liskamp, Combinatorial solid-phase synthesis and screening of a diverse tripodal triazacyclophane (TAC)-based synthetic receptor library showing a remarkable selectivity towards a D-Ala-D-Ala containing ligand, *Tetrahedron* **2004**, *60*, 8691.

[22] M. Hijnen, D. J. van Zoelen, C. Chamorro, P. van Gageldonk, F. R. Mooi, G. Berbers, R. M. J. Liskamp, A novel strategy to mimic discontinuous protective epitopes using a synthetic scaffold, *Vaccine* **2007**, *25*, 6807.

[23] D. J. van Zoelen, M. R. Egmond, R. J. Pieters, R. M. J. Liskamp, Synthesis and evaluation of TAC-based inhibitors of papain as mimics of cystatin b, *Chembiochem* **2007**, *8*, 1950.

[24] H. B. Albada, R. M. J. Liskamp, TAC-Scaffolded tripeptides as artificial hydrolytic receptors: A combinatorial approach toward esterase mimics, *J. Comb. Chem.* **2008**, *10*, 814.

[25] C. J. C. de Haas, K. E. Veldkamp, A. Peschel, F. Weerkamp, W. J. B. Van Wamel, E. C. J. M. Heezius, M. J. J. G. Poppelier, K. P. M. Van Kessel, J. A. G. van Strijp, Chemotaxis inhibitory protein of *Staphylococcus aureus*, a bacterial antiinflammatory agent, *J. Exp. Med.* **2004**, *199*, 687.

[26] P. J. Haas, C. J. C. de Haas, M. J. J. C. Poppelier, K. P. M. van Kessel, J. A. G. van Strijp, K. Dijkstra, R. M. Scheek, H. Fan, J. A. W. Kruijtzer, R. M. J. Liskamp, J. Kemmink, The structure of the C5a receptor-blocking domain of chemotaxis inhibitory protein of *Staphylococcus aureus* is related to a group of immune evasive molecules, *J. Mol. Biol.* **2005**, *353*, 859.

[27] P. J. Haas, *Staphylococcal* drug discovery, PhD thesis, Utrecht University (Utrecht), **2006**, 73.

[28] A. J. Wright, A. Higginbottom, D. Philippe, A. Upadhyay, S. Bagby, R. C. Read, P. N. Monk, L. J. Partridge, Characterisation of receptor binding by the chemotaxis inhibitory protein of *Staphylococcus aureus* and the effects of the host immune response, *Mol. Immunol.* **2007**, *44*, 2507.

[29] J. H. Ippel, C. J. C. De Haas, A. Bunschoten, J. A. G. van Strijp, J. A. W. Kruijtzer, R. M. J. Liskamp, J. Kemmink, Structure of the tyrosine-sulfated C5a-receptor N-terminus in complex with chemotaxis inhibitory protein of Staphylococcus aureus, *J. Biol. Chem.* **2009**, *284*, 12363.

[30] T. Opatz, R. M. J. Liskamp, Synthesis and screening of libraries of synthetic tripodal receptor molecules with three different amino acid or peptide arms: Identification of iron binders, *J. Comb. Chem.* **2001**, *4*, 275.

[31] T. Opatz, R. M. J. Liskamp, A selectively deprotectable triazacyclophane scaffold for the construction of artificial receptors, *Org. Lett.* **2001**, *3*, 3499.

[32] M. C. F. Monnee, A. J. Brouwer, R. M. J. Liskamp, Synthesis, screening and evaluation of a combined library of tweezer- and tripodal synthetic receptors, *QSAR & Comb. Sci.* **2004**, *23*, 546.

[33] H. B. Albada, F. Soulimani, B. M. Weckhuysen, R. M. J. Liskamp, Scaffolded amino acids as a close structural mimic of type-3 copper binding sites, *Chem. Commun.* **2007**, 4895.

[34] C. Chamorro, J. A. W. Kruijtzer, M. Farsaraki, J. Balzarini, R. M. J. Liskamp, A general approach for the non-stop solid phase synthesis of TAC-scaffolded loops towards protein mimics containing discontinuous epitopes, *Chem. Commun.* **2009**, 821.

[35] E. Gustafsson, A. Rosen, K. Barchan, K. P. M. van Kessel, K. Haraldsson, S. Lindman, C. Forsberg, L. Ljung, K. Bryder, B. Walse, P. J. Haas, J. A. G. van Strijp, C. Furebring, Directed evolution of chemotaxis inhibitory protein of *Staphylococcus aureus* generates biologically functional variants with reduced interaction with human antibodies, *Protein Eng., Des. Sel.* **2010**, *23*, 91.

[36] A. Bunschoten, J. A. W. Kruijtzer, J. H. Ippel, C. J. C. de Haas, J. A. G. van Strijp, J. Kemmink, R. M. J. Liskamp, A general sequence independent solid phase method for the site specific synthesis of multiple sulfated-tyrosine containing peptides, *Chem. Commun.* **2009**, 2999.

[37] E. von Arx, M. Faupel, M. Brugger, Das 4,4´-tetramethyldiamino-diphenylmethan reagens (TDM). Eine modifikation der chlor-o-tolidin farbereaktion fur die dunnschichtchromatographie, *J. Chromatogr., A* **1976**, *120*, 224.

[38] T. Vojkovsky, Detection of Secondary-Amines on Solid-Phase, *Pept. Res.* **1995**, *8*, 236.

[39] E. Kaiser, R. L. Colescott, C. D. Bossinger, P. I. Cook, Color test for detection of free terminal amino groups in the solid-phase synthesis of peptides, *Anal. Biochem.* **1970**, *34*, 595.

[40] S. Komiya, *Synthesis of Organomateallic Compounds*, John Wiley & Sons Ltd., **1997**.

[41] A. Biosystems, *Applied Biosystems Model 433A Peptide Synthesizer User´s Manual* **June 1993**, version 1.0.

[42] A. Biosystems, *Applied Biosystems Research News* **June 1993**, Model 433A Peptide Synthesizer.

Appendices

Summary

Samenvatting

Curriculum Vitae

List of publications

Summary

Post-translational modifications are modification of peptides or proteins after they have been synthesized in the ribosomes. These post-translational modifications (PTM's) are intended to augment functional diversity of the 20 natural L-amino acids of which proteins are constructed. PTM's have important functions and most are crucial for the tasks of the modified proteins. Phosphorylation and dephosphorylation of serine, threonine and tyrosine, for instance, is crucial for multiple intracellular signalling pathways, while acetylation and deacetylation of histones is highly involved in gene transcription.

Sulfation of small aromatic compounds in the human body has first been described in 1876 and was recognized as a post-translational modification of proteins in 1954. Slowly it was realized that tyrosine sulfation is a widespread modification of excreted and membrane bound peptides and proteins. Sulfation is catalyzed by two membrane bound tyrosylprotein sulfotransferases (TPST), which are located in the trans Golgi. These enzymes and the universal sulfate donor PAPS were found in all examined tissues of the human body. Although sulfation is believed to be a widespread and biologically very important PTM, it has not been studied in great detail. This is mainly because of the instability of the sulfate group, especially under acidic conditions. This represents a major hurdle for its identification in cell lysates or complex protein mixtures, for its localization within peptide sequences and for the synthesis of biological important sulfated peptides.

In **chapter 1** the *in vivo* occurrence of sulfation is discussed as well as the efforts to analyze and identify sulfated tyrosine residues within peptides and proteins. Isotope labeling, inhibition of sulfation, sulfotyrosine selective antibodies and mass spectrometry are described in the literature as methods for the identification of sulfated tyrosine residues and to determine their role within sulfated peptides and proteins. A very important and useful method especially for the elucidation of the role of sulfated tyrosine residues within peptides and proteins is the chemical synthesis of sulfated peptides for *in vitro* and *in vivo* studies. Several methods for the chemical synthesis of sulfated peptides have been described in the literature, like the use of global sulfating reagents, introduction of protected and unprotected sulfated building blocks, the introduction of a sulfate isostere and enzymatic sulfation (Fig. A1). Each method has its advantages and its shortcomings. Within this thesis a new general applicable sequence independent method for the synthesis of multiple sulfated peptides will be described and applied.

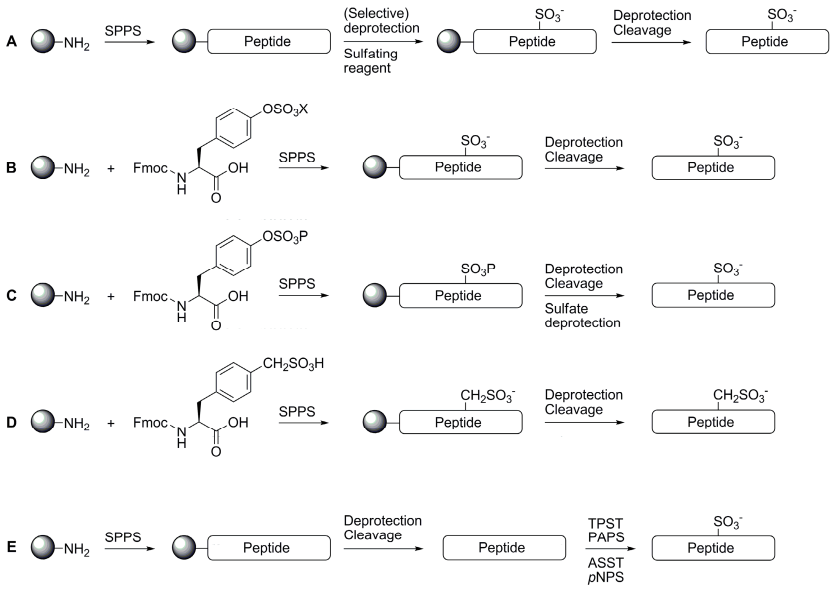

Figure A1 Sulfating methods described in the literature. A) global sulfating reagents, B) Unprotected sulfated Fmoc-building blocks with appropriate counterion (X), C) Protected sulfated Fmoc-building blocks with appropriate protecting group (P), D) Sulfotyrosine isostere, E) Enzymatic sulfation.

The C5a-receptor (C5aR) is a crucial protein involved in the human complement system. Activation of this receptor by its natural ligand C5a leads to the migration of specific white blood cells towards the site of infection to kill invading pathogens. This very sensitive and effective defense mechanism depends on the presence of two sulfated tyrosine residues in the N-terminal part of the C5a-receptor. Although this complement system is a crucial defense mechanism against invading pathogens, unnecessary, excessive or chronic activation of C5aR has been linked to several inflammatory diseases. Therefore several inhibitors for the C5aR have been developed targeting the activation site in the receptor core. A new approach for the inhibition of the C5aR is inspired by the **Ch**emotaxis **I**nhibitory **P**rotein of ***S**taphylococcus aureus* (CHIPS) (Fig. A2). CHIPS is found in the supernatant of most strains of the bacterium *S. aureus*, which is capable of blocking the C5aR by binding to its extracellular N-terminus. Knowledge about the interactions of CHIPS with the sulfated N-terminus of the C5a-recepter might open the way for new anti-inflammatory compounds.

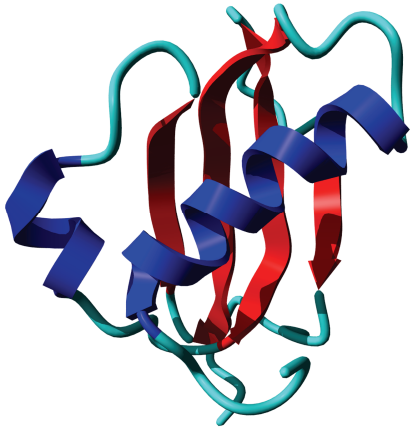

Figure A2 An NMR structure of $CHIPS_{31\text{-}121}$ (PDB: 1XEE)

In **chapter 2** a new convenient strategy for the solid phase synthesis of sulfated peptides is described. By selective deprotection of the tyrosine residues that have to be sulfated and the introduction of a trichloroethyl (TCE) protected sulfate on these tyrosine residues, an acid stable (protected) sulfated peptide is synthesized. This peptide can be cleaved and deprotected with 95% trifluoroacetic acid (TFA) and purified by TFA-buffers without cleaving the protected sulfates. After purification, the TCE group can be removed under mild conditions yielding the sulfated peptide as ammonium salt. With this strategy a small library of sulfated C5aR mimics was synthesized containing peptides ranging from nine to thirty-five amino acids. Site selective introduction is shown with one or two sulfated tyrosine residues next to unmodified tyrosines and the compatibility with the cysteine side chain is demonstrated. One hurdle in the synthesis of these C5aR mimics had to be taken, the trityl protecting group of histidine had to be replaced by the dimethoxybenzoyl protecting group to prevent sulfation of this residue. This protecting group was conveniently removed in the final stage by 7 M NH_3 in methanol. Next to the sulfating reagent applied in this chapter, 2,2,2-trichloroethyl chlorosulfate, the more stable 2,2,2-trichloroethyl methylimidazoliumsulfate salt was synthesized and tested on a small peptide. This reagents was at least as reactive as 2,2,2-trichloroethyl chlorosulfate and showed no degradation upon 9 months storage at room temperature.

In **chapter 3** the small library of C5aR mimics is used for binding experiments. The affinity of CHIPS for the C5aR mimics is determined by Isothermal Titration Calorimetry (ITC) and their potency to compete with the native receptor is explored in a biological assay with C5aR expressing cells. The strongest binder appeared to be the doubly sulfated $C5aR_{7\text{-}28}S_2$ (K_d = 8.4 nM) (residue numbers based on Swiss-Prot entry P21730). Both sulfated tyrosine residues were necessary to obtain low nanomolar binding. $C5aR_{7\text{-}28}S_2$ was selected to form a complex with $CHIPS_{31\text{-}121}$ for structural studies by NMR spectroscopy. Based on long range NOE contacts within CHIPS, the $C5aR_{7\text{-}28}S_2$ and between these two molecules, the structure of the $CHIPS_{31\text{-}121}$:$C5aR_{7\text{-}28}S_2$ complex could be solved.

(Fig. A3A) The structure of this complex revealed a number of key interactions, amongst which especially the interactions of the sulfated tyrosine residues demonstrated the importance of this post-translational modification of the C5a-receptor. Structural information of the complex is crucial for the design of a new class of CHIPS-based C5aR inhibitors.

In **chapter 4** we explored the possibility of replacing the sulfate groups, naturally present *in vivo* on the N-terminus of the C5a-receptor, with the synthetically more amenable and stable phosphate groups. Several phosphorylated C5aR mimics were synthesized and their binding to CHIPS was studied by ITC, NMR and in a biological assay. The phosphorylated C5aR mimics showed a comparable nanomolar binding affinity in for CHIPS. The influence of the doubly phosporlylated C5aR mimic on the chemical shifts of the backbone amides of CHIPS was strikingly similar to the original sulfated C5aR mimics. However, in a biological assay the phosphorylated C5aR mimics were significantly less potent compared to the sulfated versions.

In **chapter 5** the knowledge, we obtained from studying the CHIPS:C5a$R_{7\text{-}28}S_2$ complex was employed to design a mimic of CHIPS. We coined this mimic '**CH**emotaxis inhibitory c**O**nstruct **P**rotein of ***S****taphylococcus aureus*' (CHOPS) (Fig. A3B). CHOPS consists of two fragments of CHIPS, which are in direct contact with the C5aR. Those two fragments were linked together via a small β-turn inducing sequence to form a single small protein. This 50 residue long protein was able to bind to C5a$R_{7\text{-}28}S_2$ with a dissociation constant of 3.6 μM, while it showed no affinity towards the unsulfated C5aR mimic. While free CHOPS is unstructured in solution, upon binding to C5a$R_{7\text{-}28}S_2$ several long-range NOE contacts could be identified, which were also observed in NMR spectra of the $CHIPS_{31\text{-}121}$:C5a$R_{7\text{-}28}S_2$ complex. This suggests that CHOPS, upon binding C5a$R_{7\text{-}28}S_2$, adopts a similar fold compared to native CHIPS.

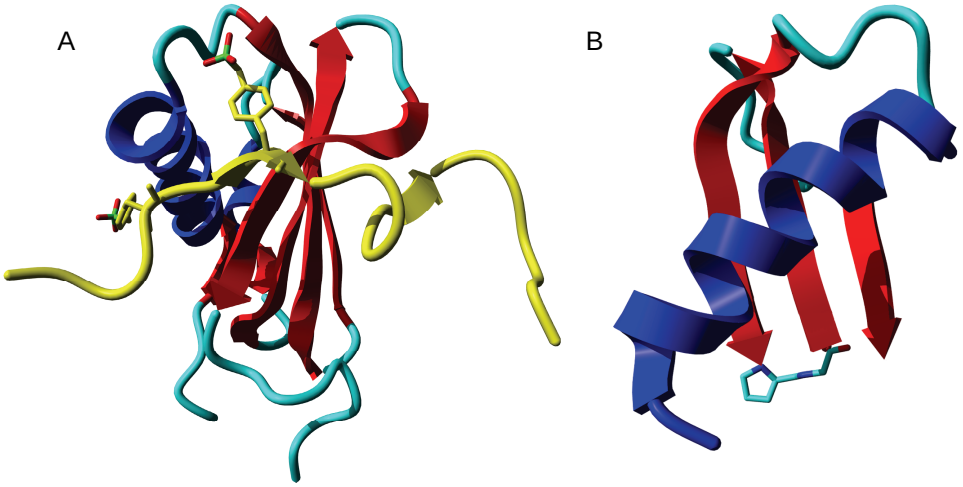

Figure A3 A) A NMR structure of the $CHIPS_{31\text{-}121}$:C5a$R_{7\text{-}28}S_2$ complex, B) A model of CHOPS.

After the successful development of this first mimic of CHIPS we attempted to further reduce the size of CHIPS mimics. In **chapter 6** a different approach to mimic CHIPS was explored. Several small peptide fragments of CHIPS, which are important for the interaction with the C5aR, are selected and brought together on a scaffold. The TAC scaffold with three orthogonal protecting groups was selected, which made it possible to attach three different peptides to the same scaffold. Four mimics of CHIPS were successfully synthesized, unfortunately none of them demonstrated affinity for the sulfated or unsulfated C5aR mimic in ITC experiments.

Nederlandse samenvatting

Post-translationele modificaties (PTM's) zijn aanpassingen aan peptiden of eiwitten die plaatsvinden na hun synthese door de ribosomen, de eiwitfabrieken van de cel. Deze post-translationele modificaties zijn bedoeld om de varieteit en functionaliteit van eiwitten te vergroten buiten de eigenschappen die al ingebouwd zijn via de 20 L-aminozuren waaruit eiwitten zijn opgebouwd. PTM's hebben belangrijke functies en zijn cruciaal voor de gemodificeerde eiwitten om hun taken uit te voeren. Phosphorylering en dephosphorylering van serine, threonine en tyrosine residuen is cruciaal bij het doorgeven van signalen binnen in een cel en acetylering en deacetylering van histonen is van enorm belang bij het goed vertalen van de juiste stukken genetisch materiaal.

De sulfatering van kleine aromatisch moleculen in het menselijk lichaam is voor het eerst beschreven in de literatuur in 1876 en de reactie werd erkend als een post-translationele modificatie van eiwitten in 1954. Langzaam zag men in dat de sulfatering van tyrosine residuen in eiwitten een veel voorkomende modificatie is en dat het vooral voorkomt bij peptiden en eiwitten die de cel verlaten of membraan gebonden zijn. De sulfatering van tyrosine residuen in eiwitten wordt uitgevoerd door twee membraan gebonden enzymen, tyrosylprotein sulfotransferases (TPST) genaamd, die zich bevinden in het trans Golgi. Deze twee enzymen, samen met de sulfaat donor PAPS, zijn aangetoond in alle onderzochte weefsels in het menselijk lichaam. Ondanks dat sulfatering een veel voorkomende PTM is, is er nog niet heel veel over bekend en zijn er nog maar weinig gesulfateerde eiwitten beschreven. Dit komt vooral door de chemische instabiliteit van deze sulfaat groepen, vooral onder zure condities. Dit is een groot obstakel voor het aantonen van gesulfateerde tyrosines in cel lysaten of complexe eiwit mengsels, voor het lokaliseren van de gesulfateerde tyrosine residuen in een peptide sequenties en voor de synthese van biologisch actieve gesulfateerde peptiden.

In **hoofdstuk 1** wordt zowel sulfatering *in vivo* besproken als het onderzoek dat wordt verricht om sulfatering *in vivo* aan te tonen. Isotoop labelling, het inhiberen van sulfatering, antilichamen tegen sulfotyrosine en massa spectrometrie worden in de literatuur beschreven als methodes voor het identifiseren van gesulfateerde peptiden en eiwitten en voor het ophelderen van de rol van het gesulfateerde tyrosine residuen in het betreffende eiwit of peptide. De functie van de sulfaat groep binnen een peptide of eiwit kan goed bestudeerd worden d.m.v. *in vitro* en *in vivo* binding studies met behulp van synthetisch gesulfateerde peptiden. Via chemische synthese kunnen grotere hoeveelheden van een zuiver gesulfateerd peptide worden verkregen. In de literatuur zijn meerdere synthese routes beschreven zoals: globale sulfaterings reagentia, het inbouwen van beschermde of onbeschermde gesulfateerde bouwstenen, het introduceren van een sulfaat mimeticum en het enzymatische sulfateren (Fig. A1). Elke methode heeft zo zijn voor- en nadelen. In dit proefschrift zal een nieuwe, breed toepasbare synthese van gesulfateerde peptiden worden beschreven die onafhankelijk is van de peptide sequentie. Deze nieuwe methode zal toegepast worden op de synthese van een collectie gesulfateerde C5a-receptor mimetica.

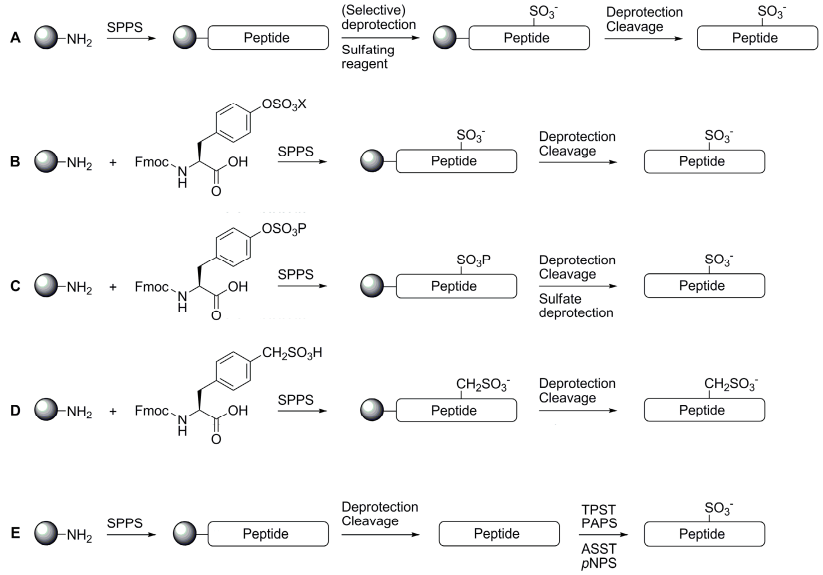

Figuur A1 Sulfaterings methods beschreven in de literatuur. A) algemene sulfaterings reagentia, B) Onbeschermd gesulfateerde Fmoc-bouwstenen met geschikt tegen-ion (X), C) Beschermd gesulfateerd Fmoc-bouwsteen met geschikte beschermgroep (P), D) Sulfotyrosine mimeticum, E) Enzymatische sulfatering.

De C5a-receptor is een cruciaal eiwit dat betrokken is bij het humane complement systeem. Activatie van deze receptor door zijn natuurlijke ligand C5a resulteert in de migratie van specifieke witte bloedlichamen richting de plaats van een infectie om de oorzaak aan te pakken. Dit gevoelige en effectieve mechanisme is afhankelijk van twee gesulfateerde tyrosine residuen in het N-terminale gedeelte van de C5a-receptor. Alhoewel het complement systeem een onmisbare bescherming tegen binnendringende ziekteverwekkers is, speelt onnodige, onnodig sterke of chronische activatie van de C5aR een rol bij verschillende ontstekingsziektes. Daarom is er een actieve zoektocht naar remmers van deze receptor gaande. De meeste remmers die op dit moment bekend zijn, zijn gericht op de activatie plek van de receptor in zijn kern. Een nieuwe benadering heeft men gevonden in het eiwit **Ch**emotaxis **I**nhibitory **P**rotein of ***S****taphylococcus aureus* (CHIPS) (Fig. A2). Dit eiwit is ontdekt in het supernatant van de bacterie *S. aureus* en dit eiwit blokkeert de receptor door aan het N-terminale gedeelte van de receptor te binden. Als we exact weten welke interacties tussen CHIPS en de C5aR belangrijk zijn, kan dit gebruikt worden voor de ontwikkeling van nieuwe ontstekingsremmers.

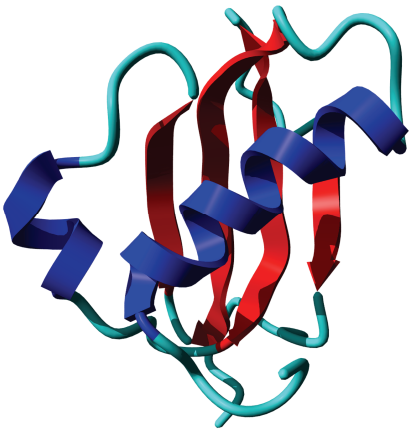

Figuur A2 Een NMR structuur van $CHIPS_{31-121}$ (PDB: 1XEE)

In **hoofdstuk 2** wordt een nieuwe strategie voor de synthese van gesulfateerde peptiden op de vaste drager beschreven. Allereerst worden de tyrosine residuen, die gesulfateerd moeten worden, selectief ontschermd. Vervolgens wordt er een sulfaat groep geintroduceerd die beschermd is met een trichloroethyl (TCE) group, waardoor deze sulfaat groep nu zuur stabiel is. Hierdoor kan het peptide ontschermd en van de vaste drager gesplitst worden met 95 % trifluoro azijnzuur (TFA) en kan het gezuiverd worden met TFA buffers zonder dat de sulfaat groep wordt aangetast. Na zuivering kan de TCE groep worden verwijderd onder milde omstandigheden waardoor het gesulfateerde peptide wordt verkregen als ammonium zout. Met deze methode is een kleine collectie gesulfateerde mimetica van de C5a-receptor gemaakt, waaronder peptiden van 9 tot 35 residuen lang. De gesulfateerde tyrosines konden worden ingebouwd naast ongemodificeerde tyrosines. Bovendien is het met deze methode mogelijk om cysteine residuen in te bouwen in de gesulfateerde peptiden. Een hindernis die genomen moest worden was het vervangen van de trityl beschermgroep van histidine door de dimethoxybenzoyl groep om sulfatering van histidine te voorkomen. Deze beschermgroep kon gemakkelijk worden verwijderd met 7M NH_3 in methanol, aan het eind van de peptide synthese Naast het sulfaterings reagens dat in dit hoofdstuk is gebruikt, 2,2,2-trichloroethyl chloorsulfaat, is ook het stabielere 2,2,2-trichloroethyl methylimidazoliumsulfaat zout gemaakt en getest op een klein peptide. Dit reagens was minstens zo actief als het gebruikte 2,2,2-trichloroethyl chlorosulfaat en liet geen degradatie zijn na 9 maanden opslag bij kamertemperatuur.

In **hoofdstuk 3** wordt de collectie van C5aR mimetica getest op affiniteit voor CHIPS. Deze affiniteit is bepaald met ‘Isothermal Titration Calorimetry’ (ITC). De C5aR mimic met de hoogste affiniteit voor CHIPS bleek de dubbel gesulfateerde $C5aR_{7-28}S_2$ te zijn met een dissociatie constante van 8.4 nM. (nummering van de C5aR mimics is gebaseerd op Swiss-prot artikel P21730). De potentie van deze C5aR mimic is ook bestudeerd in een biologisch assay waar dit peptide kon competeren met de natieve C5a-receptor op een C5aR dragende cellijn. In beide experimenten bleken de twee

gesulfateerde tyrosine residuen op positie 11 en 14 cruciaal te zijn voor de hoge bindingsaffiniteit. $C5aR_{7\text{-}28}S_2$ is geselecteerd om een complex te vormen met CHIPS waarna de structuur van dit complex opgehelderd kon worden met NMR spectroscopy (Fig. A3A). Met behulp van lange afstands NOE contacten binnen CHIPS, het $C5aR_{7\text{-}28}S_2$ peptide en tussen hen beide, kon de structuur van het $CHIPS_{31\text{-}121}$:$C5aR_{7\text{-}28}S_2$ opgelost worden. De structuur van dit complex onthulde verschillende cruciale interacties, waarvan vooral de contacten tussen de gesulfateerde tyrosines van $C5aR_{7\text{-}28}S_2$ en $CHIPS_{31\text{-}121}$ de belangrijke rol van de gesulfateerde tyrosine residuen bevestigde. De structurele informatie van dit complex levert zeer belangrijke informatie op voor het ontwerpen van een nieuwe klasse van C5aR remmers gebaseerd op CHIPS.

In **hoofdstuk 4** zijn de C5a-receptor mimetica gesynthetiseerd met phosphaat groepen op de plek waar in de natuur sulfaat groepen zitten (tyrosines 11 en 14). Deze phosphaat groepen lijken qua structuur en lading veel op sulfaat groepen en de synthese van gephosporyleerde peptiden is al beter beschreven en de phosphaat groepen zijn stabieler. In dit hoofdstuk is getest of deze gephosphoryleerde C5aR mimitica ook kunnen binden aan CHIPS en of ze kunnen concurreren met de gesulfateerde receptor. Het bleek dat *in vitro*, de gephosphoryleerde C5aR mimetica vergelijkbare affiniteit voor CHIPS laten zien in vergelijking met de gesulfateerde mimetica. Ook de invloed van de gephosphoryleerde C5aR mimic op de chemical shifts van de amides in de peptideketen van CHIPS bleek vrijwel hetzelfde te zijn in vergelijking met de gesulfateerde C5aR mimic. Bij de biologische experimenten met C5aR presenterende cellen bleek echter dat de gephosphoryleerde C5aR mimetica minder goed in staat waren te concurreren met de natieve receptor. Dit in tegenstelling tot de gesulfateerde mimitica beschreven in hoofdstuk 3.

In **hoofdstuk 5** wordt de kennis over de structuur van het $CHIPS_{31\text{-}121}$:$C5aR_{7\text{-}28}S_2$ complex, beschreven in hoofdstuk 3, gebruikt voor het ontwerpen van een CHIPS mimic. Deze mimic is '**CH**emotaxis inhibitory c**O**nstruct **P**rotein of ***S****taphylococcus aureus*' (CHOPS) genoemd (Fig. A3B). CHOPS bestaat uit twee fragmenten van CHIPS die in direct contact zijn met de C5a-receptor. Deze twee fragmenten zijn aan elkaar gekoppeld met een kleine peptide sequentie die een bocht in de peptide keten induceert. Dit 50 amino zuren grote peptide bond aan het gesulfateerde $C5aR_{7\text{-}28}S_2$ met een dissociatie constante van 3.6 μM, terwijl het geen binding aan het ongesulfateerde peptide vertoonde. Terwijl het kleine eiwit geen structuur vertoonde in oplossing, konden verschillende lange afstands NOE contacten worden gemeten zodra het bond aan $C5aR_{7\text{-}28}S_2$. Deze contacten suggereren dat CHOPS een vergelijkbare structuur aanneemt als CHIPS zodra het bind aan de gesulfateerde receptor mimetica.

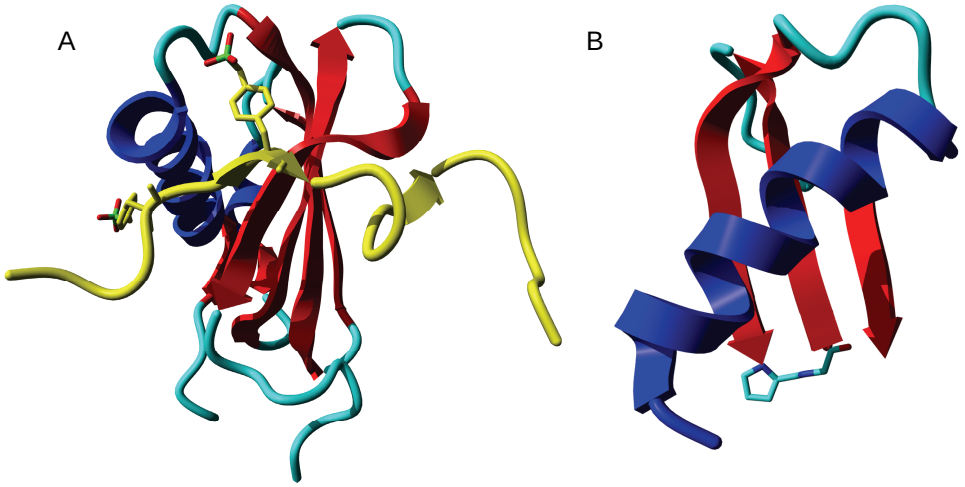

Figuur A3 A) Een NMR structuur van het $CHIPS_{31-121}$:$C5aR_{7-18}S_2$ complex, B) Een model van CHOPS.

Na het succes van het ontwerpen en synthetiseren van de eerste mimic van CHIPS, beschreven in hoofdstuk 5, zijn we gaan proberen om nog kleinere mimetica te ontwerpen. In **hoofdstuk 6** hebben we gekozen voor een andere aanpak om CHIPS na te bootsen. In dit hoofdstuk zijn er verschillende kleine peptide fragmenten van CHIPS geselecteerd welke, volgens de NMR structuur van het complex, belangrijk zijn voor binding aan C5aR. Deze kleine fragmenten zijn samen gebracht op de TAC-scaffold in een dusdanige oriëntatie dat ze de structuur van CHIPS zouden kunnen benaderen. De speciale eigenschappen van de TAC-scaffold maakte het mogelijk om drie verschillende peptide sequenties te koppelen en dat allemaal op de vaste drager. Vier op TAC gebaseerde CHIPS mimetica werden ontworpen en succesvol gesynthetiseerd. Helaas bleken deze mimetica geen affiniteit te vertonen voor de C5aR mimetica in ITC experimenten en konden ze ook de activering van de C5aR niet voorkomen in biologische testen met C5aR presenterende cellen.

Curriculum Vitae

De auteur van dit proefschrift werd geboren op 28 september 1981 te Soest en is vanaf zijn 3e levensjaar opgegroeid in Amersfoort. Na het behalen van het VWO diploma in juni 1999 aan het Farel College te Amersfoort koos hij voor een studie Scheikunde aan Universiteit Utrecht. Na het behalen van zijn propedeuse scheikunde Cum Laude in augustus 2000 koos hij voor de studierichting 'Geneesmiddelchemie', een gezamenlijke opleiding van de faculteiten Farmacie en Scheikunde. Aan het eind van het derde studie jaar liep hij een stage bij de discipline groep Biochemie van lipiden o.l.v. Dr. Dimitri S. Sakharov, waar onderzoek werd gedaan naar 'photodynamic therapy' wat resulteerde in zijn eerste co-auteurschap. Zijn major stage werd gedaan bij de onderzoeksgroep Medicinal Chemistry o.l.v. ing. Arwin J. Brouwer. Er werd onderzoek gedaan naar de synthese van op aminozuur gebaseerde chloromethyl sulfoxides en hun toepassing in het inhiberen van cysteine proteases, wat resulteerde in een publicatie. Zijn externe stage werd gevolgd bij Altana Pharma bv. te Amsterdam o.l.v. Dr. J. A. M. Christiaans waar hij werkte aan de synthese van nieuwe klasse medicijn kandidaten. Het doctoraaldiploma Cum Laude werd behaald op 25 augustus 2005. Van september 2005 tot september 2009 was de auteur werkzaam als assistent in opleiding o.l.v. Dr. Johan Kemmink, Dr. Ir. John A. W. Kruijtzer and Prof. Dr. Rob M. J. Liskamp bij de disciplinegroep Medicinal Chemistry & Chemical Biology aan de Universiteit Utrecht. Het verrichte onderzoek is beschreven in dit proefschrift en heeft geresulteerd in vier publicaties. Dit onderzoek werd ondermeer gepresenteerd op het 30th European Peptide Symposium (Augustus/September 2008, Helsinki, Finland) en het 21th American Peptide Symposium (Junie 2009, Bloomington, USA). Vanaf 1 april 2010 is de auteur werkzaam als postdoc bij het NKI-AvL o.l.v. Dr. Fijs W. van Leeuwen.

List of publications

A. Bunschoten, J. H. Ippel, J. A. W. Kruijtzer, L. Feitsma, C. J. C. de Haas, R. M. J. Liskamp, J. Kemmink, A peptide mimic of the Chemotaxis Inhibitory Protein of *Staphylococcus aureus*: Towards the development of novel anti-inflammatory compounds, *Amino Acids*, **2010**, in press.

A. Bunschoten, L. J. Feitsma, J. A. W. Kruijtzer, C. J. C. de Haas, R. M. J. Liskamp, J. Kemmink, CHIPS binds to the phosphorylated N-terminus of the C5a-receptor, *Bioorganic & Medicinal Chemistry Letters*, **2010**, *20*, 3338.

A. Bunschoten, J. A. W. Kruijtzer, J. H. Ippel, C. J. C. de Haas, J. A. G. van Strijp, J. Kemmink, R. M. J. Liskamp, A general sequence independent solid phase method for the site specific synthesis of multiple sulfated-tyrosine containing peptides, *Chemical Communications*, **2009**, 2999

J. H. Ippel, C. J. C. de Haas, A. Bunschoten, J. A. G. van Strijp, J. A. W. Kruijtzer, R. M. J. Liskamp, J. Kemmink, Structure of the tyrosine-sulfated C5a Receptor N-terminus in complex with chemotaxis inhibitory protein of Staphylococcus Aureus, *Journal of Biological Chemistry*, **2009**, 12363.

J. Brouwer, A. Bunschoten, R. M. J. Liskamp, Synthesis and evaluation of chloromethyl sulfoxides as a new class of selective irreversible cysteine proteases inhibitors, *Bioorganic & Medicinal Chemistry*, **2007**, 6985.

D. V. Sakharov, A. Bunschoten, H. van Weelden, K. W. A. Wirtz, Photodynamic treatment and H_2O_2-induced oxidative stress result in different patterns of cellular protein oxidation, *European Journal of Biochemistry*, **2003**, 4859.

International symposia
Abstracts

30th European Peptide Symposium, August 2008, Helsinki, Finland
Preparation of a close mimic of the N-terminal part of the C5a-receptor (C5aR) by selective introductions of sulfated tyrosine residues, A. Bunschoten, Hans Ippel, Johan Kemmink, John A. W. Kruijtzer, Carla J. C. de Haas, Jos A. G. van Strijp, Rob M. J. Liskamp, *J. Pept. Sci.*, **2008**, *14*, S1, 106.

21th American Peptide Symposium, June 2009, Bloomington, USA.
Synthesis of multiple *O*-tyrosine sulfated peptides by Fmoc/*t*Bu solid phase peptide synthesis to study the C5a-receptor, A. Bunschoten, J. H. Ippel, J. Kemmink, J. A. W. Kruijtzer, C. J. C. de Haas, J. A. G. van Strijp, R. M. J. Liskamp, *Biopolymers, peptide science*, **2009**, *92*, 320.

Posters

30th European Peptide Symposium, August 2008, Helsinki, Finland

Preparation of a close mimic of the N-terminal part of the C5a-receptor (C5aR) by selective introductions of sulfated tyrosine residues, A. Bunschoten, J. H. Ippel, J. Kemmink, J. A. W. Kruijtzer, C. J. C. de Haas, J. A. G. van Strijp, R. M. J. Liskamp.

21th American Peptide Symposium, June 2009, Bloomington, USA.

Synthesis of multiple *O*-tyrosine sulfated peptides by Fmoc/*t*Bu solid phase peptide synthesis to study the C5a-receptor, A. Bunschoten, J. H. Ippel, J. Kemmink, J. A. W. Kruijtzer, C. J. C. de Haas, J. A. G. van Strijp, R. M. J. Liskamp.

Oral presentations

14th Dutch Peptide Symposium, 27 April 2007, Utrecht University, Utrecht

Synthesis of sulfated peptides for resolving the binding site of CHIPS on the C5a-receptor.

CW-NWO 'Design & Synthesis', KNCV 'Organic Chemistry', 15 June 2007, Vrije University, Amsterdam

Synthesis of sulfated peptides for resolving the binding site of CHIPS on the C5a-receptor.

Dankwoord

Dit zijn dan de laatste pagina's van dit proefschrift waarin het werk van 4 jaar en een beetje beschreven staat. Ook al staat mijn naam dan voor op dit proefschrift, dat wil zeker niet zeggen dat ik dit werk ook allemaal alleen heb gedaan. In tegendeel zelfs, het meeste werk heb ik samen met anderen gedaan, of had ik niet zonder de hulp van anderen kunnen doen. En dan is dit, naast een paar biertjes op de receptie en het promotiefeest, de juiste plek om hen te bedanken.

Allereerst wil ik mijn promotor Rob Liskamp bedanken voor zijn enthousiasme en inspiratie. Vanaf het eerste moment dat ik als studentje wat experimenten bij MedChem mocht doen werd ik gegrepen door de stimulerende energie die van jou uitgaat. Al kon die eeuwige positiviteit af en toe wel eens frustrerend zijn als je zelf het idee had dat de plannen of resultaten helemaal niet zo positief waren, maar zelfs dan werkte het nog motiverend en kon de glimlach op mijn gezicht niet lang wegblijven. Bedankt hiervoor Rob.

Ook mijn twee copromotoren waren onmisbaar in de afgelopen jaren. John en Johan (die namen heb ik meer dan eens door elkaar gebruikt) bedankt voor jullie inspanningen, adviezen en geduld, ik heb veel van jullie beiden geleerd. Johan, bedankt voor al je uitleg over NMR, ik ben die techniek erg gaan waarderen. Ook van jouw manier van het schrijven van publicaties heb ik erg veel opgestoken. Je wist mijn verhalen, zonder de inhoud al te veel aan te passen, om te vormen in logische en duidelijke manuscripten. John, je was voor mij de wandelende encyclopedie op het gebied van peptidechemie. En ook al werd je als maar drukker met faculteitszaken en de nieuwbouw, toch wist je altijd wel de tijd te vinden voor onze chemische overlegjes en de films en concerten buiten het werk. En ik ben nog steeds verbaasd dat je altijd de juiste referenties op peptidegebied had liggen en dat je ze ook nog eens binnen zeer korte tijd wist te vinden.

Dirk, ook jij bedankt voor het feit dat ik altijd bij je terecht kon voor zinnige discussies en gesprekken en je kennis op het gebied van de organische synthese. Als John de Yin is dan ben jij de Yang van Medchem, of andersom natuurlijk. Het was altijd weer grappig om de tegenstellingen bij jullie op de kamer te zien.

Voor een zeer cruciaal onderdeel van het CHIPS project wil ik mijn dank uitspreken richting Hans Ippel. Zonder jouw inspanningen om het complex van CHIPS met de C5a-receptor op te lossen had het eerste deel van mijn proefschrift een doel minder gehad en was het tweede deel van mijn proefschrift niet mogelijk geweest. Bedankt voor je inzet en hulp.

Het CHIPS project was een samenwerking met de medische microbiologie groep in het UMC van Prof. Jos van Strijp en dan in het bijzonder met Carla de Haas. Bedankt voor het maken van de enorme hoeveelheden CHIPS die wij verbruikte voor onze experimenten, ik heb nooit zonder hoeven

te zitten. Ook jouw input van de biologische data in dit proefschrift was zeer waardevol. Ik hoop dat jouw samenwerking met Johan nog vele mooie resultaten zullen opleveren.

Verder wil ik Eefjan Breukink bedanken voor de introductie met Isothermal Titration Calorimetry. Het is een zeer waardevolle techniek gebleken die nu ruimschoots vertegenwoordigd is binnen Medchem. Kees Versluis wil ik bedanken voor zijn zeer waardevolle massa spectrometrie metingen van mijn gesulfateerde peptiden.

En natuurlijk wil ik al mijn studenten bedanken voor hun bijdrage aan dit proefschrift. Naast dat ik hopelijk jullie wat bij heb kunnen brengen van de organische chemie heb ik ook veel van jullie geleerd. Tima, jij was mijn eerste (master)student en dat was voor mij een aardig leerproces. Je hebt een paar hele mooie constructen gemaakt om CHIPS na te bootsen waarvan iets in hoofdstuk 6 beschreven staat. Tijdens het schrijven van mijn proefschrift heb ik regelmatig een grote glimlach op mijn gezicht gekregen wanneer ik weer door jouw labjournaal bladerde. Aan de opmerkingen onder aan de bladzijde kon je vaak zien of je tevreden was over het verloop van het experiment en daar kwamen regelmatig flinke krachttermen aan te pas, vooral bij die TFA ontscherming op de schudbank tijdens jouw dinsdagmiddag presentatie.

Loek, jij hebt vooral een theoretische bijdrage geleverd aan mijn kennis over synthetische sulfateringen en phosphoryleringen door jou literatuurscriptie over deze twee onderwerpen. Marcel, jij hebt met jouw bachelorondersoek naar een nieuw sulfateringsreagens perfect aangetoond waar ons bijproduct bij de synthese van gesulfateerde peptiden vandaan kwam en je hebt gelukkig ook aan kunnen tonen dat onze keuzes hierin de juiste zijn geweest. Louris, jij hebt mee kunnen helpen aan het afronden van het onderzoek beschreven in dit proefschrift en een mooie brug kunnen slaan naar eventueel vervolg onderzoek. Als beginner in de chemie heb je de peptide chemie snel opgepakt en jou ervaring met moleculaire biologie was zeer welkom bij de labelling van CHIPS en de testen die we met TPST hebben gedaan. Hopelijk gaat dit nog mooie resultaten opleveren in de toekomst.

Naast het interessante onderzoek vind ik zelf een goede werksfeer altijd erg belangrijk. En gelukkig heb ik hier zelden wat te klagen over gehad bij Medchem in zijn geheel en op Z601 in het bijzonder. De niet te missen persoon op het ‘Lovina Hofmeyer lab’ was klein van stuk maar groot van woorden. Hans bedankt voor alles wat je voor mij en de groep hebt betekend, zowel wat betreft de sfeer op het lab, de algemene ondersteuning voor HPLC en chemicaliën en voor alle zaken buiten het werk. Jij had altijd een lek luchtbed voor me klaar liggen en een ontbijt voor me klaar staan als dat nodig was. Ik wil je daarbovenop nog eens extra bedanken dat je mij wil bijstaan als paranimf bij de laatste lootjes van mijn promotie, super gozert!

En natuurlijk ook alle andere labgenootjes van Z601 bedankt voor de werksfeer. In het begin Remco van wie ik de zuurkast heb mogen erven, Maarten met zijn clickpolymeren en Cheng bij wie je altijd

als eerste moest zoeken als je iets kwijt was. Cheng, heel veel succes met het afronden van jouw proefschrift, volgens mij ben jij de volgende. Cristina, bedankt voor alle diepgaande gesprekken en veel succes als docent aan de hogeschool Utrecht. Jin en Helmus, de nieuwe bezetting van Z601, succes met jullie onderzoek de komende jaren. Jin and Helmus, the new occupants of Z601, thanks for the nice working atmosphere and good luck with your research in the coming years.

Naast mijn luidruchtige labgenoot, liep er nog eentje rond die Hans zonder moeite kon overstemmen, zowel qua geluid als qua zinloze argumenten in al even zinloze discussies. Arwin, bedankt voor al je adviezen en sfeer, ik zal het lezen van de gebruikelijke advertenties in de krant zeker missen, maar ik zal mijn ogen open houden voor onze 'sportmomenten', niemand kan zo juichen als Schumacher. Gelukkig hoor ik nu geen smurfenhouse en bambam radio meer komen van het lab naast mij, maar stiekem mis ik het wel heel af en toe.

Ik hoop dat we de activiteiten buiten het werk gaan blijven houden. De concerten, de films in Ede, het vissen en al die andere dingen. Die hebben de afgelopen 4 jaar extra leuk gemaakt en zijn volgens mij zeer belangrijk voor de sfeer in de groep.

Ik wil alle huidige AIO's van Medchem veel succes wensen met hun onderzoek en uiteindelijke promotie. Monique, Timo, Jack, Steffen, Helmus, Jinqiang, Gwen, Jacqeline, Francesca, Ou, Hilde, Loek, Thierry en Rik zet hem op. Marjolein, sterkte met het afronden en je verdere carrière.

En natuurlijk alle andere collega's van Medchem, bedankt voor de sfeer en de openheid. Ik ben nooit een dichte deur of een onvriendelijk woord tegengekomen op de zesde en zevende verdieping van het Went.

Marcel en Sandra, bedankt voor jullie vriendschap sinds ongeveer het eerste jaar van onze studie en voor onze wekelijkse ontspanning op de bank, achter de computer of op de sportschool. Jullie staan altijd voor mij klaar, of het nou met een glimlach, filmpie, auto of motor is, ik kan altijd op jullie rekenen. Marcel, bedankt dat ik ook op deze laatste dag van mijn promotieweg op jou kan rekenen als paranimf, zien we je toch nog een keer in een net pak.

Pap en Mam, bedankt dat jullie mij de kans hebben gegeven om te gaan studeren en mij hier altijd in gesteund hebben. Zonder deze steun had ik het niet gered.

Anton Bunschoten, Juli 2010.